Tumor targeted drug delivery: fate of the encapsulated and released drug

Evelien Smits

Tumor targeted drug delivery: fate of the encapsulated and released drug

Eveline Alida Wilhelmina Smits

The research in this thesis was performed at NV Organon | Schering-Plough Corporation | MSD Oss BV in Oss and the Department of Pharmaceutical Sciences at Utrecht University in collaboration with others.

Printing of this thesis was financially supported by:
MSD Oss BV
Utrecht Institute for Pharmaceutical Sciences
InProcess-LSP

ISBN: 978-94-6361-280-7

Lay out and printing: Optima Grafische Communicatie, Rotterdam

Tumor targeted drug delivery: fate of the encapsulated and released drug

Selectieve medicijnafgifte in tumoren:
farmacokinetiek van het ingesloten en vrijgekomen farmacon

(met een samenvatting in het Nederlands)

Proefschrift

ter verkrijging van de graad van doctor aan de
Universiteit Utrecht
op gezag van de
rector magnificus, prof.dr. H.R.B.M. Kummeling,
ingevolge het besluit van het college voor promoties
in het openbaar te verdedigen op

woensdag 19 juni 2019 des ochtends te 10.30 uur

door

Eveline Alida Wilhelmina Smits

geboren op 22 september 1983
te Arcen en Velden

Promotor:
Prof. dr. H. Vromans

Copromotor:
Dr. N. de Wijs-Rot

The research in this thesis was financially supported by MediTrans, an Integrated Project funded by the European Commission under the "nanotechnologies and nano-sciences, knowledge-based multifunctional materials and new production processes and devices" (NMP), thematic priority of the Sixth Framework Program.

CONTENTS

Chapter 1

General introduction

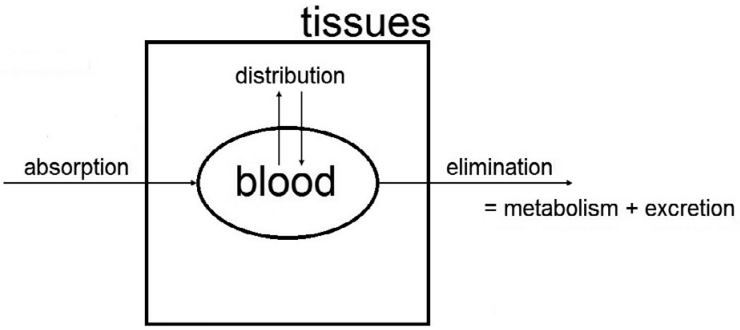

Figure 1: Schematic representation of (systemic) absorption, distribution, metabolism and excretion (ADME)
Elimination results in the loss of unchanged drug and involves both metabolism and excretion.

GENERAL INTRODUCTION

The industrial drug development process comprises multiple sequential and parallel steps [1, 2]. After the identification of new compounds and/or new drug targets, development of the dosage form follows. In this process, knowledge of the pharmacokinetics (PK) and pharmacodynamics (PD) is most useful, which describe "the relationship between the drug input and the concentration achieved with time" and "the relationship between the concentration and both the desired and adverse effects with time", respectively. During drug development four important PK processes are studied mainly quantitatively:

- **the (systemic) absorption,** i.e. the transfer of drug from the site of administration to the site of measurement which is mostly the plasma;
- **distribution,** the reversible transfer of drug between the site of measurement and the rest of the body;
- **metabolism,** the conversion of drug into another chemical structure; and
- **excretion,** the irreversible removal of drug from the site of measurement.

These PK processes are especially known by their joint abbreviation "ADME" and the individual processes are interrelated as shown in Figure 1. The ADME processes determine the local drug concentrations with time and strongly influence the performance of the drug. Studies which identify the underlying causes and which quantify the variability of the PK as well as PD provide mechanistic information that supports the development of the most safe and effective dosage form and corresponding regimen.

This thesis focusses on the targeting of solid tumors by liposomal drug delivery systems. Encapsulation of drugs in liposomes can alter the PK processes of distribution and elimination yielding an improved ratio between efficacy and

safety [3-6]. However, the PK of liposomal formulations contains an additional PK parameter of key importance, i.e. the liberation from the liposomal carrier and subsequent fate of the drug, and is not yet completely understood.

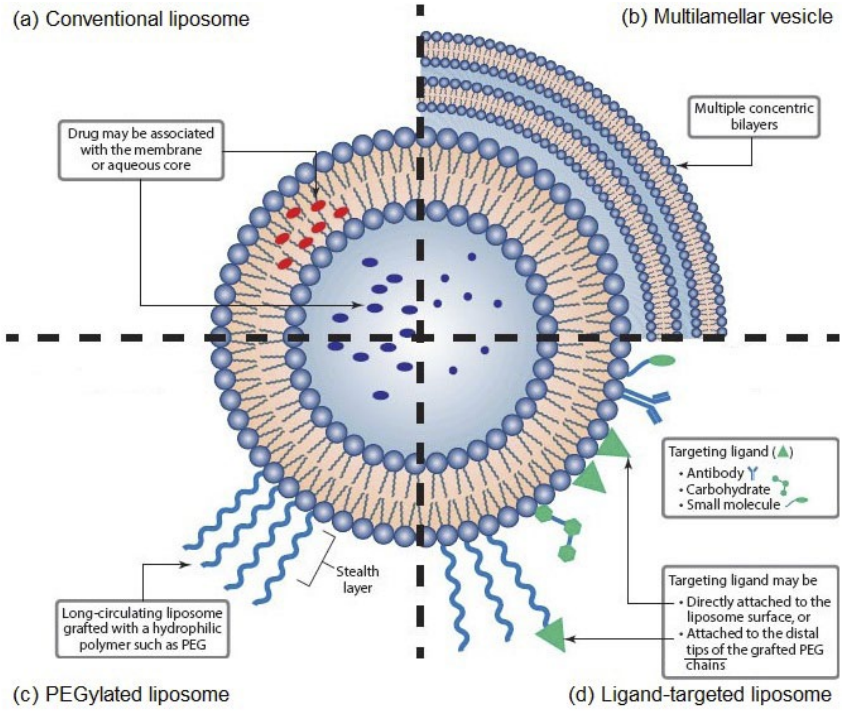

Figure 2: Schematic representation of liposomal drug delivery systems
Liposomes are vesicles in which therapeutic agents can be entrapped and consist of one (a) or more (b) lipid bilayers. Conventional liposomes (a) are composed of phospholipids to which often cholesterol is added in order to increase the liposomal stability. PEGylated liposomes (c) have an additional stealth coat of polyethylene glycol (PEG) to delay the recognition and clearance of liposomes by the macrophages of the mononuclear phagocyte system. Ligands (d) can be attached to the liposomal surface or to the terminal end of the PEG chains aiming for specific targeting. The figure is slightly adapted from Florence and Crommelin [117] with permission.

The promise of tumor targeted drug delivery by liposomes

The targeting of solid tumors by liposomal drug delivery systems has been considered a promise for quite a few decades now. Liposomes are described as vesicles in which therapeutic agents can be entrapped and which are composed of one or more (phospho) lipid bilayers (see Figure 2) [7, 8]. Ideally, the liposomal-encapsulated drug efficaciously accumulates at the intended target cells while significantly avoiding healthy tissue. At the target site the drug should be released inducing a level within the therapeutic window for a sufficient period of time. In this way, the liposomal-encapsulated drug is protected against elimination, healthy tissue is protected against the toxicity of the

drug and an optimized therapeutic activity is obtained [9, 10, 11]. This approaches the concept of the "magic bullet" as postulated by Paul Ehrlich around 1900 [12].

Table 1: Reduction of the risk of cardiotoxicity and congestive heart failure due to the encapsulation of doxorubicin in PEGylated liposomes

	Number of patients	
	liposomal (n = 254)	non-encapsulated (n = 255)
Patients who developed cardiotoxicity	10	48
Cardiotoxicity with signs and symptoms of congestive heart failure	0	10
Cardiotoxicity without signs and symptoms of congestive heart failure	10	38
Patients with signs and symptoms of congestive heart failure only	2	2

Cardiotoxicity (based on the left ventricular ejection fraction) and congestive heart failure during treatment and follow-up in a phase III trial concerning metastatic breast cancer are shown. Patients in the PEGylated liposomal doxorubicin arm (Doxil®/Caelyx®) had a median cumulative anthracycline dose of 293 mg/m^2 (including prior anthracycline exposure; doxorubicin belongs to the class of anthracyclines). For patients in the conventional non-encapsulated doxorubicin arm this was 361 mg/m^2. The overall risk of cardiotoxicity was significantly higher for non-encapsulated doxorubicin than for PEGylated liposomal doxorubicin (hazard ratio = 3.16; 95% confidence interval 1.58-6.31; p <0.001). The table is reproduced from O'Brien et al. [18] by permission of Oxford University Press on behalf of the European Society for Medical Oncology.

Improvement of pharmacokinetics, biodistribution and therapeutic index

In practice, liposomes do not meet all the criteria of an ideal tumor targeting drug delivery system as described above. However, the encapsulation of drugs in liposomes can change the PK and biodistribution compared to non-encapsulated drug formulations [3-5] yielding an increased therapeutic index mostly through reduced side effects [6, 13, 14]. To be more concrete, results from polyethylene glycol (PEG)-coated liposomes containing doxorubicin, marketed as Doxil® or Caelyx® [15], are shown as example. Doxorubicin belongs to the class of anthracyclines, which are drugs derived from *Streptomyces* bacteria and which are used in cancer chemotherapy. Their use is limited by cardiotoxic side effects that are related to the lifetime cumulative exposure [16, 17]. Yet, during the treatment of metastatic breast cancer with Doxil® a significantly reduced risk of cardiotoxicity was observed compared to the non-encapsulated drug (see Table 1 and Figure 3) [18]. Alopecia, nausea, vomiting and neutropenia are also considerable reduced, while the efficacy, i.e. the progression-free survival in months, was comparable for the liposomal and non-encapsulated formulation (6.9 versus 7.8 months, respectively; hazard ratio = 1.00; 95% confidence interval 0.82-1.22).

The achievement of an expanded therapeutic index depends on a combination of liposome features and biological characteristics of the host. Firstly, a well-balanced liposome composition reduces the drug permeability of the liposome membrane and increases the liposomal stability [8, 19]. In this respect, the phase transition temperature

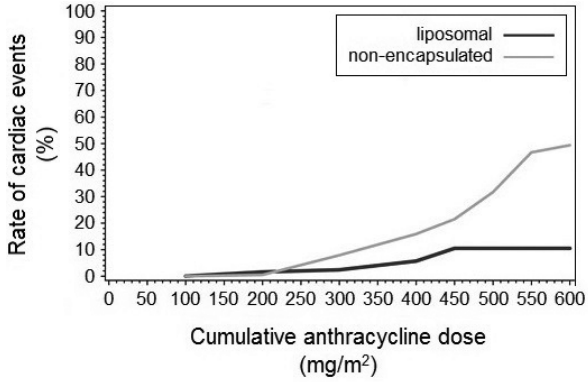

Figure 3: Reduction of the percentage of cardiac events due to the encapsulation of doxorubicin in PEGylated liposomes

The cumulative percentage of cardiac events (based on the left ventricular ejection fraction; Kaplan-Meier) is shown as a function of the cumulative anthracycline dose (including prior anthracycline exposure; doxorubicin belongs to the class of anthracyclines) for patients receiving PEGylated liposomal doxorubicin (Doxil®/Caelyx®) or non-encapsulated doxorubicin during a phase III trial concerning metastatic breast cancer. The overall risk of cardiotoxicity was significantly higher for non-encapsulated doxorubicin than for PEGylated liposomal doxorubicin (hazard ratio = 3.16; 95% confidence interval 1.58-6.31; p <0.001). The figure is reproduced from O'Brien et al. [18] by permission of Oxford University Press on behalf of the European Society for Medical Oncology.

(T_T), at which the liposome membrane transforms from a rigid state into a "fluid" state, plays an important role. Below T_T the lipids are ordered and packed, whereas above T_T the lipids are able to move freely within their own lipid layer yielding a permeable liposome membrane [8, 20]. In addition, highly permeable interfaces between domains of lipids which are still in the rigid phase and domains of lipids which are already in the fluid phase are formed upon heating [20]. Thus, liposomes composed of lipids which show a T_T above the body temperature have less-permeable bilayers after administration and also avoid large drug release during heating from storage to *in vivo* conditions, because the temperature range does not include the T_T [8, 21]. In addition, incorporation of cholesterol (see Figure 2) can decrease the permeability of liposome membranes which exhibit a fluid phase by increasing the order and packing of the lipids. The inclusion of cholesterol can even eliminate the phase transition yielding only one single phase that is neither rigid nor fluid, in which the acyl chains of the lipids are highly ordered but the lipid molecules maintain the possibility of diffusion within the lipid layer [22, 23]. The charge of the liposomal bilayers [8, 24] and the encapsulated drug as well as the drug characteristics in general, e.g. hydrophilicity, [19, 25] can also contribute to drug retention. Further, remote loading may also decrease the leakage of drug. During remote loading the drug is loaded into the liposomes after vesicle formation and it is driven by a transmembrane gradient [19, 26]. The presence of intra-liposomal trapping agents like (poly)anions or the induction of intra-liposomal drug concentrations above

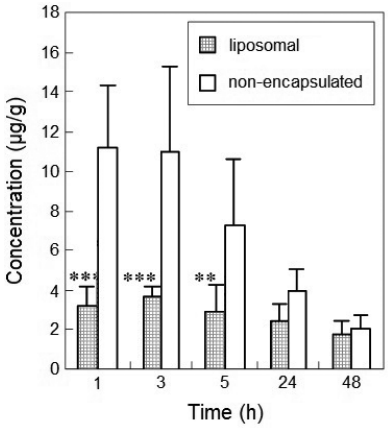

Figure 4: Example of reduced doxorubicin levels in a healthy tissue, i.e. the heart, due to liposomal encapsulation

Doxorubicin concentrations after a single intravenous injection (5 mg/kg) of PEGylated liposomal doxorubicin or non-encapsulated doxorubicin in mice are shown with time. The liposomes were composed of egg phosphatidylcholine, cholesterol, and PEG-distearoyl phosphosphatidyl ethanol amine in a molar ratio of 55:40:5. Doxorubicin was detected by HPLC-UV. Each column shows the mean and the corresponding standard error (n = 6 for each). ** indicates p <0.01 and *** indicates p <0.001 versus non-encapsulated doxorubicin at the same sampling time-point, respectively. The figure is reprinted from Lu et al. [35] with permission from Elsevier on behalf of the Japanese Pharmacological Society.

the solubility limit followed by precipitation increases the encapsulation efficiency and can also enhance drug retention [26-28].

Secondly, the liposome size strongly influences the PK of the liposomal formulation. Liposome diameters are typically about 30-500 nm and preferably about 200 nm or less [11, 29]. Such dimensions prevent the glomerular filtration of liposomes [30] and are believed to impede liposome extravasation towards healthy tissues [29, 31-33]. Provided that the drugs are stable encapsulated as described above, this is believed to be the cause of a reduction in the (total) drug levels in healthy tissues [29, 34]. For example, the encapsulation of doxorubicin in PEGylated liposomes reduces the total doxorubicin levels in the heart during the first hours after administration in mice (see Figure 4) [35]. Further, a reduced size and the addition of a stealth coat of hydrophilic polymers like PEG (see Figure 2), which interferes with the adsorption of serum proteins, reduces the recognition and delays the clearance of liposomes by phagocytic cells like macrophages of the mononuclear phagocyte system (MPS) [7, 36-39]. E.g. Scherphof et al. observed a significant reduction of the quantity of total lipids in the rat spleen and in the Kupffer cells of the liver when the average liposome size decreased from 130 nm to 85 nm as shown in Figure 5 [39]. Similarly, PEGylation also reduced the lipid quantity in the spleen and Kupffer cells. Note that for these liposomes uptake by hepatocytes also seems to play a role.

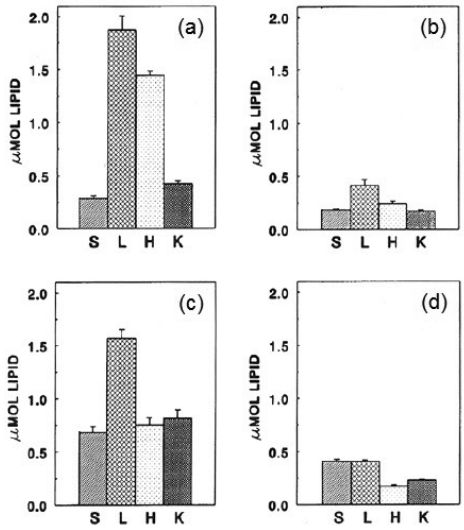

Figure 5: The effect of the liposome size and of PEGylation on the uptake of liposomes by the organs of the MPS

The distribution of non-PEGylated (a) and PEGylated (b) liposomes with an average liposome size of 85 nm, and non-PEGylated (c) and PEGylated (d) liposomes with an average liposome size of 130 nm after i.v. injection of 5 pmol total lipid in rats are shown. The liposomes were composed of egg phosphatidylcholine, cholesterol and (optional) PEG distearoyl phosphatidylethanolamine in a molar ratio of 2:1:0.12 and were radiolabeled with a trace of [^{14}C]cholesteryl oleylether. After 20 h the spleen (S), whole liver (L) and purified hepatocyte (H) and Kupffer cell (K) fractions were assayed for radioactivity and the radioactivity data was transformed into quantities of total lipid per whole organ or cell population. The figure is reprinted from Scherphof et al. [39] with permission from Elsevier.

Together with the characteristics of the healthy tissues as described above, the aforementioned liposome features can result in a considerably reduced distribution volume and an increased circulation time [4, 5, 40]. Doxil®, for example, exhibits a volume of distribution at steady state (V_{SS}) which approximates the blood volume and exhibits a half-life ($t_{1/2}$) in the range of 50-80 h in adults with cancer [5]. In contradiction, non-encapsulated doxorubicin shows a rapid decline of the initial plasma concentration due to a fast and large distribution ($t_{1/2}$: 0.06 h; V_{SS}: 365 L) followed by elimination exhibiting a $t_{1/2}$ of about 10.4 h [5, 41]. Due to the prolonged presence in the circulation, liposomes can accumulate in tumor tissue that shows specific characteristics: relative large fenestrations in the tumor vasculature allow liposomes to extravasate into the tumor interstitial fluid (see Figure 6), whereas the absence of well-functioning lymphatic drainage in the tumor results in enhanced liposome retention. This is called the enhanced permeation and retention (EPR) effect [32, 42]. As for the example of with Doxil®, at 72 h after treatment the total doxorubicin concentration in biopsy specimens of lesions from nine patients suffering from AIDS-related Kaposi's sarcoma was 5.2-11.4 fold larger than after treatment with equivalent doses of non-encapsulated doxorubicin [43].

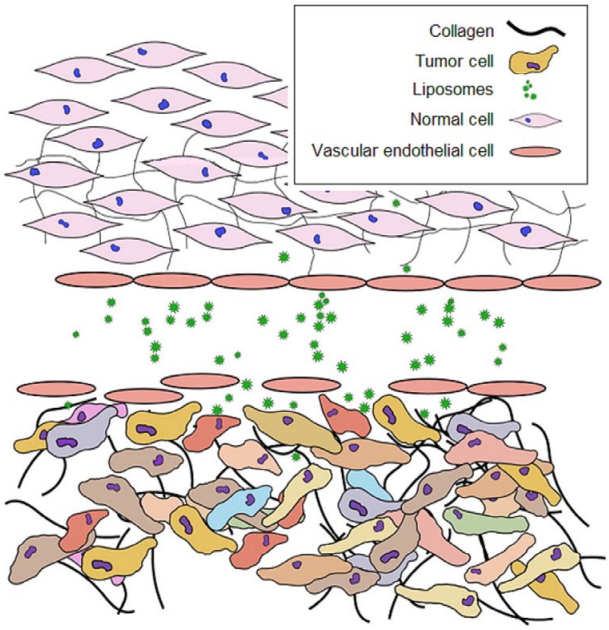

Figure 6: Extravasation of liposomes through large fenestrations in the tumor vasculature
The figure is reprinted from Nichols and Bae [32] with permission from Elsevier.

An overview of approved liposomal formulations for cancer therapy is listed in Table 2. Despite extensive research and the preclinical development of dozens of liposomal drug formulations during the past decades [15], until now, only about a dozen liposomal formulations received approval for the treatment of cancer. Hence, the usefulness of liposomal targeted delivery towards tumors is a subject of discussion [13, 15, 44-46]. The remaining challenges will be discussed in the next section.

Liposomes: challenges of tumor targeted delivery

The success of tumor targeting by nanomedicines like liposomes and the corresponding EPR effect have been discussed lately [32, 44, 47]. Various challenges in liposomal tumor targeting still remain. These are discussed in this section.

Heterogeneity of the EPR effect

The EPR effect is a variable phenomenon and it can vary between animal models and humans, between different types of cancer, between individuals and even within individual tumors [13, 32, 47-49]. E.g. Harrington et al. [48] used nuclear medicine whole body gamma camera imaging to study the differences in accumulation of ^{111}In-DTPA-labeled PEGylated liposomes in various solid tumors in patients with locally advanced cancers. At 72 h, the reported tumor accumulation ranged from 5.3 ± 2.6% of the

Table 2: Approved liposomal formulations for tumor targeted drug delivery

Name	Year of first approval	Cargo	Indication
Doxil®/ Caelyx®	1995 (FDA)	doxorubicin	AIDS-related Kaposi's sarcoma, ovarian cancer, multiple myeloma (combination therapy with bortezomib), metastatic breast cancer
DaunoXome®	1996 (FDA) *partly discontinued*	daunorubicin	AIDS-related Kaposi's sarcoma
DepoCyt(e)®	1999 (FDA) *discontinued*	cytarabin	lymphomatous meningitis
Myocet®	2000 (EMA)	doxorubicin	metastatic breast cancer (combination therapy with cyclophosphamide)
Lipusu®	2003 (China)	paclitaxel	ovarian cancer, non-small cell lung cancer, breast cancer (in combination with cisplatin or without)
Mepact®	2009 (EMA)	mifamurtide	high-grade non-metastatic osteosarcoma (used with other anticancer medicines after the cancer has been removed by surgery)
Marqibo®	2012 (FDA)	vincristine	acute lymphoblastic leukemia
Onivyde®	2015 (FDA)	irinotecan	metastatic adenocarcinoma of the pancreas (combination therapy with fluorouracil and leucovorin)
Vyxeos®	2017 (FDA)	daunorubicin, cytarabine	acute myeloid leukemia

The table is derived using the following sources: Belfiore et al. [15], College ter Beoordeling van Geneesmiddelen [111], European Medicine Agency (EMA) [112], Leadiant Biosciences [113], Sofias et al. [114], U.S. Food and Drug Administration (FDA) [115], and Zylberberg and Matosevic [46]. Generic equivalents are not included.

injected dose/kg in breast cancers to 33.0 ± 15.8% of the injected dose/kg in head and neck cancers. However, the "% of the injected dose/kg" as units of measurement might be confusing, because the tumor mass was rather in the order of g instead of kg. I.e. the estimated tumor mass ranged from 36.2 ± 18.0 g (for head and neck cancers) to 234.7 ± 101.4 g (for breast tumors). Consequently, the estimated levels of tumor liposome uptake expressed as % of the injected dose were only about 0.5-3.5%. A meta-analysis of the literature on studies performed in animal tumor models from 2005-2015 shows that on average only 0.5% of the injected dose is delivered to tumors with a maximum of about 10% [49]. In addition, the EPR effect is most probably more pronounced in animal models than in humans [32]. The sub-optimal efficiency of the EPR effect has been recognized by the scientific community [32, 44, 47, 50, 51]. To control and enhance the liposome extravasation towards tumors, pharmacological (e.g. tumor penetrating peptides, histamine, tumor necrosis factor-alpha) and physical (e.g. hyperthermia, radiotherapy) strategies to modulate the tumor vasculature have been attempted [50, 51]. For instance, liposome extravasation initiated by local hyperthermia was observed as shown in Figure 7 [52]. Physical strategies like hyperthermia can also trigger the release of drug from the liposomes and are further discussed below.

Due to irregular vascular distribution and permeability as well as heterogeneous blood flow within a single tumor, large regions of the tumor are inaccessible by means of the EPR effect alone [32]. Diffusion of the liposomes to cover for the remaining distance is hindered due to an increased interstitial fluid pressure and biological interactions with cells and proteins like collagen in the tumor tissue [32, 50]. This results in the inhomogeneous distribution of liposomes in the tumor including large regions that are not accessible to liposomes (see Figure 8) [120]. Attempted strategies for the enhanced intratumoral penetration include the modification of the liposome (e.g. the addition of tumor penetration peptides) as well as modification of the interstitial fluid pressure and extracellular tumor matrix [50, 53]. The latter strategies include the application of enzymes that catalyze the degradation of collagen and hyaluronic acid as well as inhibitors that suppress the synthesis of these constituents of the extracellular tumor matrix, which are a barrier for liposome movement and contribute to the high interstitial fluid pressure [50, 54].

Intracellular drug availability

After accumulation of the liposomal carrier in the interstitial fluid of the tumor tissue, ideally, the encapsulated drug has to end-up in the (cancer) cell and has to be released to become available and manifest its activity. However, the internalization of PEGylated liposomes by cancer cells is believed to be minimal and, rather, the drug is released by slow, nonspecific degradation of the liposome in the interstitial fluid followed by transfer of the released drug into the cancer cells [55, 56]. The exact release mechanism is often not well known, although the degradation of the liposomes by endocytic cells like macrophages can play a role [57, 58]. Several approaches to increase the intracellular availability of released drug in the cancer cells are attempted and can be roughly divided into two groups: (1) ligand-based targeting to increase the selective uptake of the liposomes by the target cell and/or (2) triggered-based release to induce (the controlled) release from the liposomes locally [8, 59]. These approaches will be illustrated below.

The attachment of targeting ligands on the surface of liposomes (e.g. antibodies, growth factors), of which the corresponding binding partner is either exclusively expressed on the target cell or is expressed in relatively high amounts compared to normal cells, can induce direct liposome-target cell binding [8, 59]. Additionally, ligand-target binding can induce liposome internalization usually by endocytosis [15, 59]. Aiming for drug release into the cytoplasm, the drug should be released from the liposome by liposome degradation or a pH-triggered release mechanism in the acidic and enzyme rich endosomes/lysosomes followed by escape of the drug from the harsh environment [19, 59, 60]. Additionally, cell penetrating peptides are added to liposome preparations in order to attempt translocation of the encapsulated drug through the cell or endosomal membrane [8, 61].

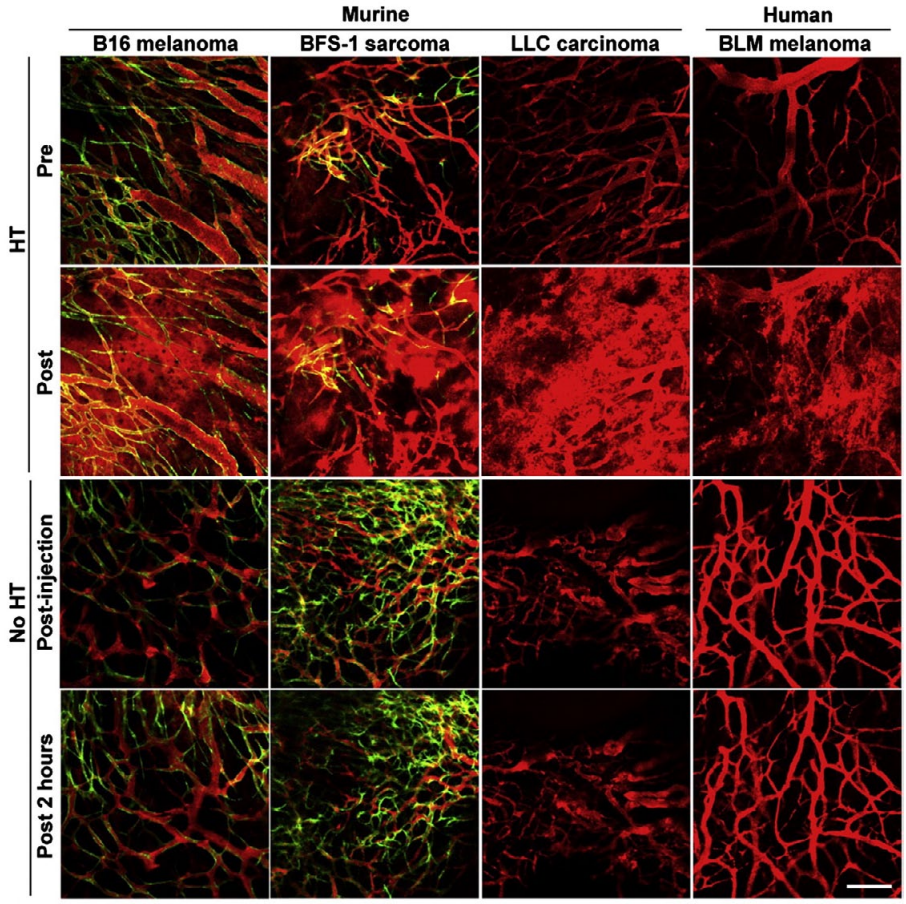

Figure 7: Hyperthermia enhances the extravasation of PEGylated liposomes

The extravascular localization of PEGylated liposomes is shown by intravital confocal microscopy using a dorsal skin flap window chamber, at which the liposomes (red) and tumor vasculature (green) were labelled. Optionally, mild hyperthermia (HT) at 41°C was applied for 1 h. Four tumor models in mice were used: murine B16 melanoma, BFS-1 sarcoma, Lewis lung carcinoma (LLC) and human BLM melanoma.

Extravascular liposome accumulation was observed upon mild HT, while without mild HT the liposomes remained located within the tumor vasculature in all selected locations up to 2 h post-injection. The liposome extravasation was attributed to the observed increase of the vascular permeability. Depending on the tumor model, the permeable tumor vascular surface showed at minimum a more than 50 fold increase due to HT [52].

The liposomes were composed of 1,2-dipalmityol-sn-glycero-3-phosphocholine, 1,2-distearoyl-sn-glycero-3-phosphocholine and 1,2-distearoyl-sn-glycero-3-phosphoethanolamine-*N*-PEG2000 in a molar ratio of 80:15:5 and were labeled with 1,2-dioleoyl-sn-glycero-3-phosphoethanolamine-*N*-(lissamine rhodamine B sulfonyl) in the lipid membrane (0.1 mol%). The liposome diameter was about 85 nm. The scale bar represents 200 µm. The figure is reprinted from Li et al. [52] with permission from Elsevier.

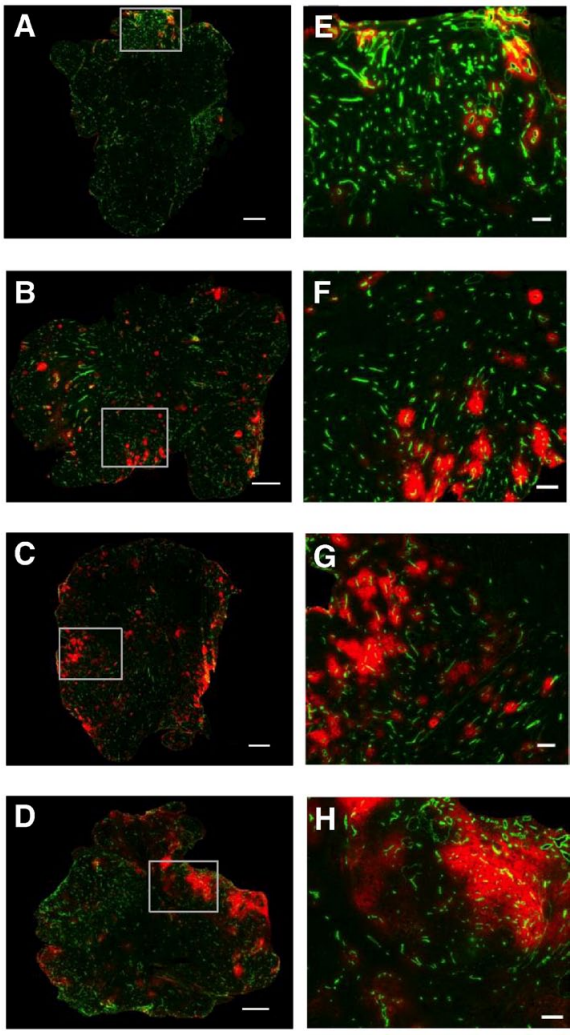

Figure 8: The inhomogeneous distribution of PEGylated liposomes within a tumor

The intratumoral distribution of PEGylated liposomes is shown by fluorescence microscopy of whole ME-180 tumor tissue sections from a murine tumor model, at which the liposomes (red) and tumor blood vessels (green) are labeled. Fluorescence images were recorded at 2 (a,e), 18 (b,f), 48 (c,g) and 120 (d,h) h after injection. The images in the second column present the enlargements of the indicated sections in the first column.

Roughly, the signal corresponding to extravascular liposomes in the rim and periphery seems to increase with time, whereas the liposome localization in the core remains relatively low and unaltered [120]. Note that large regions (with or without showing the green signal corresponding to the vessels) do not show the red liposome signal.

The liposomes were composed of 1,2-dipalmitoyl-sn-glycero-3-phosphocholine, cholesterol and *N*-(carbonyl-methoxyPEG-2000)-1,2-distearoyl-sn-glycero-3-phosphoethanolamine in a molar ratio of 55:40:5 and the liposome diameter was 96.4 ± 5.4 nm. The scale bars represent 1 mm in the first column and 200 μm in the second. The figure is reprinted from Ekdawi et al. [120] with permission from Elsevier.

If the drug release from PEGylated as well as ligand-targeted liposomes is insufficient, a triggered release mechanism could be implemented. Different triggered release approaches are attempted, which can be roughly divided into two categories: physiology-dependent release and external stimuli-dependent release [8, 46, 62]. During physiology-dependent release the deviant characteristics of the tumor tissue or of cellular organelles (e.g. low pH, elevated enzyme levels) are exploited to trigger drug release, whereas during external stimuli-dependent release a remote trigger (e.g. heat, ultrasound, light) is applied [8, 46, 62]. If the triggered release occurs in the tumor vasculature [63] or tumor interstitial fluid [64], the drug itself should still transfer into the target cell [55, 56]. Hyperthermia is a multifunctional strategy. Besides direct tumor tissue destruction by heat ablation, thermal sensitization of tumor cells prior to radiation and/or chemotherapy and the permeabilization of the tumor vasculature, mild hyperthermia in combination with (low)-thermosensitive liposomes can also be attempted to trigger drug release increasing the local available drug concentrations [50, 65]. These thermosensitive liposomes contain lipid bilayers exhibiting a phase transition temperature in the range of the applied temperature, lysolipids and/or thermosensitive polymers. Note, drug release from thermosensitive liposomes often occurs in the vasculature of the tumor avoiding the necessity of the EPR effect [63, 66]. This in contradiction to "plain" PEGylated liposomes that are aiming for extravasation from the vasculature into the tumor. An example of the benefit of local hyperthermia as well as thermosensitive liposomes is shown in Figure 9 [67]: low-thermosensitive liposomes administered during local hyperthermia showed a rapid signal enhancement at the tumor periphery that remained elevated until the end of the experiment. As discussed by the authors, this illustrated rapid release kinetics, which is so fast that all drug is released before the liposomes reached the tumor center. On the contrary, low-thermosensitive liposomes administered without local hyperthermia showed a smaller, but relatively homogeneous distributed signal enhancement in the tumor with a maximum at 5 min followed by a decline due to clearance of liposomes from the vasculature. Meanwhile, administration of non-thermosensitive liposomes during hyperthermia showed a heterogeneous distributed signal enhancement that increased throughout the experiment. However, at 5 min after administration of non-thermosensitive liposomes without hyperthermia only minimal enhancement was observed in the tumor. The minimal enhancement reflected the presence of liposomes in the vasculature. No enhancement was observed for the other time points. These differences between non-thermosensitive liposomes with and without hyperthermia showed the improved liposome extravasation and accumulation due to hyperthermia.

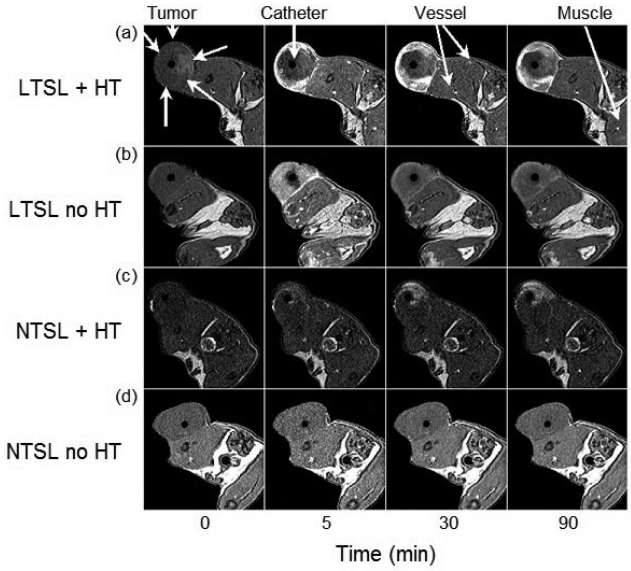

Figure 9: The benefit of local hyperthermia as well as thermosensitive liposomes
The MRI signal enhancement is shown as a function of time for rats with transplanted flank fibrosarcomas treated with the following $MnSO_4$/doxorubicin loaded liposomes (10 mg/kg of doxorubicin) with or without hyperthermia (HT): (a) low-temperature sensitive liposomes (LTSL) with HT, (b) LTSL without HT, (c) non-thermally sensitive formulation (NTSL) with HT, and (d) NTSL without HT. The MRI signal enhancement is mainly representative for the released drug, although there is also some signal from the $MnSO_4$ in the liposomes (due to the water inside the liposomes). The flank tumor, heating catheter, venous vessels and unheated muscle are indicated in the first row. The figure is reproduced from Viglianti et al. [88] with permission from Wiley. © 2004 Wiley-Liss, Inc.

Accumulation in healthy tissues

Besides challenges concerning the tumor, PEGylated liposomes still localize in healthy tissues like the liver and the spleen [5, 68, 69]. Probably, the accumulation of PEGylated liposomes in the liver and the spleen still involves the MPS, since PEGylation only reduces the uptake by macrophages and does not completely avoid it [39, 70]. However, the different anatomy of the vasculature of these organs may also play a role [30]. Figure 10 shows the considerable uptake of radiolabeled PEGylated liposomes in the liver, spleen and in this case also the bone marrow in a patient with a lung tumor [5]. Additionally, dose-limiting side effects can be observed. In the previous section the treatment of breast cancer by Doxil® was shown as an example of the reduction of certain side effects. However, in the same study, the risk of other side effects increased. Due to the changed PK, hand-foot syndrome (48% versus 2%), stomatitis (22% versus 15%) and mucositis (23% versus 13%) were more often associated with the liposomal formulation in comparison to the non-encapsulated doxorubicin [18]. Besides the introduction or increase of side effects, liposomes accumulating in healthy tissues do, of course, not

reach the tumor, which represents another deviation from the ideal tumor targeting drug delivery system.

Alternatively, optimization of the liposome characteristics as well as priming of the biological environment have been investigated in order to reduce the uptake by the MPS [36, 61]. This includes (1) liposome properties that bind plasma proteins which decrease interactions with macrophages, (2) the attachment of PEG to multiple phospholipids which increases the stability and circulation half-life and decreases the accumulation in liver and spleen, (3) mimicking the transport features of naturally occurring components, and (4) saturation and depletion of macrophages [36, 61].

Although strategies to reduce the uptake by the MPS, to optimize liposome extravasation towards the tumor and the liposome distribution in the tumor, and to deliver the released drug intracellularly are believed to be promising, they are often accompanied by their own complications and/or more research is required [15, 36, 46, 50, 51, 53, 59, 61]. Moreover, due to the heterogeneity of cancer it is not likely that there will be one single strategy suitable to deal with all challenges and the need for personalized medicine is rising [50, 51, 54]. The clinical value of these approaches will be apparent in the future.

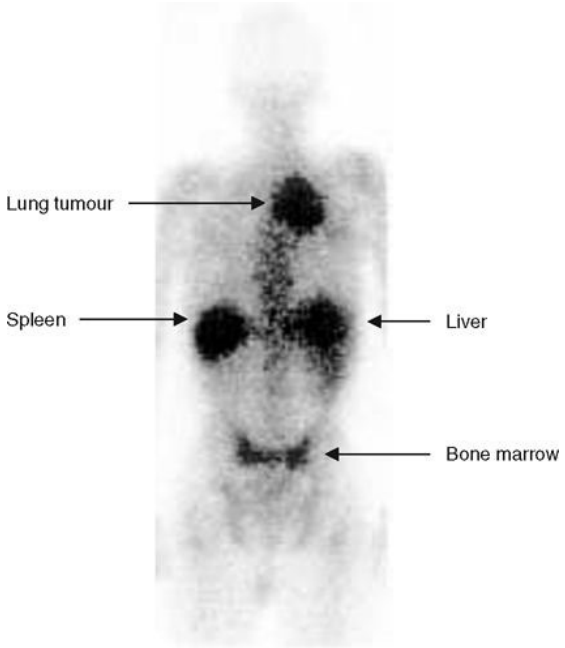

Figure 10: Tissue distribution of PEGylated liposomes in a patient with lung cancer
The image was recorded by gamma scintigraphy (posterior view) 48 h after the injection of ^{111}In-radiolabelled PEGylated liposomes. Prominent liposome uptake was seen in the lung tumor, liver, spleen and bone marrow [5]. The figure is reprinted from Gabizon et al. [5]. The figure from Gabizon et al. is reprinted from Harrington et al. [48]. Reprinted with permission from AACR and by permission from Springer Nature.

Direct and accurate quantification of released drug

Successes and challenges of drug formulations are determined by the PK and PD. Consequently, analysis of the PKPD is an integral part of the drug development process as described above. However, the complete PKPD of liposomal formulations intended for the targeting of solid tumors is often not known. Besides knowledge of ADME of the liposomal formulation, another PK process is of crucial importance for the success of liposomal drug delivery systems. As already shortly mentioned above, the biological activity is not related to the drug that is still entrapped in the liposomes (in this chapter further referred to as encapsulated drug). Only the released drug is available and can induce efficacy and toxicity (in this chapter further referred to as released drug) [71, 72, 73]. The availability of released drug and the corresponding fate (i.e. retention, distribution, elimination) are as least as important as the behavior of the liposomal carrier [71, 74]. Thus, the individual quantification of the encapsulated drug and the released drug in the circulation, tumor as well as healthy tissues is essential to understand and improve the PK and PD of liposomal targeted delivery. This is stressed by the example of PEGylated liposomal cisplatin for which poor clinical results were observed [73]. Zamboni et al. suggested that, while larger amounts of liposomal cisplatin accumulated in the tumor as compared to the corresponding non-encapsulated drug formulation, less platinum was released into the extracellular fluid and less platinum-DNA adducts were formed, to which cytotoxicity is related.

Such individual concentration profiles have been measured in plasma (and other body fluids) using techniques such as solid phase extraction and size-exclusion chromatography. These techniques separate the liposomes and released drug based on their different physicochemical properties like charge, size and hydrophobicity [75-81]. However, these separation techniques are problematic for the separate quantification with regard to solid tissue samples, since tissue homogenization is required prior to their application. Homogenization tends to induce liposome rupture and release of encapsulated drug which leads to overestimations of the released drug concentration [82]. Nevertheless, Su et al. [119] claim they developed a homogenization method without disrupting nanoliposomes by using a ball mill with mild conditions. Unfortunately, at the time of writing of this introduction, the specific study has not been published yet.

It is probably due to these practical complications that the separate quantification of encapsulated and released drug in tissues is still not common. A small number of methods are explored to work around these practical difficulties. These will be discussed here. The measurement of the drug-to-lipid ratio can provide some valuable insights about the *in vivo* release [83]. If the clearance of the liposomal lipids and the encapsulated drug from the circulation or tissue is negligible compared to the clearance of the released drug, lower drug-to-lipid ratios indicate that more drug is released from the liposomes and is metabolized, diffused and/or excreted [84, 85]. The drug-to-lipid

ratio thus cannot differentiate between encapsulated drug and released drug that is still present in the tissue.

The co-encapsulation of MRI contrast agents like Gd^{3+}- and Mn^{2+}-complexes which are liberated simultaneously with the drug can also allow the visualization and quantification of drug release from the liposomes in tissues in a minimally invasive, temporal and spatial manner [63, 66, 74, 121]. Usually, these MRI contrast agents modify the signal of the surrounding water by altering the longitudinal relaxation time T_1 of the water protons [63, 66, 86-88]: inside the liposomes this effect is considerable less visible, because the exchange of water molecules across the liposomal membrane is limited. After release of the contrast agent (and drug), the water exchange increases resulting in an increased amount of water protons with an altered T_1, which induces contrast enhancement. Shortly after (i.e. 90 min) the intravascular triggered release from thermosensitive liposomes by locally applied hyperthermia, the co-localization of drug and contrast agent in the tumor seems sufficient in order to calculate the released drug concentrations in the tumor based on the observed relaxivity of the contrast agent [67]. However, finding ideal contrast agents which also mimic the complete PK profile of the released drug for hours and days (i.e. retention, biodistribution, metabolism and excretion) is believed to be quite challenging [66, 74, 89].

Similarly, the co-encapsulation of fluorophores (e.g. carboxyfluorescein, calcein) that are released simultaneously with the encapsulated drug could visualize drug release from the liposomes in tissues [90-92]. The differentiation of encapsulated and released fluorophore is based on self-quenching [92, 122]. Self-quenching means that the fluorescence intensity is considerably decreased at high fluorophore concentrations, whereas at sufficiently low concentrations the fluorescence intensity correlates linearly with the concentration. The fluorophore concentration inside the liposomes is sufficiently high to result in minimization of the fluorescence signal, while upon release the fluorophore is diluted to a level at which quenching is not apparent. Most probably, imaging of the complete PK profile of released drug by analysis of the fluorophore faces similar challenges as discussed for MRI contrast agents. However, the encapsulation of drugs exhibiting fluorescent properties themselves (e.g. doxorubicin) allow the visualization of the biodistribution of the released drug [92-95]. To do so, homogenization of dissected tissue samples should, of course, be avoided. Herewith, fluorescence microscopy of excised, thin tissue slices (μm range) [93] or in combination with window frames which are surgical implanted onto small tumors at a skin flap [92, 94, 95] can offer a solution. However, accurate quantitative analysis of released doxorubicin by fluorescence microscopy is difficult, because doxorubicin fluorescence is partially quenched upon DNA binding [5, 56, 96, 97]. Moreover, the applicability of multiple windows to also visualize the release in large healthy tissues like the liver and the spleen seems questionable.

Laginha et al. used the affinity of doxorubicin for DNA in the cell nucleus to estimate released doxorubicin levels in tumor tissue [72]. More specific, after release from the liposomes in the tumor interstitium, doxorubicin was assumed to quickly diffuse into surrounding cells [98]. Hereafter, the nucleus functions as a "sink" for doxorubicin, at which doxorubicin strongly binds to DNA, even when the drug was first located in other organelles [99, 100]. Indeed, after injection of non-encapsulated doxorubicin the drug located in the nucleus of tumor cells showed an area under the concentration-time curve (AUC) from 0 to 24 h which was 95% of the corresponding AUC for the total drug in the tumor. This confirms the sink characteristics of the nucleus for doxorubicin. The C_{max} of total doxorubicin was reached at 30 min after injection, whereas the C_{max} of doxorubicin in the nucleus was only reached after 4 h. This indicates a lag time between drug release and accumulation in the nucleus of several hours. The advantage is that the method approximates the available drug at one [101] of the sites of action. Based on an AUC from 0 to 7 days for drug in the nuclei relative to the total tumor, Doxil® resulted in an availability of 49.4 and 41.3% for a dose of 9 and 16 mg/kg, respectively. The availability of released drug in healthy tissues was not included.

Finally, microdialysis allows the measurement of the non-protein-bound fraction of the released drug but solely in the fluids of tissues. It involves passive diffusion from the interstitial fluid across the semi-permeable membrane of a microdialysis catheter [102].

Without the intention to devaluate the aforementioned methods, the encapsulation of phosphate prodrugs in liposomes can provide a direct and accurate method for the individual quantitation of encapsulated and release drug concentrations in solid tumors and tissue. This will be explained in the next sections.

Liposomal prednisolone phosphate

The encapsulation of the phosphate prodrug of prednisolone (P) allows the individual quantification of encapsulated and released drug concentrations in tissues after administration of the liposomal formulation [103]. Prednisolone phosphate (PP) is known for its rapid dephosphorylation into P *in vivo* [103-105]. Immediate conversion of PP into P after release from the liposomes *in vivo* provides a means to differentiate between encapsulated and released drug also in tissues. As will be discussed in the next section, the thorough development and implementation of such methodology form the aim of this thesis. PEGylated liposomes containing glucocorticoids like PP are not only applied for drug delivery with regard to typical inflammatory diseases like rheumatic arthritis and multiple sclerosis, but also with regard to cancer-related inflammation [106]. In contradiction to the non-encapsulated drug formulation, the liposomal formulation of PP was able to reduce tumor growth in tumor mouse models as shown in Figure 11 [107]. Often the inhibition of the production of pro-angiogenic/pro-inflammatory factors by tumor associated macrophages [108, 109] is designated as the main underlying

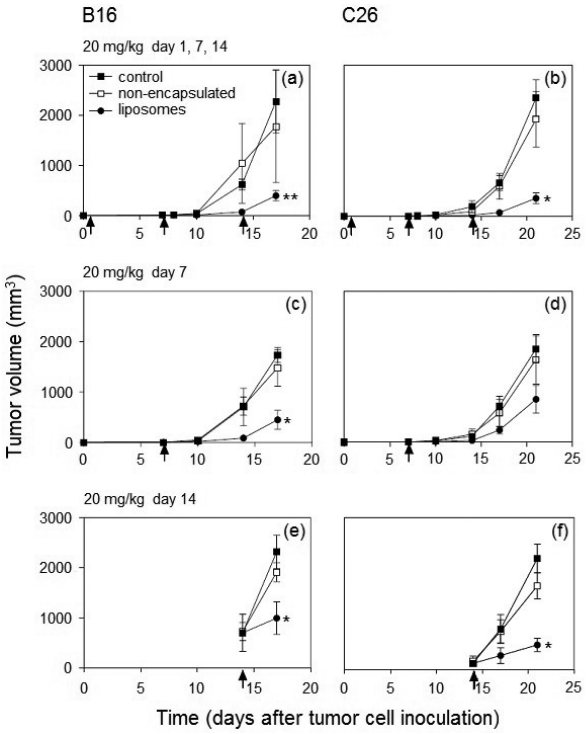

Figure 11: Inhibition of tumor growth by PEGylated liposomal PP in tumor mouse models
The tumor volume as a function of time is shown after different treatment schedules of PEGylated liposomal PP, non-encapsulated PP and saline (control). Multiple injections (a, b) or a single injection (c-f) of 20 mg/kg of liposomal PP or non-encapsulated PP were administered to B16F10 (a, c, e) and C26 tumor-bearing mice (b, d, f). The liposomes were composed of dipalmitoylphosphatidylcholine, cholesterol and PEG2000-distearoylphosphatidylethanolamine in a molar ratio of 1.85:1.0:0.15. Means ± standard deviation are represented and $n = 5$ animals per experimental group. The figure is reprinted from Schiffelers et al. [107] with permission from Elsevier.

mechanism. Additionally, Kluza et al. [118] postulated a systemic, immunosuppressive effect that may also contribute to the inhibition of tumor growth: they observed a large depletion of circulating white blood cells in mice treated with PEGylated liposomal PP. While immunosuppression can yield adverse effects, this depletion may also decrease tumor infiltration of monocytes, which stimulate angiogenesis.

The tissue distribution in tumor-bearing mice of ^{111}In-labeled PEGylated liposomes, which are similar to the PEGylated liposomal PP formulation, is shown in Figure 12. At 24 h after injection, 7-10% of the injected dose was observed in the tumor tissues of the B16F10 and C26 murine tumor models. However, relevant percentages of the injected dose also end up in the liver, spleen and kidneys. Consequently, this results in considerable liposome concentrations in healthy tissues and especially the spleen when considering its small weight (≈ 0.09 g; which was calculated from the relative organ

weight as published by Brown et al. [116] and assuming a total body weight of 25 g). From a toxicity/efficacy point of view it is important to determine the encapsulated and released drug concentrations in tumor as well as liver, spleen and kidneys.

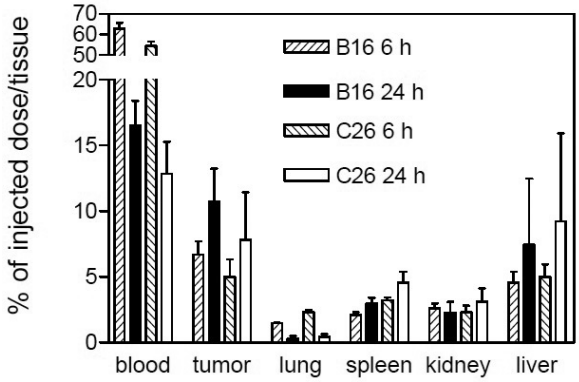

Figure 12: Tissue distribution of ^{111}In-labeled PEGylated liposomes in tumor-bearing mice
At a tumor volume of about 1 cm^3, 25 µmol/kg lipid was administered in B16F10 tumor-bearing C57BL/6 mice or C26 tumor-bearing BALB/c mice. Radioactivity in blood and tissue samples was counted using a liquid scintillation counter. Tumors weighed approximately 1 g. Means ± standard deviation are represented and n = 5 animals per experimental group. The figure is reprinted from Schiffelers et al. [107] with permission from Elsevier.

General aim of this dissertation

The aim of this thesis is to provide additional understanding of the PK of liposomal targeted delivery using PEGylated liposomal PP as a model formulation. To do so, a new analytical approach was developed for the accurate quantification of encapsulated and released drug in blood and tissues after administration of PEGylated liposomal PP in mice. The differentiation of encapsulated and released drug is based on the rapid *in vivo* dephosphorylation of PP into P after its release from the liposomes [103]: whereas the PP concentration represents the encapsulated drug concentration, the released drug concentration is assessed by quantification of the parent compound P. To obtain reliable results the methodology was thoroughly developed and validated using criteria adapted from the guidelines of the Food and Drug Administration (FDA) [110], which were in agreement with accuracy criteria from internal, industrial guidelines for preclinical bioanalytical methods. Finally, the developed methodology was implemented in a PK study in mice.

In **chapter 2** the rapid dephosphorylation of PP by murine liver and kidney phosphatases after release from the liposomes is verified *in vitro* using representative tissue homogenates and data modelling.

Chapter 3 presents the development of a method for the quantification of encapsulated and non-encapsulated drug in liposomal preparations of PP. Besides that the determination of the non-encapsulated amount is an essential part of the quality assurance of liposomal preparations, quantitative information about the encapsulated and non-encapsulated fraction in the liposome preparation itself is also required for the semi-validation of the methodology to quantitate individual encapsulated and released drug concentrations in blood and tissues *in vivo*.

Chapter 4 discusses the development and semi-validation of a suitable sample preparation method for the quantification of encapsulated PP and released P in plasma, blood and liver tissue. Besides common requirements for sample preparation (e.g. sufficient sample clean-up, extraction recovery, accuracy and precision), complete liposome rupture as well as the prevention of dephosphorylation of PP during homogenization was ensured.

Chapter 5 presents the development and semi-validation of an LC-MS method which, together with the previous developed sample preparation method, enables the simultaneous quantification of separate encapsulated PP and released P concentrations in whole blood and liver tissue. Optimized liquid chromatography, negative electrospray ionization and Orbitrap-MS analysis were applied to overcome the high-intensity matrix background of tissues samples.

Chapter 6 presents the implementation of above developed methodology during a PK study in B16F10 tumor-bearing mice. Encapsulated and released drug concentrations were measured in whole blood, tumor, liver, spleen and kidneys after administration of PEGylated liposomal PP. The released drug concentrations in the tumor were compared to the released drug concentrations in the healthy tissues. To further understand the PK, the tissue influx of encapsulated PP and the rate of release from the liposomes were modelled for all tissues separately. The results provide better understanding of the PK. Corresponding positive as well as fragile points are indicated and targeted drug delivery by liposomes is put into perspective.

REFERENCES

1. M. Rowland and T.N. Tozer, Clinical pharmacokinetics and pharmacodynamics: concepts and applications, Wolters Kluwer Health | Lippincott Williams & Wilkins, Philadelphia, 2011.
2. U.S. Food and Drug Administration, The drug development process, https://www.fda.gov/ForPatients/Approvals/Drugs/default.htm, (accessed January 2019).
3. A.Y. Bedikian, A. Vardeleon, T. Smith, S. Campbell and R. Namdari, Pharmacokinetics and urinary excretion of vincristine sulfate liposomes injection in metastatic melanoma patients, *J. Clin. Pharmacol.*, 2006, **46**, 727-737.
4. T.C. Chang, H.S. Shiah, C.H. Yang, K.H. Yeh, A.L. Cheng, B.N. Shen, Y.W. Wang, C.G. Yeh, N.J. Chiang, J.Y. Chang and L.T. Chen, Phase I study of nanoliposomal irinotecan (PEP02) in advanced solid tumor patients, *Cancer Chemother. Pharmacol.*, 2015, **75**, 579-586.
5. A. Gabizon, H. Shmeeda and Y. Barenholz, Pharmacokinetics of PEGylated liposomal doxorubicin: review of animal and human studies, *Clin. Pharmacokinet.*, 2003, **42** (5), 419-436, DOI: 10.2165/00003088-200342050-00002. Figure 10 is reprinted with permission from AACR and by permission from Springer Nature.
6. G.H. Petersen, S.K. Alzghari, W. Chee, S.S. Sankari and N.M. La-Beck, Meta-analysis of clinical and preclinical studies comparing the anticancer efficacy of liposomal versus conventional non-liposomal doxorubicin, *J. Controlled Release*, 2016, **232**, 255-264.
7. A. Bunker, A. Magarkar, and T. Viitala, Rational design of liposomal drug delivery systems, a review: combined experimental and computational studies of lipid membranes, liposomes and their PEGylation, *Biochim. Biophys. Acta*, 2016, **1858**, 2334-2352.
8. B.S. Pattni, V.V. Chupin and V.P. Torchilin, New developments in liposomal drug delivery, *Chem. Rev.*, 2015, **115**, 10938-10966.
9. Y.H. Bae and K. Park, Targeted drug delivery to tumors: myths, reality and possibility, *J. Controlled Release*, 2011, **153**, 198-205.
10. T. Lammers, W.E. Hennink and G. Storm, Tumour-targeted nanomedicines: principles and practice, *Br. J. Cancer*, 2008, **99**, 392-397.
11. S. Qian, C. Li and Z. Zuo, Pharmacokinetics and disposition of various drug loaded liposomes, *Curr. Drug Metab.*, 2012, **13**, 372-395.
12. K. Strebhardt and A. Ullrich, Paul Ehrlich's magic bullet concept: 100 years of progress, *Nat. Rev. Cancer*, 2008, **8**, 473-480.
13. J.I. Hare, T. Lammers, M. B. Ashford, S. Puri, G. Storm and S.T. Barry, Challenges and strategies in anti-cancer nanomedicine development: an industry perspective, *Adv. Drug Delivery Rev.*, 2017, **108**, 25-38.
14. M. Xing, F. Yan, S. Yu and P. Shen, Efficacy and cardiotoxicity of liposomal doxorubicin-based chemotherapy in advanced breast cancer: a meta-analysis of ten randomized controlled trials, *PLoS One*, 2015, **10**, e0133569.
15. L. Belfiore, D.N. Saunders, M. Ranson, K.J. Thurecht, G. Storm and K.L. Vinea, Towards clinical translation of ligand-functionalized liposomes in targeted cancer therapy: challenges and opportunities, *J. Controlled Release*, 2018, **277**, 1-13.
16. M.S. Ewer and S.M. Ewer, Cardiotoxicity of anticancer treatments, *Nat. Rev. Cardiol.*, 2015, **12**, 547-558.
17. J.V. McGowan, R. Chung, A. Maulik, I. Piotrowska, J.M. Walker and D.M. Yellon, Anthracycline chemotherapy and cardiotoxicity, *Cardiovasc. Drugs Ther.*, 2017, **31**, 63-75.

18. M.E.R. O'Brien, N. Wigler, M. Inbar, R. Rosso, E. Grischke, A. Santoro, R. Catane, D.G. Kieback, P. Tomczak, S.P. Ackland, F. Orlandi, L. Mellars, L. Alland and C. Tendler, Reduced cardiotoxicity and comparable efficacy in a phase III trial of PEGylated liposomal doxorubicin HCl (Caelyx™/Doxil®) versus conventional doxorubicin for first-line treatment of metastatic breast cancer, *Ann. Oncol.*, 2004, **15** (3), 440-449, DOI: 10.1093/annonc/mdh097. Table 1 and Figure 3 are reproduced by permission of Oxford University Press on behalf of the European Society for Medical Oncology.
19. T.M. Allen and P.R. Cullis, Liposomal drug delivery systems: from concept to clinical applications, *Adv. Drug Delivery Rev.*, 2013, **65**, 36-48.
20. T. Ta and T.M. Porter, Thermosensitive liposomes for localized delivery and triggered release of chemotherapy, *J. Controlled Release*, 2013, **169**, 112-125.
21. T.M. Allen and L.G. Cleland, Serum-induced leakage of liposome contents, *Biochim. Biophys. Acta*, 1980, **597**, 418-426.
22. A. Filippov, G. Orädd and G. Lindblom, The effect of cholesterol on the lateral diffusion of phospholipids in oriented bilayers, *Biophys. J.*, 2003, **84**, 3079-3086.
23. H. Saito and W. Shinoda, Cholesterol effect on water permeability through DPPC and PSM lipid bilayers: a molecular dynamics study, *J. Phys. Chem. B*, 2011, **115**, 15241-15250.
24. M. Grit and D.J.A. Crommelin, Chemical stability of liposomes: implications for their physical stability, *Chem. Phys. Lipids*, 1993, **64**, 3-18.
25. I.V. Zhigaltsev, G. Winters, M. Srinivasulu, J. Crawford, M. Wong, L. Amankwa, D. Waterhouse, D. Masin, M. Webb, N. Harasym, L. Heller, M.B. Bally, M.A. Ciufolini, P.R. Cullis and N. Maurer, Development of a weak-base docetaxel derivative that can be loaded into lipid nanoparticles, *J. Controlled Release*, 2010, **144**, 332-340.
26. G. Haran, R. Cohen, L.K. Bar and Y. Barenholz, Transmembrane ammonium sulfate gradients in liposomes produce efficient and stable entrapment of amphipathic weak bases, *Biochim. Biophys. Acta*, 1993, **1151**, 201-215.
27. D.C. Drummond, C.O. Noble, Z. Guo, K. Hong, J.W. Park and D.B. Kirpotin, Development of a highly active nanoliposomal irinotecan using a novel intraliposomal stabilization strategy, *Cancer Res.*, 2006, **66**, 3271-3277.
28. M.J.W. Johnston, K. Edwards, G. Karlsson and P.R. Cullis, Influence of drug-to-lipid ratio on drug release properties and liposome integrity in liposomal doxorubicin formulations, *J. Liposome Res.*, 2008, **18**, 145-157.
29. E. Tahover, Y.P. Patil and A.A. Gabizon, Emerging delivery systems to reduce doxorubicin cardiotoxicity and improve therapeutic index: focus on liposomes, *Anti-Cancer Drugs*, 2015, **26**, 241-258.
30. N. Bertrand and J.-C. Leroux, The journey of a drug-carrier in the body: an anatomo-physiological perspective, *J. Controlled Release*, 2012, **161**, 152-163.
31. S.K. Hobbs, W.L. Monsky, F. Yuan, W.G. Roberts, L. Griffith, V.P. Torchilin and R.K. Jain, Regulation of transport pathways in tumor vessels: role of tumor type and microenvironment, *Proc. Natl. Acad. Sci. USA*, 1998, **95**, 4607-4612.
32. J.W. Nichols and Y.H. Bae, EPR: evidence and fallacy, *J. Controlled Release*, 2014, **190**, 451-464, DOI: 10.1016/j.jconrel.2014.03.057. Figure 6 is reprinted with permission from Elsevier.
33. F. Yuan, M. Dellian, D. Fukumura, M. Leunig, D.A. Berk, V.P. Torchilin and R.K. Jain, Vascular permeability in a human tumor xenograft: molecular size dependence and cutoff size, *Cancer Res.*, 1995, **55**, 3752-3756.

34. R. Luo, Y. Li, M. He, H. Zhang, H. Yuan, M. Johnson, M. Palmisano, S. Zhou and D. Sun, Distinct biodistribution of doxorubicin and the altered dispositions mediated by different liposomal formulations, *Int. J. Pharm.*, 2017, **219**, 1-10.
35. W.-L. Lu, X.-R. Qi, Q. Zhang, R.-Y. Li, G.-L. Wang, R.-J. Zhang and S.-L. Wei, A PEGylated liposomal platform: pharmacokinetics, pharmacodynamics, and toxicity in mice using doxorubicin as a model drug, *J. Pharmacol. Sci.*, 2004, **95** (3), 381-389, DOI: 10.1254/jphs.FPJ04001X. Figure 4 is reprinted with permission from Elsevier on behalf of the Japanese Pharmacological Society.
36. A. Khalid, S. Persano, H. Shen, Y. Zhao, E. Blanco, M. Ferrari and J. Wolfram, Strategies for improving drug delivery: nanocarriers and microenvironmental priming, *Expert Opin. Drug Delivery*, 2017, **14**, 865-877.
37. A.L.Klibanov, K. Maruyama, A.M. Beckerleg, V.P. Torchilin and L. Huang, Activity of amphipathic poly(ethylene glycol) 5000 to prolong the circulation time of liposomes depends on the liposome size and is unfavorable for immunoliposome binding to target, *Biochim. Biophys. Acta*, 1991, **1062**, 142-148.
38. T. Lian and R.J.Y. Ho, Trends and developments in liposome drug delivery systems, *J. Pharm. Sci.*, 2001, **90**, 667-680.
39. G.L. Scherphof, M. Velinova, J. Kamps, J. Donga, H. van der Want, F. Kuipers, L. Havekes and T. Daemen, Modulation of pharmacokinetic behavior of liposomes, *Adv. Drug Delivery Rev.*, 1997, **24** (2-3), 179-191, DOI: 10.1016/S0169-409X(96)00457-7. Figure 5 is reprinted with permission from Elsevier.
40. T. Golan, T. Grenader, P. Ohana, Y. Amitay, H. Shmeeda, N.M. La-Beck, E. Tahover, R. Berger and A.A. Gabizon, PEGylated liposomal mitomycin C prodrug enhances tolerance of mitomycin C: a phase 1 study in advanced solid tumor patients, *Cancer Med.*, 2015, **4**, 1472-1483.
41. A. Gabizon, R. Catane, B. Uziely, B. Kaufman, T. Safra, R. Cohen, F. Martin, A. Huang and Y. Barenholz, Prolonged circulation time and enhanced accumulation in malignant exudates of doxorubicin encapsulated in polyethylene-glycol coated liposomes, *Cancer Res.*, 1994, **54**, 987-992.
42. R.K. Jain and T. Stylianopoulos, Delivering nanomedicine to solid tumors, *Nat. Rev. Clin. Oncol.*, 2010, **7**, 653-664.
43. D.W. Northfelt, F.J. Martin, P. Working, P.A. Volberding, J. Russell, M. Newman, M.A. Amantea and L.D. Kaplan, Doxorubicin encapsulated in liposomes containing surface-bound polyethylene glycol: pharmacokinetics, tumor localization, and safety in patients with AIDS-related Kaposi's sarcoma, *J. Clin. Pharmacol.*, 1996, **36**, 55-63.
44. K. Park, The drug delivery field at the inflection point: time to fight its way out of the egg, *J. Control Release*, 2017, **267**, 2-14.
45. R. van der Meel, T. Lammers and W.E. Hennink, Cancer nanomedicines: oversold or underappreciated?, *Expert Opin. Drug Delivery*, 2017, **14**, 1-5.
46. C. Zylberberg and S. Matosevic, Pharmaceutical liposomal drug delivery: a review of new delivery systems and a look at the regulatory landscape, *Drug Delivery*, 2016, **23**, 3319-3329.
47. H. Maeda, Toward a full understanding of the EPR effect in primary and metastatic tumors as well as issues related to its heterogeneity, *Adv. Drug Delivery Rev.*, 2015, **91**, 3-6.
48. K.J. Harrington, S. Mohammadtaghi, P.S. Uster, D. Glass, A.M. Peters, R.G. Vile and J.S.W. Stewart, Effective targeting of solid tumors in patients with locally advanced cancers by radiolabeled PEGylated liposomes, *Clin. Cancer Res.*, 2001, **7** (2), 243-254. Figure 10 is reprinted with permission from AACR and by permission from Springer Nature.
49. S. Wilhelm, A.J. Tavares, Q. Dai, S. Ohta, J. Audet, H.F. Dvorak and W.C.W. Chan, Analysis of nanoparticle delivery to tumours, *Nat. Rev. Mater.*, 2016, **1**, 16014.

50. B. Goins, W.T. Phillips and A. Bao, Strategies for improving the intratumoral distribution of liposomal drugs in cancer therapy, *Expert Opin. Drug Delivery*, 2016, **13**, 873-889.
51. T. Ohja, V. Pathak, Y. Shi, W.E. Hennink, C.T.W. Moonen, G. Storm, F. Kiessling and T. Lammers, Pharmacological and physical vessel modulation strategies to improve EPR-mediated drug targeting to tumors, *Adv. Drug Delivery Rev.*, 2017, **119**, 44-60.
52. L. Li, T.L.M. ten Hagen, M. Bolkestein, A. Gasselhuber, J. Yatvin, G.C. van Rhoon, A.M.M. Eggermont, D. Haemmerich and G.A. Koning, Improved intratumoral nanoparticle extravasation and penetration by mild hyperthermia, *J. Controlled Release*, 2013, **167** (2), 130-137, DOI: 10.1016/j.jconrel.2013.01.026. Figure 7 is reprinted with permission from Elsevier.
53. J.W. Nichols, Y. Sakurai, H. Harashima and Y.H. Bae, Nano-sized drug carriers: extravasation, intratumoral distribution, and their modeling, *J. Controlled Release*, 2017, **267**, 31-46.
54. A.G. Kohli, S. Kivimäe, M.R. Tiffany and F.C. Szoka, Improving the distribution of Doxil® in the tumormatrix by depletion of tumor hyaluronan, *J. Controlled Release*, 2014, **191**, 105-114.
55. Z. Al-Ahmady and K. Kostarelos, Chemical components for the design of temperature-responsive vesicles as cancer therapeutics, *Chem. Rev.*, 2016, **116**, 3883-391.
56. Y. Barenholz, Doxil® - The first FDA-approved nano-drug: lessons learned, *J. Controlled Release*, 2012, **160**, 117-134.
57. B.J. Crielaard, T. Lammers, M.E. Morgan, L. Chaabane, S. Carboni, B. Greco, P. Zaratin, A.D. Kraneveld and G. Storm, Macrophages and liposomes in inflammatory disease: friends or foes?, *Int. J. Pharm.*, 2011, **416**, 499-506.
58. C.W. Wong, B. Czarny, J.M. Metselaar, C. Ho, S.R. Ng, A.V. Barathi, G. Storm and T.T. Wong, Evaluation of subconjunctival liposomal steroids for the treatment of experimental uveitis, *Sci. Rep.*, 2018, **8**, e6604.
59. M. Merino, S. Zalba and M.J. Garrido, Immunoliposomes in clinical oncology: state of the art and future perspectives, *J. Controlled Release*, 2018, **275**, 162-176.
60. S.R. Paliwal, R. Paliwal and S.P. Vyas, A review of mechanistic insight and application of pH-sensitive liposomes in drug delivery, *Drug Delivery*, 2015, **22**, 231-242.
61. D. Zhang, J. Wang and D. Xu, Cell-penetrating peptides as noninvasive transmembrane vectors for the development of novel multifunctional drug-delivery systems, *J. Controlled Release*, 2016, **229**, 130-139.
62. Y. Lee and D.H. Thompson, Stimuli-responsive liposomes for drug delivery, *Wiley Interdiscip. Rev.: Nanomed. Nanobiotechnol.*, 2017, **9**, e1450.
63. T. Tagami, W.D. Foltz, M.J. Ernsting, C.M. Lee, I.F. Tannock, J.P. May and S.-D. Li, MRI monitoring of intratumoral drug delivery and prediction of the therapeutic effect with a multifunctional thermosensitive liposome, *Biomaterials*, 2011, **32**, 6570-6578.
64. A. Bandekar, S. Karve, M.-Y. Chang, Q. Mu, J. Rotolo and S. Sofou, Antitumor efficacy following the intracellular and interstitial release of liposomal doxorubicin, *Biomaterials*, 2012, **33**, 4345-4352.
65. Y. Dou, K. Hynynen and C. Allen, To heat or not to heat: challenges with clinical translation of thermosensitive liposomes, *J. Controlled Release*, 2017, **249**, 63-73.
66. F. Reeßing and W. Szymanski, Following nanomedicine activation with magnetic resonance imaging: why, how, and what's next?, *Curr. Opin. Biotechnol.*, 2019, **58**, 9-18.
67. B.L. Viglianti, A.M. Ponce, C.R. Michelich, D. Yu, S.A. Abraham, L. Sanders, P.S. Yarmolenko, T. Schroeder, J.R. MacFall, D.P. Barboriak, O.M. Colvin, M.B. Bally and M.W. Dewhirst, Chemodosimetry of *in vivo* tumor liposomal drug concentration using MRI, *Magn. Reson. Med.*, 2006, **56**, 1011-1018.

68. E. Cittadino, M. Ferraretto, E. Torres, A. Maiocchi, B.J. Crielaard, T. Lammers, G. Storm, S. Aime and E. Terreno, MRI evaluation of the antitumor activity of paramagnetic liposomes loaded with prednisolone phosphate, *Eur. J. Pharm. Sci.*, 2012, **45**, 436-441.
69. X. Liu, A. Situ, Y. Kang, K.R. Villabroza, Y. Liao, C.H. Chang, T. Donahue, A.E. Nel and H. Meng, Irinotecan delivery by lipid-coated mesoporous silica nanoparticles shows improved efficacy and safety over liposomes for pancreatic cancer, *ACS Nano*, 2016, **10**, 2702-2715.
70. C.D. Walkey, J.B. Olsen, H. Guo, A. Emili and W.C.W. Chan, Nanoparticle size and surface chemistry determine serum protein adsorption and macrophage uptake, *J. Am. Chem. Soc.*, 2012, **134**, 2139-2147.
71. H.M. Kieler-Ferguson, D. Chanc, J. Sockolosky, L. Finney, E. Maxey, S. Vogt and F.C. Szoka Jr, Encapsulation, controlled release, and antitumor efficacy of cisplatin delivered in liposomes composed of sterol-modified phospholipids, *Eur. J. Pharm. Sci.*, 2017, **103**, 85-93.
72. K.M. Laginha, S. Verwoert, G.J.R. Charrois and T.M. Allen, Determination of doxorubicin levels in whole tumor and tumor nuclei in murine breast cancer tumors, *Clin. Cancer Res.*, 2005, **11**, 6944-6949.
73. W.C. Zamboni, A.C. Gervais, M.J. Egorin, J.H.M. Schellens, E.G. Zuhowski, D. Pluim, E. Joseph, D.R. Hamburger, P.K. Working, G. Colbern, M.E. Tonda, D.M. Potter and J.L. Eiseman, Systemic and tumor disposition of platinum after administration of cisplatin or Stealth liposomal-cisplatin formulations (SPI-077 and SPI-077 B103) in a preclinical tumor model of melanoma, *Cancer Chemother. Pharmacol.*, 2004, **53**, 329-336.
74. M. de Smet, E. Heijman, S. Langereis, N.M. Hijnen and H. Grüll, Magnetic resonance imaging of high intensity focused ultrasound mediated drug delivery from temperature-sensitive liposomes: an *in vivo* proof-of-concept study, *J. Controlled Release*, 2011, **150**, 102-110.
75. R. Bellott, P. Pouna and J. Robert, Separation and determination of liposomal and non-liposomal daunorubicin from the plasma of patients treated with DaunoXome, *J. Chromatogr. B*, 2001, **757**, 257-267.
76. N.M. Deshpande, M.G. Gangrade, M.B. Kekare and V.V. Vaidya, Determination of free and liposomal amphotericin B in human plasma by liquid chromatography-mass spectroscopy with solid phase extraction and protein precipitation techniques, *J. Chromatogr. B*, 2010, **878**, 315-326.
77. S. Druckmann, A. Gabizon and Y. Barenholz, Separation of liposome-associated doxorubicin from non-liposome-associated doxorubicin in human plasma: implications for pharmacokinetic studies, *Biochim. Biophys. Acta*, 1989, **980**, 381-384.
78. R. Krishna, M.S. Webb, G. St-Onge and L.D. Mayer, Liposomal and nonliposomal drug pharmacokinetics after administration of liposome-encapsulated vincristine and their contribution to drug tissue distribution properties, *J. Pharmacol. Exp. Ther.*, 2001, **298**, 1206-1212.
79. L.D. Mayer and G. St-Onge, Determination of free and liposome-associated doxorubicin and vincristine levels in plasma under equilibrium conditions employing ultrafiltration techniques, *Anal. Biochem.*, 1995, **232,** 149-157.
80. A.A. Srigritsanapol and K.K. Chan KK, A rapid method for the separation and analysis of leaked and liposomal entrapped phosphoramide mustard in plasma, *J. Pharm. Biomed. Anal.*, 1994, **12**, 961-968.
81. Y. Xie, N. Shao, Y. Jin, L. Zhang, H. Jiang, N. Xiong, F. Su and H. Xu, Determination of non-liposomal and liposomal doxorubicin in plasma by LC-MS/MS coupled with an effective solid phase extraction: in comparison with ultrafiltration technique and application to a pharmacokinetic study, *J. Chromatogr. B*, 2018, **1072**, 149-160.

82. A.N. Schorzman, A.T. Lucas, J.R. Kagel and W.C. Zamboni, Methods and study designs for characterizing the pharmacokinetics and pharmacodynamics of carrier-mediated agents, in *Targeted drug delivery methods and protocols*, eds. R.W. Sirianni and B. Behkam, Humana Press, New York, 2018, pp 201-228.
83. G.J.R. Charrois and T.M. Allen, Drug release rate influences the pharmacokinetics, biodistribution, therapeutic activity, and toxicity of PEGylated liposomal doxorubicin formulations in murine breast cancer, *Biochim. Biophys. Acta*, 2004, **1663**, 167-177.
84. D.C. Drummond, C.O. Noble, M.E. Hayes, J.W. Park and D.B. Kirpotin, Pharmacokinetics and *in vivo* drug release rates in liposomal nanocarrier development, *J. Pharm. Sci.*, 2008, **97**, 4696-4740.
85. A. Gabizon, A.T. Horowitz, D. Goren, D. Tzemach, H. Shmeeda and S. Zalipsky, *In vivo* fate of folate-targeted polyethylene-glycol liposomes in tumor-bearing mice, *Clin. Cancer Res.*, 2003, **9**, 6551-6559.
86. A.H. Negussie, P.S. Yarmolenko, A. Partanen, A. Ranjan, G. Jacobs, D. Woods, H. Bryant, D. Thomasson, M.W. Dewhirst, B.J. Wood and M.R. Dreher, Formulation and characterisation of magnetic resonance imageable thermally sensitive liposomes for use with magnetic resonance-guided high intensity focused ultrasound, *Int. J. Hyperthermia*, 2011, **27**, 140-155.
87. R. Salomir, J. Palussière, S.L. Fossheim, A. Rogstad, U.N. Wiggen, N. Grenier and C.T.W. Moonen, Local delivery of magnetic resonance (MR) contrast agent in kidney using thermosensitive liposomes and MR imaging-guided local hyperthermia: a feasibility study *in vivo*, *J. Magn. Reson. Imaging*, 2005, **22**, 534-540.
88. B.L. Viglianti, S.A. Abraham, C.R. Michelich, P.S. Yarmolenko, J.R. MacFall, M.B. Bally and M.W. Dewhirst, *In vivo* monitoring of tissue pharmacokinetics of liposome/drug using MRI: illustration of targeted delivery, *Magn. Reson. Med.*, 2004, **51** (6), 1153-1162, DOI: 10.1002/mrm.20074. Figure 9 is reproduced with permission from Wiley. © 2004 Wiley-Liss, Inc.
89. F. Man, T. Lammers and R.T. M. de Rosales, Imaging nanomedicine-based drug delivery: a review of clinical studies, *Mol. Imaging Biol.*, 2018, **20**, 683-695.
90. K. Djanashvili, T.L.M. ten Hagen, R. Blangé, D. Schipper, J.A. Peters and G.A. Koning, Development of a liposomal delivery system for temperature-triggered release of a tumor targeting agent, Ln(III)-DOTA-phenylboronate, *Bioorg. Med. Chem.*, 2011, **19**, 1123-1130.
91. S.C. Offerman, A.V. Kamra Verma, B.A. Telfer, D.A. Berk, D.J. Clarke and H.S. Aojula, Ability of co-administered peptide liposome nanoparticles to exploit tumour acidity for drug delivery, *RSC Adv.*, 2014, **4**, 10779-10790.
92. N.Z. Wu, R.D. Braun, M.H. Gaber, G.M. Lin, E.T. Ong, S. Shan, D. Papahadjopoulos and M.W. Dewhirst, Simultaneous measurement of liposome extravasation and content release in tumors, *Microcirculation*, 1997, **4**, 83-101.
93. S. Eggen, M. Afadzi, E.A. Nilssen, S.B. Haugstad, B. Angelsen and C. de L. Davies, Ultrasound improves the uptake and distribution of liposomal doxorubicin in prostate cancer xenografts, *Ultrasound Med. Biol.*, 2013, **39**, 1255-1266.
94. L. Li, T.L.M. ten Hagen, M. Hossann, R. Süss, G.C. van Rhoon, A.M.M. Eggermont, D. Haemmerich and G.A. Koning, Mild hyperthermia triggered doxorubicin release from optimized stealth thermosensitive liposomes improves intratumoral drug delivery and efficacy, *J. Controlled Release*, 2013, **168**, 142-150.
95. W.J.M. Lokerse, E.C.M. Kneepkens, T.L.M. ten Hagen, A.M.M. Eggermont, H. Grüll and G.A. Koning, In depth study on thermosensitive liposomes: optimizing formulations for tumor specific therapy and *in vitro* to *in vivo* relations, *Biomaterials*, 2016, **82**, 138-150.

96. T. Etrych, H. Lucas, O. Janoušková, P. Chytil, T. Mueller and K. Mäder, Fluorescence optical imaging in anticancer drug delivery, *J. Controlled Release*, 2016, **226**, 168-181.
97. M. Gigli, S.M. Doglia, J.M. Millot, L. Valentini and M. Manfait, Quantitative study of doxorubicin in living cell nuclei by microspectrofluorometry, *Biochim. Biophys. Acta*, 1988, **950**, 13-20.
98. D.E. Lopes de Menezes, M.J. Kirchmeier, J.-F. Gagne, L.M. Pilarski and T.M. Allen, Cellular trafficking and cytotoxicity of anti-CD19-targeted liposomal doxorubicin in B lymphoma cells, *J. Liposome Res.*, 1999, **9**, 199-228.
99. B.J. Marafino, S.N. Giri and D.M. Siegel, Pharmacokinetics, covalent binding and subcellular distribution of [3H]doxorubicin after intravenous administration in the mouse, *J. Pharmacol. Exp. Ther.*, 1981, **216**, 55-61.
100. T. Terasaki, T. Iga, Y. Sugiyama, Y. Sawada and M. Hanano, Nuclear binding as a determinant of tissue distribution of adriamycin, daunomycin, adriamycinol, daunorubicinol and actinomycin D, *J. Pharmacobio-Dyn.*, 1984, **7**, 269-277.
101. G.R. Chamberlain, D.V. Tulumello and S.O. Kelley, Targeted delivery of doxorubicin to mitochondria, *ACS Chem. Biol.*, 2013, **8**, 1389-1395.
102. W.C. Zamboni, S. Strychor, E. Joseph, D.R. Walsh, B.A. Zamboni, R.A. Parise, M.E. Tonda, N.Y. Yu, C. Engbers and J.L. Eiseman, Plasma, tumor, and tissue disposition of Stealth liposomal CKD-602 (S-CKD602) and nonliposomal CKD-602 in mice bearing A375 human melanoma xenografts, *Clin. Cancer Res.*, 2007, **13**, 7217-7223.
103. J.M. Metselaar, M.H.M Wauben, J.P.A. Wagenaar-Hilbers, O.C. Boerman and G. Storm, Complete remission of experimental arthritis by joint targeting of glucocorticoids with long-circulating liposomes, *Arthritis Rheum.*, 2003, **48**, 2059-2066.
104. V. Garg and W.J. Jusko, Bioavailability and reversible metabolism of prednisone and prednisolone in man, *Biopharm. Drug Dispos.*, 1994, **15**, 163-172.
105. H. Möllmann, S. Balbach, G. Hochhaus, J. Barth and H. Derendorf, Pharmacokinetic-pharmacodynamic correlations of corticosteroids, in *Handbook of pharmacokinetic/ pharmacodynamic correlation*, eds. H. Derendorf and G. Hochhaus, CRC Press, Boca Raton, 1995, pp 323-361.
106. B. Ozbakir, B.J. Crielaard, J.M. Metselaar, G. Storm and T. Lammers, Liposomal corticosteroids for the treatment of inflammatory disorders and cancer, *J. Controlled Release*, 2014, **190**, 624-636.
107. R.M. Schiffelers, J.M. Metselaar, M.H.A.M. Fens, A.P.C.A. Janssen, G. Molema and G. Storm, Liposome-encapsulated prednisolone phosphate inhibits growth of established tumors in mice, *Neoplasia*, 2005, **7** (2), 118-127, DOI: 10.1593/neo.04340. Figure 11 and 12 are reprinted with permission from Elsevier.
108. M. Banciu, J.M. Metselaar, R.M. Schiffelers and G. Storm, Antitumor activity of liposomal prednisolone phosphate depends on the presence of functional tumor-associated macrophages in tumor tissue, *Neoplasia*, 2008, **10**, 108-117.
109. M. Banciu, J.M. Metselaar, R.M. Schiffelers and G. Storm, Liposomal glucocorticoids as tumor-targeted anti-angiogenic nanomedicine in B16 melanoma-bearing mice, *J. Steroid Biochem. Mol. Biol.*, 2008, **111**, 101-110.
110. U.S. Department of Health and Human Services, Food and Drug Administration, Center for Drug Evaluation and Research, Center for Veterinary Medicine, Guidance for industry: bioanalytical method validation, http://www.fda.gov/downloads/Drugs/Guidances/ucm070107.pdf, 2001.
111. College ter Beoordeling van Geneesmiddelen, Geneesmiddeleninformatiebank, https://www.geneesmiddeleninformatiebank.nl/, (accessed September 2018).

112. European Medicine Agency, https://www.ema.europa.eu/en/medicines, (accessed September 2018).
113. Leadiant Biosciences, website DepoCyt® (cytarabine liposome injection), http://www.depocyt.com, (accessed September 2018).
114. A.M. Sofias, M. Dunne, G. Storm and C. Allen, The battle of "nano" paclitaxel, *Adv. Drug Delivery Rev.*, 2017, **122**, 20-30.
115. U.S. Food and Drug Administration, Drugs@FDA: FDA approved drug products, https://www.accessdata.fda.gov/scripts/cder/daf/, (accessed September 2018).
116. R.P. Brown, M.D. Delp, S.L. Lindstedt, L.R. Rhomberg and R.P. Beliles, Physiological parameter values for physiologically based pharmacokinetic models, *Toxicol. Ind. Health*, 1997, **13**, 407-484.
117. A.T. Florence and D.J.A. Crommelin, Nanotechnologies for drug delivery and targeting: opportunities and obstacles, *Basicmedical Key*, https://basicmedicalkey.com/nanotechnologies-for-drug-delivery-and-targeting-opportunities-and-obstacles/, (accessed September 2018). Figure 2 is slightly adapted with permission.
118. E. Kluza, S.Y. Yeo, S. Schmid, D.W.J. van der Schaft, R.W. Boekhoven, R.M. Schiffelers, G. Storm, G.J. Strijkers and K. Nicolay, Anti-tumor activity of liposomal glucocorticoids: the relevance of liposome-mediated drug delivery, intratumoral localization and systemic activity, *J. Controlled Release*, 2011, **151**, 10-17.
119. C. Su, Y. Liu, Y. He and J. Gu, Analytical methods for investigating *in vivo* fate of nanoliposomes: a review, *J.Pharm. Anal.*, 2018, **8**, 219-225.
120. S.N. Ekdawi, J.M.P. Stewart, M. Dunne, S. Stapleton, N. Mitsakakis, Y.N. Dou, D.A. Jaffray and C. Allen, Spatial and temporal mapping of heterogeneity in liposome uptake and microvascular distribution in an orthotopic tumor xenograft model, *J. Controlled Release*, 2015, **207**, 101-111, DOI: 10.1016/j.jconrel.2015.04.006. Figure 8 is reprinted with permission from Elsevier.
121. S. Rizzitelli, P. Giustetto, J.C. Cutrina, D. Delli Castelli, C. Boffa, M. Ruzza, V. Menchise, F. Molinari, S. Aime and E. Terreno, Sonosensitive theranostic liposomes for preclinical *in vivo* MRI-guided visualization of doxorubicin release stimulated by pulsed low intensity non-focused ultrasound, *J. Controlled Release*, 2015, **202**, 21-30.
122. R.F. Chen and J.R. Knutson, Mechanism of fluorescence concentration quenching of carboxyfluorescein in liposomes: energy transfer to nonfluorescent dimers, *Anal. Biochem.*, 1988, **172**, 61-77.

Chapter 2

In vitro confirmation of the quantitative differentiation of liposomal encapsulated and non-encapsulated prednisolone (phosphate) tissue concentrations by murine phosphatases

Determination of the dephosphorylation rate of murine phosphatases to enable the quantitative differentiation between liposomal encapsulated and non-encapsulated drug in tissues after administration of liposomal prednisolone phosphate in mice

Evelien A. W. Smits, José A. Soetekouw and Herman Vromans

This is an Accepted Manuscript of an article published by Taylor & Francis in *Journal of Liposome Research* in *June 2014*, available online:
https://www.tandfonline.com/10.3109/08982104.2013.850593

ABSTRACT

The quantitative differentiation of liposomal encapsulated and non-encapsulated drug tissue concentrations is desirable, since the efficacy and toxicity are only related to the level of non-encapsulated drug. However, such separate concentration profiles in tissues have rarely been reported due to lacking analytical methodology. The encapsulation of prodrugs like prednisolone phosphate (PP) in liposomes offers new, analytical opportunities. Instantaneous dephosphorylation of PP into prednisolone (P) by phosphatases after its release from the liposome *in vivo* makes it possible to differentiate between the encapsulated and the non-encapsulated drug for preparations of liposomal PP: PP represents the encapsulated drug, while P represents the non-encapsulated drug. In the here described study, the instantaneous dephosphorylation of PP by murine liver and kidney phosphatases has been verified by incubation of PP in liver and kidney homogenates followed by estimation of the dephosphorylation rate constants *k* and the dephosphorylation time of the expected maximal *in vivo* non-encapsulated drug concentrations. *In vitro* PP has been rapidly converted into P in the presence of homogenate from the excretory organs. The calculated values for *k* have shown that the liver contains more active sites per gram of tissue than the kidneys. However, the dephosphorylation of PP by these active sites is slower compared with the kidneys.

As compared to the time frame of drug release from polyethylene glycol-coated liposomes, which is rather in the order of hours than minutes, the estimated dephosphorylation times of the expected maximal *in vivo* non-encapsulated drug concentrations in the liver and the kidneys are considered to be instantaneous. This enables the separate determination of the encapsulated and non-encapsulated drug concentrations in the excretory organs after administration of liposomal PP in mice. This can also gain important insights into the pharmacokinetics of liposomal formulations in general.

INTRODUCTION

Prodrugs are drug substances which are modified by attaching, for example, a solubility enhancing group and which transform *in vivo* into the active parent compound [1]. Depending on the route of administration, e.g. oral or intravenous, the bioconversion of these prodrugs occurs in the intestine, liver or in the circulation. Nowadays, prodrugs are also applied in combination with drug delivery systems. Metselaar et al. have encapsulated the prodrug prednisolone phosphate (PP) in polyethylene glycol (PEG)-coated liposomes [2]. Due to the encapsulation of this phosphate prodrug in liposomes, the prodrug does not become available until the liposomes accumulate at the pathological site (e.g. tumors and inflammations caused by rheumatic arthritis) or in the liver, spleen and kidneys, where the prodrug is supposed to be released from the liposomes. The non-encapsulated, further referred to as free[1], PP is transformed *in vivo* into its active compound prednisolone (P) by phosphatases like alkaline phosphatase [1]. To our knowledge, (quantitative) information about the *in vivo* or *in vitro* dephosphorylation of PP in P in above organs has not been published before. However, immediate dephosphorylation of PP into P after its release from the liposome *in vivo* makes it possible to differentiate between the encapsulated and free drug and quantitate their tissue concentrations separately after administration of a preparation of liposomal PP. Such separate concentrations have rarely been described until now, but are of significant importance: the drug must be released from the liposomes to become active and the anti-tumor efficacy as well as the toxicity to healthy tissues are only related to the level of free drug.

In this study, the *in vivo* hydrolysis rate of PP into P by murine phosphatases in tissues, where significant amounts of liposomes accumulate *in vivo*, has been approximated *in vitro*. The obtained data has been used to verify the instantaneous dephosphorylation in the tissues.

MATERIALS AND METHODS

Materials

Prednisolone disodium phosphate was obtained from Bufa (IJsselstein, the Netherlands). Dexamethasone, dexamethasone disodium phosphate, 4-(2-hydroxyethyl)-1-piperazineethanesulfonic acid (HEPES) BioUltra, and prednisolone were purchased from Sigma (St. Louis, MO, USA). Fresh liver, kidney and splenic tissue from male C57BL/6J

1 Here, free drug is defined as the non-encapsulated drug including non-protein-bound drug as well as protein-bound drug.

mice were from Janvier (Le Genest-Saint-Isle, France). The tissues were stored at -20°C until use. Acetonitrile LiChrosolv was obtained from Merck (Darmstadt, Germany). Absolute ethanol and methanol HPLC gradient grade were from Mallinckrodt Baker BV (Deventer, The Netherlands). Trifluoroacetic acid, which was used during preparation of the mobile phase for high-performance liquid chromatography (HPLC), was from Fisher Scientific (Loughborough, UK). For all aqueous solutions purified water was used, which was prepared using a Milli-Q system from Millipore Corporation (Billerica, MA, USA).

HPLC

HPLC analysis was performed on an Agilent 1100 system equipped with a G1322A degasser, a G1312A high pressure binary pump, a G1329A autosampler with a 100 µL injection loop, a G1316A column compartment and a G1314A variable wavelength UV detector with a 10 mm flowcel (Agilent Technologies, Palo Alto, CA, USA). Empower Pro Software (Waters, Milford, MA, USA) controlled all modules.

Reference solutions were prepared by dissolving PP in purified water and P in purified water containing 5% ethanol at a final concentration of 568 and 611.9 µM, respectively. Subsequent dilution of these concentrated solutions using purified water yielded concentrations down to 2.22 µM for PP and 2.39 µM for P. Prior to HPLC analysis 800 µL methanol containing the internal standards dexamethasone phosphate (DP) and dexamethasone (D) (69.97 and 68.99 µM, respectively) were added to 200 µL of the above PP and P solutions followed by vortexing for 30 s.

PP, DP, P and D could be measured in one single run. A Zorbax SB-C18 column (2.1 × 150 mm, 3.5 µm particle size; Agilent Technologies) was used, which was maintained at 40°C during analysis. The mobile phase consisted of (A) 0.1% (v/v) trifluoroacetic acid in water and (B) acetonitrile. A gradient was performed from 95% (v/v) to 70% (v/v) A in 2 min, followed by a gradient from 70% (v/v) to 40% (v/v) A in 8 min. Prior to the next run, the system was rinsed using 100% (v/v) B during 4 min, followed by an 8-min equilibration step at 95% (v/v) A. The flow rate was kept at 0.25 mL/min at all times. The eluate was monitored at 245 nm. During the first run, the injection volume was set at 5 µL to prevent peak splitting of higher PP and P concentrations. In a second run, samples containing low concentrations were analyzed again applying an injection volume of 30 µL.

High-intensity focused ultrasound

Samples were subjected to high-intensity focused ultrasound (HIFU) using a Covaris E210x (Covaris Inc., Woburn, MA, USA) controlled by Covaris SonoLab Software version Ev4.3.3 (Covaris Inc.). The Covaris was equipped with a metal, custom made 4 × 6 tube rack from KBioscience (Hoddesdon, UK). Prior to the HIFU treatment the sample was transferred to a HIFU resistant 15 × 19 mm glass vial with screw cap (Covaris Inc.).

The tube was placed in the metal rack held in a water bath with a maximal temperature limit of 15°C. Then, the sample was exposed to HIFU three times by running the following process configuration for 60 s: duty cycle, 20%; intensity, 10.0; cycles/burst, 1000; frequency sweep: vertical, ± 1.0 mm; vertical rate, 20.0 cpm. In between the three runs the sample was allowed to cool down for at least 60 s.

Tissue homogenization

The aim of the *in vitro* incubation was to simulate the *in vivo* dephosphorylation of PP. Since inorganic phosphate is an inhibitor of the dephosphorylation of phosphate ester prodrugs by phosphatases like alkaline phosphatase [3], the incubation was performed in an environment containing similar inorganic phosphate concentrations compared to the *in vivo* situation. To do so, first a biorelevant, isotonic (300-305 mOsm/L) HEPES buffer [4] was prepared, containing (1) 25 mM HEPES, (2) a physiological, interstitial pH of 7.4 [5, 6], and (3) a physiological, interstitial inorganic phosphate concentration of 2.75 mmol/L [7, 8, 9, 10]. Prior to incubation frozen tissues were freshly homogenized in 5 mL of this HEPES buffer/g tissue using a General Laboratory Homogenizer (Omni, Kennesaw, GA, USA).

In vitro hydrolysis

Since accumulation of PEGylated liposomes has been observed in tumor, kidneys, liver and spleen after i.v. administration in tumor-bearing mice [11], these tissues were the tissues of interest in this study. Unfortunately, representative tumor tissue was not available and the hydrolysis of PP due to incubation in tumor homogenate could not be studied. To assess the hydrolysis of PP into P by murine phosphatases in liver, kidneys and spleen, a high (~3.1×10^3 nmol/g tissue in the homogenate) and a low (191 nmol/g tissue in the liver homogenate; 2.6×10^2 nmol/g for kidney) PP concentration were incubated in duplicate with freshly homogenized tissue. The incubation assay was as follows. 1162.5 µL fresh homogenate were preheated at 37°C for 10 min in a Thermomixer Compact (Eppendorf, Hamburg, Germany) stirring at 500 rpm. The incubation was started by the addition of 37.5 µL of 1.58×10^4 (high) or 986 (low) µM PP in HEPES buffer with exception of the splenic homogenate, which was only incubated using a high PP concentration due to the limited availability of splenic tissue. After distinct time intervals an aliquot of 50 µL was sampled from the incubation mixture. Prior to HPLC analysis the samples were processed according to the developed sample preparation method for whole blood samples as described in chapter 4. This sample preparation method was as follows. Immediately after sampling 200 µL methanol containing the internal standards DP and D (69.97 and 68.99 µM, respectively) were added and the sample was vortexed for 30 s, which stops phosphatase activity and induces protein precipitation. Hereafter, HIFU was applied using the Covaris E210x as described above in order to rupture cells

present in the sample and extract all drug from these cells. The sample was centrifuged at 20817 RCF for 15 min. The clear supernatants were transferred to HPLC vials and the PP and P concentrations were determined using HPLC as described above.

The developed sample preparation method was designed in such a way to prevent the dephosphorylation of PP in whole blood samples after sampling (see chapter 4). The prevention of the dephosphorylation of PP after sampling, when applying this sample preparation method to above samples containing kidney, liver and splenic homogenate, was verified as follows. In duplicate, 50 µL tissue homogenate were heated for 10 min at 37°C in a Thermomixer Compact stirring at 500 rpm. Hereafter, 200 µL of a PP solution in methanol (~125 µM) were added and the samples were vortexed for 30 s. After 30 min, HIFU was applied as described above, and, again after a second period of 30 min, the samples were centrifuged at 20817 RCF for 15 min. The clear supernatants were used for HPLC analysis.

The pH was measured prior and after incubation in order to monitor the quality of the homogenate. To check the chemical stability of PP during incubation, the assay was repeated in duplicate using the HEPES buffer instead of homogenate.

Data analysis

To determine whether the data sets corresponding to the different tissue/concentration combinations show statistical significant decreases, the Kruskal-Wallis test was applied using SigmaPlot version 8.02 from Systat Software Inc. (San Jose, CA, USA).

Subsequently, the data sets were fitted using Equations (1) and (2) [12]:

$$[PP]_t = [PP]_0 \times e^{-k \times t} \quad (1)$$

$$[P]_t = [PP]_0 \times (1 - e^{-k \times t}) \quad (2)$$

where $[PP]_t$ and $[P]_t$ are the PP and P concentration, respectively, at a time t, $[PP]_0$ is the initial PP concentration and k is the pseudo-first-order rate constant for the enzymatic hydrolysis. The rate constant k was determined by multiple function least squares non-linear regression of the data sets in SigmaPlot version 8.02 using Equations (1) and (2). To determine the goodness of fit the coefficient of determination (R^2), the standard error and p-value of the determined value of k were calculated.

Equations (1) and (2) were differentiated with respect to t. For $t = 0$, this yielded the reaction rate v_0 for the dephosphorylation of PP (v_{0PP}) as well as the formation of P (v_{0P}):

$$v_{0PP} = -k \times [PP]_0 \quad (3)$$

$$v_{0P} = k \times [PP]_0 \quad (4)$$

Equations (3) and (4) were used to calculate the v_0 corresponding to each data set.

Although mammalian alkaline phosphatases, which are expected to be among the phosphatases responsible for PP dephosphorylation, probably belong to the group of enzymes which do not follow Michaelis-Menten kinetics [13, 14], the Michaelis-Menten equation (see Equation (5)) could still be used to yield information about the magnitude of the reaction time t_{vivo} that is necessary to convert specific amounts of $[PP]_0$, which are similar to the maximal expected free drug concentrations *in vivo*. This, to verify the immediate hydrolysis of PP after its release from the liposome. To do so, v_0 was plotted as a function of $[PP]_0$ for each tissue separately. Fitting of this plot, including the origin, to the Michaelis-Menten equation using SigmaPlot version 8.02 yielded the maximal reaction rate at saturating $[PP]_0$ (v_{max}) and the Michaelis constant (K_M). Initial guesses for v_{max} and K_M were obtained using a Hanes-Woolf plot. The Michaelis-Menten equation is as follows [13]:

$$v_0 = \frac{v_{max} \times [PP]_0}{K_M + [PP]_0} \tag{5}$$

and the percentage of active sites filled (f_{ES}) were calculated using Equation 6 [13]:

$$f_{ES} = \frac{[PP]_0}{K_M + [PP]_0} \times 100 \tag{6}$$

Hereafter, the Michaelis-Menten equation was modified giving a function for $[PP]_0$ as a function of v_0:

$$[PP]_0 = \frac{v_0 \times K_M}{v_{max} - v_0} \tag{7}$$

Differentiation of Equation (7) with respect to v_0 yielded the following equation for the reaction time:

$$t_{vivo} = \frac{K_M}{v_{max} - v_0} \times (1 + \frac{v_0}{v_{max} - v_0}) \tag{8}$$

The reaction time that is necessary to convert various amounts of PP in the different tissues *in vivo* (t_{vivo}) was estimated using Equations (5) and (8).

In case both the low and the high $[PP]_0$ yield equal values for k, a plot showing v_0 as a function of $[PP]_0$ gives a linear correlation described by Equations (3)/(4) and fitting of the data to the Michaelis-Menten equation is impossible. Then, the reaction time t_{vivo} was calculated by:

$$t_{vivo} = \frac{1}{k} \tag{9}$$

RESULTS AND DISCUSSION

In vitro hydrolysis

A low and a high PP concentration were incubated in liver, kidney and splenic homogenate as described above. Subsequent application of the developed sample preparation method (from chapter 4) did not yield artificial high P concentrations due to unwanted dephosphorylation of PP after sampling: no significant amounts of P have been observed in the control samples. The insignificant amounts of P that have been observed were below 1 area% and can be contributed to the prednisolone present in the raw PP product.

The resulting reaction progress curves of the dephosphorylation of PP into P are shown in Figure 1. The difference in the median PP concentrations among the different time points are greater than would be expected by chance and a statistical significant decrease of the PP concentration in homogenate of the liver and kidneys is observed (p <0.05) regardless of the used $[PP]_0$. However, with regard to the splenic homogenate, which was only incubated using a high $[PP]_0$, the difference in the median values among the different time points is not great enough to exclude the possibility that the difference is due to random sample variability (p = 0.162). Thus, Figure 1 displays no statistical significant decrease of the high $[PP]_0$ in splenic homogenate.

As can be seen in Figure 1, PP has been rapidly converted into P in the presence of homogenate from the excretory organs, i.e. the liver and the kidneys. Even when incubated with a high $[PP]_0$ already after 10 min the majority of the $[PP]_0$ has been converted into P. Whereas similar reaction progress curves have been observed for the high $[PP]_0$ in liver and kidney homogenate, for the low $[PP]_0$ the highest conversion has been observed in the kidneys. This is in line with previous results from a study on the pharmacological properties of a dopamine phosphate ester [4]. In the present study, the reaction rate v_0 in 1 g of liver was about 30% of the v_0 in 1 g of kidneys.

Extrapolation to *in vivo*

The *in vivo* hydrolysis of PP into P by murine tissue phosphatases was approximated using the results of above *in vitro* incubation. As can be seen in Figure 1, the conversion of PP into P has been plotted and fitted on a time scale from 0 to 10 min only. The latter data points have been discarded. There are basically two reasons for this: (1) the incubations in all homogenates have showed a gradually decreasing mass balance in time. Since the incubation of PP in the HEPES buffer has always resulted in recoveries slightly above 100%, PP is chemically stable under the incubation conditions used and the degradation of PP in the presence of tissue homogenate can be assigned to enzyme activity. Thus, the decreasing mass balance observed during the incubations in the homogenates probably indicates that PP and/or P are also degraded by at least one

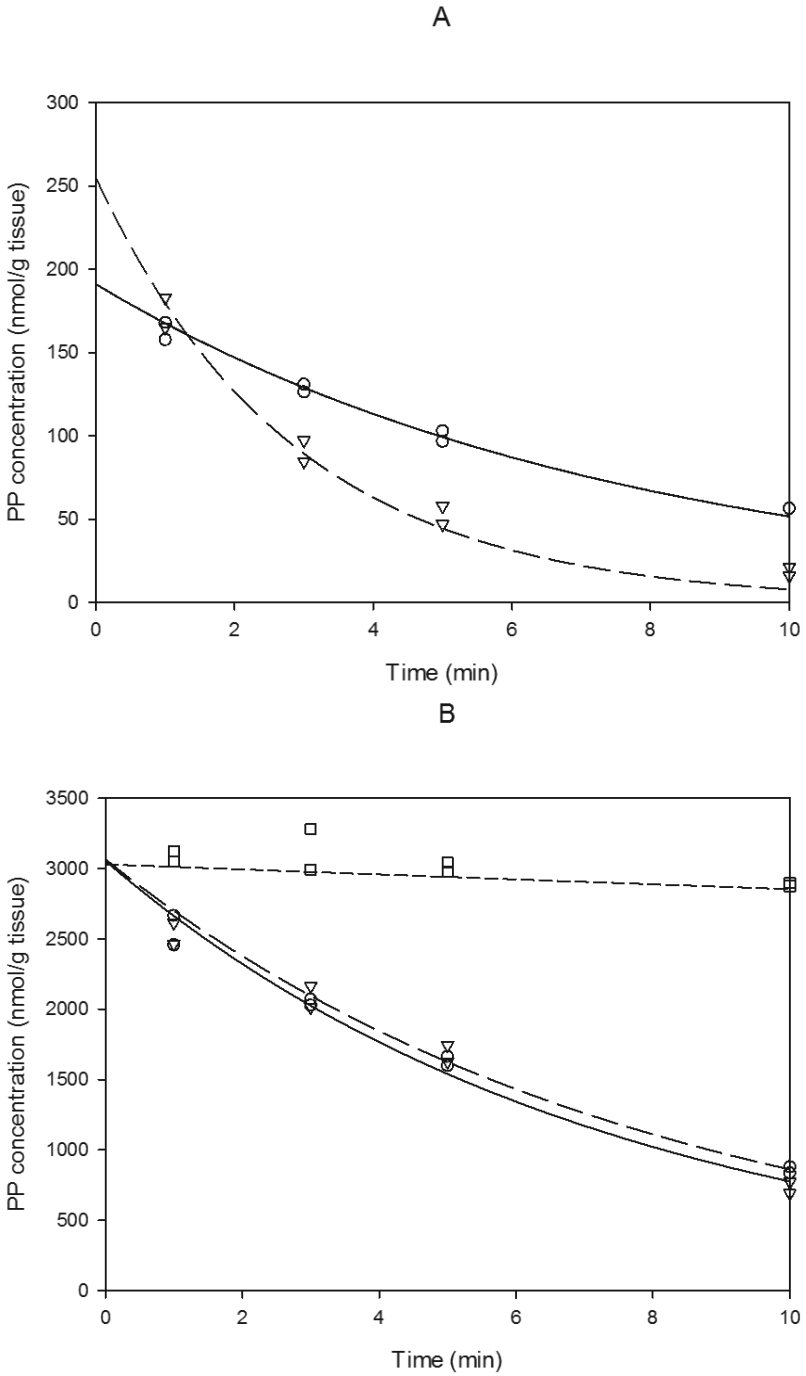

Figure 1: The conversion of low (a) and high (b) PP concentrations into P by murine tissue phosphatases in liver (○), kidneys (▽) and spleen (□)

The incubation mixtures were prepared in duplo.

other mechanism. Since the decrease in the mass balance and the decrease in the P concentration run parallel to each other, the observed decline is most probably caused by further metabolism of P after it is formed by dephosphorylation of PP. (2) After almost complete hydrolysis of PP a regeneration of PP has been observed. The hydrolysis reaction of PP by phosphatases, like for example alkaline phosphatase, exists of multiple equilibrium steps depending on environmental factors like pH [15]. The pH values of the tissue homogenates, measured prior and after incubation, are summarized in Table 1. During incubation the pH values dropped in all tissue homogenates. Such pH shifts are probably caused by the acting metabolism or by deterioration of the homogenates and probably cause the equilibrium to shift towards the product or, as in this case, towards the substrate side. Although the incubation mixtures contain numerous different compounds and it is too complicated to pinpoint the cause of the observed additional metabolism and change in pH, they are both reproducible. However, this situation is not particular relevant with regard to *in vivo* conditions, where sink conditions are prevalent: metabolic products nor degradants significantly affect the environment *in vivo*. Hence, the latter data points of the *in vitro* study are not representative for the *in vivo* situation.

Table 1: pH values of the used tissue homogenates prior and after incubation with a low or a high $[PP]_0$

Matrix	Prior to incubation	After incubation	
		low $[PP]_0$	high $[PP]_0$
Kidney homogenate	7.15	6.60	6.68
Liver homogenate	7.11	6.64	6.77
Splenic homogenate	6.96	NA	6.09

Dephosphorylation rate constants

The parts of the *in vitro* reaction progress curves representative with regard to the *in vivo* situation have been fitted as described previously. The resulting values for the rate constant k, the standard error of k, the corresponding p-value and R^2 are shown in Table 2. R^2 was always above 0.95 and the p-value was always below 0.05 indicating the values derived for k were statistically significant at a confidence interval of 95%.

Table 2 shows that for the liver a similar value of k has been observed for the low and the high $[PP]_0$. This indicates that v_0 is directly proportional to $[PP]_0$ and that unsaturated enzyme conditions apply for the substrate range from low $[PP]_0$ to high $[PP]_0$ in liver. This becomes more clear when the calculated values of v_0 are plotted against $[PP]_0$, which results in a linear correlation through the origin. Logically, it was not possible to determine v_{max} and K_M. With regard to the kidneys the value of k was decreasing with increasing $[PP]_0$, which indicates that the enzyme conditions change towards saturation when $[PP]_0$ increases from low to high: the corresponding f_{ES} increases from 16% to 70%.

Table 2: Summary of the determined values for the rate constant *k* and the corresponding goodness of fit after multiple function least squares non-linear regression

Matrix	$[PP]_0$	*k* (min^{-1})	Standard error of *k* (min^{-1})	*p*-value *k*	R^2
Kidney homogenate	low	0.35	0.02	<0.0001	0.962
	high	0.127	0.004	<0.0001	0.978
Liver homogenate	low	0.131	0.003	<0.0001	0.988
	high	0.137	0.005	<0.0001	0.968
Splenic homogenate	high	0.006	0.001	0.0011	0.996

Assuming phosphatases are non-cooperative enzymes [14], the results of the liver and the kidneys learn that the liver probably exhibits more active sites per gram of tissue than the kidneys. However, these are apparently less active compared with the active sites of the kidneys. Such observations are not very surprising: different phosphatase activities in rat tissues have already been observed by Frank et al. using *p*-nitrophenylphosphate as substrate [16].

Estimated dephosphorylation time of free PP *in vivo*

The time required to dephosphorylate a specific amount of free PP *in vivo* has been estimated applying Equations (8) or (9). Suppose a worst-case situation in which the *in vivo* maximal total drug concentration in the kidneys of about 60 nmol/g[2] is released at once from the liposomes. Then, according to Equation (8), the phosphatases present in the kidneys convert all of the free PP in P in only 2.6 min. Since the drug release from PEGylated liposomes is rather in the order of hours than minutes [17, 18], a conversion time of several minutes is considered to be immediately. The actual *in vivo* free drug concentrations are lower than determined for the above worst-case situation and so is the conversion time. Similarly, a free drug concentration equal to the *in vivo* maximal total drug concentration of about 70 nmol/g liver[2] would be hydrolyzed into P within 7.5 ± 0.2 min according to Equation (9). Due to the observed large amounts of active sites per gram liver, even in the case of an extreme worst-case, in which the total dose would target the liver and would be released at once, the present phosphatases would still face unsaturated conditions and the free drug concentration of about 705 nmol/g liver would also be converted into P in 7.5 ± 0.2 min. Thus, such large amounts of free PP in the liver are also hydrolyzed into P in the order of several minutes and is considered to be immediately. The data about the conversion in splenic tissue is too poor to draw any conclusions.

2 *In vivo* data presenting the blood and tissue concentration-time profiles of total, encapsulated and free drug after i.v. administration of liposomal PP in mice is presented in chapter 6.

CONCLUSIONS

Quantitation of separate encapsulated and free drug tissue concentrations after administration of liposomal PP by measuring the encapsulated prodrug PP and free P, requires the instantaneous conversion of free PP to P *in vivo*. In this study, the immediate dephosphorylation of PP into P in murine liver and kidney *in vivo* has been verified through an *in vitro* study followed by data analysis.

In vitro PP has been rapidly converted into P in the presence of homogenate from the excretory organs. The values calculated for the rate constant *k* have showed that the murine liver contains more active sites per gram tissue than the kidneys. However, the dephosphorylation of PP by these active sites is slower compared with the kidneys.

Based on the extrapolation of the *in vitro* data and subsequent data analysis, the *in vivo* conversion of free PP by liver and kidneys is estimated to be instantaneous compared with the drug release from PEGylated liposomes. This enables the determination of encapsulated and free drug concentrations in the excretory organs after administration of liposomal PP. This can also gain important insights into the pharmacokinetics of liposomal formulations in general.

ACKNOWLEDGMENTS

Jon Curtis and Niels Kruize from KBioscience are acknowledged for their assistance during the application of the Covaris. The authors thank Hester Kramer from MSD Oss BV for reviewing this article. The authors acknowledge MediTrans for the financial support.

DECLARATION OF INTEREST

This study was supported by MediTrans, an Integrated Project funded by financial support from the Commission of the European Communities, Priority 3 "Nanotechnologies and Nanosciences, Knowledge Based Multifunctional Materials, New Production Processes and Devices" of the Sixth Framework Programme for Research and Technological Development (Targeted Delivery of Nanomedicine: NMP4-CT-2006-026668). It does not necessarily reflect its views and in no way anticipates the Commission's future policy in this area. The authors declare no conflicts of interests. The authors alone are responsible for the content and writing of this.

REFERENCES

1. J. Rautio, H. Kumpulainen, T. Heimbach, R. Oliyai, D. Oh, T. Järvinen and J. Savolainen, Prodrugs: design and clinical applications, *Nat. Rev. Drug Discovery*, 2008, **7**, 255-270.
2. J.M. Metselaar, M.H.M. Wauben, J.P.A. Wagenaar-Hilbers, O.C. Boerman and G. Storm, Complete remission of experimental arthritis by joint targeting of glucocorticoids with long-circulating liposomes, *Arthritis Rheum.*, 2003, **48**, 2059-2066.
3. J. Brouwers, J. Tack and P. Augustijns, *In vitro* behavior of a phosphate ester prodrug of amprenavir in human intestinal fluids and in the Caco-2 system: illustration of intraluminal supersaturation, *Int. J. Pharm.*, 2007, **336**, 302-309.
4. K.H. Byington, Pharmacologic properties of a phosphate ester of dopamine, *Life Sci.*, 1987, **40**, 2091-2095.
5. M. Stubbs, Z.M. Bhujwalla, G.M. Tozer, L.M. Rodrigues, R.J. Maxwell, R. Morgan, F.A. Howe and J.R. Griffiths, An assessment of ^{31}P MRS as a method of measuring pH in rat tumours, *NMR Biomed.*, 1992, **5**, 351-359.
6. J.L. Wike-Hooley, J. Haveman and H.S. Reinhold, The relevance of tumour pH to the treatment of malignant disease, *Radiother. Oncol.*, 1984, **2**, 343-366.
7. M. Kuro-o, Y. Matsumura, H. Aizawa, H. Kawaguchi, T. Suga, T. Utsugi, Y. Ohyama, M. Kurabayashi, T. Kaname, E. Kume, H. Iwasaki, A. Iida, T. Shiraki-Iida, S. Nishikawa, R. Nagai and Y.-I. Nabeshima, Mutation of the mouse *klotho* gene leads to a syndrome resembling ageing, *Nature*, 1997, **390**, 45-51.
8. J.R. Stubbs, S. Liu, W. Tang, J. Zhou, Y. Wang, X. Yao and L.D. Quarles, Role of hyperphospatemia and 1,25-dihydroxyvitamin D in vascular calcification and mortality in fibroblastic growth factor 23 null mice, *J. Am. Soc. Nephrol.*, 2007, **18**, 2116-2124.
9. U. Till, D. Brox and H. Frunder, Orthophosphate turnover in the extracellular and intracellular space of mouse liver, *Eur. J. Biochem.*, 1969, **11**, 541-548.
10. H. Tsujikawa, Y. Kurotaki, T. Fujimori, K. Fukuda and Y.-I. Nabeshima, *Klotho*, a gene related to a syndrome resembling human premature aging, functions in a negative regulatory circuit of vitamin D endocrine system, *Mol. Endocrinol.*, 2003, **17**, 2393-2403.
11. R.M. Schiffelers, J.M. Metselaar, M.H.A.M. Fens, A.P.C.A. Janssen, G. Molema and G. Storm, Liposome-encapsulated prednisolone phosphate inhibits growth of established tumors in mice, *Neoplasia*, 2005, **7**, 118-127.
12. E.A.W. Smits, C.J.P. Smits and H. Vromans, The development of a method to quantify encapsulated and free prednisolone phosphate in liposomal formulations, *J. Pharm. Biomed. Anal.*, 2013, **75**, 47-54.
13. J.M. Berg, J.L. Tymoczko and L. Stryer, Biochemistry, W.H. Freeman, New York, 5th edition, 2002. (5th ed).
14. M.F. Hoylaerts, T. Manes and J.L. Millán, Mammalian alkaline phosphatases are allosteric enzymes, *J. Biol. Chem.*, 1997, **272**, 22781-22787.
15. J.E. Coleman, Structure and mechanism of alkaline phosphatase, *Annu. Rev. Biophys. Biomol. Struct.*, 1992, **21**, 441-483.
16. N. Frank, E. Frei and M. Wiessler, Metabolism of *N*-nitroso-hydroxyethyl-alkylamine phosphate esters in the rat, *Toxicology*, 1989, **57**, 59-67.
17. A. El-Kareh and T.W. Secomb, A mathematical model for comparison of bolus injection, continuous infusion, and liposomal delivery of doxorubicin to tumor cells, *Neoplasia*, 2000, **2**, 325-338.
18. K.M. Laginha, S. Verwoert, G.J.R. Charrois and T.M. Allen, Determination of doxorubicin levels in whole tumor and tumor nuclei in murine breast cancer tumors, *Clin. Cancer Res.*, 2005, **11**, 6944-6949.

Chapter 3

The development of a method to quantify encapsulated and free prednisolone phosphate in liposomal formulations

Evelien A.W. Smits, Coen J.P. Smits, Herman Vromans

This is an Accepted Manuscript of an article published by Elsevier. This article was published in *Journal of Pharmaceutical and Biomedical Analysis*, 2013, **75**, 47-54, Copyright Elsevier (2012).

ABSTRACT

This paper presents the development of a new method for the simple and reliable quantification of the free drug amount in liposomal preparations of prednisolone phosphate (PP). In this method the free drug is distinguished from the encapsulated drug by means of hydrolysis of the free PP into prednisolone by alkaline phosphatase (AP).

During method development reaction progress curves were recorded to determine the required AP concentration and the corresponding incubation time to achieve hydrolysis of all free PP. Reaction progress curves also showed that small changes in the amount of weighted AP and the incubation periods used do not cause a change in outcome. Further, several organic solvents were tested as precipitation solvent and the use of tetrahydrofuran yielded clean chromatograms, rapid AP deactivation and complete liposome rupture avoiding under- and overestimations of the encapsulated and free drug concentrations.

Method accuracy was evaluated during a cross-validation involving dialysis. Intra- and interday precision were evaluated by determining the standard deviation and relative standard deviation after applying the new method on one day ($n = 4$) and on different days ($n = 3$). The accuracy of the developed method is comparable to the accuracy determined by dialysis, while clearly the method using AP is more precise.

In conclusion, comprehensive method development yielded an accurate and precise method, which can replace traditional methods like dialysis and solid phase extraction. With little effort the method can be upgraded and become part of the liposome certification prior to human use. The overall principle behind the method offers possibilities for many drug carrier systems.

INTRODUCTION

Liposomes are nanovesicles which can be applied as a drug delivery system for tumor targeting. They are composed of one or more phospholipid bilayers surrounding an aqueous core, in which water-soluble drugs can be entrapped, while lipid-soluble drugs can be encapsulated in the bilayers [1,2]. When encapsulated in liposomes the drug is protected against clearance and metabolism, while the host is protected against the toxicity of the drug. In addition, due to the enhanced permeation and retention effect [3], the liposomal drug is expected to accumulate in the tumor avoiding the healthy tissue. The resulting reduction of severe side effects and the possible increased efficacy compared to free drug formulations increases the possibilities to survive severe cancer [4].

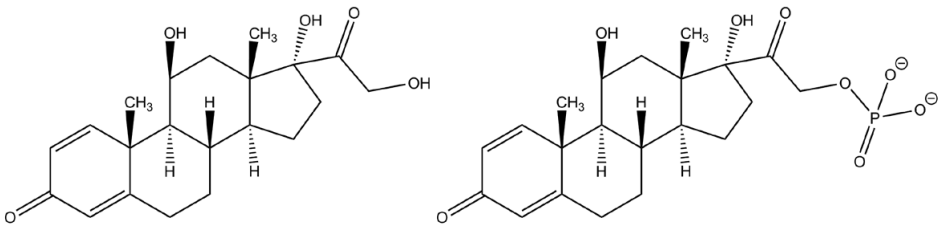

Figure 1: Structure of prednisolone (left) and its phosphate prodrug prednisolone phosphate (right)

There are various methods to prepare liposomes [5]. In all cases a minor free drug concentration is present. Quantification of this non-encapsulated amount is an essential part of the quality assurance of liposomes. This paper presents the development of a new method for the accurate quantification of the amount of free drug in preparations of liposomal prednisolone phosphate as described by Metselaar et al [6]. Commonly, determinations of the non-encapsulated drug involved the physical separation of the liposomes and the free drug followed by quantitative drug analysis. To separate the liposomes and the free drug several methods have been attempted: size-exclusion chromatography [7,8], solid phase extraction (SPE) [9,10], ion exchange chromatography [11], ultracentrifugation [12], ultrafiltration [12,13], dialysis [7,12], and also more exotic methods like the use of a Ficoll density gradient or protamine aggregation [7]. Combinations of the above mentioned methods are also possible [7]. All these techniques have their advantages and disadvantages. For example, dialysis is simple, but it requires non-recoverable large sample volumes, it is extremely time-consuming and is not precise. Accurate and fast methods like SPE can induce liposome release during column passage or the liposomes might co-elute with the free drug (or vice versa) requiring extensive method optimization. Methods like ultracentrifugation require expensive equipment, which is not available in every laboratory. Therefore, there is still need

for a method which is assessable, fast as well as reliable. We describe such a method for liposomes containing prednisolone phosphate (PP) where the aforementioned separation techniques are avoided by making use of the esterase alkaline phosphatase (AP). After addition of AP to the sample, free PP is hydrolyzed rapidly by AP into prednisolone (P), whereas the liposome protects the enclosed PP against conversion. Hereafter, liposome rupture and enzyme precipitation followed by high-performance liquid chromatography (HPLC) analysis of PP and P, of which the structures are shown in Figure 1, yield the encapsulated and free drug concentrations, respectively. To our knowledge such a method and the corresponding method optimization and cross-validation have not been published before.

MATERIALS AND METHODS

Materials

Unless mentioned otherwise, all materials were used as received. Dipalmitoylphosphatidylcholine (DPPC) and poly(ethylene glycol)2000-distearoy lphosphatidylethanolamine (PEG2000-DSPE) were purchased from Lipoid GmbH (Ludwigshafen, Germany). Prednisolone disodium phosphate was from Bufa (IJsselstein, the Netherlands). AP from rabbit intestine, cholesterol, phosphate buffered saline (PBS) powder in foil pouches, and prednisolone were from Sigma (St. Louis, MO, USA). The PBS pH 7.4 (0.01 M), which was used for dialysis and liposome dilution, was prepared as described by the supplier.

Nuclepore™ Track-Etch polycarbonate membrane filters used for liposome sizing were from Whatman GmbH (Dassel, Germany). To monitor liposome size disposable 1.5 mL plastic cuvettes with a path length of 10 mm from Brand GmbH (Wertheim, Germany) were used. Slide-A-Lyzer dialysis cassettes with a molecular weight cut-off of 10,000 were from Pierce (Rockford, IL, USA).

Acetonitrile (ACN) LiChrosolv® and tetrahydrofuran (THF) Uvasol® were obtained from Merck (Darmstadt, Germany). Dimethyl sulfoxide (DMSO) p.a., absolute ethanol and methanol HPLC gradient grade were from Mallinckrodt Baker BV (Deventer, The Netherlands). Phosphoric acid, which was used for adjusting the HPLC eluent to pH 2, was from Fisher Scientific (Loughborough, UK). Purified water for preparing HPLC eluent and PBS was prepared using a Milli-Q system from Millipore Corporation (Billerica, MA, USA).

Liposome preparation

Polyethylene glycol (PEG)-coated liposomes encapsulating PP were prepared according to the film-extrusion method as described previously [6]. In short, a mixture of DPPC, cholesterol and PEG2000-DSPE in a molar ratio of 1.85:1.0:0.15, respectively, was

dissolved in absolute ethanol. Hereafter, ethanol was evaporated under reduced pressure using a rotary evaporator yielding a thin lipid film, which was additionally dried under a stream of nitrogen. Subsequently, the lipid film was hydrated with a 100 mg/mL prednisolone disodium phosphate aqueous solution inducing the self-assembly of the lipids and, consequently, the encapsulation of PP. The resulting liposome dispersion was sized by repeated extrusion through a variety of polycarbonate membrane filters of decreasing pore size from 600 to 50 nm. Finally, the free PP was removed by dialysis using dialysis cassettes of 0.5-3 mL capacity against PBS pH 7.4 at 2-8°C.

Liposome characterization

In order to determine the total PP content, lipids were extracted using chloroform followed by HPLC analysis of the aqueous phase as described by Metselaar et al [6].

Liposome size was determined by dynamic light scattering. Prior to the measurement liposome samples were diluted with PBS pH 7.4. Approximately 1.2 mL of the diluted liposomes was transferred to plastic cuvettes. Subsequently, the peak diameter, corresponding width and the polydispersity index were recorded on a Malvern Zetasizer Nano ZS (Malvern Instruments Ltd., Hereford and Worcester, UK) equipped with a 633-nm He-Ne laser using non-invasive backscatter at an angle of 173° at 22°C. The Dispersion Technology Software version 6.01 (Malvern Instruments Ltd.) was used for data collection and analysis, which automatically determined the optimal settings.

HPLC

HPLC analysis was performed on an Agilent 1100 system equipped with a G1322A degasser, a G1312A high pressure binary pump, a G1329A autosampler with a 100 µL injection loop, a G1316A column compartment and a G1314A variable wavelength UV detector with a 10 mm flowcel (Agilent Technologies, Palo Alto, CA, USA).

Reference solutions of PP and P were prepared in PBS pH 7.4 and PBS pH 7.4 containing ≤5% ethanol (v/v), respectively. The range of the calibration curves was always chosen in such way to accommodate the expected sample concentrations. The reference solutions were stored at 2-8°C and used within one week after preparation. For the quantification of aqueous samples the calibration solutions were used as such. For the quantification of samples containing organic solvents (e.g. ACN, THF), prior to HPLC analysis 400 µL of the solvent was added to 200 µL of the above calibration solutions followed by vortexing for 30 s.

P and PP could be measured in one single run using an adapted method from Metselaar et al [6]. An XTerra™ RP_{18} column (4.6 × 150 mm, 5 µm particle size; Waters, Milford, MA, USA) was used, which was maintained at 30°C during analysis. The mobile phase consisted of 25% (v/v) ACN in water of pH 2 set at a flow rate of 1 mL/min. The eluate was monitored at 254 nm using a sample rate of >0.05 min (1 s). For the quantification of

aqueous samples an injection volume of 10 µL was used, whereas for samples containing organic solvent the injection volume was decreased to 5 µL to prevent peak splitting. After every run the column was rinsed properly using 100% ACN for 5 min, followed by a 5-min equilibration step using water pH 2-ACN (75:25 v/v).

Empower Pro Software (Waters) controlled all modules and was used for data handling.

Table 1: Summary of the various initial PP concentrations ($[PP]_0$), AP concentrations ($[AP]$) and incubation periods (t_i) used

$[PP]_0$ (mM)	$[AP]$ (mM)	$[PP]_0/[AP]$	t_i (min)
2.427×10^{1}	1.45×10^{-2}	1.67×10^{3}	120
2.425×10^{1}	7.44×10^{-2}	3.26×10^{2}	30, 60, 90, 120
1.950	1.43×10^{-2}	1.36×10^{2}	0, 30, 60, 90, 120
1.950×10^{-1}	1.43×10^{-2}	1.36×10^{1}	0, 30, 60

For comparison the number of initial PP per enzyme ($[PP]_0/[AP]$) was also calculated.

Determination of the optimal AP concentration and corresponding incubation time

To determine the required AP concentration and the corresponding incubation time to achieve complete hydrolysis of the free PP, reaction progress curves were determined as follows: one equivalent of various PP solutions in PBS pH 7.4 was incubated with one equivalent of several AP solutions, also in PBS pH 7.4, for 0, 30, 60, 90 or 120 min. AP solutions were always freshly prepared by the addition of PBS pH 7.4 to a specific amount of AP followed by gently mixing using the pipette. The used combinations of PP and AP solutions are shown in Table 1. For each incubation period of a specific $[PP]_0/[AP]$ combination two separate incubation mixture were prepared. Incubations were stopped by adding four equivalents of ACN followed by vortexing for 30 s. Hereafter, the samples were cooled for at least 15 min at 2-8°C and centrifuged at 8.8×10^{2} RCF for 10 min at room temperature. If necessary, centrifugation was repeated until a clear supernatant was obtained. The clear supernatants were transferred to HPLC vials and PP and P concentrations were determined using a HPLC method slightly different as described above: the mobile phase consisted of 30% (v/v) ACN in water of pH 2 set at a flow rate of 0.5 mL/min. The P reference solutions were prepared by dissolving P in the ACN followed by mixing with plain PBS pH 7.4.

The recorded absolute PP and P concentrations were plotted against the incubation period yielding the so-called reaction progress curves. Such time-courses can be well modeled by first-order kinetics [14]:

$$[S]_t = [S]_0 \times e^{-k \times t} \quad (1)$$

where $[S]_t$ is the substrate concentration at time t, $[S]_0$ is the initial substrate concentration and k is the pseudo-first-order rate constant for the reaction. In addition, the model for the hydrolysis of PP into P by AP should also meet the following constraint:

$$[PP]_t + [P]_t = [PP]_0 \quad (2)$$

where $[PP]_t$ and $[P]_t$ are the PP and P concentration, respectively, at a time t, and $[PP]_0$ is the initial PP concentration. Combination of Equations (1) and (2) gives first-order equations for the PP and P concentration during dephosphorylation by AP:

$$[PP]_t = [PP]_0 \times e^{-k \times t} \quad (3)$$

$$[P]_t = [PP]_0 \times (1 - e^{-k \times t}) \quad (4)$$

The rate constant k was determined by multiple function least squares non-linear regression of Equations (3) and (4) in SigmaPlot version 8.02 from Systat Software Inc. (San Jose, CA, USA). To determine the goodness of fit the coefficient of determination (R^2), the standard error (*SE*) and *p*-value for the determined value of k were calculated.

Choice of precipitation solvent

Liposome rupture by several organic solvents (ACN, DMSO, methanol, THF) was determined by addition of an aliquot of solvent to an aliquot of liposomes followed by mixing. Lipid solubility was evaluated visually.

Subsequently, the recovery of PP after liposome rupture using the promising solvents, ACN and THF, was measured as follows: liposomes were diluted hundred times using PBS pH 7.4 and to 200 µL of this dilution 400 µL of ACN or THF was added. The resulting mixtures were vortexed for 30 s, stirred using a Thermomixer Comfort (Eppendorf, Hamburg, Germany) at 1400 rpm for 30 min at 22°C, vortexed again for 30 s, cooled for 15 min at 2-8°C, and centrifuged at 8.8×10^2 RCF for 30 min. The clear supernatants were transferred to HPLC vials and the PP concentrations were determined using HPLC. The recovery of the samples was calculated using the PP content of the liposomes as determined as described above in the section "Liposome characterization".

Deactivation of AP

To 8.612 mg of frozen AP 1.5 mL of PBS pH 7.4 was added followed by gently mixing. The AP solution was stored at room temperature for at least 1 h before continuing the experiment. Then, to validate the complete deactivation of AP after addition of THF, 80 µL of PBS pH 7.4 was added to 100 µL of the AP solution in PBS pH 7.4 and the resulting sample was mixed with the pipette. Subsequently, 400 µL of THF was added and the

samples were vortexed for 30 s. Hereafter, immediately 20 µL of a PP solution in PBS pH 7.4 (2.06 mM) was added. Then, the samples were mixed using the pipette, mixed using a Thermomixer Comfort at 1400 rpm for 30 min at 22°C, vortexed for 30 s, cooled for 15 min at 2-8°C, and centrifuged at 8.8×10^2 RCF for 15 min. The supernatants were transferred to HPLC vials and the PP and P concentrations were determined using HPLC.

Stability of liposomes in the presence of AP

Possible drug release due to the presence of AP was evaluated as follows. First, on the day of the experiment a solution of AP in PBS pH 7.4 was prepared, at which 24.815 mg frozen AP was mixed gently with 4.5 mL of PBS pH 7.4. The AP solution was stored at room temperature for at least 1 h before continuing the experiment. Meanwhile, a liposomal dispersion containing 9.51 mM PP was diluted 10 times using PBS pH 7.4. Then, 100 µL of the freshly prepared AP solution in PBS pH 7.4 was added to 100 µL of this dilution. 100 µL of a free PP solution of about 426 µM was used as a control for enzyme activity. The resulting mixtures were mixed using the pipette. After 1, 2 and 3 h the enzymatic reaction was stopped by addition of 400 µL of THF and vortexing for 30 s. The samples were stirred using a Thermomixer Comfort at 1400 rpm for 30 min at 22°C, vortexed again for 30 s, cooled for 15 min at 2-8°C, and centrifuged at 8.8×10^2 RCF for 15 min. Finally, 0.5 mL of the supernatants was transferred to HPLC vials and the PP and P concentrations were determined using HPLC.

Cross-validation

To define the accuracy of the new method involving AP, encapsulated and free drug amounts were determined during a cross-validation using AP as well as dialysis. The determination using AP according to the newly developed standard operating procedure was as follows. First, a solution of AP in PBS pH 7.4 was prepared on the day of the experiment, at which at least 6.960 mg frozen AP was mixed gently with 1.5 mL of PBS pH 7.4. The AP solution was stored at room temperature for at least 1 h before continuing the experiment. Then, 100 µL of the AP solution was added to: 100 µL of (1) the pure liposome batch, (2) a hundred times liposome dilution, (3) a ten times liposome dilution, and (4) a free PP solution of 500 µM (control for enzyme activity). The resulting mixtures were mixed gently using the pipette. After 60 min enzyme activity was stopped by the addition of 400 µL of THF. The samples were vortexed for 30 s, cooled at 2-8°C for 15 min and centrifuged at 8.8×10^2 RCF for 15 min. 0.5 mL of the supernatants was transferred to HPLC vials. PP and P concentrations were determined as described in the above section "HPLC". To determine total drug concentrations 200 µL of a hundred times liposome dilution was used and the incubation step using AP was skipped.

With regard to dialysis the encapsulated and free drug amounts were determined as follows. First, a volume of 0.5 mL of pure liposomes was measured in duplo using

a Gilson pipette. Hereafter, an 18-gauge needle was pre-rinsed with liposomes to minimize sample loss and used to fill two Slide-A-Lyzer cassettes of 0.1-0.5 mL capacity with the 0.5 mL of liposomes. To separate the liposomal PP from the free PP, the cassettes were dialyzed against 250 mL of PBS pH 7.4 for ~26 h at ~7°C. The buffer was changed twice and buffer samples were taken at different time points. Hereafter, the cassettes were removed from the PBS and emptied using an 18-gauge needle. PP concentrations in the donor and buffer phase were determined using HPLC. Plotting the amount of PP that diffused into the buffer versus time showed a curve reaching a plateau. The plateau indicates the complete removal of all free PP and its value yields the free drug amount in the liposome preparation. The removal of all free PP was also confirmed by measuring the encapsulated and free drug concentrations in the donor phase using AP, in which the free drug amount was below the lower limit of quantification (LLOQ).

Determination of the precision

To determine the intraday precision the total, encapsulated and free PP concentrations of a freshly prepared liposome batch containing 8.07 mM PP were determined using the above developed method (for details see the procedure described in the above section "Cross-validation"; for a schematic representation see Table 2) for $n = 4$. Averages, standard deviations (*SD*s) and relative standard deviations (*RSD*s) were calculated.

This was repeated on two different days. The data resulting from the three days (day 1, 25 and 33) was averaged and *SD*s as well as *RSD*s were calculated to express the interday precision.

Table 2: Schematic representation of the procedure to determine liposome-encapsulated and free PP concentrations in a liposomal preparation using AP

1. Incubation
a. Gently mix AP solution (100 µL) + liposomes/liposome dilution (100 µL)
b. Wait for 60 min
2. Enzyme deactivation and liposome rupture
a. Add THF (400 µL)
b. Vortex 30 s
3. Protein precipitation
a. Cool samples at 2-8°C for 15 min
b. Centrifuge at 8.8×10^2 RCF for 15 min
c. Transfer supernatant to HPLC vials (0.5 mL)

RESULTS AND DISCUSSION

Liposome characterization

The liposome preparations contained about 12 mmol PP/L. The peak diameter appeared to be around 95 nm and the corresponding width was about 30 nm. The polydispersity index was always below 0.2 indicating that the liposome preparation is monodisperse. The phospholipid content was 60 mM [6].

Method development

Reaction progress curves of the dephosphorylation of PP by AP were recorded. Progress curves provide more insight in the amount of AP and the duration of incubation required to ensure complete hydrolysis of all free PP. Drug leakage from the liposomes during incubation should be prevented to avoid overestimations of the free drug concentration. With regard to drug release, preparations of liposomal PP are stable at room temperature in PBS pH 7.4 for at least 168 h (less than 2% leakage; data not shown). Liposome stability is however not self-evident [15,16] and to ensure liposome stability the reaction progress curves should be performed at room temperature in PBS pH 7.4 at the expense of AP activity: the maximal activity of AP is observed at alkaline pH [17,18] and inorganic phosphate inhibits the AP activity [18]. On top of it all, divalent metal cations like Mg^{2+}, which can be used to activate AP [19,20], can induce liposome fusion and aggregation [16,21]. Therefore, the use of these cations should be avoided. To our knowledge the dephosphorylation kinetics of PP by AP at above optimal conditions with regard to liposome stability, which are deviating from the common experimental conditions to obtain maximal enzyme activity when using AP, is not reported yet.

A chromatogram of PP and P in the beginning and near the end of the enzymatic hydrolysis is shown in Figure 2. Clearly, the peak corresponding to P is increasing during the reaction process at the expense of the peak corresponding to PP. The resulting reaction progress curves are shown in Figure 3. The total drug concentration of liposomal PP preparations can amount up to about 20 mM of which the ratio encapsulated/free drug is unknown. In the worst case, all PP is unencapsulated and present as free drug. Therefore, the AP concentration used should be able to convert ~20 mM PP. The dotted line in Figure 3 shows the formation of P when ~20 mM PP is incubated with an AP concentration of $\sim 1.5 \times 10^{-2}$ mM. After 120 min only 13% of the PP is hydrolyzed into P. Using a five times higher enzyme concentration (–..–..–) yielded already in a similar conversion after 20 min, while after 120 min 58% of the PP was dephosphorylated. Although further increase of the AP concentration and/or prolongation of the incubation time would give complete PP hydrolysis eventually, due to pragmatic reasons (e.g. AP solubility) the use of higher enzyme concentrations is undesirable. Instead, to ensure that the reaction of all free drug goes to completion the PP concentration was decreased

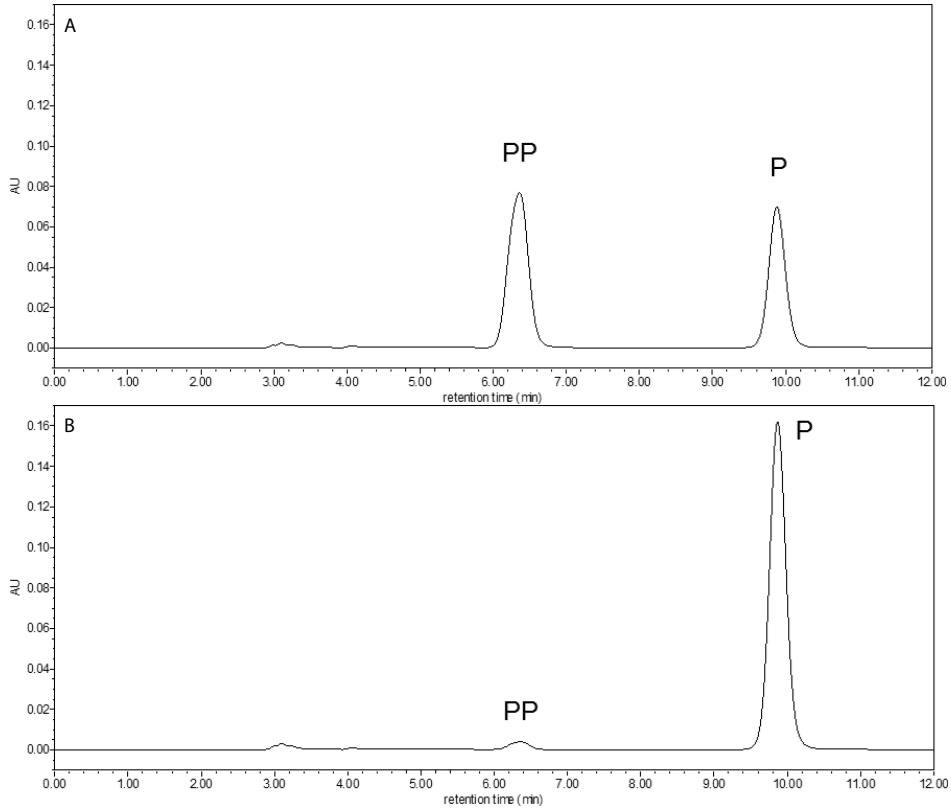

Figure 2: Representative chromatograms of PP and P at the beginning (after 30 min, A) and near the end (after 120 min, B) of the enzymatic hydrolysis

The chromatograms are recorded during the determination of the reaction progress curves as described in the section "Determination of the optimal AP concentration and corresponding incubation time" in "Materials and methods". The ratio $[PP]_0/[AP]$ used was 1.36×10^2. Retention times for PP and P are 6.4 and 9.9 min, respectively. AP produced no interfering peaks.

by dilution of the liposome samples. Low PP concentrations of about 2 and 0.2 mM, representing a 10 and 100 times dilution of the liposomes (assuming 100% free drug) respectively, were also incubated using an AP concentration of ~1.5×10^{-2} mM. As can be seen in Figure 3 (———), the complete hydrolysis of all free PP can be achieved within 60 min at a 100 times dilution of the liposome batch using ~1.5×10^{-2} mM AP.

While the $[PP]_0/[AP]$ combinations of 1.36×10^2 and 1.36×10^1 resulted in clear exponential curves, the data corresponding to the $[PP]_0/[AP]$ ratio of 3.26×10^2 is nearly linear probably due to saturated AP conditions. From these findings, $[PP]_0/[AP]$ ratios can be chosen at which AP is not saturated and is not functioning at (nearly) maximal capacity as would be the case for much higher substrate concentrations. Therefore, slight changes in the experimental set-up, like using smaller AP concentrations than planned, will still yield complete hydrolysis creating a robust method.

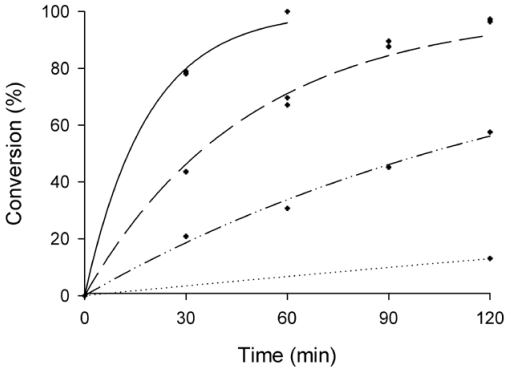

Figure 3: Reaction progress curves of the formation of P due to the dephosphorylation of PP by AP in PBS pH 7.4 at room temperature

The lines were prepared as described in the section "Determination of the optimal AP concentration and corresponding incubation time" in "Materials and methods". For each incubation period of a specific $[PP]_0/[AP]$ combination incubation mixtures were prepared in duplo. The corresponding fit results were:
$k \pm SE = 0.00116 \pm 0.00001$ min^{-1} and $R^2 = 1.00$ for $[PP]_0/[AP] = 1.67 \times 10^3$ (·····);
$k \pm SE = 0.0069 \pm 0.0002$ min^{-1} and $R^2 = 0.978$ for $[PP]_0/[AP] = 3.26 \times 10^2$ (–··–··–);
$k \pm SE = 0.0207 \pm 0.0006$ min^{-1} and $R^2 = 0.992$ for $[PP]_0/[AP] = 1.36 \times 10^2$ (– – – – –); and
$k \pm SE = 0.054 \pm 0.002$ min^{-1} and $R^2 = 0.997$ for $[PP]_0/[AP] = 1.36 \times 10^1$ (———).
The p-value was always below 0.0001.

Like with every HPLC analysis of samples containing biological compounds, sample clean-up is inevitable in order to promote chromatographic separation and to prevent malfunctioning of the column material. In this study, protein precipitation is preferred to other clean-up methods used in bioanalysis like liquid-liquid extraction and SPE. PP and P exhibit very different characteristics resulting in different partitioning during liquid-liquid extraction or SPE, whereas protein precipitation is easy and fast and also applicable for small sample volumes. Moreover, the samples will only contain AP instead of a multitude of biological compounds and, therefore, protein precipitation is expected to yield sufficiently clean samples. Prior to HPLC analysis the liposomes should be disrupted. To avoid too many steps during sample preparation, the precipitation solvent used was also anticipated to disrupt the liposomes. This may be critical as simultaneously with the liposome disruption, AP should be deactivated to prevent any hydrolysis of the released PP. Thus, besides sample clean-up and liposome rupture, the precipitation solvent should also be able to deactivate AP immediately.

Most organic solvents were expected to be able to precipitate proteins and to deactivate enzymes, therefore, a first selection was based on the visual liposome dissolving capability of the organic solvents used. THF appeared to be the only solvent able to fully dissolve the liposomes. ACN resulted in slightly cloudy samples, although complete liposome rupture by ACN was reported by Demers et al. [22]. Other solvents like methanol resulted in white, jelly-like samples.

To evaluate whether the liposome rupture induced by THF or ACN yielded the release of all encapsulated drug, the recovery of PP was determined after mixing liposomes and THF or ACN as precipitation solvent. Liposome size determinations were not included, since liposome size and drug release are not correlated by definition: for example, liposome fusion without release of vesicle contents is observed by Goñi and Alonso [23]. Moreover, any change of the liposome characteristics during the method are not of importance as long as the determined encapsulated and free drug concentrations are valid and reliable. In contrast to what has been reported by Demers et al., ACN yielded a recovery of only 79%. Thus, with regard to our experimental set-up, ACN is not suitable for complete liposome rupture. Apart from the small differences in liposome formulation, the use of significantly smaller liposome concentrations as used by Demers et al., might result in a full recovery of PP. Fortunately, the PP recovery observed after addition of THF amounts 100%. Thus, THF appeared to be the only solvent able to dissolve the liposomes completely resulting in quantification of all encapsulated PP during UV detection.

To ensure the immediate and complete deactivation of AP by THF, THF was added to AP immediately followed by addition of PP. PP and P concentrations were measured. After three days the samples were measured again to verify the stability of the samples. The following results were obtained: at the first day a small amount (~3%) of PP was converted into P, but within three days the amount of P increased only insignificantly from 3.3 to 3.6%, which is within the variation of the determination. Probably, THF did not deactivate the enzymes instantaneously and since even a few seconds are sufficient for AP to hydrolyze PP into P, a minor amount of P was observed. However, when free drug was separated from the liposomes using dialysis during above described cross-validation, free drug determination with AP (in duplo) of the donor phase yielded a free drug concentration smaller than the LLOQ. Probably, the liposome dissolution by THF is slower compared to the enzyme deactivation by THF and the encapsulated drug is still protected by the liposome until THF completely deactivated the present AP.

Finally, clean chromatograms showing no interferences of impurities and analytes were observed after protein precipitation using THF.

For the past decades, liposomal stability was already a point of discussion. In addition, enzymes are rather used to trigger liposomal drug release [16,24] and the idea of using an enzyme to differentiate between encapsulated and free drug lead to suspicion by other researchers in the field. During the triggered release of liposomal formulations comparable to the preparation used in this study, (phospho)lipases cleave one of the acyl chains of the phospholipids, which can lead to liposome fusion, pore formation in the bilayer and/or liposome lysis possibly yielding liposomal drug release. However, AP is mainly a phosphomonoesterase [18,25], which removes phosphate groups from its substrate, and, consequently, the used lipids are not expected to be a substrate for AP. This was confirmed experimentally, at which liposomes were incubated for 1, 2 or 3 h

and encapsulated and free drug ratios were measured. If AP destabilizes liposomes, a larger free fraction would be observed after a longer incubation time. Figure 4 shows the encapsulated and free drug amounts using different incubation periods. The free drug amount does not increase due to longer AP incubation times. Thus, no drug is released and liposomes are stable in the presence of AP.

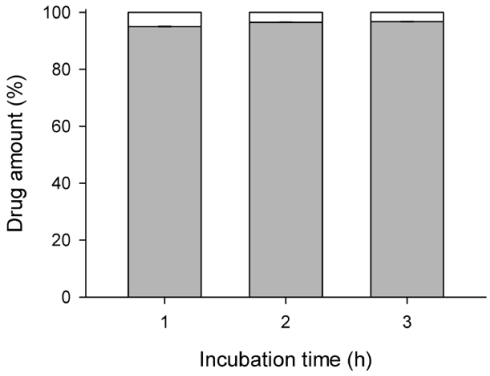

Figure 4: Measured encapsulated (gray) and free (white) drug amounts using different incubation periods
Values are means ± *SD* of two determinations per incubation period.

Cross-validation

Above method development resulted in the procedure shown in Table 2 (for details see the procedure described in section "Cross-validation" in "Materials and methods"). To evaluate the accuracy of this new method, the encapsulated and free drug amount obtained using AP were compared to the encapsulated and free drug amount obtained by dialysis. Data are shown in Figure 5. The free drug amount observed for the AP method and dialysis equal 36.0% and 34%, respectively. Taking into account the high *SD* observed for the dialysis data (± 5%), no evidence of a difference between the accuracy of both methods was observed. Note, the precision using the AP method is much higher compared to the method involving dialysis, which occasionally suffers from poor recoveries (81%).

Method validation

In the conditions as described in the section "HPLC" in "Materials and methods" for THF threated samples, retention times of 4.9 and 8.9 min were observed for PP and P, respectively. For aqueous samples a similar retention time was observed for PP. As already mentioned in the above section "Method development" no interfering peaks were observed. During the quantification of aqueous samples linearity of the calibration curves was observed over a range of 19.6-491 µM for PP. During the quantification of

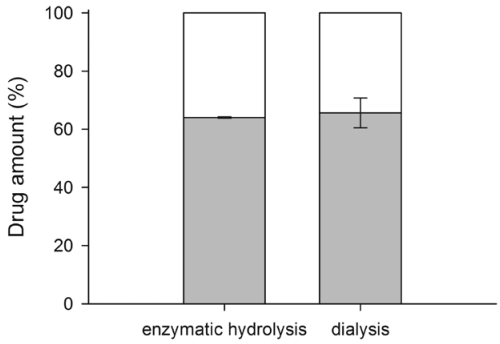

Figure 5: Encapsulated (gray) and free (white) drug amounts measured using AP or dialysis cassettes
Values are means ± *SD* of two determinations per method.

samples threated with THF linearity was observed over a range of 4.85-1055 µM for PP and 14.79-742.4 µM for P. The coefficient of determination was always ≥0.9998 and fractions were in the range 0.98-1.02. The PP solutions were stable for at least eight days (less than 1% deviation), when stored at 2-8°C. The LLOQ for THF threated samples was considered to be 4.85 µM for PP and 14.79 µM for P. The LLOQ for aqueous samples was below the concentration range used and, therefore, not determined.

The real encapsulated and free drug concentrations were not known yet. Hence, the need for this method. However, the accuracy was verified during extensive method development and cross-validation as described above. In addition, any deviation due to pH mediated hydrolysis of PP is not likely. As is following from above observed stability for the PP reference solutions, PP is stable at pH 7.4 for the course of the method. During the reaction the alcoxide of P and inorganic phosphate are formed. The formation of these (side)-products could yield a pH shift toward the alkaline range. However, dexamethasone phosphate, a similar phosphate prodrug like PP, is stable at alkaline pH [26] and this is also expected for PP. Furthermore, an extreme pH increase (ΔpH >1) is prevented by the PBS buffer for the concentrations of the (side)-products in this study.

The method precision with regard to the total, encapsulated and free PP concentrations determined using AP is shown in Table 3. For both the total and encapsulated PP amounts the *SD* and *RSD* in one series as well as on different days are small. Although the intraday *SD* and the interday *SD* for the free drug amount are also small (<1%), the intraday and interday *RSD* of the free drug amounts seem rather large. This is due to the rather small amounts of free PP present in the samples: relative standard deviations increase when the observed absolute corresponding values decrease. Nevertheless, with regard to the homogeneity of liposome dispersions and the fact that biological materials (AP) were used, a *SD* of 0.7% in the free PP amount is still very acceptable.

CONCLUSIONS

The quantitative knowledge of the free drug amount in a liposome preparation is desirable. The developed method enables a simple and reliable determination of encapsulated and free drug concentrations in a preparation of PEGylated liposomes containing prednisolone phosphate. Reliability was ensured by careful determination of the operating procedure. Reaction progress curve analysis showed that small changes in the amount of weighted AP and the incubation periods used do not cause a change in outcome. Moreover, the use of THF as precipitation solvent yields clean chromatograms, rapid deactivation of AP and ensures complete liposome rupture avoiding under- and overestimations of the encapsulated and free drug concentrations.

The accuracy of the developed method is comparable to the accuracy determined by dialysis. Since expected under- and overestimations were investigated thoroughly and could be excluded, the accuracy of this method easily meets the requirements for preclinical studies.

With regard to intra- as well as interday precision, small *SD*s and *RSD*s were found for total, free and encapsulated PP concentrations. An exception was the *RSD* of the free drug amounts, which was caused by the small absolute free drug concentrations present. Clearly, the method involving AP is more precise compared to dialysis.

This method as summarized by Table 2 is accessible and inexpensive, because the use of sophisticated techniques or equipment, like SPE or ultracentrifugation, is avoided. In addition, it is fast, can be applied using small sample volumes and is applicable for the analysis of a large number of samples. Therefore, it can replace other techniques like the slow and less precise dialysis or the complex SPE. With little effort the method can be upgraded and become part of the liposome certification prior to human use.

Besides the separate determination of free and encapsulated drug concentrations in preparations of liposomal PP, most likely, this method can also be employed for all liposomal formulations of phosphate prodrugs. After additional experiments implementation of this method with regard to liposomal preparations of different prodrugs or phosphate prodrugs conjugated to other carrier systems is possible. Overall, the principle behind the developed method enables the separate determination of free and conjugated drug concentrations in any drug substance-carrier system combination, as long as the drug is metabolized reasonably fast in some way and the conjugated drug is protected against degradation. It then offers possibilities for many drug carrier systems.

This study is a sophisticated example of how different fields of sciences, like for example biotechnology, can contribute during analytics.

Table 3: Precision of the assay in one series and on different days, in which *[PP_T]* is the total PP concentration, *[PP_{lipo}]* is the encapsulated PP concentration and *[PP_{free}]* is the free PP concentration

mean *[PP_T]* ± *SD* (mM)	*RSD* (%)	mean *[PP_{lipo}]* ± *SD* (%)	*RSD* (%)	mean *[PP_{free}]* ± *SD* (%)	*RSD* (%)
Intraday precision (n = 4)					
8.11 ± 0.08	1	95.2 ± 0.3	0.3	4.8 ± 0.3	6
Interday precision (n = 3)					
8.07 ± 0.03	0.4	95.1 ± 0.7	0.7	4.9 ± 0.7	13

CONFLICT OF INTEREST

This study has been carried out with financial support from the Commission of the European Communities, Priority 3 "Nanotechnologies and Nanosciences, Knowledge Based Multifunctional Materials, New Production Processes and Devices" of the Sixth Framework Programme for Research and Technological Development (Targeted Delivery of Nanomedicine: NMP4-CT-2006-026668). It does not necessarily reflect its views and in no way anticipates the Commission's future policy in this area.

ACKNOWLEDGMENTS

We thank Louis van Bloois from Utrecht University for his technical assistance with regard to the preparation of the liposomes. Jurgen Ketelaars and John den Engelsman from MSD Oss BV are thanked for their support concerning dynamic light scattering. We acknowledge MediTrans for the financial support.

REFERENCES

1. R. Schwendener and H. Schott, Incorporation of lipophilic antitumor and antiviral drugs into the lipid bilayer of small unilamellar liposomes, in *Liposome technology: volume II, entrapment of drugs and other materials into liposomes*, ed. G. Gregoriadis, Informa Healthcare, New York, 2007, pp 51-62.
2. V.P. Torchilin, Recent advances with liposomes as pharmaceutical carriers, *Nat. Rev. Drug Discovery*, 2005, **4**, 145-160.
3. S.H. Jang, M.G. Wientjes, D. Lu and J.L.-S. Au, Drug delivery and transport to solid tumors, *Pharm. Res.*, 2003, **20**, 1337-1350.
4. T. Lammers, W.E. Hennink and G. Storm, Tumour-targeted nanomedicines: principles and practice, *Br. J. Cancer*, 2008, **99**, 392-397.
5. J. Lasch, V. Weissig and M. Brandl, Preparation of liposomes, in *Liposomes: a practical approach*, eds. V.P. Torchilin and V**.** Weissig, Oxford University Press, Oxford, 2003, pp 3-29.
6. J.M. Metselaar, M.H.M. Wauben, J.P.A. Wagenaar-Hilbers, O.C. Boerman and G. Storm, Complete remission of experimental arthritis by joint targeting of glucocorticoids with long-circulating liposomes, *Arthritis Rheum.*, 2003, **48**, 2059-2066.
7. S.R. Dipali, S.B. Kulkarni and G.V. Betageri, Comparative study of separation of non-encapsulated drug from unilamellar liposomes by various methods, *J. Pharm. Pharmacol.*, 1996, **48**, 1112-1115.
8. T. Ruysschaert, A. Marque, J.-L. Duteyrat, S. Lesieur, M. Winterhalter and D. Fournier, Liposome retention in size exclusion chromatography, *BMC Biotechnol.*, 2005, **5**, 11-23.
9. R. Bellott, P. Pouna and J. Robert, Separation and determination of liposomal and non-liposomal daunorubicin from the plasma of patients treated with DaunoXome, *J. Chromatogr. B*, 2001, **757**, 257-267.
10. P. Egger, R. Bellmann and C.J. Wiedermann, Determination of amphotericin B, liposomal amphotericin B, and amphotericin B colloidal dispersion in plasma by high-performance liquid chromatography, *J. Chromatogr. B*, 2001, **760**, 307-313.
11. S. Druckmann, A. Gabizon and Y. Barenholz, Separation of liposome-associated doxorubicin from non-liposome-associated doxorubicin in human plasma: implications for pharmacokinetic studies, *Biochim. Biophys. Acta*, 1989, **980**, 381-384.
12. R.L. Magin and H.-C. Chan, Rapid separation of liposomes using ultrafiltration, *Biotechnol. Tech.*, 1987, **1**, 185-188.
13. R. Krishna, M.S. Webb, G. St. Onge and L.D. Mayer, Liposomal and nonliposomal drug pharmacokinetics after administration of liposome-encapsulated vincristine and their contribution to drug tissue distribution properties, *J. Pharmacol. Exp. Ther.*, 2001, **298**, 1206-1212.
14. R.A. Copeland, Enzymes: a practical introduction to structure, mechanism, and data analysis, Wiley-VCH, New York, 2nd edition, 2000.
15. B. Heurtault, P. Saulnier, B. Pech, J.-E. Proust and J.-P. Benoit, Physico-chemical stability of colloidal lipid particles, *Biomaterials*, 2003, **24**, 4283-4300.
16. M. Riaz, Stability and uses of liposomes, *Pak. J. Pharm. Sci.*, 1995, **8**, 69-79.
17. G. Cathala and C. Brunel, Bovine kidney alkaline phosphatase: catalytic properties, subunit interactions in the catalytic process, and mechanism of Mg^{2+} stimulation, *J. Biol. Chem.*, 1975, **250**, 6046-6053.
18. J.E. Coleman, Structure and mechanism of alkaline phosphatase, *Annu. Rev. Biophys. Biomol. Struct.*, 1992, **21**, 441-483.

19. C. PetitClerc, M. Delisle, M. Martel, C. Fecteau and N. Brière, Mechanism of action of Mg^{2+} and Zn^{2+} on rat placental alkaline phosphatase. I. Studies on the soluble Zn^{2+} and Mg^{2+} alkaline phosphatases, *Can. J. Biochem.*, 1975, **53**, 1089-1100.
20. K. Sorimachi, Activation of alkaline phosphatase with Mg^{2+} and Zn^{2+} in rat hepatoma cells: accumulation of apoenzyme, *J. Biol. Chem.*, 1987, **262**, 1535-1541.
21. R. Sundler and D. Papahadjopoulos, Control of membrane fusion by phospholipid head groups: I. phosphatidate/phosphatidylinositol specificity, *Biochim. Biophys. Acta*, 1981, **649**, 743-750.
22. R.D.D. Demers, D.L. Wentzel, A.L. McGrath and S. Klepfer, Novel approaches to developing LC/MS/MS bioanalytical methods for liposomal encapsulations, website Tandem Labs™, http://www.tandemlabs.com/documents/Web_RogerD.pdf, (last accessed January 2012).
23. F.M. Goñi and A. Alonso, Membrane fusion induced by phospholipase C and sphingomyelinases, *Biosci. Rep.*, 2000, **20**, 443-463.
24. T.L. Andresen, S.S. Jensen and K. Jørgensen, Advanced strategies in liposomal cancer therapy: problems and prospects of active and tumor specific drug release, *Prog. Lipid Res.*, 2005, **44**, 68-97.
25. J.L. Millán, Alkaline phosphatases: structure, substrate specificity and functional relatedness to other members of a large superfamily of enzymes, *Purinergic Signalling*, 2006, **2**, 335-341.
26. R. Gonzalo-Lumbreras, A. Santos-Montes, E. Garcia-Moreno and R. Izquierdo-Hornillos, High-performance liquid chromatographic separation of corticoid alcohols and their derivatives: a hydrolysis study including application to pharmaceuticals, *J. Chromatogr. Sci.*, 1997, **35**, 439-445.

Chapter 4

Plasma, blood and liver tissue sample preparation methods for the separate quantification of liposomal-encapsulated prednisolone phosphate and non-encapsulated prednisolone

Evelien A.W. Smits, José A. Soetekouw, Peter F.A. Bakker, Bart J.H. Baijens and Herman Vromans

This is an Accepted Manuscript of an article published by Taylor & Francis in *Journal of Liposome Research* in *March 2015*, available online: *https://www.tandfonline.com/10.3109/08982104.2014.928887*

ABSTRACT

Besides the development of sample preparation methods for the determination of separate liposomal-encapsulated prednisolone phosphate and non-encapsulated prednisolone concentrations in murine plasma and blood, this article also presents the first description of an accurate sample preparation method for the determination of such separate concentrations in the murine liver. The quantitative differentiation is based on the immediate hydrolysis of prednisolone phosphate (PP) into prednisolone (P) after its release from the liposomes *in vivo*: PP represents the encapsulated drug, while P represents the non-encapsulated drug. The use of 10 mL methanol/g tissue during homogenization of liver tissue ensures complete liposome rupture, prevention of the dephosphorylation of PP released during homogenization, sufficient clean supernatants, excellent extraction of P and sufficient extraction of PP, and excellent accuracies and precision complying with the internal guidelines for preclinical studies (80-120% and maximal 20%, respectively). Similarly, the matching sample preparation methods for plasma and blood involve protein precipitation with four equivalents of methanol also ensuring accuracies and precision complying with the internal guidelines for preclinical studies. Application of these sample preparation methods is going to generate the pharmacokinetic profile of liposomal PP, in which also the encapsulated and non-encapsulated drug concentrations in a tissue are measured separately. Such separated concentration profiles can gain important insights into the pharmacokinetics of liposomal PP and probably also with regard to liposomal formulations in general, like the quantification of the *in vivo* drug release from the liposomes.

INTRODUCTION

The use of stealth liposomal drug delivery systems can be very valuable in the treatment of cancer, infections and inflammations. Due to the encapsulation of drugs in stealth liposomes its pharmacokinetics (PK) and corresponding biodistribution is changed. Consequently, an increased therapeutic index and a significant reduction of severe side effects, like myelosuppression, mucositis and alopecia in the case of cytostatics, were observed compared to free drug formulations [1]. However, numerous biodistribution studies showed not only the accumulation of liposomes in target tissue, but also in heavily perfused organs like the liver and the spleen [2-5]. Since liposomes are often used for the formulation of very toxic compounds like cytostatics, this accumulation of liposomes in healthy organs yielded new, dose-limiting, side effects like hand-foot syndrome [2] and the significant reduction of the phagocytic activity of the liver macrophages resulting in a significantly reduced bacterial blood clearance [6, 7].

The explanation for the above described increased therapeutic index and new side effects rests in the PK profile of these liposomal formulations. Though, the complete PK of liposomal drugs is still not elucidated. Although hundreds of biodistribution studies are performed (708 publications in PubMed, search terms "liposome" AND "biodistribution"), mainly liposome concentrations or total drug concentrations in the tissues of interest were determined [2, 3, 8]. However, efficacy as well as toxicity can only be related to the level of non-encapsulated drug (further referred to as free drug). In order to have a full PK profile, the free drug concentration profiles in plasma, whole blood, tumor and healthy tissues should be known separately from the encapsulated drug profiles. Such separate drug concentrations yield significant fundamental insights with regard to the functioning of liposomal formulations, like values for the drug release from the liposomes in different tissues *in vivo*. Once the complete PK profile is understood it will be possible to optimize liposomal formulations with regard to efficacy and side effects.

While the separate quantification of encapsulated and free drug in plasma *in vivo* is becoming less rare [9-14], it is still scarce in tumor and healthy tissues. Techniques, which were successful for the separate quantification of encapsulated and free drug in plasma, use the different physicochemical properties of the liposome and the free drug like charge, size and hydrophobicity. Unfortunately, these techniques are not suitable for the separate determination in tissues, since homogenization is required prior to their application. Homogenization induces liposome rupture followed by the release of encapsulated drug and, consequently, too high free drug concentrations would be obtained. Until now, the separate quantitative assessment of encapsulated and free drug in tissues was approximated by techniques like dual-labelling and microdialysis or by using the "sink" characteristics of the nucleus in the case of doxorubicin. As for dual-labelling the drug/lipid ratio in various tissues is measured by labelling the lipid as well as

the drug, for example by using radiolabels [15]. However, the drug/lipid ratio is not able to distinct between a lipid organized in a liposome and a free lipid. Moreover, the drug/lipid ratio resulting from encapsulated drug is equal to the drug/lipid ratio of free drug, which is already released from the liposome, but is still present in the tissue. Essentially, it is necessary to measure the true encapsulated and free drug concentrations instead of the "liposome" and free drug concentrations. During microdialysis [14], which is based on the passive diffusion of non-protein associated drug across the semi-permeable membrane of the microdialysis catheter, the non-protein-bound part of the free drug is determined. Quantification of the non-protein-bound free drug can yield information about the efficacy and toxicity of the liposome formulation. However, it does not yield information about the underlying PK, since only an indication about the drug release from the liposomes is obtained instead of an accurate quantification. Further, the necessity to estimate the so-called probe recovery gives less accurate results of the non-protein-bound drug concentration. Laginha and co-workers [16] used a different, creative approach to approximate the separate concentrations in tumor tissue after intravenous administration of Doxil®: once doxorubicin is released from the liposomes into the interstitium in solid tumors it rapidly diffuses into cells. Then, a large proportion of the free doxorubicin accumulates in the cell nucleus and strongly binds to the DNA in the nucleus. Since the nucleus acts like a sink for doxorubicin, Laginha et al. used the doxorubicin concentration in the nucleus as a measure for the free doxorubicin concentration. As already stated by the authors themselves this method yielded only a reasonable first approximation.

Therefore, there is still need for the development of an accurate, quantitative bioanalytical method, which is able to distinguish between the encapsulated and free drug in tumors and healthy tissues *in vivo*. The key behind the success of such a method lays in the careful development of the corresponding sample preparation method: the free drug has to be distinguished from the encapsulated drug in an accurate manner.

This study presents the development of a tissue sample preparation method, which enables the relatively simple determination of encapsulated and free drug concentrations in murine liver for a liposomal preparation of prednisolone phosphate. In addition, the development of a matching sample preparation method suitable for plasma and whole blood samples was shown. Phosphate prodrugs like prednisolone phosphate (PP) are known for their rapid *in vivo* dephosphorylation by phosphatases [17, 18] and, even more specific, the immediate dephosphorylation of PP that is released from the liposomes is demonstrated for murine tissues, i.e. liver and kidneys [19], and whole blood (internal study similar to [19]). Hence, the encapsulated concentration will then simply be represented by PP, whereas prednisolone (P) represents the free drug concentration [3]. In order to avoid overestimations of the free drug concentration, any conversion of PP released from the liposomes during storage and during sample preparation was prevented.

MATERIALS AND METHODS

Materials

Unless mentioned otherwise, all materials were used as received. Dipalmitoylphosphatidylcholine (DPPC) and poly(ethylene glycol)2000-distearoy lphosphatidylethanolamine (PEG2000-DSPE) were purchased from Lipoid GmbH (Ludwigshafen, Germany). Prednisolone disodium phosphate was from Bufa (IJsselstein, the Netherlands). Alkaline phosphatase from rabbit intestine, 4-(2-aminoethyl) benzenesulfonyl fluoride hydrochloride (AEBSF), cholesterol, dexamethasone, dexamethasone disodium phosphate, prednisolone, rolipram and anhydrous sodium hydroxide pellets (≥98%) were from Sigma (St. Louis, MO, USA). 0.01 M phosphate buffered saline (PBS) pH 7.4 was prepared using PBS powder in foil pouches from Sigma as described by the supplier. The commercial available phosphatase and protease inhibitor cocktails were from Sigma as well as from Roche Diagnostics (Mannheim, Germany). Methyl arachidonyl fluorophosphonate (MAFP) was from Tocris Bioscience (Bristol, UK). Acetonitrile (ACN) LiChrosolv, ethyl acetate and tetrahydrofuran Uvasol® were obtained from Merck (Darmstadt, Germany). Dimethyl sulfoxide (DMSO) p.a., absolute ethanol and methanol HPLC gradient grade were from Mallinckrodt Baker BV (Deventer, The Netherlands). Hydrochloric acid for analysis, ~37% solution in water, was from Acros Organics (Geel, Belgium). Trifluoroacetic acid was from Fisher Scientific (Loughborough, UK). All water used was purified water prepared using a Milli-Q system from Millipore Corporation (Billerica, MA, USA). Liver tissue, ethylenediaminetetraacetic acid (EDTA)-stabilized plasma and EDTA-stabilized whole blood from male C57BL/6J mice were from Janvier (Le Genest-Saint-Isle, France). Nuclepore™ Track-Etch polycarbonate membrane filters used for liposome sizing were from Whatman GmbH (Dassel, Germany) and Slide-A-Lyzer dialysis cassettes with a molecular weight cut-off of 10,000 were from Pierce (Rockford, IL, USA). 10 mL TC16 borosilicate glass tubes with matching polypropylene screw caps, both resistant to high-intensity focused ultrasound (HIFU), were from KBioscience (Hoddesdon, UK).

Liposome preparation and characterization

A batch of polyethylene glycol (PEG)-coated liposomes encapsulating PP as described by Metselaar et al. [3] were prepared. In short, a mixture of DPPC, cholesterol and PEG2000-DSPE in a molar ratio of 1.85:1.0:0.15, respectively, was dissolved in absolute ethanol. Hereafter, the ethanol was evaporated under reduced pressure using a rotary evaporator yielding a thin lipid film, which was additionally dried under a stream of nitrogen. Subsequently, the lipid film was hydrated with a 100 mg/mL prednisolone disodium phosphate aqueous solution inducing the self-assembly of the lipids and, consequently, the encapsulation of PP. The resulting liposome dispersion was sized by

repeated extrusion through a variety of polycarbonate membrane filters of decreasing pore size from 600 to 50 nm. Finally, non-encapsulated PP was removed by dialysis using dialysis cassettes of 0.5-3 mL capacity against PBS pH 7.4 at 2-8°C.

The total, encapsulated and free PP content of the liposome preparation were determined using a new method, in which the free PP is distinguished from the encapsulated PP by dephosphorylation into P using alkaline phosphatase [20]. In short, for the determination of the encapsulated and free PP content, 100 µL of an appropriate dilution of the liposome preparation were incubated with 100 µL of alkaline phosphatase solution (≥4.6 mg/mL). After 60 min, 400 µL of tetrahydrofuran were used for enzyme deactivation, liposome rupture and protein precipitation. After centrifugation, PP and P concentrations were determined using high-performance liquid chromatography (HPLC). To determine the total drug concentration, 200 µL of a hundred times diluted liposome preparation were used and the incubation step using alkaline phosphatase was skipped.

The mean liposome size was determined by dynamic light scattering as also described previously [20].

HPLC

HPLC analysis was performed on an Agilent 1100 system equipped with a G1322A degasser, a G1312A high pressure binary pump, a G1329A autosampler with a 100 µL injection loop, a G1316A column compartment and a G1314A variable wavelength UV detector with a 10 mm flowcel (Agilent Technologies, Palo Alto, CA, USA). Empower Pro Software (Waters, Milford, MA, USA) controlled all modules and was used for peak integration. PP, dexamethasone phosphate (DP), P and dexamethasone (D) could be measured in one single run using a Zorbax SB-C18 column (2.1 × 150 mm, 3.5 µm particle size, Agilent Technologies), which was maintained at 40°C during analysis. The injection volume was set at 5 µL. When a higher sensitivity was required, the injection volume was increased to 10 µL. The mobile phase consisted of (A) 0.1% (v/v) trifluoroacetic acid in water and (B) acetonitrile. A gradient was performed from 95% to 70% A over 2 min, followed by a gradient from 70% to 40% A over 8 min. Prior to the next run, the system was rinsed using 100% B for 4 min, followed by an 8-min equilibration step at 95% A. The flow rate was kept at 0.25 mL/min at all times and the eluate was monitored at 245 nm.

Tissue samples: During the development of the tissue sample preparation method, external calibration solutions of PP and P were prepared in methanol and in methanol-water (70:30, v/v). Additionally, the methanol and methanol-water, which was used during validation, contained the internal standards DP and D.

Plasma/whole blood samples: PP calibration samples were prepared by mixing one equivalent of a series of PP solutions in PBS pH 7.4 and a specific number of equivalents of

methanol, followed by vortexing (30 s). During method validation, methanol containing the internal standards was used. Calibration curves for P were prepared in a similar way.

The range of the calibration curve was always chosen in such way to cover the expected sample concentrations. All calibration standards had to be within 15% of their nominal values after back-calculation.

High-intensity focused ultrasound

Drugs can be located within the cells of the tissues. In order to rupture these cells and to extract drug from these cells, HIFU was applied to the samples using a Covaris E210x (Covaris Inc., Woburn, MA, USA) controlled by Covaris SonoLab Software version Ev4.3.3 (Covaris Inc.). The Covaris was equipped with a metal rack holding a 12-well plate (Covaris Inc.).

The tubes containing the samples were placed in the metal rack held in a water bath with a maximal temperature limit of 15°C. Then, the samples were exposed to HIFU by running the following process configuration, which is an adapted version of the treatment settings used by Melarange et al. [21] for the sample preparation of rat liver. The progress configuration entails: 100 cycles/burst for 60 s, 1000 cycles/burst for 60 s, 100 cycles/burst for 30 s, 1000 cycles/burst for 30 s. The Power Tracking mode was chosen from the Frequency Tuning menu and the duty cycle and intensity were always kept at 50% and 10, respectively.

Selection of tissue homogenization solvent

Since accumulation of PEGylated liposomes has been observed in the tumors, kidneys, livers and spleens of tumor-bearing mice after i.v. administration [5], these tissues are the tissues of interest. The presence of phospholipids in the final sample is considered to be the major cause of matrix interference by endogenous compounds [22]. Based on the phospholipid volume tissue fraction [23] the liver contains the largest amount of phospholipids as compared to the kidneys and spleen (no data was available for tumor tissue). Moreover, the liver contains numerous amounts of phosphatases [19]. Therefore, the development of a sample preparation method suitable for liver tissue was expected to be the most challenging and, initially, the method development was performed using murine liver tissue.

To find a suitable manner to prevent the enzymatic hydrolysis of free PP, which is released after sampling, during and after tissue homogenization, phosphatase deactivation by various inhibitors and solvents (acetonitrile, 17.99 mM AEBSF, commercial available phosphatase and protease inhibitor cocktails, 7.80 mM EDTA, ethanol, ethanol-water (70:30, v/v), ethyl acetate, 0.01 M HCl, 16.2 µM MAFP, methanol, methanol-water (7:2, v/v), 2 M NaOH, 200.0 µM rolipram, saturated ammonium sulphate solution, tetrahydrofuran, water of 100°C) was evaluated as follows. Several murine

livers were thawed at room temperature and homogenized using a General Laboratory Homogenizer (Omni, Kennesaw, GA, USA). Aliquots of homogenate were transferred to 10 mL glass tubes. 2.5 mL of one of the inhibitors or solvents was added and the sample was vortexed immediately. To one of the aliquots of homogenate only 2.5 mL of water was added as control. After at least 30 min of incubation of the homogenate with the inhibitors/solvents, 150-200 µL of a PP solution (70.5 µM) were added and the samples were vortexed shortly. After incubation (overnight or for 30 min) acetonitrile was added, the samples were vortexed and proteins were precipitated by centrifugation. The resulting supernatants were transferred to HPLC vials and analyzed using HPLC as described above. The percentage of P present in the different samples was estimated by calculating the percentage of the area of P compared to the sum total area (area PP + area P).

Liposome rupture

Tissue samples: To verify the complete liposome rupture by methanol during tissue sample preparation, different amounts of methanol were mixed with liposomes yielding final concentrations of 0.0030-0.45 mmol PP/L. These concentrations simulate the addition of 1, 2, 5, 10 and 35 mL methanol/g tissue to various tissues, among which the liver, containing their expected maximal *in vivo* liposome concentrations [24]. A similar dilution series of liposomes was prepared in methanol-water (70:30, v/v). About 1 mL of each dilution was transferred to HPLC vials. Commonly, tissue samples are immersed in liquid nitrogen prior to homogenization. To determine the influence of this liquid nitrogen step on the recovery of PP, another 1 mL of each dilution was transferred to centrifuge tubes and cooled for about 10 s using liquid nitrogen. These samples were allowed to come to room temperature for at least 30 min and were also transferred to HPLC vials. PP concentrations were determined using HPLC as described above. Recoveries were calculated using the nominal concentrations, which were calculated based on the total drug content of the liposome preparation.

Plasma samples: The amount of methanol[3] required to induce the complete liposome rupture in plasma samples was determined as follows. In duplicate, to 100 µL of a liposome dilution containing a PP concentration of 0.44 mM, which is similar to the expected maximal liposomal PP plasma concentration [24], 100 up to 500 µL of methanol were added. The resulting samples were vortexed for 30 s. As described above, PP concentrations were determined using HPLC yielding the recovery of PP after liposome rupture.

3 After finishing the method development for the preparation of tissues, methanol appeared to be the solvent of choice (see section "Selection of the homogenization and precipitation solvent"). Therefore, method development with regard to plasma sample preparation continued using methanol only.

Whole blood samples: The complete liposome rupture of 0.52 mM liposomal PP, which is similar to the expected maximal liposomal PP blood concentration (based on the dose and mouse blood volume [25]), by four equivalents of methanol[4] was verified in a similar way as described above for the plasma samples.

Immediate deactivation of phosphatases

Tissue samples: The volume of methanol or methanol-water (70:30, v/v) required to immediately stop the complete phosphatase activity during tissue sample preparation was determined as follows. Liver tissue was immersed for about 5 s in liquid nitrogen and homogenized using a General Laboratory Homogenizer. 11 aliquots of 250 mg homogenate were transferred to separate glass tubes. In duplicate, 1, 2, 5, 10 and 35 mL methanol/g homogenate containing 98.1 µM PP was added to ten aliquots. To the eleventh aliquot an amount of 2 mL/g of plain methanol was added as control. The samples were vortexed and only one of the two samples per added amount of methanol was subjected to HIFU as described above. Subsequently, all samples were centrifuged at 2890 *g* for 15 min. The resulting supernatants were used for HPLC analysis. This procedure was repeated similarly for methanol-water. The percentage of P present in the samples treated with methanol was estimated using the calculated total area, which was based on the observed response of the above PP solution in methanol. The percentage of P present in the samples treated with methanol-water was estimated using the corresponding sum total response of the sample (area PP + area P).

Plasma samples: To determine the volume of methanol (refer footnote 3) necessary to immediately deactivate the plasma phosphatase activity, to 100 µL of plasma 100 up to 500 µL of a solution of PP in methanol (488 µM) was added in duplicate. Samples were vortexed for about 30 s and, after 30 min, the samples were centrifuged for 15 min at 8.8×10^2 *g*. The supernatant was used for HPLC analysis and analyzed using HPLC as described above. The percentage of P after the addition of different volumes of methanol was estimated using the sum total response measured for the sample (area PP + area P).

Whole blood samples: The immediate phosphatase deactivation of whole blood samples by four equivalents of methanol (refer footnote 4) was verified in a similar way as described above for plasma samples. However, an additional step was introduced after vortexing, at which the samples were subjected to HIFU as described above.

Recovery, accuracy and precision

Tissue samples: The recovery and accuracy of PP as well as P after tissue sample preparation using different volumes of methanol or methanol-water (70:30, v/v) were

4 After development of the plasma sample preparation method it was evaluated whether the method could also be freely applied to whole blood samples.

determined as follows. Six murine livers were transferred to large centrifuge tubes of 50 mL. 25 µL of a P solution in DMSO (4.86 mM) were added to all six liver tissues. After ten minutes, also 25 µL of a liposome dilution in PBS pH 7.4 (4.6 mM PP) were added. The tissue samples were cooled in liquid nitrogen for 10 s. Immediately, 5, 10 or 35 mL methanol/g tissue containing the internal standards D and DP were added and the tissues were homogenized using a General Laboratory Homogenizer. A representative aliquot of the resulting homogenates was transferred to 10 mL glass tubes and HIFU was applied as described above. Subsequently, the samples were centrifuged at 2890 *g* for 15 min and the resulting supernatants were transferred to HPLC vials. PP and P concentrations were determined using HPLC as described above.

Again this procedure was repeated using methanol-water containing the internal standards D and DP, at which 10 or 35 mL/g tissue was added. To improve the purity of the supernatants of samples treated with methanol-water, also a second aliquot of homogenate was transferred to 10 mL glass tubes for all methanol-water samples. These samples were treated as described above with the exception that the samples were cooled for 15 min at 2-8°C prior to centrifugation. If necessary, the ultracentrifuge was applied additionally.

Plasma samples: The amount of methanol (refer footnote 3), yielding a good recovery and accuracy after plasma sample preparation, was determined as follows: in sextuple, 10 µL of a P solution in DMSO (260.0 µM) were added to 180 µL of plasma and the samples were mixed gently using the pipette. After 10 min, 10 µL of a liposomal PP dilution in PBS pH 7.4 (3.8 mM PP) were added to the samples and again the samples were mixed gently using the pipette. Hereafter, either 600, 800 or 1000 µL of methanol containing the internal standards was added. The samples were vortexed for 30 s, cooled for 15 min at 2-8°C and centrifuged for 15 min at 8.8×10^2 *g*. The supernatants were used for HPLC analysis. PP and P concentrations were determined using HPLC as described above.

Whole blood samples: The recovery and accuracy after processing blood samples containing either a high (PP: 0.45 mM; P: 0.4748 mM) or a low (PP: 45 µM; P: 47.5 µM) drug concentration using four equivalents of methanol (refer footnote 4) was determined similarly as compared to the plasma samples. After vortexing, these samples were subjected to HIFU as described above. The samples were centrifuged at 20817 *g* for 15 min. Samples were analyzed using HPLC as described above.

Recoveries were determined by comparing the nominal concentrations and the measured PP and P concentrations obtained without the use of the internal standards. The nominal concentrations were corrected for the small spiking volumes and for concentrating due to precipitation of solid (tissue) matter during centrifugation. To do so, the water contents of the liver tissue, plasma or whole blood was used and the density of biological matter was assumed to be equal to 1 mL/g. The liver (70.81%) and plasma (93.33%) water contents were determined in-house by freeze-drying and

loss-on-drying. The used water content of whole blood, as determined by Sahin and co-workers [26], was 81.1%. To determine the accuracies, the nominal concentrations and the PP and P concentrations obtained when using the internal standards were compared. In this case, the internal standards correct for the volume contribution of the biological matter and the small spiking volume. The precision is expressed by the relative standard deviation (*RSD*) of the calculated PP and P accuracies. The accuracy and precision were assessed according to internal guidelines for preclinical studies aiming for an accuracy of 80-120% and an *RSD* of maximal 20%, respectively.

Freeze-thaw stability of whole blood samples

The freeze-thaw stability of whole blood samples was assessed as follows: 15 µL liposome dispersion were added to 235 µL of whole blood yielding samples containing a high concentration of 0.54 mM PP and samples containing a low concentration of 0.10 mM PP. After gently mixing of the samples none, one or three freeze-thaw cycles were applied. One freeze-thaw cycle included storage at -20°C for at least 24 h, followed by storage at room temperature for about 7.5 h with exception of the last thawing step, which was always shorter in order to process the samples. In addition, four samples were subjected to three freeze-thaw cycles containing a freezing step at -20°C for at least 24 h and a thawing step of only 30 min. After the required number of freeze-thaw cycles, the samples were gently homogenized and divided into two aliquots of 100 µL. To determine the "true" encapsulated and free drug ratio, the first aliquot was processed by an adapted version of the method described by Smits et al. [20]. In short, 100 µL of an alkaline phosphatase solution in PBS pH 7.4 (4.64 mg/mL) was added and the sample was gently mixed. After 60 min the enzymatic activity was stopped by the addition of 800 µL methanol containing the internal standards. After mixing using the vortexer for 30 s, the samples were subjected to HIFU as described above and centrifuged for 15 min at 20817 *g*. The supernatants were injected into the HPLC. To evaluate the validity of the here developed sample preparation method after storage, 400 µL of methanol containing the internal standards were added to the second aliquot. After vortexing for 30 s, HIFU and centrifugation (15 min at 20817 *g*), also these supernatants were injected into the HPLC.

Statistical analysis

To reinforce the observed results, the following statistical tests were performed using SigmaPlot version 8.02 from Systat Software Inc. (San Jose, CA, USA). To evaluate whether one can expect the recovery corresponding to a sample treatment to be different from the nominal value of 100%, *p*-values were calculated by performing a one-sample *t*-test using 100 as the test mean. To verify significant differences between various groups a two-sample *t*-test or one-way ANOVA was performed. For pairwise

comparisons after ANOVA the Holm-Sidak test was applied. To evaluate whether one can expect the accuracy corresponding to a sample treatment to be between 80 and 120%, (1) the observed accuracies should be between 80 and 120 and (2) *p*-values were calculated by performing two one-sample *t*-tests using 80 and 120 as the test mean. To evaluate whether one can expect the precision corresponding to a sample treatment to be smaller than 20%, a two-sample *t*-test was performed using the individual results of the two injections of each sample within one treatment group, at which the results of the injections corresponding to the sample exhibiting the lowest results were multiplied by 1.2. *p*-Values of <0.05 were considered statistically significant. Only results, at which the null hypothesis was rejected, were taken into consideration.

When the data were too limited, the estimated standard deviations (*SD*) and *RSD*s between the various treatments were compared to the (*R*)*SD*s due to sample and HPLC variability as observed during this study.

RESULTS AND DISCUSSION

To avoid overestimations of the free drug concentration and to develop accurate methods, any conversion of PP released from the liposomes during storage and during sample preparation had to be prevented. To safeguard this, it was chosen to freeze the tissue samples directly after sampling and to not thaw them prior to homogenization. At such low temperatures phosphatases are not active. Since the sample temperature will increase and major drug release from the liposomes is expected during homogenization, the sample preparation method must be so that during homogenization phosphatases are deactivated immediately. In addition, prior to HPLC analysis, liposome rupture should be complete. Thus, in this case the tissue sample preparation method should not only involve (1) homogenization, (2) analyte extraction and (3) sample clean-up, but also (4) immediate deactivation of the phosphatases during homogenization and (5) complete liposome rupture. To avoid too many steps during sample preparation, the homogenization solvent is not only anticipated to perform analyte extraction and sample clean-up, but also to immediately deactivate the present phosphatases and ensure the complete liposome rupture.

Similarly, it was also chosen to freeze plasma and blood samples immediately. However, plasma and blood samples have to be thawed prior to processing. Therefore, EDTA, which reduces phosphate prodrug dephosphorylation in plasma [27], was chosen as anticoagulant and additional experiments were performed to verify the prevention of the hydrolysis of significant amounts of PP in EDTA-stabilized plasma and blood samples due to freeze-thaw. Since EDTA does not prevent the dephosphorylation reaction completely [27] causing the hydrolysis of large amounts of PP in the long-term, the

precipitation solvent used during the matching sample preparation method for plasma and whole blood samples should meet similar criteria as described above for the tissue sample preparation method.

Since the methodology is intended for use during fundamental research, it is not restricted to extensive bioanalytical method validation as defined by the Food and Drug Administration (FDA) authorities [28]. Still, to guarantee suitable and reliable performance characteristics, the selectivity, linearity, freeze-thaw stability (of plasma and whole blood samples), recovery, accuracy and precision were evaluated in an appropriate way.

Liposome characteristics

The total drug content, liposome size and polydispersity was similar as described by Metselaar [24]: the liposome batch contained 8.9 ± 0.3 mM PP, of which 9.1 ± 0.7% is present as free drug. The presence of a minor free drug amount in liposome preparations is common [11, 29, 30]. After self-assembly of the liposomes during liposome preparation, the non-encapsulated drug is removed by dialysis. Dialysis is based on an equilibrium between the donor and acceptor phase leaving always a small amount of free drug in the donor phase. Although a smaller free drug amount can be desirable for certain liposome formulations during clinical applications, the observed free drug amount in this study is very acceptable with regard to the analytical scope. The peak diameter appeared to be around 98 ± 27 nm. The polydispersity index was 0.055 indicating that the liposome preparation is monodisperse. The phospholipid content was 60 mM [3].

Selectivity

During the evaluation of blanks containing liver, plasma or whole blood matrix no evidence of significant interfering impurities was observed: either no impurities or only insignificant amounts of impurities eluted together with PP, DP, P and D. Peak areas of the co-eluting impurities were always ≤7% compared to peaks corresponding to the smallest PP, DP, P and D concentrations present in the samples. Such amounts of impurities are considered insignificant, because accuracies were still between 80-120% regardless whether the impurity peak area was included in the peak area of the analytes and internal standards.

PP, DP, P and D eluted at 8.7-9.1, 9.4-9.8, 10.1-10.5 and 11.2-11.6 min, respectively. The variation in retention time was caused by the use of multiple Zorbax columns and Agilent 1100 systems and it is not caused by the variation in matrices.

Linearity

During the development of the tissue sample preparation method, linearity was observed for all used calibration curves in methanol as well as methanol-water (70:30,

v/v). Noteworthy are: 48.8-488 µM PP in methanol (injection volume: 5 µL); 0.976-97.6 µM PP in methanol (injection volume: 10 µL); 47.3-473 µM PP in methanol-water (injection volume: 5 µL); 1.18-118 µM PP in methanol-water (injection volume: 10 µL); 1.03-25.6 µM for P in methanol (injection volume: 5 µL); and 1.00-25.0 µM for P in methanol-water (injection volume: 5 µL). The coefficient of determination (R^2) was always ≥0.9998 and after back-calculation almost all calibration standards were within 4% of their nominal values. Exceptions were found for the calibration standards containing the lowest drug concentrations, which were within 10% of their nominal values.

With regard to the development of a plasma preparation method, linearity was observed for all calibration curves used (injection volume was always 5 µL): 184-584 µM for PP (PBS pH 7.4-methanol ratio 1:1-1:5); 49.4-247 µM for PP (PBS pH 7.4-methanol ratio 1:3-1:5; ratio 1:1 and 1:2 not tested); and 5.40-26.98 µM for P (PBS pH 7.4-methanol ratio 1:3-1:5; ratio 1:1 and 1:2 not tested). R^2 was always ≥0.9997 for PP and ≥0.9986 for P. All calibration standards were within 2% and 3% of their nominal values for the PP and P calibration curves, respectively.

During the analysis of whole blood samples linearity was observed for the PP calibration curves in the range 50.3-654 µM and for P over 51.0-664 µM, at which almost all calibration standards were within 6% of their nominal values. This with exception of the lowest calibration standards, at which the determined concentrations were within 15% and 12% of their nominal values for PP and P, respectively. The R^2 for calibration curves of PP was always ≥0.9945, for P ≥0.9976. The linearity of calibration curves using internal standards was superior to calibration curves without the use of internal standards.

For all three matrices, the analyte responses of the calibration standards containing the lowest analyte concentrations were larger than five times the response of the liver, plasma or blood containing blank. Therefore, the analyte concentrations in these calibration standards were considered to be the lower limit of quantification.

Selection of the homogenization and precipitation solvent

PP and P exhibit very different physical characteristics yielding different partitioning during sample clean-up methods like liquid-liquid extraction (unpublished data) and solid phase extraction. This in disservice of the recovery for at least one of the compounds. Therefore, sample clean-up by protein precipitation is preferred.

A large variety of solvents and inhibitors, including acetonitrile and methanol, was tested for their capability as homogenization solvent to deactivate the liver phosphatase activity. Methanol and methanol-water (7:2, v/v) offered the best perspective. In contrast to most solvents and inhibitors tested, they were able to prevent any conversion of PP in P completely. After 30 min of incubation of PP with liver homogenate, which was treated overnight with these solvents, no measurable P amounts were observed. It

should be noted that this does not mean that these solvents deactivate phosphatases "immediately". This is evaluated in the section "Immediate deactivation of phosphatases" below. Furthermore, the largest UV response was observed in favor of methanol and methanol-water.

Although acetonitrile is widely used in bioanalysis to initiate protein precipitation in plasma samples and it is assumed to denaturate enzymes, the solvent was not able to deactivate liver phosphatase activity completely and a P amount of ~47 area% was observed. In comparison, in the control sample a P amount of ~81 area% was observed. It appeared that the phosphatase activity in EDTA plasma at room temperature is only significant for small PP concentrations (data not shown), which clarifies the accurate results obtained worldwide when using acetonitrile. Further, also the use of commercial available inhibitor cocktails did not yield complete phosphatase inhibition.

Plasma and whole blood, both anticoagulated with EDTA, contain less impurities and active phosphatases compared to liver tissue. Therefore, because of the above promising results with regard to tissue sample preparation, methanol was also selected as the solvent of choice for the sample processing of plasma and whole blood samples.

Liposome rupture

The PP recovery of samples representing the expected *in vivo* tissue concentrations after liposome rupture by different volumes of methanol and methanol-water (70:30, v/v) was determined. In addition, the influence of the immersion in liquid nitrogen on the recovery of PP was evaluated. Full recoveries (99-107%) were observed for the samples representing the liposome rupture by the smallest volumes of solvent (0.045-0.45 mmol PP/L). Considering the random sample variability, variability of the HPLC analysis and the *SD* of the total drug content of the liposome preparation, which is used for the calculation of the nominal values, it is not worthwhile to compare different treatments. However, for these smallest volumes of methanol and methanol-water and regardless whether liquid nitrogen was used, the recoveries were well within 80-120% also when considering the *SD* of the total drug content of the liposome preparation. This indicates the liposome rupture is sufficient to prevent inaccurate results. The samples representing the liposome rupture by the largest volumes of solvent (3.0-18 µmol PP/L) were below the linear range. However, since the smaller volumes of solvent are already able to yield sufficient liposome rupture, this most likely also applies for these larger volumes. Further, significant influence of the liquid nitrogen step on the recovery of PP is unlikely: the difference in the response (*RSD* ≤2%) is rather caused by the variability of the HPLC analysis than due to the liquid nitrogen step. Besides, considering the aimed accuracy of 80-120% these deviations observed due to the use of liquid nitrogen are not interesting. Hence, all tested treatments are suitable and the development of an accurate method was not restricted by insufficient liposome rupture. In spite of the

observed full recoveries, for methanol-water (slightly) cloudy samples were obtained for the smaller methanol-water volumes. The development of the sample preparation method was therefore continued with 1, 2, 5, 10 and 35 mL/g for methanol and 5, 10 and 35 mL/g for methanol-water only.

The liposome rupture of one equivalent containing the maximal expected *in vivo* liposomal PP plasma concentration was induced using different equivalents of methanol (refer footnote 3). The mean of the observed recoveries per group, which were treated with different amounts of methanol, varied from 106 ± 1 to 108 ± 0.1%. All recoveries were well within the aimed accuracy of 80-120%, even when considering the *SD* of the total drug content of the liposome preparation. This indicates the liposome rupture by all volumes is sufficient to prevent inaccurate results. Thus, also for plasma the development of an accurate method was not restricted by insufficient liposome rupture.

After using four equivalents of methanol (refer footnote 4) in combination with the maximal expected *in vivo* whole blood concentration, the mean of the observed recoveries yielded 96 ± 0.4%. Even when considering the *SD* of the total drug content of the liposome preparation, the recoveries were well within 80-120%. No inaccurate results are expected due to insufficient liposome rupture.

Immediate deactivation of phosphatases

The ability of different volumes of methanol or methanol-water (70:30, v/v) to immediately stop all phosphatase activity during tissue homogenization was evaluated. Logically, the higher the amount of PP converted into P, the less the immediate phosphatase activation. All observed P areas, with exception of these observed in the samples treated with 1 mL methanol/g liver, were below the linear range. This indicates the P amounts in these samples are maximally 1.3-1.8 area%. The estimated area% of P in these samples as well as the calculated area% for the samples treated with 1 mL/g of methanol are shown in Figures 1a and 1b. Since only one of the duplos was subjected to HIFU, the estimated *SD* of the percentage of P in Figure 1 represents the variation due to HIFU as well as the random sample variability and variability of the HPLC analysis. Either the corresponding *SD*s of the absolute values of the P response were rather caused due to random sample and/or HPLC variability or no significant amounts of P were observed at all. Hence, no significant differences were observed for samples subjected and samples not subjected to HIFU. Neither chemical instability of PP (or P) during HIFU nor the release of intracellular phosphatases during HIFU in the presence of methanol or methanol-water does yield significant unwanted hydrolysis of PP into P. When volumes of 5, 10 and 35 mL/g of methanol and 10 and 35 mL/g of methanol-water were used only insignificant amounts of P (<1 area%) were observed, which probably originated from the raw PP product and/or small amounts of co-eluting impurities. Volumes of 1

or 2 mL/g of methanol yielded larger percentages of P. Roughly, it seems that a larger conversion of PP is observed when smaller volumes of homogenization solvent are used. However, larger volumes of solvent did not change the partition of the impurities and the analytes between the tissue material and solvent. Therefore, the use of small volumes of homogenization solvent, but which still prevent significant hydrolysis of P, are most favorable because of the resulting smaller dilution and the most advantageous lower limit of quantification.

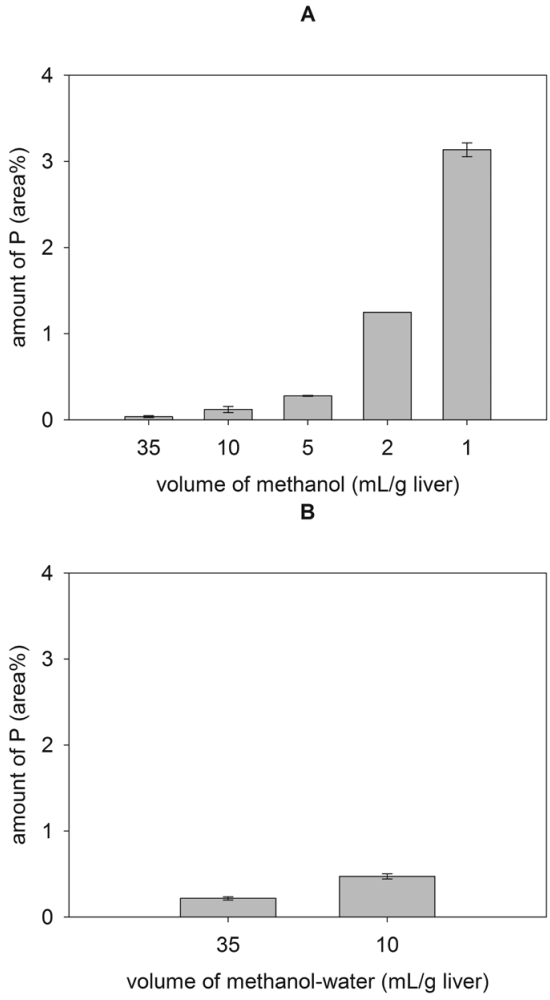

Figure 1: The ability of various volumes of methanol (a) or methanol-water (70:30, v/v) (b) to stop the phosphatase activity immediately during homogenization (*n* = 2)
This was expressed as the relative amount of PP which was converted into P by liver phosphatases in the presence of the solvents.

In addition, the ability of different equivalents of methanol (refer footnote 3) to immediately deactivate the minor amount of active phosphatases in EDTA plasma was evaluated. The use of 1 or 2 equivalents of methanol resulted in cloudy supernatants and irreversible damage of the column. In order to obtain a robust method, the use of 1 or 2 equivalents was further avoided. Larger quantities yielded clean supernatants. These contained P amounts of approximating 0.5 area%, at which the differences between the use of 3, 4 or 5 equivalents of methanol are probably caused due to random sample and HPLC variability. Most probably, such P amounts are originating from the raw PP product and/or small amounts of co-eluting impurities. Most relevant, in these samples substantial hydrolysis of PP which is released after sampling was prevented. In spite of the clean samples observed for a ratio of 1:3, the ratio 1:4 was selected. This guarantees the presence of sufficient methanol also when somewhat more impurities are present in the plasma assuring a robust method.

The processing of whole blood samples using four equivalents of methanol (refer footnote 4) yielded similar results compared to the plasma samples. The observed response for P was below the linear range and the amount of P was estimated at 0.12 ± 0.01 area%. Again, such small amounts of P are rather caused by P in the raw PP product and/or small amounts of co-eluting impurities than by dephosphorylation of PP. Thus, the use of four equivalents of methanol deactivates blood phosphatases immediately, avoiding the dephosphorylation of free PP which may be released after sampling.

Recovery, accuracy and precision

The recovery, intrarun accuracy and intrarun precision of PP and P after tissue sample preparation using different volumes of methanol (35, 10 and 5 mL/g) or methanol-water (70:30, v/v) (35 and 10 mL/g) were determined to confirm the validity of this sample preparation method. The observed recoveries and accuracies are shown in Table 1. Although nice recoveries and accuracies are observed after extraction of PP and P using different amounts of methanol-water, cloudy supernatants were observed regardless of the volume used, even when the samples were additionally cooled or centrifuged using an ultracentrifuge. As explained above such cloudy samples and thus the use of methanol-water should be avoided. Fortunately, clear supernatants were obtained for all livers homogenized in methanol. For all volumes of methanol the extraction of P from the liver tissue is excellent: all observed recoveries are within a few percentages of 100%. The recoveries observed for PP are significant lower than 100% ($p \leq 0.010$) for all volumes of methanol used. This is probably due to partitioning of PP between the tissue and methanol, which is supported by the fact that the use of larger volumes of methanol yields significant larger recoveries ($p < 0.001$). Nonetheless, the observed PP recoveries are not that dramatic, since at least about 2/3 of the PP is still recovered, and the internal standard DP can correct for this, yielding excellent accuracies as shown in Table 1. For all

Table 1: The recoveries and accuracies observed for the encapsulated PP and free P after applying the tissue sample preparation method, at which the volume of the homogenization solvents was varied

Homogenization solvent	Volume of homogenization solvent (mL/g tissue)	Recovery PP (%) ± *SD*	Accuracy PP (%) ± *SD*	Recovery P (%) ± *SD*	Accuracy P (%) ± *SD*
methanol	5	65 ± 1	102 ± 3	97.4 ± 0.9	99 ± 2
(*n* = 2)	10	67 ± 0.4	97 ± 0.3	102 ± 2	101 ± 0.3
	35	79 ± 0.3	92 ± 2	99 ± 4	95 ± 4
methanol-water	10	90 ± 4	110 ± 8	104 ± 1	107 ± 3
(*n* = 2)	35	97 ± 3	101 ± 1	103 ± 0.2	101 ± 1

The theoretical concentrations (in nmol/g ± *SD*) were: 86 ± 9 for PP and 91 ± 9 for P.

volumes of methanol used, the observed accuracies of PP and P comply with the internal guidelines for preclinical studies. Also, the FDA requirements with regard to accuracies in human clinical trials were met [28], even when the *SD* of the total drug content in the liposomal preparation was considered. The *RSD*s of the PP and P accuracies were 4% or smaller and the precision of the tissue sample preparation method complies with the internal guidelines for preclinical studies ($p \leq 0.025$). Hence, methanol yields clean supernatants, suitable recoveries and excellent accuracies and precision for all volumes tested. Since homogenization using 5 mL/g is very inconvenient from a practical point of view and the larger PP recovery observed when using 35 mL/g does not counterbalance the large sample dilution, 10 mL methanol/g tissue is favorable.

A similar validity investigation was done on the plasma sample preparation. Again, the plasma/methanol ratio was varied and the corresponding recoveries and accuracies are summarized in Table 2. Excellent recoveries approaching 100% were observed for all ratios for PP as well as P, indicating extraction of both drugs is optimal. Subsequently, the use of all plasma/methanol ratios tested results in accuracies, which comply with the internal guidelines for preclinical studies ($p \leq 0.042$) and nearly meet the FDA requirements for human clinical trials [28] ($p \leq 0.071$). Even when considering the *SD* of the total drug content of the liposome preparation. This with exception for P when using five equivalents of methanol, for which it was not possible to statistically verify

Table 2: The recoveries and accuracies observed for the encapsulated PP and free P after applying the plasma sample preparation method, at which the sample/methanol ratio was varied

Plasma/methanol ratio	Recovery PP (%) ± *SD*	Accuracy PP (%) ± *SD*	Recovery P (%) ± *SD*	Accuracy P (%) ± *SD*
1:3	97 ± 0.3	103 ± 0.3	93.1 ± 0.1	97.6 ± 0.4
1:4	96 ± 0.3	106 ± 1	95.1 ± 0.8	100 ± 1
1:5	95 ± 1	105 ± 1	93 ± 22	97 ± 22

The theoretical concentrations were: 0.19 mM for PP and 13.0 µM for P. For all ratios *n* = 2.

that the use of five equivalents yields the aimed accuracies. This is due to an exceptional large deviation (*RSD* of 22%) caused by a low recovery of one of the individual samples. However, the average and individual accuracies are still between 80-120%. The other *RSD*s of the PP and P accuracies in plasma samples were 1% or smaller and thus easily comply with the aimed precision of 20%.

Recoveries and accuracies observed after preparation of whole blood samples containing either a high or a low analyte concentration are summarized in Table 3. The observed recoveries were always sufficient at which the vast majority of PP and P was extracted from blood cells, proteins and liposomes. The observed accuracies comply with the guidelines for preclinical studies and nearly meet the FDA requirements for human clinical trials [28]. This also applies when considering the *SD* of the total drug content of the liposome preparation. The observed *RSD*s after application of the sample preparation method for blood were maximal 7%. This with exception of the precision observed for a high PP concentration in blood: a precision of 23% was determined, which was due to the large peak area observed for PP in one of the individual samples. Most probably, this large peak area is caused by carry-over from the previous injected sample. While carry-over can be prevented by injecting the samples from low to high PP

Table 3: The recoveries and accuracies observed for the encapsulated PP and free P after applying the blood sample preparation method, at which the concentrations of encapsulated PP and free P were varied

Theoretical PP concentration (mM)	Recovery PP (%) ± *SD*	Accuracy PP (%) ± *SD*	Theoretical P concentration (μM)	Recovery P (%) ± *SD*	Accuracy P (%) ± *SD*
0.45	76 ± 17	120 ± 28	475	78.4 ± 0.4	96.9 ± 0.3
0.045	79 ± 3	106 ± 7	47.5	92 ± 5	102 ± 7

For both concentrations $n = 2$.

concentration, in this case the sample order was unfavorable due to human error.

Freeze-thaw stability of whole blood samples

Unlike tissue samples, plasma and whole blood samples have to be thawed prior to processing in order to accurately transfer a known volume. Major release of PP from the liposomes is expected during freeze-thaw [31, 32] and during the thawing step the phosphatase activity will increase again. Consequently, PP, that is released during freeze-thaw, will be (partly) hydrolyzed into P yielding overestimations of the free drug concentration. To prevent such overestimations it was chosen to use EDTA as anticoagulant during sampling, since EDTA also shows phosphatase inhibiting properties [27]. However, the dephosphorylation reaction might not be completely inhibited by

Table 4: Freeze-thaw stability of whole blood samples containing high drug concentrations (0.54 mM)

Number of freeze-thaw cycles applied	"True" encapsulated/free drug ratio		PP/P drug ratio according to new method	
	[encapsulated drug] (%) ± *SD*	[free drug] (%) ± *SD*	*[PP]* (%) ± *SD*	*[P]* (%) ± *SD*
0	93 ± 0.1	7.0 ± 0.1	>99.5 ± 0.002	<0.46 ± 0.002
1	31 ± 1	69 ± 1	98 ± 0.1	1.8 ± 0.1
3	<8.4 ± 0.03	>92 ± 0.03	43 ± 1	57 ± 1
3[a]	-	-	96 ± 0.02	4.1 ± 0.02

The PP and P concentrations according to the new method are compared to the "true" ratio of the encapsulated drug concentration and free drug concentration after none, one or three freeze-thaw cycles. *SD*, standard deviation

[a]Thawing step was decreased from 7.5 h to 30 min.

EDTA [27]. To exclude significant hydrolysis of the PP released after sampling the freeze-thaw stability of the whole blood samples was investigated.

As can be seen in Table 4, PP leaks out of the liposomes significantly (p <0.001) due to freeze-thaw: after one freeze-thaw cycle only one third of the drug is still encapsulated and after three freeze-thaw cycles (almost) all encapsulated drug is released. And this might even be an underestimation of the drug release caused by freeze-thaw, since the free PP is differentiated from the encapsulated PP by hydrolysis using alkaline phosphatase and the alkaline phosphatase activity is probably reduced due to the presence of EDTA. Such major drug release during storage would lead to inaccurate results when the conventional techniques based on the physical separation of the liposomes and free drug would be used. The method described in this current paper does not lead to inaccurate results, as long as all PP, which was still encapsulated at the moment of sampling, is not converted into P. The amounts of PP and P after none, one or three freeze-thaw cycles followed by the new sample preparation procedure are also shown in Table 4. After one freeze-thaw cycle the new method yields only little amounts of P, which are significantly smaller than the free drug amount before freeze-thaw (p <0.001). Such small amounts of P are probably caused by the presence of P in the raw PP product or by dephosphorylation of non-encapsulated PP in the liposome preparation during the small period in between spiking and freezing. Hence, one freeze-thaw cycle causes no overestimations of the free drug concentration using the new method. After three freeze-thaw cycles the amount of P is significantly (p <0.001) larger than the free drug amount before freeze-thaw. Apparently, the long periods at room temperature were sufficient to "reactivate" the phosphatases and, indeed, EDTA does not prevent the dephosphorylation reaction in blood completely. Three freeze-thaw cycles should be prevented. However, if the thawing step is decreased from 7.5 h to 30 min only, which

could be the case in a situation where the samples are repeatedly removed from the freezer to remove a few and store the remaining samples again, only 4.1 ± 0.02% of P is observed. This P amount is significantly lower than the free drug amount before freeze-thaw (p <0.001) and the corresponding dephosphorylation of PP is too small to cause any underestimations of the encapsulated drug with regard to the aimed accuracy (p <0.001). Note, after such a thawing step of 30 min, the protein precipitation method must be so that phosphatases are inhibited immediately. This, was safeguarded as described in the section "Immediate deactivation of phosphatases" in "Results and discussion". Of course, the relative amount of PP converted for smaller concentrations would be expected to be larger. However, for whole blood samples containing a low PP concentration of 1.0 × 10^2 µM the relative amount of PP converted after one freeze-thaw cycle was smaller than 4.7 ± 0.04% and after three freeze-thaw cycles containing thawing steps of 30 min amounted to be 4.9 ± 0.3%. Also here, the corresponding dephosphorylation of PP is too small to cause any underestimations of the encapsulated drug with regard to the aimed accuracy (p = 0.001 and p = 0.008, respectively). Since whole blood samples exhibit more phosphatase activity compared to plasma, the defined storage conditions for whole blood samples also prevent significant free drug overestimations in plasma samples.

CONCLUSIONS

The accurate determination of separate encapsulated and free drug concentrations in tissue, plasma and whole blood is desirable. To our knowledge, suitable methodology to measure such separate concentration profiles in tissues was hardly available.

A murine liver tissue sample preparation method for the accurate determination of such separate concentrations for liposomal PP was developed. Thorough method development and optimization guarantee that under- and overestimations of encapsulated and free drug concentrations are prevented: the use of 10 mL methanol/g tissue (containing the internal standards DP and D) during tissue homogenization verifies (1) complete liposome rupture, (2) immediate phosphatase deactivation, (3) sufficient clean supernatants, (4) convenient homogenization, (5) excellent extraction of P and sufficient extraction of PP, and (6) excellent accuracies and precision complying with the internal guidelines for preclinical studies. Similarly, a matching plasma sample preparation method was developed. Here, proteins were precipitated using four equivalents of methanol containing the internal standards. By adding one step, at which the samples were subjected to HIFU to extract possible intracellular drug, the plasma sample preparation method can be freely applied to whole blood samples still yielding accurate results complying with the internal guidelines for preclinical studies. One prerequisite: more than one freeze-thaw cycle of whole blood as well as plasma samples

Table 5: Schematic representation of the sample preparation methods for murine liver, plasma and whole blood samples to determine the liposomal-encapsulated and free drug concentration profiles of liposomal PP

Liver samples
Immerse in liquid nitrogen for 5-10 s
Immediately, add 10 mL/g methanol containing the internal standards
Immediately, homogenize using a General Laboratory Homogenizer (3 × 5 s, level 6)
Apply HIFU as described above
Centrifuge for 15 min
Transfer supernatant to vial
Plasma/whole blood samples
Add four equivalents of methanol containing the internal standards
Vortex 30 s
Apply HIFU as described above[b]
Centrifuge for 15 min
Transfer supernatant to vial

[b] HIFU is only required for whole blood samples.

should preferably be prevented. The protocols corresponding to the developed sample preparation methods are summarized in Table 5.

Application of above sample preparation methods is going to generate the PK profile of liposomal PP, in which also the encapsulated and free drug concentrations in a tissue are measured separately. Through combining these data with PK modeling, the *in vivo* drug release from the liposomes can be quantified, which will form an important component in assessing the true PK.

Although these sample preparation methods are specifically suitable for liposomal-encapsulated phosphate prodrugs and possibly, after additional experiments, also for other prodrugs and carrier systems, it is not able to distinguish between a liposomal-encapsulated anthracycline and the free anthracycline drug. However, it can gain important insights into the PK of liposomal formulations in general.

ACKNOWLEDGMENTS

The authors like to thank Foppe Bakker and Hans van Laarhoven from MSD Oss BV for the determination of the water content of murine liver tissue and plasma. The authors also like to thank Laura Hermens and Bianca Huisman for their assistance during the application of the General Laboratory Homogenizer. Coen Smits is acknowledged for his advice during the statistical analysis of the obtained results. We acknowledge MediTrans for the financial support.

DECLARATION OF INTEREST

This study has been carried out with financial support from the Commission of the European Communities, Priority 3 "Nanotechnologies and Nanosciences, Knowledge Based Multifunctional Materials, New Production Processes and Devices" of the Sixth Framework Programme for Research and Technological Development (Targeted Delivery of Nanomedicine: NMP4-CT-2006-026668). It does not necessarily reflect its views and in no way anticipates the Commission's future policy in this area.

REFERENCES

1. S. Qian, C. Li and Z. Zuo, Pharmacokinetics and disposition of various drug loaded liposomes, *Curr. Drug Metab.*, 2012, **13**, 372-395.
2. A. Gabizon, H. Shmeeda and Y. Barenholz, Pharmacokinetics of PEGylated liposomal doxorubicin: review of animal and human studies, *Clin. Pharmacokinet.*, 2003, **42**, 419-436.
3. J.M. Metselaar, M.H.M. Wauben, J.P.A. Wagenaar-Hilbers, O.C. Boerman and G. Storm, Complete remission of experimental arthritis by joint targeting of glucocorticoids with long-circulating liposomes, *Arthritis Rheum.*, 2003, **48**, 2059-2066.
4. M.S. Newman, G.T. Colbern, P.K. Working, C. Engbers and M.A. Amantea, Comparative pharmacokinetics, tissue distribution, and therapeutic effectiveness of cisplatin encapsulated in long-circulating, PEGylated liposomes (SPI-077) in tumor-bearing mice, *Cancer Chemother. Pharmacol.*, 1999, **43**, 1-7.
5. R.M. Schiffelers, J.M. Metselaar, M.H.A.M. Fens, A.P.C.A. Janssen, G. Molema and G. Storm, Liposome-encapsulated prednisolone phosphate inhibits growth of established tumors in mice, *Neoplasia*, 2005, **7**, 118-127.
6. T. Daemen, J. Regts, M. Meesters, M.T. Ten Kate, I.A.J.M. Bakker-Woudenberg and G.L. Scherphof, Toxicity of doxorubicin entrapped within long-circulating liposomes, *J. Controlled Release*, 1997, **44**, 1-9.
7. G. Storm, M.T. Ten Kate, P.K. Working and I.A.J.M. Bakker-Woudenberg, Doxorubicin entrapped in sterically stabilized liposomes: effects on bacterial blood clearance capacity of the mononuclear phagocyte system, *Clin. Cancer Res.*, 1998, **4**, 111-115.
8. I.K. Kwon, S.C. Lee, B. Han and K. Park, Analysis on the current status of targeted delivery to tumors, *J. Controlled Release*, 2012, **164**, 108-114.
9. S. Druckmann, A. Gabizon and Y. Barenholz, Separation of liposome-associated doxorubicin from non-liposome-associated doxorubicin in human plasma: implications for pharmacokinetic studies, *Biochim. Biophys. Acta*, 1989, **980**, 381-384.
10. N. Griese, G. Blaschke, J. Boos and G. Hempel, Determination of free and liposome-associated daunorubicin and daunorubicinol in plasma by capillary electrophoresis, *J. Chromatogr. A*, 2002, **979**, 379-388.
11. R. Krishna, M.S. Webb, G. St. Onge and L.D. Mayer, Liposomal and nonliposomal drug pharmacokinetics after administration of liposome-encapsulated vincristine and their contribution to drug tissue distribution properties, *J. Pharmacol. Exp. Ther.*, 2001, **298**, 1206-1212.
12. L.D. Mayer and G. St.-Onge, Determination of free and liposome-associated doxorubicin and vincristine levels in plasma under equilibrium conditions employing ultrafiltration techniques, *Anal. Biochem.*, 1995, **232**, 149-157.
13. A.A. Srigritsanapol and K.K. Chan, A rapid method for the separation and analysis of leaked and liposomal entrapped phosphoramide mustard in plasma, *J. Pharm. Biomed. Anal.*, 1994, **12**, 961-968.
14. W.C. Zamboni, S. Strychor, E. Joseph, D.R. Walsh, B.A. Zamboni, R.A. Parise, M.E. Tonda, N.Y. Yu, C. Engbers and J.L. Eiseman, Plasma, tumor, and tissue disposition of Stealth liposomal CKD-602 (S-CKD602) and nonliposomal CKD-602 in mice bearing A375 human melanoma xenografts, *Clin. Cancer Res.*, 2007, **13**, 7217-7223.
15. B.S. Zolnik, S.T. Stern, J.M. Kaiser, Y. Heakal, J.D. Clogston, M. Kester and S.E. McNeil, Rapid distribution of liposomal short-chain ceramide *in vitro* and *in vivo*, *Drug Metab. Dispos.*, 2008, **36**, 1709-1715.

16. K.M. Laginha, S. Verwoert, G.J.R. Charrois and T.M. Allen, Determination of doxorubicin levels in whole tumor and tumor nuclei in murine breast cancer tumors, *Clin. Cancer Res.*, 2005, **11**, 6944-6949.
17. V. Garg and W.J. Jusko, Bioavailability and reversible metabolism of prednisone and prednisolone in man, *Biopharm. Drug Dispos.*, 1994, **15**, 163-172.
18. H. Möllmann, S. Balbach, G. Hochhaus, J. Barth and H. Derendorf, Pharmacokinetic-pharmacodynamic correlations of corticosteroids, in *Handbook of pharmacokinetic/ pharmacodynamic correlation*, eds. H. Derendorf and G. Hochhaus, CRC Press, Boca Raton, 1995, pp 323-361.
19. E.A.W. Smits, J.A. Soetekouw and H. Vromans, *In vitro* confirmation of the quantitative differentiation of liposomal encapsulated and non-encapsulated prednisolone (phosphate) tissue concentrations by murine phosphatases: determination of the dephosphorylation rate of murine phosphatases to enable the quantitative differentiation between liposomal encapsulated and non-encapsulated drug in tissues after administration of liposomal prednisolone phosphate in mice, *J. Liposome Res.*, 2013, DOI: 10.3109/08982104.2013.850593.
20. E.A.W. Smits, C.J.P. Smits and H. Vromans, The development of a method to quantify encapsulated and free prednisolone phosphate in liposomal formulations, *J. Pharm. Biomed. Anal.*, 2013, **75**, 47-54.
21. R. Melarange, P. Sadra, A. Harris, D. Clapham and J. Curtis, The use of Covaris adaptive focused acoustics in psychiatryCEDD DMPK, website Covaris®, http://covarisinc.com/wp-content/uploads/GSK_DMDG_2007.pdf, (last accessed June 2015).
22. P.K. Bennett and K.C. Van Horne, Identification of the major endogenous and persistent compounds in plasma, serum and tissue that cause matrix effects with electrospray LC/MS techniques, website Tandem Labs™, http://www.tandemlabs.com/documents/AAPS03PB.pdf, (last accessed March 2014).
23. P. Poulin and F.-P. Theil, Prediction of pharmacokinetics prior to *in vivo* studies. 1. Mechanism-based prediction of volume of distribution, *J. Pharm. Sci.*, 2002, **91**, 129-156.
24. J.M. Metselaar, Liposomal targeting of glucocorticoids: a novel treatment approach for inflammatory disorders, PhD thesis, Utrecht University, 2003.
25. J.T. Brandenburg, K. Kramer and J. van der Valk, Bloedafname en bloedonderzoek, in *Proefdierkunde: biotechnisch handboek*, ed. J.T. Brandenburg, Stichting Proefdierkundige Informatie, Oss, 2000, pp 395-407.
26. S. Sahin, Y. Karabey, M.S. Kaynak and A.A. Hincal, Potential use of freeze-drying technique for estimation of tissue water content, *Methods Find. Exp. Clin. Pharmacol.*, 2006, **28**, 211-215.
27. M.N. Samtani, M. Schwab, P.W. Nathanielsz and W.J. Jusko, Stabilization and HPLC analysis of betamethasone sodium phosphate in plasma, *J. Pharm. Sci.*, 2004, **93**, 726-732.
28. U.S. Department of Health and Human Services, Food and Drug Administration, Center for Drug Evaluation and Research, Center for Veterinary Medicine, Guidance for industry: bioanalytical method validation, http://www.fda.gov/downloads/Drugs/Guidances/ucm070107.pdf, 2001.
29. R. Bellott, P. Pouna and J. Robert, Separation and determination of liposomal and non-liposomal daunorubicin from the plasma of patients treated with DaunoXome, *J. Chromatogr. B*, 2001, **757**, 257-267.
30. D.J.A. Crommelin and G. Storm, Liposomes: from the bench to the bed, *J. Liposome Res.*, 2003, **13**, 33-36.
31. L.M. Hays, J.H. Crowe, W. Wolkers and S. Rudenko, Factors affecting leakage of trapped solutes from phospholipid vesicles during thermotropic phase transitions, *Cryobiology*, 2001, **42**, 88-102.

32. E.M.G. Van Bommel and D.J.A. Crommelin, Stability of doxorubicin-liposomes on storage: as an aqueous dispersion, frozen or freeze-dried, *Int. J. Pharm.*, 1984, **22**, 299-310.

Chapter 5

Quantitative LC-MS determination of liposomal encapsulated prednisolone phosphate and non-encapsulated prednisolone concentrations in murine whole blood and liver tissue

Evelien A.W. Smits, José A. Soetekouw, Irene van Doormalen, Bart H.J. van den Berg, Marcel P. van der Woude, Nicolette de Wijs-Rot and Herman Vromans

This is an Accepted Manuscript of an article published by Elsevier. This article was published in *Journal of Pharmaceutical and Biomedical Analysis*, 2015, **115**, 552-561, Copyright Elsevier (2015).

ABSTRACT

The underlying pharmacokinetic profile of liposomal drug delivery systems is not yet fully known. This is primarily due to the limitation of suitable quantitative bioanalytical methodology to simultaneously determine separate liposomal encapsulated and non-encapsulated drug tissue concentrations in complex biological samples. Here, a method involving liquid chromatography-mass spectrometry (LC-MS) was developed which enables the simultaneous quantification of separate liposomal encapsulated prednisolone phosphate and non-encapsulated prednisolone concentrations in whole blood and liver tissue.

Liquid chromatography, negative electrospray ionization and Orbitrap-MS analysis allowed highly accurate and sensitive detection of prednisolone phosphate (PP) and prednisolone (P) in complex matrix. Using dexamethasone phosphate and dexamethasone as internal standards, the quantitative LC-MS method was optimized and validated for high selectivity, sensitivity and quantitative accuracy of PP and P from liposomes.

The lower limits of quantitation were: 0.99 µmol/L blood and 0.53 nmol/g liver for PP, and 229 nmol/L blood and 0.514 nmol/g liver for P. Quantitative accuracies of 84-118% were observed. The intrarun precision was ≤11%.

Application of this new LC-MS method will yield the required liposomal pharmacokinetic profile showing accurate encapsulated and non-encapsulated drug tissue concentrations separately. To our knowledge, this is also the first quantitative LC-MS method for the simultaneous quantification of the prodrug PP and its parent drug P in whole blood and liver tissue samples.

INTRODUCTION

Long-circulating liposomes are known for their application as drug delivery systems in the treatment of cancer, infections and inflammations [1,2]. Liposomal drug encapsulation changes the pharmacokinetics (PK) increasing the efficacy and/or reducing severe side effects (e.g. myelosuppression, mucositis and alopecia) compared to free drug formulations [1,2]. Unfortunately, besides accumulation at the target site, liposome accumulation was also observed in the skin [3] and in heavily perfused organs (e.g. liver and spleen) [3,4,5]. Because liposomes are often used for the formulation of highly toxic compounds (e.g. cytostatics) [2,6], liposome accumulation in healthy organs yields new, dose-limiting side effects such as hand-foot syndrome [3] and the significant reduction of the phagocytic activity of the liver macrophages resulting in a significantly reduced bacterial blood clearance [7,8].

Liposomes were first described fifty years ago [9] and a wealth of scientific literature covers liposome science[5]. However, the complete underlying PK profile is still unsolved. Until now, mainly liposome concentrations or total drug concentrations in the tissues of interest [3,4,5] were determined. However, the drug must be released from the liposomes to become effective or toxic and the free[6] drug concentrations in blood, tumor and healthy tissues should be distinguished from the liposomal encapsulated drug concentrations [6,10]. Such individual concentration profiles allow further optimization of liposomal formulations and an increase of the efficacy and/or a decrease of side effects [6].

Until now, individual concentration profiles of the encapsulated and free drug in tissues could hardly be determined in an accurate manner [6,10] and have only been approximated by techniques such as dual-labelling [11] and microdialysis [12] or by using the "sink" characteristics of the cell nucleus as with doxorubicin [13]. Therefore, there is still need for the development of an accurate quantitative bioanalytical method suitable for the differentiation between encapsulated and free drug tissue concentration profiles [6,10].

This study presents the development and semi-validation of an accurate method involving liquid chromatography-mass spectrometry (LC-MS) for quantifying encapsulated and free drug in liver and whole blood after intravenous administration of liposomal prednisolone phosphate. The method simultaneously determines individual prednisolone phosphate (PP) and prednisolone (P) concentrations. Prodrugs such as PP are rapidly dephosphorylated by phosphatases *in vivo* [14,15]. PP released from the

5 24,091 publications in PubMed on August 3th, 2015, search terms "liposome" AND "drug"

6 Here, free drug is defined as the non-encapsulated drug, whether protein-bound or not protein-bound.

liposomes in the circulation [unpublished data] or liver [10] is assumed to be immediately converted into P. Accordingly, the encapsulated drug concentration is represented by PP, whereas P represents the free drug concentration [5].

Due to the very different characteristics of PP and P, sample clean-up by protein precipitation is preferred [6,16]. To avoid the interference by (biological) impurities during PP and P detection, high-resolution accurate mass Orbitrap LC-MS analysis is applied. Sufficient specificity, sensitivity and accuracy were obtained for the quantification of encapsulated PP and free P concentrations in the nM-μM range in blood and pmol/g-nmol/g range in liver samples.

LC-MS has been used to quantify PP, P and similar glucocorticosteroids in liver [17-22] and plasma/serum/blood [23-32]. However, to the best of our knowledge, this is the first quantitative LC-MS method for the simultaneous quantification of a prodrug such as PP and its parent drug P in whole blood and liver tissue samples. Additionally, this LC-MS method facilitates the required accurate quantification of individual liposomal encapsulated and free drug tissue concentrations.

MATERIALS AND METHODS

Materials

Unless mentioned otherwise, all materials were used as received. Dipalmitoylphosphatidylcholine (DPPC) and poly(ethylene glycol)2000-distearoy lphosphatidylethanolamine (PEG2000-DSPE) were purchased from Lipoid GmbH (Ludwigshafen, Germany). Alkaline phosphatase from rabbit intestine, cholesterol, dexamethasone, dexamethasone disodium phosphate, phosphate buffered saline (PBS) powder in foil pouches, and prednisolone were purchased from Sigma (St. Louis, MO, USA). PBS pH 7.4 (0.01 M) was prepared as described by Sigma. Prednisolone disodium phosphate was purchased from Bufa (IJsselstein, The Netherlands). Acetonitrile LiChrosolv and tetrahydrofuran (THF) Uvasol were purchased from Merck (Darmstadt, Germany). Dimethyl sulfoxide (DMSO) and methanol HPLC gradient grade were purchased from Mallinckrodt Baker BV (Deventer, The Netherlands). Ammonium acetate ULC/MS grade was purchased from Biosolve BV (Valkenswaard, the Netherlands). Formic acid 98+% pure was purchased from Acros Organics (Morris Plains, NJ, USA). Liver tissues and ethylenediaminetetraacetic acid (EDTA)-stabilized whole blood from male C57BL/6J mice were purchased from Janvier (Le Genest-Saint-Isle, France). All water used was purified water prepared using a Milli-Q system (Millipore Corporation, Billerica, MA, USA).

Liposome preparation and characterization

Polyethylene glycol (PEG)-coated liposomes encapsulating PP were prepared according to the film-extrusion method as described previously [5], starting from a mixture of DPPC, cholesterol and PEG2000-DSPE in a molar ratio of 1.85:1.0:0.15, respectively. To evaluate the completion of the liposome preparation, the total, encapsulated and free PP content were determined using a recently described method using alkaline phosphatase for differentiation [16]. The mean liposome size was determined by dynamic light scattering (DLS) as described previously [16].

Chromatographic conditions

Analytes were separated using an Agilent 1200 Series HPLC (high-performance liquid chromatography) system (Agilent Technologies, Palo Alto, CA, USA) and the chromatographic conditions as described in Table 1, which are adapted from a recently described HPLC-UV method [6].

To prevent inaccurate results due to carry-over from PP, which was observed during preliminary experiments [6,unpublished data], samples were injected from low to high

Table 1: Chromatographic conditions of the LC-MS method, which are adapted from a recently described HPLC-UV method [6]

Column	Zorbax SB-C18, 2.1 × 150 mm, 3.5 µm[a]				
Column temperature	40°C				
Mobile phase:	Time (min)	%A	%B	%C	%D
A: 50 mM ammonium acetate in water	0	95	5	0	0
B: acetonitrile	2	70	30	0	0
C: water	10	40	60	0	0
D: 30% THF/60% acetonitrile/10% water	12	40	60	0	0
	12.1[b]	0	60	40	0
	14[b]	0	60	40	0
	14.1[b,c]	0	0	0	100
	32[b,c]	0	0	0	100
	32.1[d]	95	5	0	0
	42[d]	95	5	0	0
Flow rate	0.250 mL/min				
Splitter	PEEK tee and tubing[e]				
Flow split ratio (prior to ESI source)	1.25:1				

[a] Agilent Technologies, Palo Alto, CA, USA

[b] Rinsing step

[c] Simultaneously, the electrospray ionization (ESI) source and MS system were cleaned using 50% acetonitrile/50% water

[d] Equilibration

[e] Upchurch Scientific, Oak Harbor, WA, USA

PP concentration and the system was washed appropriately in between the analyses of high and low concentrated samples. The standard injection volume was 5 µL. To yield a quantification range that is larger than the linearity corresponding to the standard injection volume of 5 µL, low concentrated samples were measured using an injection volume of 30 µL. Similarly, the high concentrated samples were diluted 5× with methanol and re-analyzed using an injection volume of 5 µL.

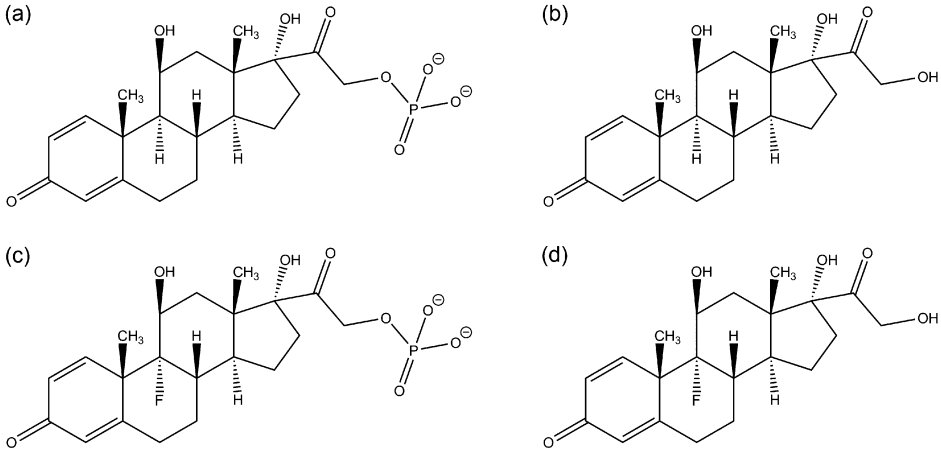

Figure 1: Chemical structures of prednisolone phosphate (a), prednisolone (b), dexamethasone phosphate (c) and dexamethasone (d)

MS optimization for detection of PP, P and internal standards

All MS measurements were done on an LTQ Orbitrap mass spectrometer equipped with an electrospray ionization (ESI) source (Thermo Fisher Scientific Inc., Waltham, MA, USA).

In order to select the optimal ions and optimal MS parameters for the detection of PP and P and the internal standards dexamethasone phosphate (DP) and dexamethasone (D) (chemical structures shown in Figure 1), an LC-flow injection analysis of a mixture of PP, DP, P and D in methanol was performed in the negative ionization mode. Preliminary, internal MS method development for PP, DP, P and D in water/THF (1:2 v/v%) [unpublished data] has shown that negative ionization mode produces less background ions and yields higher signal intensities for PP and DP compared to the positive ionization mode. For P and D in negative mode more adducts and in-source fragmentation were observed, which was used to our advantage and the ESI parameters were adjusted to in-source fragment P and D each into a single product ion. This yielded similar signal intensities compared to the positive ionization mode. Therefore, negative ionization mode was chosen for further analysis. The advanced MS scan features (e.g. analyzer, resolution, scan type) were optimized to obtain maximal signal intensities. The optimal parameters for the electrospray source (ionization), the ion optics (ion lenses)

and the FT transfer optics (multipole) were determined automatically using the LTQ Tune Plus version 2.4 SP1 Software (Thermo Electron Corporation, Waltham, MA, USA) followed by manual tuning.

High-intensity focused ultrasound

Liver and blood cell membranes were disrupted by high-intensity focused ultrasound (HIFU) to extract intracellular drug prior to LC-MS analysis. To do so, a Covaris E210x (Covaris Inc., Woburn, MA, USA) controlled by Covaris SonoLab Software version Ev4.3.3 (Covaris Inc.) was used. The sample tubes were held in a water bath of maximal 15°C [6].

Whole blood: The samples were transferred to HIFU resistant 15 × 19 mm glass vials (Covaris Inc.) and were exposed to HIFU 3× by running the following process configuration for 60 s: duty cycle, 20%; intensity, 10.0; cycles/burst, 1000; frequency sweep: vertical, ± 1.0 mm, vertical rate, 20.0 cpm. In between the three runs the samples were allowed to cool for at least 60 s.

Liver tissue: Liver homogenate was prepared as described in the section "Preparation and processing of calibration standards and quality control samples" below and was transferred to HIFU resistant 10 mL TC16 borosilicate glass tubes (KBioscience). Liver homogenates were exposed to HIFU as described recently [6]. To summarize, the samples were exposed to HIFU by running a process configuration adapted from the rat liver preparation from Melarange et al. [33]: 100 cycles/burst for 60 s, 1000 cycles/burst for 60 s, 100 cycles/burst for 30 s, 1000 cycles/burst for 30 s. The Power Tracking mode was activated and the duty cycle and intensity were kept at 50% and 10.0, respectively.

Preparation of stock and working solutions

Whole blood: Stock solutions containing 48.5 mM PP or 51.29 mM P were prepared in PBS pH 7.4 or DMSO, respectively. These stock solutions were equally diluted in PBS pH 7.4 or DMSO yielding 17 working solutions from 12.1 mM to 185 nM for PP and from 12.8 mM to 196 nM for P. These working solutions were used to prepare the calibration standards. To improve the precision, no liposomal PP was used here. Independent stock and working solutions were prepared for the preparation of the quality control (QC) samples. Whereas the liposomal preparation as such served as stock solution for liposomal PP, for P a stock solution of 7.200 mM P was prepared in DMSO. Subsequent dilution of these stock solutions using PBS pH 7.4 or DMSO yielded seven working solutions from 6.5 mmol PP/L to 1.0 µmol PP/L and from 2.880 mM to 360.0 nM for P.

Liver tissue: Stock solutions containing 48.4 mM PP or 51.08 mM P were prepared in PBS pH 7.4 or DMSO, respectively. These stock solutions were equally diluted in PBS pH 7.4 or DMSO yielding 14 working solutions from 3.02 mM to 369 nM for PP and from 3.19 mM to 390 nM for P. These working solutions were used to prepare the calibration standards. In favor of the precision, no liposomal PP was used here. Independent stock

and working solutions were prepared for the preparation of the QC samples. Whereas the liposomal preparation as such served as stock solution for liposomal PP, for P a stock/working solution of 4.468 mM P was prepared in DMSO. Subsequent dilution of these "stock" solutions using PBS pH 7.4 or DMSO yielded six working solutions in total. These ranged from 4.3 mmol PP/L to 21 µmol PP/L and from 4.468 mM to 22.3 µM for P.

Preparation and processing of calibration standards and quality control samples

Whole blood: Blood calibration standards and QC samples were prepared in duplicate by adding 8 µL of the corresponding P working solution to 84 µL of whole blood and, after gently mixing using an Eppendorf Thermomixer (500 rpm, 10 min, room temperature), by adding 8 µL of the corresponding PP working solution. This resulted in 2 × 17 calibration standards containing PP concentrations from 1.16 mmol/L blood to 17.6 nmol/L blood and P concentrations from 1.22 mmol/L blood to 18.6 nmol/L blood. The PP and P concentrations for all calibration standards are presented in the supplementary data (see Appendix A.1). Additionally, this resulted in 2 × 7 QC samples containing liposomal PP concentrations from 0.62 mmol/L blood to 99 nmol/L blood and P concentrations from 274 µmol/L blood to 34.3 nmol/L blood. Information about the intermediate concentrations is shown in Tables 2a and 2b. 8 µL of PBS pH 7.4 and 8 µL DMSO were added to 84 µL of whole blood to prepare a zero calibration standard.

Blood calibration standards and QC samples were processed according to a recently developed sample preparation method [6], at which the conversion of PP released from the liposomes during storage and during sample preparation was prevented. In short, 400 µL methanol containing the internal standards (26 µM DP and 3.754 µM D) were added. Then, the samples were thoroughly vortexed for 30 s, subjected to HIFU as described above and centrifuged (20817 RCF, 15 min). The resulting supernatants were transferred to HPLC vials. Similarly, the supernatant of 100 µL blood with 400 µL methanol was prepared as blank.

Liver tissue: Processed liver calibration standards were prepared in duplicate as follows. Four livers were immersed in liquid nitrogen for 5-10 s and immediately homogenized in 10 mL methanol/g liver using a General Laboratory Homogenizer (Omni, Kennesaw, GA, USA). The methanol contained the internal standards (3.1 µM DP and 3.08 µM D). The pooled homogenates were subjected to HIFU as described above. Subsequently, 25 µL of the corresponding P standard working solution and 25 µL of the corresponding PP standard working solution were added to an aliquot of 950 µL homogenate. After thorough vortexing for 30 s, the calibration standards were centrifuged (20817 RCF, 15 min), and the resulting supernatants were analyzed by LC-MS. This yielded 2 × 14 calibration standards in the range 0.107-875 nmol PP/g liver and 0.113-924 nmol P/g liver. The PP and P concentrations for all calibration standards are presented in the

supplementary data (see Appendix A.1). Similarly, a zero calibration standard was prepared.

Liver QC samples were prepared in duplicate by spiking and were processed according to a recently described sample preparation method [6] which prevents the conversion of PP released from the liposomes during storage and sample preparation. In detail, 25 µL of the corresponding P working solution were added to one liver. After 10 min of incubation and immersion of the liver in liquid nitrogen for 5-10 s, 10 mL methanol/g liver containing the internal standards (3.1 µM DP and 3.08 µM D) and 25 µL of the corresponding liposomal PP working solution were added. Hereafter, the liver was homogenized immediately using a General Laboratory Homogenizer, subjected to HIFU (as described above) and centrifuged (2890 RCF, 15 min). The resulting supernatants were analyzed by LC-MS. This yielded 2 × 6 QC samples in the range 0.53-107 nmol PP/g liver and 0.514-125 nmol P/g liver. The liposomal PP and P concentrations for all QC samples are presented in Tables 2a and 2b, respectively. Likewise, one liver was processed in 10 mL/g methanol to prepare a blank.

Evaluation of cell membrane disruption

The suitability of HIFU to disrupt cell membranes in the presence of methanol was evaluated as follows. Since it is impossible to prepare QC samples containing known amounts of intracellular drug (encapsulated and free) similar to *in vivo* samples, a blood sample originating from one tumor-bearing mouse administrated with liposomal PP was used. The male C57BL/6J mouse of age 6-8 weeks (Charles River, Leiden, the Netherlands) was kept in standard housing with standard rodent chow, water available *ad libitum* and a 12 h light/dark cycle. The experiment was performed according to national regulations and was approved by the animal experiment committee of Utrecht University as well as MSD Oss BV. For tumor induction, 1×10^6 murine B16F10 melanoma cells were inoculated subcutaneously in the flank of the C57BL/6J mouse. At a tumor volume of approximately 250 mm^3, the mouse received 36 µmol PP/kg by tail vein injection of liposomal PP. 40 h post-injection, blood was sampled (~240 µL) via cheek puncture into EDTA containing tubes. 100 µL of this sample were processed as described in the above section "Preparation and processing of calibration standards and quality control samples". A second aliquot of ~140 µL was processed using a slightly adapted sample preparation method, where cell membranes were disrupted prior to methanol addition using a combination of previously published cell membrane disrupting methods as follows. First, this aliquot underwent three freeze-thaw cycles [34]. One freeze-thaw cycle included liquid nitrogen immersion for ~1 h, followed by storage at -20°C for at least 24 h [35], followed by thawing at room temperature for ~6.5 h. Subsequently, the aliquot was placed in an ultrasonic bath (Transsonic 890, Elma, Singen, Germany) for 30 min [36] and subjected to HIFU as described above. Note, the phosphatase activity was

Table 2a: Accuracy and *SD* observed for the encapsulated prednisolone phosphate (PP)

Matrix	Injection volume (µL)	Nominal PP conc. (µmol/L blood) (nmol/g liver)	(Mean) observed PP conc. (µmol/L blood) (nmol/g liver)	± *SD* (µmol/L blood) (nmol/g liver)	(Mean) accuracy PP (%)	± *SD* (%)
Blood (n = 2)	30[f]	0.99	0.95	± 0.01	96	± 1
	5[g]	0.99	0.94	± 0.04	95	± 4
	5	4.9	5.81	± 0.02	118	± 0.4
	5	25	28.0	± 0.1	113	± 0.4
	5[h]	124	124	± 2	99	± 2
	5 (dilution)	124	138	± 0.9	111	± 1
	5[i] (dilution)	623	631	± 0.3	101	± 0.04
Liver	30[f]	0.53	0.466	-	88	-
	30	0.61	0.546	-	90	-
	5[g]	17	16.0	-	97	-
	5	17	17.3	-	101	-
	5	34	32.2	-	96	-
	5	35	30.5	-	86	-
	5	65	67.1	-	104	-
	5	67	62.1	-	93	-
	5	98	111	-	114	-
	5	101	104	-	102	-
	5	105	102	-	97	-
	5[h]	107	107	-	99	-

The spiked concentrations of encapsulated PP were varied. Lower (LLOQ) and upper (ULOQ) limits of quantification are indicated.

[f] LLOQ using an injection volume of 30 µL

[g] LLOQ using an injection volume of 5 µL

[h] ULOQ using an injection volume of 5 µL

[i] ULOQ after 5× sample dilution (injection volume: 5 µL)

Table 2b: Accuracy and *SD* observed for the free prednisolone (P)

Matrix	Injection volume (µL)	Nominal P conc. (µmol/L blood) (nmol/g liver)	(Mean) observed P conc. (µmol/L blood) (nmol/g liver)	± *SD* (µmol/L blood) (nmol/g liver)	(Mean) accuracy P (%)	± *SD* (%)
Blood (n = 2)	30[f]	0.229	0.25	± 0.02	110	± 8
	30	0.343	0.36	± 0.01	106	± 3
	5[g]	0.343	0.312	± 0.006	91	± 2
	5	0.686	0.71	± 0.02	104	± 3
	5	6.86	7.4	± 0.4	108	± 5
	5[h]	68.6	57	± 2	84	± 3
	5 (dilution)	68.6	67	± 5	98	± 7
	5[i] (dilution)	274	271	± 9	99	± 3
Liver	30[f]	0.514	0.548	-	107	-
	30	0.553	0.646	-	117	-
	5[g]	17.3	18.5	-	107	-
	5	17.9	18.7	-	105	-
	5	33.8	36.1	-	107	-
	5	35.0	39.5	-	113	-
	5	70.5	76.6	-	109	-
	5	74.1	79.6	-	107	-
	5	91.5	91.0	-	99.5	-
	5	110	109	-	98.9	-
	5	114	114	-	101	-
	5[h]	125	134	-	107	-

The spiked concentrations of the free P were varied. Lower (LLOQ) and upper (ULOQ) limits of quantification are indicated.

[f] LLOQ using an injection volume of 30 µL

[g] LLOQ using an injection volume of 5 µL

[h] ULOQ using an injection volume of 5 µL

[i] ULOQ after 5× sample dilution (injection volume: 5 µL)

not deliberately stopped prior to liposome rupture. PP and P concentrations in both aliquots were determined using LC-MS as described here and the sum total drug (PP + P) concentrations corresponding to the different aliquots were compared mutually. The relative standard deviation (*RSD*) between both cell disrupting protocols yields information regarding the deviation in drug quantitation due to possible inadequate cell membrane disruption.

Data analysis

The LCquan Software (Thermo Electron Corporation) was used for method development, data collection, and extracted peak integration. The accurate masses of the selected ions of PP, DP, P and D were extracted from the raw MS data and integrated in LCquan. Calibration curves based on peak areas were used to quantitate the drug levels in the QC samples using Microsoft Excel 2010 (Microsoft Corporation, Redmond, WA, USA). Linearity of the calibration curves was assessed by least squares linear regression after normalization of the x- (concentration ratio of the analyte to the internal standard) and y-axis (peak area ratio of the analyte versus the internal standard) using the decimal logarithm. The quantitative accuracy of the calibration standards within the linear range was as defined below.

The method, which is intended for use during fundamental research, was validated using criteria adapted from the guidance by the U.S. Food and Drug Administration (FDA). This is in accordance with internal accuracy criteria from the internal guidelines for toxicological and preclinical bioanalytical methods. The quantitative accuracy of the calibration standards and QC samples had to be within 20% with respect to the nominal values. The precision (*RSD* of the quantitative accuracy) should not exceed 20%. Because the calibration standards were prepared using free PP instead of liposomal PP and the liver calibration standards were prepared by spiking aliquots of liver homogenate instead of livers, the lower limit (LLOQ) and upper limit of quantification (ULOQ) were determined from the QC samples. The linearity of the method was considered as the range from LLOQ to ULOQ, at which linearity had to be verified for this range of the corresponding calibration curve. Also, a quantitative accuracy of 80-120% and a maximal precision of 20% had to be observed for the intermediate QC samples. Besides careful method development, the specificity, selectivity, limits of quantification, linearity, quantitative accuracy, precision and blood extraction recovery were evaluated in an appropriate way to guarantee suitable and reliable performance characteristics.

RESULTS AND DISCUSSION

Liposome preparation characteristics

The liposome preparation contained 8.9 ± 0.3 mmol PP/L, of which about 9% is present as free drug. The presence of a minor free drug amount in liposome preparations is common [37-39]. After self-assembly of the liposomes, the non-encapsulated drug was removed by dialysis leaving a small amount of free drug in the liposome preparation. The liposome diameter determined by DLS was 98 ± 27 nm. The dispersity was 0.055 indicating that the liposome preparation is monodisperse. The phospholipid content was 60 mM [5].

MS optimization for PP, DP, P and D detection

The negative mode MS parameters for PP, DP, P and D were optimized via infusion into the LC-flow into the LTQ Orbitrap. Besides the expected $[M-H]^-$, in-source fragmentation ions $[M-CH_2OH]^-$ of P and D were observed similarly to [20,40]. Preliminary experiments already ruled out that the in-source fragmentation is caused by the formation of instable structures due to protonation in acidic environment prior to ionization. Most likely, the in-source fragmentation of P and D is caused by thermal degradation [31]. Since the stability of P and D could not be sufficiently improved, these $[M-CH_2OH]^-$ fragments of P and D (*m/z* 329.17 and 361.18, respectively) were chosen for quantitative analysis in favor of the sensitivity. These together with the $[M-H]^-$ ions of PP and DP (*m/z* 439.15 and 471.15, respectively).

Maximal sensitivity and selectivity was obtained by using the Orbitrap analyzer and detector (without use of the linear ion trap) by applying the following optimized settings: AGC 5.00e+05, injection time 500 ms, resolution 7500, mass extraction window of 0.02 Da. During validation full-scan mass spectra of analytes and internal standards were acquired from *m/z* 300 to 525 only. The electrospray source parameters were manually adapted to fully in-source fragment P and D towards $[M-CH_2OH]^-$. The corresponding optimal parameters for ionization were: sheath gas flow rate (arb.): 40; auxiliary gas flow rate (arb.): 10; sweep gas flow rate (arb.): 10; I spray voltage (kV): 3.50; capillary temperature (°C): 300.00; capillary voltage (V): -27.00; tube lens (V): -138.70.

Specificity

Extracted ion chromatograms (EICs) of *m/z* 439.15, 471.15, 329.17 and 361.18, corresponding to PP, DP, P and D, respectively, were generated for the blood and liver matrix containing blank samples. No evidence of detrimental interfering peaks at the retention times of PP, DP, P and D was observed. Peak areas of co-eluting impurities were <1.8% compared to the peak areas of the lowest PP, DP, P and D concentrations present in the calibration standards and QC samples for which an accuracy of 80-120% and a

precision of maximally 20% was observed. Additionally, no overlapping isotopic peak clusters were observed in the target analyte isotopic cluster as detected in the MS. This proves a high specificity of this method for PP, DP, P and D detection. Comparable, such specificity is hard to obtain using a triple-quadrupole MS used in routine clinical screening and quantification assays. As illustrated in Figure 2, the shown EICs of $[P\text{-}CH_2OH]^-$ were acquired by applying different scan resolutions, showing: (a) the 7500 resolution of the Orbitrap used in this study and (b) 0.1 unit resolution similar to highly selective triple-quadrupole MS instruments [41]. The Orbitrap analysis allows clear identification of $[P\text{-}CH_2OH]^-$ with *m/z* 329.17 from a liver matrix impurity at *m/z* 329.23 (see Figure 2c). The triple-quadrupole mass spectrometers with 0.1 unit resolution cannot differentiate between these two compounds and peak integration of $[P\text{-}CH_2OH]^-$ for quantification is hampered. Using a strategy involving multiple reaction monitoring to reconstruct an EIC of product-ions could distinguish the target compound from matrix impurities. However, the development of these assays is time-consuming and often suffers from limited sensitivities. To reliably and swiftly quantify the target compounds in complex matrices, LC-MS assays rely strongly on the combination of high mass accuracy and high resolution as shown here.

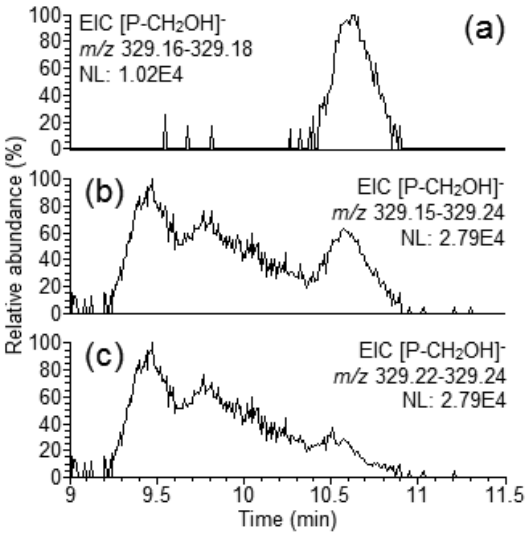

Figure 2: EICs corresponding to $[P\text{-}CH_2OH]^-$ for a liver sample (0.553 nmol P/g liver):
(a) ion extraction of *m/z* 329.17 ($[P\text{-}CH_2OH]^-$) recorded by the Orbitrap at resolving power of 7500, (b) ion extraction of *m/z* 329.2 ($[P\text{-}CH_2OH]^-$ and impurity) recorded by the Orbitrap with a resolving power comparable to the 0.1 unit resolution of highly selective triple-quadrupole MS instruments [41], and (c) ion extraction of the impurity with *m/z* 329.23 using the Orbitrap resolution from this study

Selectivity

Analytes and internal standards in the complex matrices were identified based on the retention time and accurate mass of the selected ions (see the above section "MS optimization for PP, DP, P and D detection"). PP, DP, P and D, from blood as well as liver containing matrices, eluted at the retention time windows of 8.1-8.3, 8.5-8.7, 10.4-10.7 and 11.5-11.8 min, respectively. Initially, the MS data suffered from numerous impurities (co-eluting and late-eluting carry-over impurities) that caused ion suppression and reduced the absolute amount of analyte ions collected by the c-trap. This affected the linearity, quantitative accuracy, precision and sensitivity. The amount of late-eluting carry-over impurities was significantly reduced by thorough washing of the HPLC system after every run (see the above section "Chromatographic conditions"). PP, DP, P and D were differentiated from co-eluting impurities by means of their accurate mass. The total ion chromatograms (TICs), EICs and full MS spectra of a representative blood and liver QC sample are shown in Figure 3. Certainly, for the liver QC sample the TIC shows broad high-intensity peaks caused by matrix background. This is also reflected by the ion complexity present in the MS spectra. EIC generation using accurate mass allowed proper analyte peak area integration for quantification (as described in the sections "Linearity and limits of quantification" and "Quantitative accuracy and precision" below).

The endogenous glucocorticosteroid cortisone is described by the same molecular formula and mass as P and could interfere in the accurate detection and quantification of P. Additional experiments with cortisone standards (data not shown) revealed that cortisone elutes around 10.6-10.8 min. In addition, the blank and zero blood and liver samples showed no evidence for the presence of cortisone.

Linearity and limits of quantification

In favor of the precision, free PP instead of liposomal PP was used to prepare the calibration standards. In addition, the liver calibration standards were prepared by spiking aliquots of liver homogenate instead of whole livers. Since the presence of lipids from the liposomes and the order with regard to homogenization and spiking can influence the limits of quantification, the LLOQ and ULOQ were determined from the QC samples and the linearity was defined as the range from LLOQ to ULOQ, at which a quantitative accuracy of 80-120% and a maximal precision of 20% had to be observed for the intermediate QC samples. Also, linearity had to be verified for this range of the corresponding calibration curve. The calibration curves, accuracies per calibration standard and the corresponding coefficients of determination are presented in the supplementary data (see Appendix A.1).

The LLOQ and ULOQ for PP as well as P using a 5 µL injection are indicated in Tables 2a and b, respectively. The corresponding LLOQ and ULOQ could be enhanced by increasing the injection volume to 30 µL or by 5× dilution, respectively (see also Tables 2a and b).

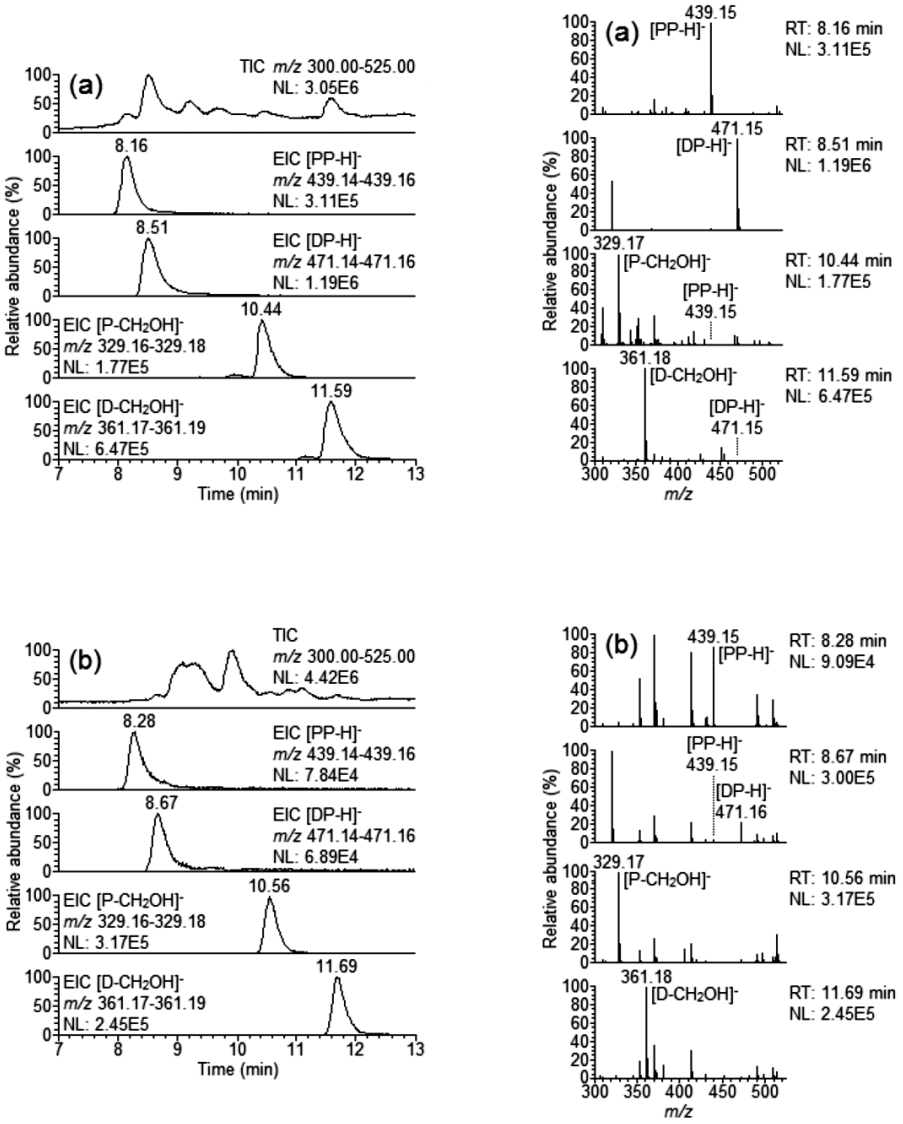

Figure 3: Representative TICs, EICs and full MS spectra after 5 µL injection of a blood (a) and liver (b) QC sample

The MS spectra correspond to the retention times of PP, DP, P and D. The nominal concentrations of PP, DP, P and D in blood/liver were: 25 µmol PP/L blood, 0.12 mmol DP/L blood, 6.86 µmol P/L blood, and 17.9 µmol D/L blood; and 35 nmol PP/g liver, 31 nmol DP/g liver, 74.1 nmol P/g liver, and 30.7 nmol D/g liver.

Considering the scheduled intravenous administration of 36 µmol/kg liposomal prednisolone phosphate in mice, an estimated murine total blood volume of 1.75 mL [42] and the indication that the majority of the drug in the blood is expected to be liposome-encapsulated [5], the expected maximal *in vivo* blood concentrations for PP

and P are estimated to be 520 and 230 μM, respectively. The expected maximal sum total drug concentration in liver is about 100 nmol/g [43]. Of this, the partition encapsulated/free drug is unknown and the maximal liver concentrations for PP as well as P can be equal to the expected maximal sum total concentrations. Measuring a representative PK profile including low PP and P concentrations, requires accurate measurement of the maximal drug concentrations down to concentrations <1% of these maximal concentrations. Such concentration ranges are covered entirely by the linearity of the method (Tables 2a and 2b).

The observed sensitivity in this study is satisfactory with regard to the expected *in vivo* concentrations as described above. The sample preparation used in this study involves a single protein precipitation step yielding samples containing more (biological) impurities. These impurities can influence the sensitivity; however, they are not a problem for result interpretation due to the high specificity of Orbitrap MS. To further improve the sensitivity, the use of later Orbitrap MS models than used here is recommended.

Quantitative accuracy and precision

Tables 2a and 2b show the QC samples for which both duplicates show a quantitative accuracy of 80-120% and therefore comply with the criteria adapted from the FDA guidance. The exact observed values of the quantitative accuracies of these QC samples are also shown in Tables 2a and 2b. The corresponding encapsulated PP and free P concentrations in blood and liver cover the required concentration ranges as described in the above section "Linearity and limits of quantification". The intrarun precision of these QC samples was ≤4% and ≤8% for PP and P in blood, respectively. For PP and P in liver, this was ≤11% and ≤6%, respectively. Therewith, the precision was consistently lower than 20% deviation.

Cell membrane disruption

To extract all intracellular drug, HIFU should disrupt cell membranes adequately. A blood sample originating from a tumor-bearing mouse administrated with liposomal PP was used to study the cell membrane disruption in methanol by HIFU. The observed sum total drug concentration of the blood sample which was subjected to HIFU as described in this paper, was compared to the observed sum total drug concentration of the blood sample after application of a combination of previously published cell membrane disrupting methods [34,36] and HIFU prior to methanol addition. This yielded a recovery of 90%. In addition, the calculated *RSD* (8%) between the determined sum total concentration using HIFU after methanol addition and the determined sum total concentration using previously published methods and HIFU prior to methanol addition was not greater than the observed maximal precision for blood as described

in the above section "Quantitative accuracy and precision". This indicates that any deviation due to insufficient cell membrane disruption in methanol by HIFU is probably not noteworthy compared to the deviation due to further sample preparation and LC-MS analysis, yielding accurate results complying with the adapted FDA criteria.

CONCLUSIONS

Here, the required LC-MS method allowing the simultaneous, accurate quantification of separate (liposome-encapsulated) PP and (non-encapsulated) P concentration profiles in blood and liver tissue is presented. Because sample clean-up by protein precipitation is preferred [6,16], the final samples contained a large amount of impurities. Sufficient specificity was obtained by using the Orbitrap. And sufficient selectivity was obtained through optimizing the chromatography. The sensitivity was adequate for the intended purpose. The quantitative accuracy and intrarun precision complied with the criteria adapted from the FDA guidance (84-118% and maximal 11%, respectively).

Application of this LC-MS method will yield the required PK profile of a liposomal formulation showing separate encapsulated and free drug concentrations in a tissue.

CONFLICT OF INTEREST

This study has been carried out with financial support from the Commission of the European Communities, Priority 3 "Nanotechnologies and Nanosciences, Knowledge Based Multifunctional Materials, New Production Processes and Devices" of the Sixth Framework Programme for Research and Technological Development (Targeted Delivery of Nanomedicine: NMP4-CT-2006-026668). It does not necessarily reflect its views and in no way anticipates the Commission's future policy in this area.

ACKNOWLEDGMENTS

The authors gratefully thank Ebel Pieters from Utrecht University for performing tumor inoculation, monitoring of the tumor size, liposomal PP administration and blood sample collection. Jon Curtis and Niels Kruize from KBioscience are acknowledged for their assistance during the application of the Covaris. The authors acknowledge Peter Bakker, Wouter Hoeberichts and Theo Janssen from MSD Oss BV for their assistance and participation in discussions. We thank MediTrans for the financial support (Targeted Delivery of Nanomedicine: NMP4-CT-2006-026668).

REFERENCES

1. T.M. Allen and P.R. Cullis, Liposomal drug delivery systems: from concept to clinical applications, *Adv. Drug Delivery Rev.*, 2013, **65**, 36-48.
2. S. Qian, C. Li and Z. Zuo, Pharmacokinetics and disposition of various drug loaded liposomes, *Curr. Drug Metab.*, 2012, **13**, 372-395.
3. A. Gabizon, H. Shmeeda and Y. Barenholz, Pharmacokinetics of PEGylated liposomal doxorubicin: review of animal and human studies, *Clin. Pharmacokinet.*, 2003, **42**, 419-436.
4. I.K. Kwon, S.C. Lee, B. Han and K. Park, Analysis on the current status of targeted delivery to tumors, *J. Controlled Release*, 2012, **164**, 108-114.
5. J.M. Metselaar, M.H.M. Wauben, J.P.A. Wagenaar-Hilbers, O.C. Boerman and G. Storm, Complete remission of experimental arthritis by joint targeting of glucocorticoids with long-circulating liposomes, *Arthritis Rheum.*, 2003, **48**, 2059-2066.
6. E.A.W. Smits, J.A. Soetekouw, P.F.A. Bakker, B.J.H. Baijens and H. Vromans, Plasma, blood and liver tissue sample preparation methods for the separate quantification of liposomal-encapsulated prednisolone phosphate and non-encapsulated prednisolone, *J. Liposome Res.*, 2015, **25**, 46-57.
7. T. Daemen, J. Regts, M. Meesters, M.T. Ten Kate, I.A.J.M. Bakker-Woudenberg and G.L. Scherphof, Toxicity of doxorubicin entrapped within long-circulating liposomes, *J. Controlled Release*, 1997, **44**, 1-9.
8. G. Storm, M.T. Ten Kate, P.K. Working and I.A.J.M. Bakker-Woudenberg, Doxorubicin entrapped in sterically stabilized liposomes: effects on bacterial blood clearance capacity of the mononuclear phagocyte system, *Clin. Cancer Res.*, 1998, **4**, 111-115.
9. A.D. Bangham and R.W. Horne, Negative staining of phospholipids and their structural modification by surface-active agents as observed in the electron microscope, *J. Mol. Biol.*, 1964, **8**, 660-668.
10. E.A.W. Smits, J.A. Soetekouw and H. Vromans, *In vitro* confirmation of the quantitative differentiation of liposomal encapsulated and non-encapsulated prednisolone (phosphate) tissue concentrations by murine phosphatases, *J. Liposome Res.*, 2014, **24**, 130-135.
11. B.S. Zolnik, S.T. Stern, J.M. Kaiser, Y. Heakal, J.D. Clogston, M. Kester and S.E. McNeil, Rapid distribution of liposomal short-chain ceramide *in vitro* and *in vivo*, *Drug Metab. Dispos.*, 2008, **36**, 1709-1715.
12. W.C. Zamboni, S. Strychor, E. Joseph, D.R. Walsh, B.A. Zamboni, R.A. Parise, M.E. Tonda, N.Y. Yu, C. Engbers and J.L. Eiseman, Plasma, tumor, and tissue disposition of Stealth liposomal CKD-602 (S-CKD602) and nonliposomal CKD-602 in mice bearing A375 human melanoma xenografts, *Clin. Cancer Res.*, 2007, **13**, 7217-7223.
13. K.M. Laginha, S. Verwoert, G.J.R. Charrois and T.M. Allen, Determination of doxorubicin levels in whole tumor and tumor nuclei in murine breast cancer tumors, *Clin. Cancer Res.*, 2005, **11**, 6944-6949.
14. V. Garg and W.J. Jusko, Bioavailability and reversible metabolism of prednisone and prednisolone in man, *Biopharm. Drug Dispos.*, 1994, **15**, 163-172.
15. H. Möllmann, S. Balbach, G. Hochhaus, J. Barth and H. Derendorf, Pharmacokinetic-pharmacodynamic correlations of corticosteroids, in *Handbook of pharmacokinetic/ pharmacodynamic correlation*, eds. H. Derendorf and G. Hochhaus, CRC Press, Boca Raton, 1995, pp 323-361.

16. E.A.W. Smits, C.J.P. Smits and H. Vromans, The development of a method to quantify encapsulated and free prednisolone phosphate in liposomal formulations, *J. Pharm. Biomed. Anal.*, 2013, **75**, 47-54.
17. R. Anderson, A. Franch, M. Castell, F.J. Perez-Cano, R. Bräuer, D. Pohlers, M. Gajda, A.P. Siskos, T. Katsila, C. Tamvakopoulos, U. Rauchhaus, S. Panzner and R.W. Kinne, Liposomal encapsulation enhances and prolongs the anti-inflammatory effects of water-soluble dexamethasone phosphate in experimental adjuvant arthritis, *Arthritis Res. Ther.*, 2010, **12**, R147.
18. C. Baiocchi, M. Brussino, M. Pazzi, C. Medana, C. Marini and E. Genta, Separation and determination of synthetic corticosteroids in bovine liver by LC-ion-trap-MS-MS on porous graphite, *Chromatographia*, 2003, **58**, 11-14.
19. J. Chrusch, S. Lee, R. Fedeniuk and J.O. Boison, Determination of the performance characteristics of a new multi-residue method for non-steroidal anti-inflammatory drugs, corticosteroids and anabolic steroids in food animal tissues, *Food Addit. Contam., Part A*, 2008, **25**, 1482-1496.
20. R. Draisci, C. Marchiafava, L. Palleschi, P. Cammarata and S. Cavalli, Accelerated solvent extraction and liquid chromatography-tandem mass spectrometry quantitation of corticosteroid residues in bovine liver, *J. Chromatogr. B*, 2001, **753**, 217-223.
21. Á. Tölgyesi, V.K. Sharma, S. Fekete, D. Lukonics and J. Fekete, Simultaneous determination of eight corticosteroids in bovine tissues using liquid chromatography-tandem mass spectrometry, *J. Chromatogr. B*, 2012, **906**, 75-84.
22. O. Van den hauwe, J. Castro Perez, J. Claereboudt and C. Van Peteghem, Simultaneous determination of betamethasone and dexamethasone residues in bovine liver by liquid chromatography/tandem mass spectrocscopy, *Rapid Commun. Mass Spectrom.*, 2001, **15**, 857-861.
23. R. DiFrancesco, V. Frerichs, J. Donnelly, C. Hagler, J. Hochreiter and K.M. Tornatore, Simultaneous determination of cortisol, dexamethasone, methylprednisolone, prednisone, prednisolone, mycophenolic acid and mycophenolic acid glucuronide in human plasma utilizing liquid chromatography-tandem mass spectrometry, *J. Chromatogr. B*, 2007, **859**, 42-51.
24. E.N. Fung, Y.-Q. Xia, A.F. Aubry, J. Zeng, T. Olah and M. Jemal, Full-scan high resolution accurate mass spectrometry (HRMS) in regulated bioanalysis: LC-HRMS for the quantitation of prednisone and prednisolone in human plasma, *J. Chromatogr. B*, 2011, **879**, 2919-2927.
25. K. Hosseini, D. Matsushima, J. Johnson, G. Widera, K. Nyam, L. Kim, Y. Xu, Y. Yao and M. Cormier, Pharmacokinetic study of dexamethasone disodium phosphate using intravitreal, subconjunctival, and intravenous delivery routes in rabbits, *J. Ocul. Pharmacol. Ther.*, 2008, **24**, 301-308.
26. I.A. Ionita and F. Akhlaghi, Quantification of unbound prednisolone, prednisone, cortisol and cortisone in human plasma by ultrafiltration and direct injection into liquid chromatography tandem mass spectrometry, *Ann. Clin. Biochem.*, 2010, **47**, 350-357.
27. B.C. McWhinney, S.E. Briscoe, J.P.J. Ungerer and C.J. Pretorius, Measurement of cortisol, cortisone, prednisolone, dexamethasone and 11-deoxycortisol with ultra high performance liquid chromatography-tandem mass spectrometry: application for plasma, plasma ultrafiltrate, urine and saliva in a routine laboratory, *J. Chromatogr. B*, 2010, **878**, 2863-2869.
28. I.I. Salem, M. Alkhatib and N. Najib, LCMS/MS determination of betamethasone and its phosphate and acetate esters in human plasma after sample stabilization, *J. Pharm. Biomed. Anal.*, 2011, **56**, 983-991.
29. A. Tan, S. Hussain and F. Vallée, Evaporation-free extraction and application in high-throughput bioanalysis by LC-MS-MS, *LCGC North Am.*, 2009, **27**, 414-427.

30. A. Thomas, H. Geyer, W. Schänzer, C. Crone, M. Kellmann, T. Moehring and M. Thevis, Sensitive determination of prohibited drugs in dried blood spots (DBS) for doping controls by means of a benchtop quadrupole/Orbitrap mass spectrometer, *Anal. Bioanal. Chem.*, 2012, **403**, 1279-1289.
31. M.W.J. van Hout, C.M. Hofland, H.A.G. Niederländer, A.P. Bruins, R.A. de Zeeuw and G.J. de Jong, On-line coupling of solid-phase extraction with mass spectrometry for the analysis of biological samples: III. determination of prednisolone in serum, *J. Chromatogr. B*, 2003, **794**, 185-192.
32. M. Zhang, G.A. Moore, B.P. Jensen, E.J. Begg and P.A. Bird, Determination of dexamethasone and dexamethasone sodium phosphate in human plasma and cochlear perilymph by liquid chromatography/tandem mass spectrometry, *J. Chromatogr. B*, 2011, **879**, 17-24.
33. R. Melarange, P. Sadra, A. Harris, D. Clapham and J. Curtis, The use of Covaris adaptive focused acoustics in psychiatryCEDD DMPK, website Covaris®, http://covarisinc.com/wp-content/uploads/GSK_DMDG_2007.pdf, (last accessed June 2015).
34. M.H. Yeganeh and I. Ramzan, Determination of propofol in rat whole blood and plasma by high-performance liquid chromatography, *J. Chromatogr. B*, 1997, **691**, 478-482.
35. D.J.A. Crommelin and E.M.G. van Bommel, Stability of liposomes on storage: freeze dried, frozen or as an aqueous dispersion, *Pharm. Res.*, 1984, **1**, 159-163.
36. C.M. Moore and I.R. Tebbett, Rapid extraction of anti-inflammatory drugs in whole blood for HPLC analysis, *Forensic Sci. Int.*, 1987, **34**, 155-158.
37. R. Bellott, P. Pouna and J. Robert, Separation and determination of liposomal and non-liposomal daunorubicin from the plasma of patients treated with DaunoXome, *J. Chromatogr. B*, 2001, **757**, 257-267.
38. D.J.A. Crommelin and G. Storm, Liposomes: from the bench to the bed, *J. Liposome Res.*, 2003, **13**, 33-36.
39. R. Krishna, M.S. Webb, G. St. Onge and L.D. Mayer, Liposomal and nonliposomal drug pharmacokinetics after administration of liposome-encapsulated vincristine and their contribution to drug tissue distribution properties, *J. Pharmacol. Exp. Ther.*, 2001, **298**, 1206-1212.
40. V.A. Frerichs and K.M. Tornatore, Determination of the glucocorticoids prednisone, prednisolone, dexamethasone, and cortisol in human serum using liquid chromatography coupled to tandem mass spectrometry, *J. Chromatogr. B*, 2004, **802**, 329-338.
41. W.D. van Dongen and W.M.A. Niessen, LCMS systems for quantitative bioanalysis, *Bioanalysis*, 2012, **4**, 2391-2399.
42. J.T. Brandenburg, K. Kramer and J. van der Valk, Bloedafname en bloedonderzoek, in *Proefdierkunde: biotechnisch handboek*, ed. J.T. Brandenburg, Stichting Proefdierkundige Informatie, Oss, 2000, pp 395-407.
43. R.M. Schiffelers, J.M. Metselaar, A.P.C.A. Janssen, L. van Bloois, J. Cornelis, M.H.A.M. Fens, G. Molema and G. Storm, Liposome-encapsulated prednisolone phosphate inhibits tumor growth in mice, in J.M. Metselaar, *Liposomal targeting of glucocorticoids: a novel treatment approach for inflammatory disorders*, PhD thesis, Utrecht University, 2003, pp 91-105.

Chapter 6

The availability of drug by liposomal drug delivery

Individual kinetics and tissue distribution of encapsulated and released drug in mice after administration of PEGylated liposomal prednisolone phosphate

Evelien A.W. Smits, José A. Soetekouw, Ebel H.E. Pieters, Coen J.P. Smits, Nicolette de Wijs-Rot and Herman Vromans

This is an Accepted Manuscript of an article published by Springer Nature in *Investigational New Drugs* on *13 December 2018*, available online: *https://doi.org/10.1007/s10637-018-0708-4*.

ABSTRACT

Lately, the usefulness of liposomal drug delivery systems has been debated. To better understand the underlying pharmacokinetics of the targeted drug delivery by liposomes, individual encapsulated and non-encapsulated drug concentrations in blood, tumor, liver, spleen and kidneys were quantified after i.v. administration of liposomal prednisolone phosphate in mice. Kinetic analysis shows that the tumor influx of encapsulated drug is not dominant compared to the uptake by the other tissues. Further, from a quantitative point of view, the availability of non-encapsulated drug in the tumor tissue after liposomal delivery is not pronounced as compared to the other tissues studied. However, drug release in the tumor seems more extended than in the other tissues and the non-encapsulated drug concentration decreases more slowly in the tumor than in the liver and spleen. The spleen shows a high affinity for the uptake of encapsulated drug as well as the release of drug from the liposomes. Subsequently, released drug in the spleen, and possibly also in other tissues, is probably quickly redistributed towards the blood and other tissues. This also impairs the drug delivery effect of the liposomes. In contrast to the released drug in the central circulation, liver and spleen, the released drug concentration in the tumor remains at a fairly constant level likely due to the extended release kinetics from the liposomes. These extended release characteristics in the tumor most probably contribute to the beneficial effect. Nevertheless, it should be noted that larger released drug concentrations are formed in healthy tissues.

INTRODUCTION

Tumor targeting by liposomes has been considered a promise for quite a few decades now and can increase the therapeutic index [1,2]. Drug targeting to tumors by liposomes has been assumed to depend on the enhanced permeation and retention (EPR) effect [2-4]: due to their specific size the liposomes should not extravasate into healthy tissues and should avoid renal clearance, whereas wide fenestrations in the leaky tumor vasculature would allow the liposomes to permeate into the tumor tissue. In addition, the absence of well-functioning lymphatic drainage in the tumor should result in enhanced tumor retention. In this respect, a stealth coat of hydrophilic polymers like polyethylene glycol (PEG) is important to delay the uptake by the phagocytes of the mononuclear phagocyte system (MPS) and to attain a blood circulation time long enough for the nanoparticles to reach the tumor tissue.

Lately, however, the success of tumor targeted delivery by nanomedicines including liposomes and the corresponding EPR effect has been questioned [4-6]. One of the issues is that PEGylated liposomes still localize considerably in healthy tissues like the liver and the spleen [7-9]. It is also pointed out that efficacy and toxicity can only be related to the released, non-encapsulated drug and not to the drug that is still encapsulated in the liposomes. Hence, the availability of the released drug and the corresponding fate (i.e. retention, distribution, elimination) are as least as important as the behavior of the liposomal carrier.

To understand and improve the pharmacokinetics of targeted drug delivery by liposomes, the separate quantitation of the drug that is still encapsulated in the liposomes (further referred to as encapsulated drug) and the released drug is essential, since efficacy and toxicity can only be related to the level of the released drug as discussed above. While techniques, which use the different physicochemical properties of the liposome and the drug like charge, size and hydrophobicity, were useful for the separate quantification of encapsulated and released drug in plasma [10-16], these techniques are not suitable for the separate quantification in tissues. Homogenization is required prior to their application, which induces liposome rupture, release of encapsulated drug and, consequently, overestimations of the released drug concentration [17].

Laginha et al. defined a creative approach to approximate available, released doxorubicin levels in tumor tissue after intravenous administration of Doxil®: although the accuracy is uncertain, the cell nucleus acts like a sink for released doxorubicin and was used as a measure for the available drug concentration [18]. Alternatively, microdialysis can be applied to measure the non-protein-bound drug in tissue fluids only, through passive diffusion from the interstitial fluid across the semi-permeable membrane of the microdialysis catheter [19]. Also the measurement of the drug/lipid ratio can provide some insights in the *in vivo* release [20]. Unfortunately, the drug/lipid

ratio cannot differentiate between encapsulated drug and released drug that is still present in the tissue [21], but the released drug in the tissue is what should be known as discussed above. Without devaluing the aforementioned methods, the encapsulation of a phosphate prodrug like prednisolone phosphate (PP) into liposomes does enable the direct and accurate quantification of encapsulated and released drug in tissues [22-24] as follows. The differentiation of encapsulated and released drug is attained by the rapid dephosphorylation of PP *in vivo* [22,25,26]. The conversion of PP into prednisolone (P) after release from the liposome in whole blood [27] and various tissues, i.e. liver and kidneys [23], is determined to be instantaneously. Phosphatases are also overexpressed in tumor microenvironments [28]. Moreover, it is strongly believed that after liposome uptake by macrophages, the encapsulated drug is liberated in the endosomal/lysosomal compartment and hydrolyzed into P [29-31], because phosphatases are also present in macrophages and lysosomes [32]. Thus, it is assumed that PP is rapidly converted into P after release. Consequently, the *in vivo* PP concentration represents the encapsulated drug concentration and the *in vivo* P concentration represents the released drug concentration [22,23,27]. N.b. PEGylated liposomes containing PP showed to reduce the tumor growth in mice in contradiction to the free drug formulation [9].

To our knowledge, accurate released drug concentrations in solid tumors have rarely been compared to such concentrations in healthy tissues until now. From an efficacy/toxicity point of view, this is very essential as discussed above. Therefore, in this study, PEGylated liposomal PP was used as a model formulation in mice to quantify the encapsulated and released drug concentrations in the tumor tissue as well as in whole blood, liver, spleen and kidneys, for which previously large liposome concentrations were observed [9,33]. To further understand the pharmacokinetics, the *in vivo* tissue influx of encapsulated drug and the *in vivo* drug release from the liposomes are calculated for each of the tissues separately using kinetic modelling. The results provide quantitative data of the pharmacokinetics of liposomal targeted drug delivery and demonstrate the quantitative availability of the released drug in different tissues.

MATERIALS AND METHODS

Materials

All materials were used as received. Dipalmitoylphosphatidylcholine (DPPC) and PEG2000-distearoylphosphatidylethanolamine (PEG2000-DSPE) were purchased from Lipoid GmbH (Ludwigshafen, Germany). Alkaline phosphatase from rabbit intestine, cholesterol, dexamethasone (D), dexamethasone disodium phosphate and prednisolone were purchased from Sigma (St. Louis, MO, USA). Prednisolone disodium phosphate was purchased from Bufa (IJsselstein, The Netherlands). Methanol HPLC gradient grade,

which was used during sample preparation, was purchased from Mallinckrodt Baker BV (Deventer, The Netherlands).

Liposome preparation and characterization

PEGylated liposomes encapsulating prednisolone phosphate were prepared using the film-extrusion method as described by Metselaar et al. starting from a mixture of DPPC, cholesterol and PEG2000-DSPE in a molar ratio of 1.85:1.0:0.15, respectively [22].

During liposome characterization total, encapsulated and non-encapsulated PP concentrations in the liposome preparation were determined using a previously developed method [34], in which the non-encapsulated PP was distinguished from the encapsulated PP by dephosphorylation into P using alkaline phosphatase. Mean liposome sizes were determined by dynamic light scattering as also described previously [34].

Murine tumor model

Male C57BL/6J (15 mice; 20-25 g) were obtained from Charles River (The Netherlands). The mice were kept in standard housing with standard rodent chow and water available *ad libitum* on a 12 h light/dark cycle. Experiments were performed according to all applicable international, national, and/or institutional guidelines and were approved by the animal experiment committee of Utrecht University. For tumor induction, 1×10^6 murine B16F10 melanoma cells were inoculated subcutaneously in the flank of the mice. Tumor size was monitored manually and the tumor volume (V_T) was calculated by applying Equation (1):

$$V_T = 0.5 \times a^2 \times b \quad (1)$$

where a is the smallest diameter and b is the largest diameter.

Medication and sampling

At a tumor volume of $3 \times 10^2 \pm 1.5 \times 10^2$ mm^3, 14 mice received 36 µmol/kg PP (= 18 mg/kg of prednisolone disodium phosphate) by tail vein injection of liposomal PP. One mouse was not administered with liposomal PP and served as control. At distinct time intervals after injection blood was sampled (~200 µL) via cheek puncture into ethylenediaminetetraacetic acid (EDTA) containing tubes. Subsequently, the specific animal was sacrificed by cervical dislocation and tumor, liver, spleen and kidneys were dissected. The tissues were weighted and all samples were stored at -20°C to prevent significant dephosphorylation of PP after sampling.

Analytical methodology

The collected blood and tissue samples were processed and analyzed according to previously developed and validated methodology for the quantitative differentiation of encapsulated PP and released P in murine whole blood and liver tissue [27,35]. The suitability of this methodology for tumor, kidney and splenic tissue was verified by qualification (internal study similar to the validation as described by Smits et al. [35]). As discussed in the introduction, the encapsulation of a phosphate prodrug like PP into liposomes enables the direct and accurate quantification of encapsulated and released drug in tissues: as long as the compound is encapsulated it is assessed as a phosphate. When released in the tissue, conversion to the parent steroid is so quick that the level of this compound can be regarded as the amount of released drug.

To summarize above methodology, blood samples were removed from the freezer and thawed for 30 min only prior to sample preparation, whereas tissue samples were processed while still frozen. In this way significant dephosphorylation of PP after sampling and, consequently, significant overestimations of the released drug concentration are prevented. Hereafter, the sample preparation of whole blood samples involved protein precipitation with four equivalents of methanol containing the internal standards D and dexamethasone phosphate (DP). To do so, 100 µL of the blood samples were used. Tissue samples were homogenized in 10 mL methanol/g tissue and again the methanol contained the internal standards. The use of such amounts of methanol ensures complete liposome rupture and prevents dephosphorylation of PP that is released during sample preparation. After the samples were treated with high-intensity focused ultrasound to disrupt the cell membranes, PP and P concentrations were measured by LC-MS analysis. The used chromatographic conditions were as described by Smits et al. [35]. Comprehensive liquid chromatography together with negative electrospray ionization, in-source fragmentation of P and D and high-resolution accurate mass Orbitrap-MS analysis was used to avoid the significant interference by (biological) impurities from the complex matrix during PP and P detection. The selectivity, sensitivity and quantitative accuracy of the methodology is sufficient for the quantification of PP and P in murine blood, liver, tumor, spleen and kidneys. Peak areas of co-eluting impurities in blank samples are <20% for PP and P and <5% for DP and D compared to the lowest peak areas in calibration standards and quality control (QC) samples. The quantitative accuracy of the methodology within the used range is 80-120%.

The tumor calibration standards served also as QC samples and were prepared by using the tumor from the control mouse. Note, all calibration standards were prepared using non-encapsulated PP instead of liposomal PP in favor of the precision.

Data analysis and statistics

Correction of PP and P tissue concentrations for residual blood

The PP and P tissue concentrations that were measured by LC-MS were corrected for the PP and P in the residual blood. Because a large part of the blood in the dissected tissues is already gone after euthanasia, the literature values according to Brown et al. do not apply [36]. Since the observed large blood concentrations especially with regard to the encapsulated concentrations (see the section "Results") can yield overestimations, the tissue concentrations were corrected as follows. At five minutes after i.v. administration (0.08 h), PEGylated liposomes are assumed to be homogenously distributed over the circulation but are also assumed still to be located in the circulation only. This is supported by the observation that the distribution volume of prednisolone phosphate in PEGylated liposomes is close to the plasma volume in rats and humans with arthritis [22, 30]. For PEGylated liposomal doxorubicin similar results were found [7].

Using the above assumptions, the volume fraction of residual blood (*VFB*) was calculated for each tissue of interest by applying Equation (2):

$$VFB = \frac{\text{measured } C(0.08)_{PPX}}{C(0.08)_{PPB}} \tag{2}$$

where "measured $C(0.08)_{PPX}$" is the uncorrected encapsulated PP concentration as measured by LC-MS in the tissue "X" at $t = 0.08$ h, and where $C(0.08)_{PPB}$ is the encapsulated PP blood concentration at $t = 0.08$ h. Then, the measured PP and P tissue concentrations were corrected for the PP and P in the residual blood by applying Equation (3) for each time *t*:

$$C_{P(P)X} = \frac{\text{measured } C_{P(P)X} - C_{P(P)B} \times VFB}{(1 - VFB)} \tag{3}$$

where $C_{P(P)X}$ is the corrected PP or P tissue concentration at time *t*, "measured $C_{P(P)X}$" is the uncorrected PP or P concentration as measured by LC-MS in the tissue "X" at time *t*, and $C_{P(P)B}$ is the corresponding PP or P blood concentration at time *t*.

Whole blood and tissue densities are assumed to be 1 g/mL.

Outliers

Data derived from two subjects for which an extremely poor total drug recovery was observed were considered to be outliers and were excluded. For these subjects the recovery was a factor 3-22 lower compared to adjacent subjects when plotted versus time. Most likely, the animals were injected incorrectly. Injection in the tail vein is

a delicate exercise because of the small size. Except for these two, no outliers were removed.

The tumor tissue dissected at $t = 16.5$ h was lost during sample preparation. Therefore, the corresponding tumor concentration is lacking.

Regression of encapsulated PP and released P concentrations

The encapsulated PP and released P blood concentrations were fitted by least squares non-linear regression with a 95% confidence interval using Equations (4) and (5) (Minitab 17 Statistical Software, Minitab Inc., State College, PA, USA), which describe straightforward first-order kinetics:

$$C_{PPB}(t) = C_{PPB}(0) \times e^{-k_{PPB} \times t} \tag{4}$$

$$C_{PB}(t) = C_{PB}(0) \times e^{-k_{PB} \times t} \tag{5}$$

where $C_{PPB}(t)$ and $C_{PB}(t)$ are the encapsulated PP and released P blood concentration at time t, $C_{PPB}(0)$ and $C_{PB}(0)$ are the pseudo initial encapsulated PP and released P concentrations, and k_{PPB} and k_{PB} are the first-order decline rate constants for encapsulated PP and released P in blood, respectively. Normality of the residuals was verified ($p > 0.05$).

The encapsulated PP concentrations in the tissues of interest were fitted as follows. First, differential equations describing the kinetics of encapsulated PP in tissue "X" were generated. The influx of encapsulated PP from the blood is assumed to be a first-order process, whereas the decline of encapsulated PP in the tissue is assumed to be a zero-order (Equation (6)) or first-order (Equation (7)) process:

$$\frac{d[m_X \times C_{PPX}(t)]}{dt} = k_{PPBX} \times V_{DPP} \times C_{PPB}(t) - R_{PPX} \tag{6}$$

$$\frac{d[m_X \times C_{PPX}(t)]}{dt} = k_{PPBX} \times V_{DPP} \times C_{PPB}(t) - k_{PPX} \times m_X \times C_{PPX}(t) \tag{7}$$

where C_{PPX} is the encapsulated PP concentration in the tissue, m_x is the mass of the tissue corrected for the mass of the residual blood by: m_x = "mass uncorrected" × (1−*VFB*), k_{PPBX} is the first-order rate constant corresponding to the influx of encapsulated PP from the blood, V_{DPP} is the volume of distribution of encapsulated PP, R_{PPX} is the zero-order decline rate constant and k_{PPX} is the first-order decline rate constant. These differential equations were solved over time t yielding the following equations:

$$C_{PPX}(t) = \frac{k_{PPBX}}{k_{PPB}} \times \frac{V_{DPP}}{m_X} \times C_{PPB}(0) \times (1 - e^{-k_{PPB} \times t}) - \frac{1}{m_X} \times R_{PPX} \times t \tag{8}$$

$$C_{PPX}(t) = \frac{k_{PPBX}}{k_{PPX} - k_{PPB}} \times \frac{V_{DPP}}{m_X} \times C_{PPB}(t) - \frac{k_{PPBX}}{k_{PPX} - k_{PPB}} \times \frac{V_{DPP}}{m_X} \times C_{PPB}(0) \times e^{-k_{PPX} \times t} \tag{9}$$

However, as is discussed in the supplementary material (see Appendix A.2), the encapsulated PP tumor kinetics is better described by the following differential equations expressing the change of the encapsulated PP tumor concentration with time:

$$\frac{dC_{PPT}(t)}{dt} = k_{PPBT} \times C_{PPB}(t) - R_{PPT} \tag{10}$$

$$\frac{dC_{PPT}(t)}{dt} = k_{PPBT} \times C_{PPB}(t) - k_{PPT} \times C_{PPT}(t) \tag{11}$$

These differential equations were solved over time t yielding the following equations:

$$C_{PPT}(t) = \frac{k_{PPBT}}{k_{PPB}} \times C_{PPB}(0) \times (1 - e^{-k_{PPB} \times t}) - R_{PPT} \times t \tag{12}$$

$$C_{PPT}(t) = \frac{k_{PPBT}}{k_{PPT} - k_{PPB}} \times C_{PPB}(t) - \frac{k_{PPBT}}{k_{PPT} - k_{PPB}} \times C_{PPB}(0) \times e^{-k_{PPT} \times t} \tag{13}$$

Then, the encapsulated PP concentrations in the tissues of interest were fitted using least squares non-linear regression with a 95% confidence interval using Equations (8) and (9) or (12) and (13). If necessary, statistical weights were included to correct for an unequal distribution of data points. Further, the normality of the residuals was verified (p >0.05) and the curve fit with the smallest S-value (standard error of the regression) was preferred.

Differences between the curve fits of encapsulated PP were accepted to be statistically significant when there was no overlap of the corresponding 95% confidence intervals. Significant differences between the released P concentrations were evaluated using linear regression of the released P concentrations in blood or the specific tissue as a function of the released P concentrations in the (other) tissues.

Calculation of tissue influx

The rate of encapsulated PP tissue influx (nmol/h) is described by Equations (14) and (15), which are in line with Equations (7) and (11), respectively:

$$\text{encapsulated PP liver/spleen/kidney influx} = k_{PPBX} \times V_{DPP} \times C_{PPB}(t) \tag{14}$$

$$\text{encapsulated PP tumor influx} = k_{PPBT} \times m_T \times C_{PPB}(t) \tag{15}$$

For comparison between the different tissues, the rate of influx was also expressed per gram of tissue by Equations (16) and (17):

$$\text{encapsulated PP influx per gram of liver/spleen/kidneys} = \frac{k_{PPBX} \times V_{DPP} \times C_{PPB}(t)}{m_X} \tag{16}$$

encapsulated PP tumor influx per gram of tissue = $k_{PPBT} \times C_{PPB}(t)$ (17)

Subsequently, the influx rates per tissue were calculated using Equations (4) and (14) or (15), and the influx rates per gram of tissue were calculated using Equations (4) and (16) or (17). The resulting rates were plotted versus time.

Differences between the rate of tissue influx or the rate of influx per gram of tissue for the various tissues were considered significant when there was no overlay between the $[(k_{PPBX} \pm SE) \times (V_{DPP} \text{ or } m_T \pm SD)]$ intervals or $\frac{[(k_{PPBX} \pm SE) \times (V_{DPP} \text{ or } m_T \pm SD)]}{m_X \pm SD}$ intervals, respectively, of two tissues. *SE* is the estimated standard error and *SD* is the estimated standard deviation.

Calculation of the rate of release

Similarly, the rate of release of drug from the liposomes in the tissues of interest was determined as follows. A schematic representation of the kinetics of the drug when still encapsulated in a tissue "X" is shown in Figure 1 and can roughly be divided into three processes: (1) influx of encapsulated PP from the blood into the tissue (k_{PPBX}), (2) release of prednisolone phosphate from the liposomes (k_{relX}), and (3) transfer of encapsulated PP from the tissue towards the blood (k_{PPXB}). The accumulation of liposomes in tumor tissue is supposed to be unidirectional [3], because the lymphatic drainage in tumor tissue is highly reduced, which limits the clearance of the liposomes from the tumor and which improves liposomal tumor retention [4, 37]. Therefore, the transfer of encapsulated PP from the tumor to the blood (k_{PPTB}) is assumed to be negligible. Furthermore, liposomes containing PP localize in phagocytes of the liver and spleen as observed by Schmidt et al. for a rat model of multiple sclerosis [38,39]. And, while encapsulated PP is expected to be too large to be excreted by glomerular filtration [40], drug delivery systems with a diameter of about 75 ± 25 nm are believed to target the mesangial cells [40,41]. Consequently, due to the digestic nature of these cells, it is likely that the fate of the majority of the liposomes ends in these phagocytes [29]. Therefore, in this study, the encapsulated PP is also expected to disappear from the liver, spleen and kidneys principally through drug release from the liposomes and the transfer of encapsulated PP from these tissues towards the blood is also assumed to be negligible. Thus, for the tissues of interest k_{PPX} is assumed to equal k_{relX}.

The release of drug from liposomes in these tissues can be better described by a first-order process (see the section "Results") and, therefore, the rate of release (nmol/h) is described by Equation (18), which is in line with Equation (7) or (11):

rate of release = $k_{relX} \times m_X \times C_{PPX}(t)$ (18)

For comparison between the different tissues, the rate of release was also expressed per gram of tissue by the following equation:

$$\text{rate of release per gram of tissue} = k_{relX} \times C_{PPX}(t) \quad (19)$$

Hereafter, the rates of release per tissue were calculated using Equations (9) or (13) and (18), whereas the rates of release per gram of tissue were calculated using Equations (9) or (13) and (19). The resulting rates were plotted versus time.

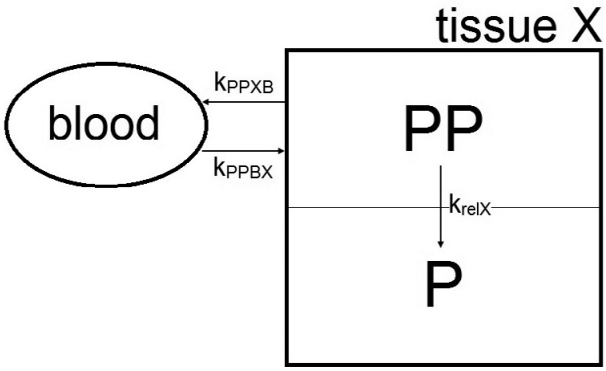

Figure 1: Basic representation of the kinetics of the drug when still encapsulated,
where k_{PPBX} is the rate constant corresponding to the influx of encapsulated PP from the blood, PP is released from the liposomes according to the rate constant k_{relX}, and k_{PPXB} represents the rate constant corresponding to the transfer of encapsulated PP to the blood. The transfer of encapsulated PP towards the blood is assumed to be negligible for all tissues studied (see the section "Calculation of the rate of release"). The subsequent kinetics of the released drug is not included in the figure.

RESULTS

Liposome characteristics

The liposome preparation used for i.v. administration contained 7.18 ± 0.06 mmol PP/L, of which 4.4 ± 0.3% was present as non-encapsulated drug. The presence of a minor non-encapsulated drug amount in liposome preparations is common [13,14,42]. After self-assembly of the liposomes, the non-encapsulated drug was removed by dialysis leaving a small amount of non-encapsulated drug in the preparation. The liposome diameter determined by dynamic light scattering was 97 ± 30 nm. The dispersity was 0.077 indicating that the liposome preparation is monodisperse. The phospholipid content was 60 mM [22]. Due to the PEGylation and the small size these liposomes are optimized for delaying uptake by the organs of the MPS [22].

Encapsulated PP and released P in the circulation

The encapsulated PP and released P blood concentrations after i.v. administration of liposomal PP are shown in Figure 2. The decline of the encapsulated PP as well as the released P concentration with time show first-order kinetics (the residuals are distributed normally: $p > 0.05$). The corresponding kinetic parameters are summarized in Table 1. The calculated half-life of encapsulated PP and released P in the circulation are 26 h and 39 h, respectively. Similar results were observed previously in the plasma of rats with adjuvant arthritis after i.v. administration of 5 mg/kg PEGylated liposomal PP (≈ 10 µmol/kg) [22].

Table 1: Kinetic parameters and the corresponding estimated standard error (*SE*) or estimated standard deviation (*SD*) for liposomal PP in male C57BL/6J mice bearing B16F10 melanoma tumors

		SE estimate	*SD* estimate
$C_{PPB}(0)$	4.0×10^2 nmol/mL	3×10^1 nmol/mL	
k_{PPB}	0.027 h^{-1}	0.004 h^{-1}	
$C_{PB}(0)$[a]	15 nmol/mL	2 nmol/mL	
k_{PB}	0.018 h^{-1}	0.004 h^{-1}	
V_{DPP}[b]	2.2 mL		
k_{PPBT}	0.004 mL/g/h	0.001 h^{-1}	
k_{relT}	0.03 h^{-1}	0.01 h^{-1}	
m_T[c]	0.9 g		0.4 g
k_{PPBL}	0.005 h^{-1}	0.002 h^{-1}	
k_{relL}	0.3 h^{-1}	0.1 h^{-1}	
m_L[d]	$= a \times t^2 + b \times t + c$	g	
a	-0.00047	0.00005	
b	0.030	0.004	
c	1.22	0.05	
k_{PPBS}	0.0033 h^{-1}	0.0009 h^{-1}	
k_{relS}	0.7 h^{-1}	0.1 h^{-1}	
m_S	0.06 g		0.02 g
k_{PPBK}	0.0007 h^{-1}	0.0001 h^{-1}	
k_{relK}	0.10 h^{-1}	0.02 h^{-1}	
m_K	0.25 g		0.02 g

[a] $\frac{C_{PB}(0)}{C_{PPB}(0) + C_{PB}(0)} \times 100\% = 3.5\%$, which is similar to the 4.4% non-encapsulated drug in the liposome preparation considering the *SE*

[b] Calculated from Figure 2 and the dose

[c] No significant trend was observed for the mass of the tumor tissue with time. Quadratic regression of the tumor mass is not significant ($p = 0.15$)

[d] The mass of the liver varies with time. During the time frame for which the encapsulated PP concentrations are above the lower limit of quantification, the data is significantly not constant and is adequately described by a parabola (*p*-values: 0.000)

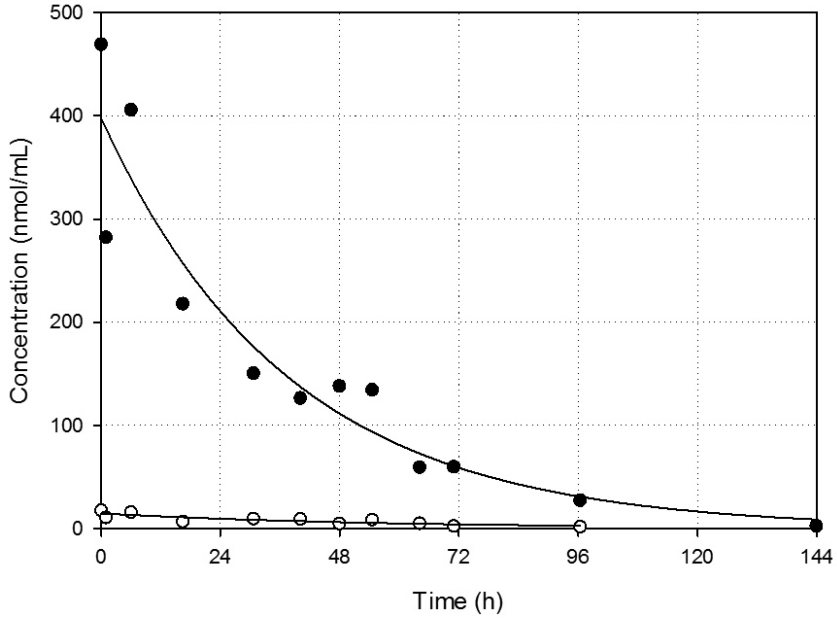

Figure 2: Individual blood concentrations of encapsulated PP (closed circles) and released P (open circles) with time after i.v. administration of 36 µmol/kg liposomal PP

The corresponding curve fits resulting from non-linear regression using Equations (4) and (5) are also plotted. The corresponding kinetic parameters are summarized in Table 1.

Encapsulated PP and released P tissue concentrations

The measured encapsulated PP and released P tissue concentrations were corrected for the drug located in the residual blood of the dissected tissues as described above. The resulting encapsulated PP and released P tissue concentrations are shown in Figure 3.

Curve fits of the encapsulated PP tissue concentrations according to Equations (9) and (13), which contain a first-order rate of drug release, are shown in Figure. 4. The corresponding values for the kinetic parameters are summarized in Table 1. For all tissues, the encapsulated PP concentration is better described using a first-order drug release (*S*-values 0.8-5.5) than by zero-order release (*S*-values 1.9-13.3). The corresponding residuals are distributed normally ($p > 0.05$). The largest encapsulated PP concentrations are observed in the spleen, for which the peak concentration is significantly larger than for tumor, liver and kidneys. The smallest encapsulated PP concentrations are observed in the liver, while the encapsulated PP tumor and kidney concentrations are in-between. These results are in line with the tissue distribution of ^{111}In-labeled liposomes at 6 and 24 h after intravenous administration in B16F10 tumor-bearing C57BL/6 mice [9].

The released P blood and tissue concentrations are compared in Figure 5. Released P is observed in whole blood as well as in all tissues of interest. The released P peak concentration at t = 6 h is significantly larger in the spleen than in the blood and the

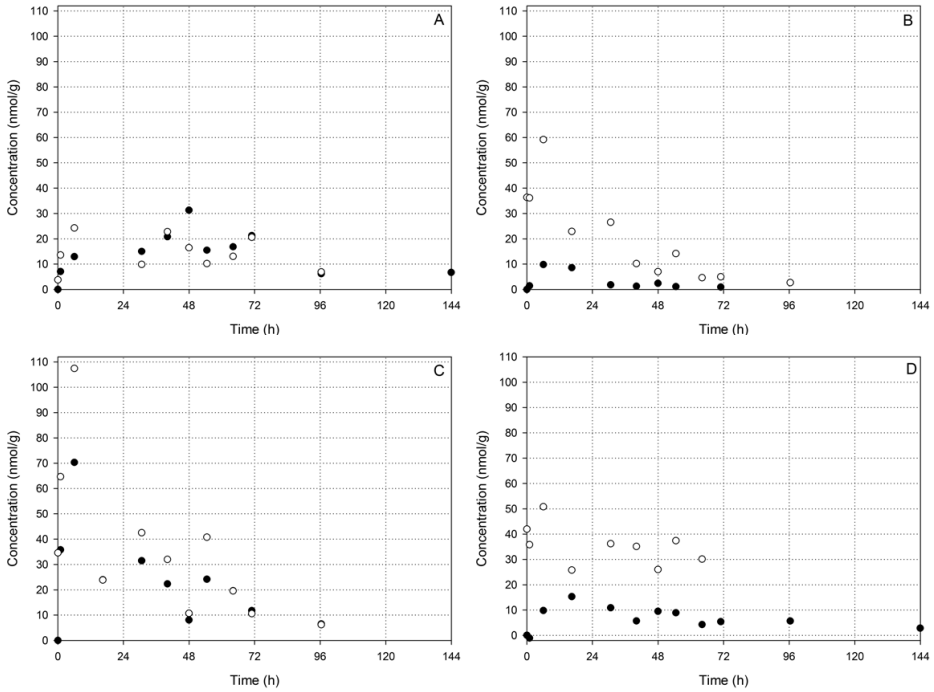

Figure 3: Individual concentrations of encapsulated PP (closed circles) and released P (open circles) with time in tumor (a), liver (b), spleen (c), and kidneys (d) after i.v. administration of 36 µmol/kg liposomal PP

other tissues. Although it was not compared to tumor tissue, similar results were observed for hydrolyzed drug in liver, spleen and kidneys after administration of liposomal 4-methylumbelliferyl phosphate in mice [24]. The concentration in the tumor at t = 6 h is significantly smaller than the peak concentrations in the liver, spleen and kidneys. A significant difference between the concentrations in the tumor and blood at t = 6 h was not observed. However, the released P concentration is decreasing slower in the tumor than in the liver and spleen. At t = 96 h, the released P tumor concentration is no longer smaller than the released P concentration in the spleen and it is significantly larger than in the blood and liver.

Tissue influx of encapsulated PP

Non-linear regression of the encapsulated PP tissue concentrations showed that the tissue influx of encapsulated PP can be well described by a first-order kinetic process for all tissues. The resulting kinetic parameters (see Table 1) were then used to model the rate of encapsulated PP tissue influx for each tissue, which is shown in Figure 6. Although there seems to be a difference in rate of encapsulated PP tissue influx (see Figure 6a), not

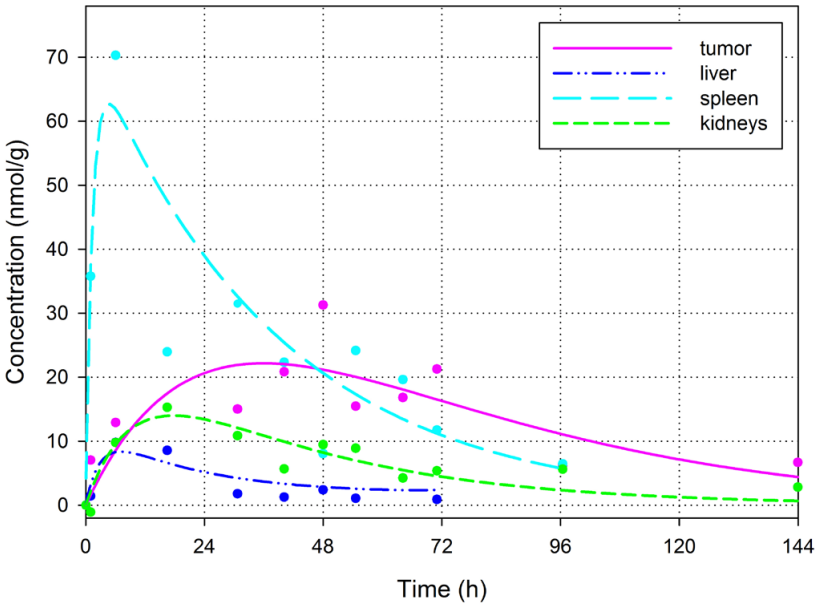

Figure 4: Non-linear regression of the encapsulated PP concentrations in tumor (purple; solid line), liver (dark blue; dash-dot-dot), spleen (cyan; long dash) and kidneys (green; short dash) according to Equations (9) and (13) describing a first-order drug release

The corresponding values for the kinetic parameters are summarized in Table 1.

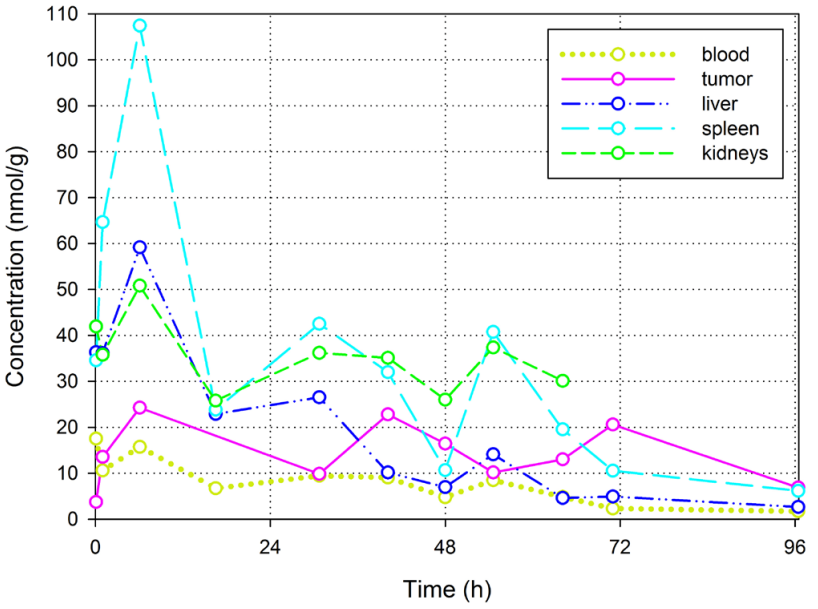

Figure 5: Released P concentrations in whole blood (lime; dotted line), tumor (purple; solid line), liver (dark blue; dash-dot-dot), spleen (cyan; long dash) and kidneys (green; short dash)

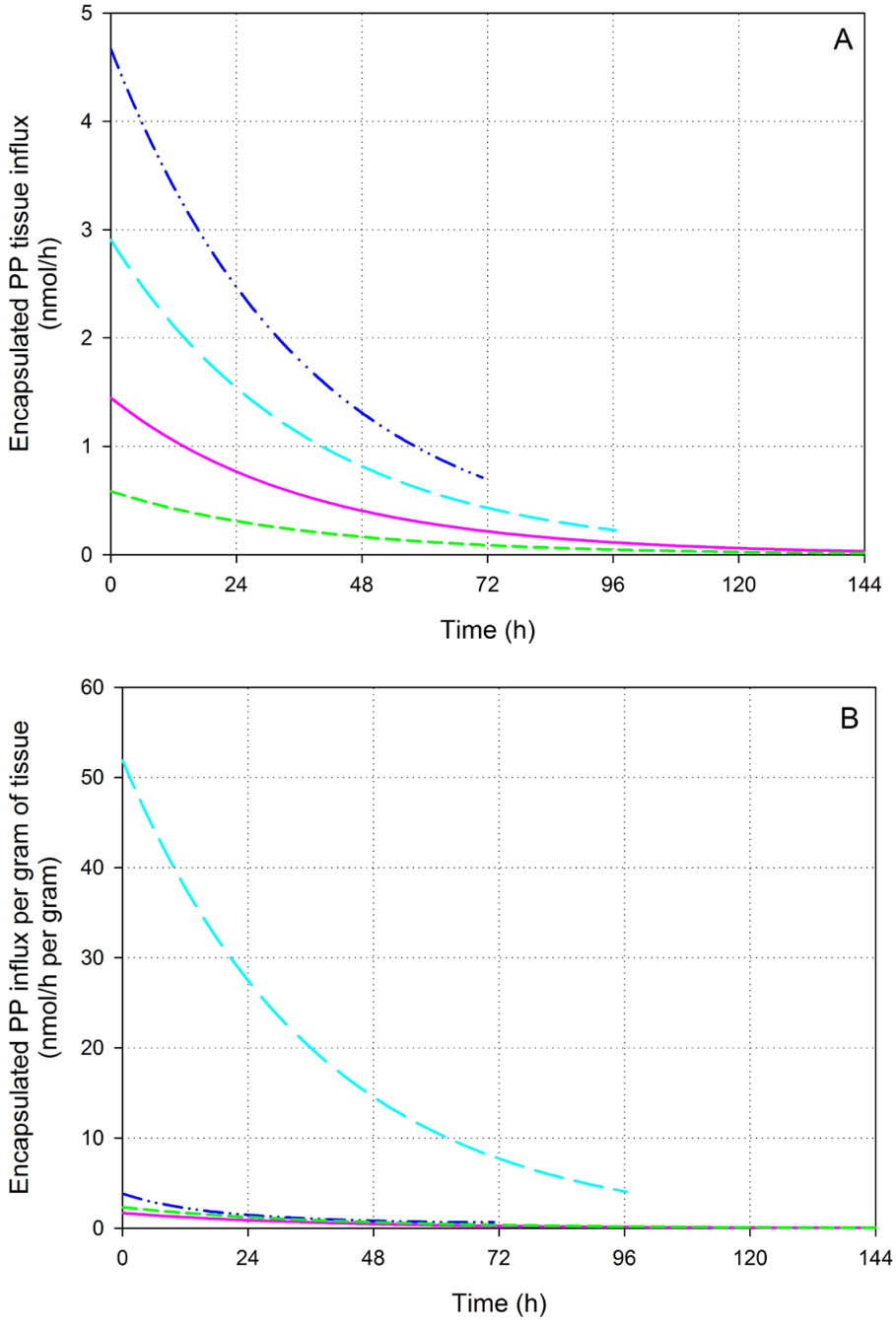

Figure 6: Calculated rate of tissue influx (a) and calculated rate of influx per gram of tissue (b) for encapsulated PP in tumor (purple; solid line), liver (dark blue; dash-dot-dot), spleen (cyan; long dash) and kidneys (green; short dash) by kinetic modelling

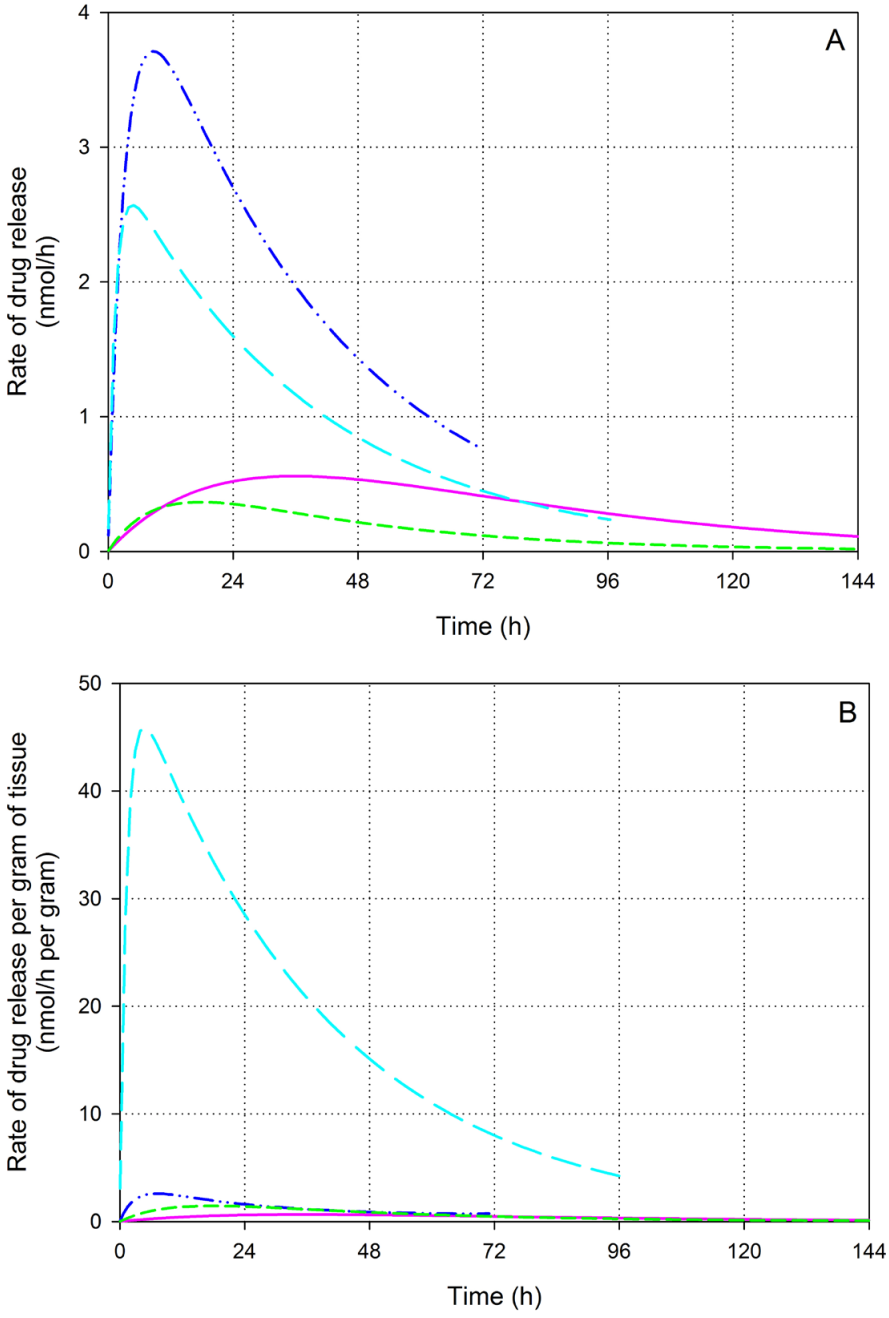

Figure 7: Calculated rate of drug release from liposomes per tissue (a) and calculated rate of drug release from liposomes per gram of tissue (b) in tumor (purple; solid line), liver (dark blue; dash-dot-dot), spleen (cyan; long dash) and kidneys (green; short dash) by kinetic modelling

Note, the rates of release are not normalized by the quantities of encapsulated PP present.

all of them are significant probably due to the relatively large *SD* of the tumor mass (see Table 1). Large *SD* of the pre- and posttreatment tumor size were observed previously [9, 43]. No significant differences were observed for the influx towards the tumor as compared to the influx towards the liver, spleen and kidneys. Significant differences were observed for the smaller influx towards the kidneys as compared to the liver and spleen.

However, when observing the influx rate per gram of tissue a high preference of encapsulated PP for the splenic tissue becomes clear (see Figure 6b). While no significant differences were observed between the encapsulated PP influx per gram of tumor, liver and kidneys, the significantly larger influx per gram of spleen is obvious.

Drug release from the liposomes

As described above, the release of drug out of the liposomes can be better described by a first-order kinetic process for all tissues. The corresponding kinetic parameters were used to model the rate of drug release from the liposomes as shown in Figure 7. The rate of drug release from the liposomes in the tumor seems smaller but more extended as compared to the liver and spleen (see Figure 7a). The extremely large capacity of the splenic tissue to release the drug becomes clear from the rate of drug release per gram of tissue shown in Figure 7b: the maximal calculated rate of release per gram of spleen is about 74 × the maximal rate in tumor, about 17 × the maximal rate in liver and about 28 × the maximal rate in the kidneys.

DISCUSSION

Extravasation of encapsulated PP towards the tumor versus the uptake by healthy tissues

Tissue concentrations of liposomes as well as the encapsulated drug depend on (1) the tissue influx and (2) the loss of the carrier or release of the encapsulated drug, respectively, in the tissue. Therefore, the tissue influx is considered a measure for the affinity of liposomes for a specific tissue. Here, the tissue influx of encapsulated PP is compared for the different tissues of interest. The encapsulated PP influx towards the tumor differs not significantly from the influx towards the liver, spleen and kidneys (as discussed above with regard to Figure 6). Hence, the extravasation towards the tumor is in the same order of magnitude as the uptake by the other organs. An exception to this is the uptake per gram of spleen, which is significantly more pronounced. Since liposomal PP localizes in the macrophages of the liver and spleen [38,39], probably, the uptake of liposomal PP by liver and spleen occurs mainly through uptake by tissue macrophages. Likely, although the liposomes are PEGylated, uptake by macrophages is still prominent. This is because PEGylation only slows down MPS uptake and does not avoid MPS uptake [4].

Figure 6b shows the high preference of encapsulated PP for the splenic tissue. Besides the larger macrophage density in the spleen as compared to most other tissues like the liver [44,45], this is most probably due to the characteristics of the spleen. The spleen provides an enormous contact surface area and is able to reduce the blood flow yielding low shear rates of the liposomes, increased retention of the particles and prolonged contact with the macrophages [45].

Drug targeting by liposomes

As discussed before, efficacy and toxicity are not determined by the liposomal concentration. Only released drug may induce efficacy/toxicity. Most probably, after uptake of liposomes by macrophages, PP is liberated in the endosomal/lysosomal compartment where it is dephosphorylated into P [29,30]. Because of the previous observed efficacy [9,29] and because P can easily pass membranes [46], it is assumed that the released P is not trapped in the lysosome, but can be available intra- and possibly also extracellularly [31]. Hence, the released P tissue concentrations shown in Figures 3 and 5 are a measure of drug targeting. Note that, from a quantitative point of view, tumor targeting by released P is not more pronounced than the targeting of the liver, spleen and kidneys. The released P peak concentration at $t = 6$ h is even significantly smaller in the tumor than in the liver, spleen and kidneys. However, the released P concentration in the tumor tissue is more persistent compared to liver and spleen.

The released P tissue concentrations are a result of the liposomal tissue influx, the subsequent drug release out of the liposomes and the subsequent fate of the released P (i.e. retention, distribution, metabolism, excretion). The rate of drug release from the liposomes in the tumor seems smaller but more extended than in the liver and spleen (see Figure 7), which is in accordance with the more persistent released P tumor concentrations observed. Possibly, this is due to (1) a smaller amount of macrophages in the tumor as compared to the liver and spleen, (2) different types in the tumor macrophage population as compared to the liver and spleen, and/or (3) the difficult accessibility of macrophages in distant areas of the tumor tissue. An extremely large rate of release is calculated per gram of spleen (see Figure 7b). However, the released P spleen concentrations remain relatively small considering this extremely large release rate. Either P is rapidly metabolized in the spleen, and/or, more probably, the released P distributes quickly out of the spleen, which is to expect from a compound like P exhibiting biopharmaceutical properties to pass membranes [46].

In fact, a rapid redistribution of released P is expected in general and it would explain the observed P concentrations in the blood as shown in Figure 2 as hypothesized previously by Schiffelers et al. [9,22]. As discussed above, about 4% of the drug in the liposome preparation was not encapsulated. Since the half-life of P in mice is short, i.e. 16 min after i.v. administration of 10 μmol/kg in female BALB/c mice (internal study),

P originating from the non-encapsulated drug amount in the liposome preparation leaves the circulation quickly within a couple of hours. In contrast, the netto P blood concentration after liposomal PP administration is decreasing more gradually yielding a pseudo half-life of 39 h. Such P concentrations were also observed in the plasma (max 0.9% of the sum total concentration) after i.v. administration of 5 mg/kg liposomal PP (≈ 10 µmol/kg) in rats with adjuvant arthritis [22] and can be explained as follows. Since liposomal PP is probably stable in the circulation [22], it suggests that P is introduced to the circulation by redistribution of released P from spleen and other tissues for multiple days. This is supported by the relatively large and persistent P concentrations in the kidneys in comparison to the calculated drug release per gram of kidneys. Basically, it reveals a mechanism of sustained release for liposomal PP.

P itself exhibits non-linear pharmacokinetics in plasma mainly due to its non-linear protein binding but also due to reversible metabolism between P and prednisone [26,47,48]. P is predominantly metabolized to the inactive metabolite and prodrug prednisone in the liver [48,49,50] and to some extend in other organs such as the kidneys [51]. In addition, other phase 1 metabolites of P are formed, e.g. 20β-hydroxyprednisone, 6β-, 20α- and 20β-hydroxyprednisolone [52,53], which are conjugated or not conjugated [54], and rapidly excreted via the kidneys together with a considerable amount of unchanged prednisolone. Metabolism of P (after PP release from the liposomes and conversion to P) was out of the scope of this study.

CONCLUSIONS

To our knowledge, accurately measured released drug concentrations in solid tumors and in healthy tissues have not been compared after administration of liposome formulations. Combined with kinetic analysis, it provides important insights into the pharmacokinetics of liposomal drug delivery systems.

The calculated rate of tumor influx of encapsulated PP appears not to be significantly larger compared to that for the other tissues. Subsequently, the rate of drug release from the liposomes seems not larger in the tumor than in the liver and spleen and the released P peak concentration at t = 6 h is smaller in the tumor than in the other tissues. From a quantitative point of view, tumor targeting by released P is not more pronounced. However, drug release in the tumor seems more extended and the netto released P concentration decreases more slowly in the tumor than in the liver and spleen.

A high capacity with regard to the encapsulated PP tissue influx as well as the drug release from the liposomes is calculated for the spleen. This is probably due to the anatomy and high macrophage density of the spleen. Likely, the released P in the spleen (and possibly also in other tissues) is quickly redistributed towards the blood and other tissues.

A fast redistribution of the released drug counteracts the targeted drug delivery by the liposomes. However, drug release in the tumor seems to be maintained for an extended period and at $t = 96$ h the released drug concentration in the tumor is significantly larger than that in the central circulation. This in contrast to the released P concentration at $t = 96$ h in the liver and spleen. These extended release characteristics in the tumor probably contribute to the beneficial effect. It should be noted however that higher released drug concentrations are formed in other tissues.

ACKNOWLEDGMENTS

The authors like to thank Pieter Vader from Utrecht University for culturing the murine B16F10 melanoma cells. Raymond Schiffelers from Utrecht University and Roel Arends from Synthon Biopharmaceuticals are acknowledged for sharing their professional expertise. MediTrans is acknowledged for the financial support.

FUNDING

This study has been carried out with financial support from the Commission of the European Communities, Priority 3 "Nanotechnologies and Nanosciences, Knowledge Based Multifunctional Materials, New Production Processes and Devices" of the Sixth Framework Programme for Research and Technological Development (Targeted Delivery of Nanomedicine: NMP4-CT-2006-026668). It does not necessarily reflect its views and in no way anticipates the Commission's future policy in this area.

COMPLIANCE WITH ETHICAL STANDARDS

Conflict of interest

All authors declare that they have no conflict of interest.

Ethical approval

This article does not contain any studies with human participants performed by any of the authors. All applicable international, national, and/or institutional guidelines for the care and use of animals were followed.

Informed consent

For this type of study, formal consent is not required.

REFERENCES

1. T.M. Allen and P.R. Cullis, Liposomal drug delivery systems: from concept to clinical applications, *Adv. Drug Delivery Rev.*, 2013, **65**, 36-48.
2. S. Qian, C. Li and Z. Zuo, Pharmacokinetics and disposition of various drug loaded liposomes, *Curr. Drug Metab.*, 2012, **13**, 372-395.
3. R. Ngoune, A. Peters, D. von Elverfeldt, K. Winkler and G. Pütz, Accumulating nanoparticles by EPR: a route of no return, *J. Controlled Release*, 2016, **238**, 58-70.
4. J.W. Nichols and Y.H. Bae, EPR: evidence and fallacy, *J. Controlled Release*, 2014, **190**, 451-464.
5. H. Maeda, Toward a full understanding of the EPR effect in primary and metastatic tumors as well as issues related to its heterogeneity, *Adv. Drug Delivery Rev.*, 2015, **91**, 3-6.
6. K. Park, The drug delivery field at the inflection point: time to fight its way out of the egg, *J. Controlled Release*, 2017, **267**, 2-14.
7. A. Gabizon, H. Shmeeda and Y. Barenholz, Pharmacokinetics of PEGylated liposomal doxorubicin: review of animal and human studies, *Clin. Pharmacokinet.*, **42**, 419-436.
8. X. Liu, A. Situ, Y. Kang, K.R. Villabroza, Y. Liao, C.H. Chang, T. Donahue, A.E. Nel and H. Meng, Irinotecan delivery by lipid-coated mesoporous silica nanoparticles shows improved efficacy and safety over liposomes for pancreatic cancer, *ACS Nano*, 2016, **10**, 2702−2715.
9. R.M. Schiffelers, J.M. Metselaar, M.H.A.M. Fens, A.P.C.A. Janssen, G. Molema and G. Storm, Liposome-encapsulated prednisolone phosphate inhibits growth of established tumors in mice, *Neoplasia*, 2005, **7**, 118-127.
10. S. Druckmann, A. Gabizon and Y. Barenholz, Separation of liposome-associated doxorubicin from non-liposome-associated doxorubicin in human plasma: implications for pharmacokinetic studies, *Biochim. Biophys. Acta*, 1989, **980**, 381-384.
11. A.A. Srigritsanapol and K.K. Chan, A rapid method for the separation and analysis of leaked and liposomal entrapped phosphoramide mustard in plasma, *J. Pharm. Biomed. Anal.*, 1994, **12**, 961-968.
12. L.D. Mayer and G. St.-Onge, Determination of free and liposome-associated doxorubicin and vincristine levels in plasma under equilibrium conditions employing ultrafiltration techniques, *Anal. Biochem.*, 1995, **232**, 149-157.
13. R. Krishna, M.S. Webb, G. St. Onge and L.D. Mayer, Liposomal and nonliposomal drug pharmacokinetics after administration of liposome-encapsulated vincristine and their contribution to drug tissue distribution properties, *J. Pharmacol. Exp. Ther.*, 2001, **298**, 1206-1212.
14. R. Bellott, P. Pouna and J. Robert, Separation and determination of liposomal and non-liposomal daunorubicin from the plasma of patients treated with DaunoXome, *J. Chromatogr. B*, 2001, **757**, 257-267.
15. N.M. Deshpande, M.G. Gangrade, M.B. Kekare and V.V. Vaidya, Determination of free and liposomal amphotericin B in human plasma by liquid chromatography-mass spectroscopy with solid phase extraction and protein precipitation techniques, *J. Chromatogr. B*, 2010, **878**, 315-326.
16. Y. Xie, N. Shao, Y. Jin, L. Zhang, H. Jiang, N. Xiong, F. Su and H. Xu, Determination of non-liposomal and liposomal doxorubicin in plasma by LC-MS/MS coupled with an effective solid phase extraction: in comparison with ultrafiltration technique and application to a pharmacokinetic study, *J. Chromatogr. B*, 2018, **1072**, 149-160.
17. A.N. Schorzman, A.T. Lucas, J.R. Kagel and W.C. Zamboni, Methods and study designs for characterizing the pharmacokinetics and pharmacodynamics of carrier-mediated agents, in

Targeted drug delivery methods and protocols, eds. R.W. Sirianni and B. Behkam, Humana Press, New York, 2018, pp 201-228.

18. K.M. Laginha, S. Verwoert, G.J.R. Charrois and T.M. Allen, Determination of doxorubicin levels in whole tumor and tumor nuclei in murine breast cancer tumors, *Clin. Cancer Res.*, 2005, **11**, 6944-6949.
19. W.C. Zamboni, S. Strychor, E. Joseph, D.R. Walsh, B.A. Zamboni, R.A. Parise, M.E. Tonda, N.Y. Yu, C. Engbers and J.L. Eiseman, Plasma, tumor, and tissue disposition of Stealth liposomal CKD-602 (S-CKD602) and nonliposomal CKD-602 in mice bearing A375 human melanoma xenografts, *Clin. Cancer Res.*, 2007, **13**, 7217-7223.
20. G.J.R. Charrois and T.M. Allen, Drug release rate influences the pharmacokinetics, biodistribution, therapeutic activity, and toxicity of PEGylated liposomal doxorubicin formulations in murine breast cancer, *Biochim. Biophys. Acta*, 2004, **1663**, 167-177.
21. A. Gabizon, A.T. Horowitz, D. Goren, D. Tzemach, H. Shmeeda and S. Zalipsky, *In vivo* fate of folate-targeted polyethylene-glycol liposomes in tumor-bearing mice, *Clin. Cancer Res.*, 2003, **9**, 6551-6559.
22. J.M. Metselaar, M.H.M. Wauben, J.P.A. Wagenaar-Hilbers, O.C. Boerman and G. Storm, Complete remission of experimental arthritis by joint targeting of glucocorticoids with long-circulating liposomes, *Arthritis Rheum.*, 2003, **48**, 2059-2066.
23. E.A.W. Smits, J.A. Soetekouw and H. Vromans, *In vitro* confirmation of the quantitative differentiation of liposomal encapsulated and non-encapsulated prednisolone (phosphate) tissue concentrations by murine phosphatases, *J. Liposome Res.*, 2014, **24**, 130-135.
24. A.G. Kohli, H.M. Kieler-Ferguson, D. Chan and F.C. Szoka, A robust and quantitative method for tracking liposome contents after intravenous administration, *J. Controlled Release*, 2014, **176**, 86-93.
25. V. Garg and W.J. Jusko, Bioavailability and reversible metabolism of prednisone and prednisolone in man, *Biopharm. Drug Dispos.*, 1994, **15**, 163-172.
26. H. Möllmann, S. Balbach, G. Hochhaus, J. Barth and H. Derendorf, Pharmacokinetic-pharmacodynamic correlations of corticosteroids, in *Handbook of pharmacokinetic/pharmacodynamic correlation*, eds. H. Derendorf and G. Hochhaus, CRC Press, Boca Raton, 1995, pp 323-361.
27. E.A.W. Smits, J.A. Soetekouw, P.F.A. Bakker, B.J.H. Baijens and H. Vromans, Plasma, blood and liver tissue sample preparation methods for the separate quantification of liposomal-encapsulated prednisolone phosphate and non-encapsulated prednisolone, *J. Liposome Res.*, 2015, **25**, 46-57.
28. J.P.M. Motion, J. Nguyen and F.C. Szoka, Phosphatase-triggered fusogenic liposomes for cytoplasmic delivery of cell-impermeable compounds, *Angew. Chem.*, 2012, **124**, 9181-9185.
29. B.J. Crielaard, T. Lammers, M.E. Morgan, L. Chaabane, S. Carboni, B. Greco, P. Zaratin, A.D. Kraneveld and G. Storm, Macrophages and liposomes in inflammatory disease: friends or foes?, *Int. J. Pharm.*, 2011, **416**, 499-506.
30. P. Barrera, J.M. Metselaar, J.M. van den Hoven, S. Mulder, B. Nuijen, C. Wortel, G. Storm, J.H. Beijnen and P.L.C.M. van Riel, Long-circulating liposomal prednisolone versus pulse intramuscular methylprednisolone in patients with active rheumatoid arthritis, in J.M. van den Hoven, *Liposomal glucocorticoids: pharmaceutical, preclinical and clinical aspects*, PhD thesis, Utrecht University, 2012, pp 101-116.
31. C.W. Wong, B. Czarny, J.M. Metselaar, C. Ho, S.R. Ng, A.V. Barathi, G. Storm and T.T. Wong, Evaluation of subconjunctival liposomal steroids for the treatment of experimental uveitis, *Sci. Rep.*, 2018, **8**, e6604.

32. H. Bull, P.G. Murray, D. Thomas, A.M. Fraser and P.N. Nelson, Acid phosphatases, *J. Clin. Pathol.: Mol. Pathol.*, 2002, **55**, 65-72.
33. E. Cittadino, M. Ferraretto, E. Torres, A. Maiocchi, B.J. Crielaard, T. Lammers, G. Storm, S. Aime and E. Terreno, MRI evaluation of the antitumor activity of paramagnetic liposomes loaded with prednisolone phosphate, *Eur. J. Pharm. Sci.*, 2012, **45**, 436-441.
34. E.A.W. Smits, C.J.P. Smits and H. Vromans, The development of a method to quantify encapsulated and free prednisolone phosphate in liposomal formulations, *J. Pharm. Biomed. Anal.*, 2013, **75**, 47-54.
35. E.A.W. Smits, J.A. Soetekouw, I. van Doormalen, B.H.J. van den Berg, M.P. van der Woude, N. de Wijs-Rot and H. Vromans, Quantitative LC-MS determination of liposomal encapsulated prednisolone phosphate and non-encapsulated prednisolone concentrations in murine whole blood and liver tissue, *J. Pharm. Biomed. Anal.*, 2015, **115**, 552-561.
36. R.P. Brown, M.D. Delp, S.L. Lindstedt, L.R. Rhomberg and R.P. Beliles, Physiological parameter values for physiologically based pharmacokinetic models, *Toxicol. Ind. Health*, 1997, **13**, 407-484.
37. H. Maeda, H. Nakamura and J. Fang, The EPR effect for macromolecular drug delivery to solid tumors: improvement of tumor uptake, lowering of systemic toxicity, and distinct tumor imaging *in vivo*, *Adv. Drug Delivery Rev.*, 2013, **65**, 71-79.
38. J. Schmidt, J.M. Metselaar, M.H.M. Wauben, K.V. Toyka, G. Storm and R. Gold, Drug targeting by long-circulating liposomal glucocorticosteroids increases therapeutic efficacy in a model of multiple sclerosis, *Brain*, 2003, **126**, 1895-1904.
39. B. Ozbakir, B.J. Crielaard, J.M. Metselaar, G. Storm and T. Lammers, Liposomal corticosteroids for the treatment of inflammatory disorders and cancer, *J. Controlled Release*, 2014, **190**, 624-636.
40. N. Bertrand and J.-C. Leroux, The journal of a drug-carrier in the body: an anatomo-physiological perspective, *J. Controlled Release*, 2012, **161**, 152-163.
41. D. Sarko and R.B. Georges, Kidney-specific drug delivery: review of opportunities, achievements, and challenges, *J. Anal. Pharm. Res.*, 2016, **2**, 33-38.
42. D.J.A. Crommelin and G. Storm, Liposomes: from the bench to the bed, *J. Liposome Res.*, 2003, **13**, 33-36.
43. E. Kluza, S.Y. Yeo, S. Schmid, D.W.J. van der Schaft, R.W. Boekhoven, R.M. Schiffelers, G. Storm, G.J. Strijkers and K. Nicolay, Anti-tumor activity of liposomal glucocorticoids: the relevance of liposome-mediated drug delivery, intratumoral localization and systemic activity, *J. Controlled Release*, 2011, **151**, 10-17.
44. S.H. Lee, P.M. Starkey and S. Gordon, Quantitative analysis of total macrophage content in adult mouse tissues: immunochemical studies with monoclonal antibody F4/80, *J. Exp. Med.*, 1985, **161**, 475-489.
45. S.M. Moghimi, Mechanisms of splenic clearance of blood cells and particles: towards development of new splenotropic agents, *Adv. Drug Delivery Rev.*, 1995, **17**,103-115.
46. C.R. Yates, C. Chang, J.D. Kearbey, K. Yasuda, E.G. Schuetz, D.D. Miller, J.T. Dalton and P.W. Swaan, Structural determinants of P-glycoprotein-mediated transport of glucocorticoids, *Pharm. Res.*, 2003, **20**, 1794-1803.
47. B.M. Frey and F.J. Frey, Clinical pharmacokinetics of prednisone and prednisolone, *Clin. Pharmacokinet.*, 1990, **19**, 126-146.
48. J. Xu, J. Winkler and H. Derendorf, A pharmacokinetic/pharmacodynamic approach to predict total prednisolone concentrations in human plasma, *J. Pharmacokinet. Pharmacodyn.*, 2007, **34**, 355-372.

49. D. Czock, F. Keller, F.M. Rasche and U. Häussler, Pharmacokinetics and pharmacodynamics of systemically administered glucocorticoids, *Clin. Pharmacokinet.*, 2005, **44**, 61-98.
50. T.K. Bergmann, K.A. Barraclough, K.J. Lee and C.E. Staatz, Clinical pharmacokinetics and pharmacodynamics of prednisolone and prednisone in solid organ transplantation, *Clin. Pharmacokinet.*, 2012, **51**, 711-741.
51. M.L. Rocci Jr., S.J. Szefler, M. Acara and W.J. Jusko, Prednisolone metabolism and excretion in the isolated perfused rat kidney, *Drug Metab. Dispos.*, 1981, **9**, 177-182.
52. V. Garg and W.J. Jusko, Simultaneous analysis of prednisone, prednisolone and their major hydroxylated metabolites in urine by high-performance liquid chromatography, *J. Chromatogr., Biomed. Appl.*, 1991, **567**, 39-47.
53. S. Ahi, A. Beotra, S. Dubey, A. Upadhyaym and S. Jain, Simultaneous identification of prednisolone and its ten metabolites in human urine by high performance liquid chromatography-tandem mass spectrometry, *Drug Test. Anal.*, 2012, **4**, 460-467.
54. G.M. Rodchenkov, A.N. Vedenin, V.P. Uralets and V.A. Semenov, Characterization of prednisone, prednisolone and their metabolites by gas chromatography-mass spectrometry, *J. Chromatogr., Biomed. Appl.*, 1991, **565**, 45-51.

Chapter 7

General discussion

GENERAL DISCUSSION

Tumor targeted drug delivery by liposomes has been considered a promise for decades now. The encapsulation of a drug into a liposomal drug delivery system can significantly alter the pharmacokinetics which can result in an increased therapeutic index in comparison to the corresponding, non-encapsulated drug formulation as shown in chapter 1. However, despite thousands of studies (i.e. 11,738 publications in PubMed on January 21st, 2019, search terms "liposome" AND "cancer"), only about a dozen liposome formulations received approval for cancer and various challenges are still open as illustrated in chapter 1.

The successes and challenges of liposomal drug delivery formulations depend on the underlying pharmacokinetics (PK) and pharmacodynamics (PD). PK processes like absorption, distribution, metabolism and excretion (ADME) are usually investigated during development of the drug product [1]. However, as discussed in chapter 1, the PKPD of liposomes intended for tumor targeted drug delivery is often not fully determined: besides ADME of the liposomal formulation another PK process is of crucial importance, i.e. the liberation of the drug. Only after release from the liposomes the drug can exert its biological activity [2-4]. Thus, efficacy and toxicity are not related to the drug which is still encapsulated in the liposomes (further referred to as encapsulated drug). Consequently, to understand and improve the PK and subsequent efficacy and toxicity, the individual quantification of encapsulated and released drug concentrations in plasma/blood, tumor and healthy tissues is essential. In general, the quantitative analysis of such concentration profiles in tissues is hampered by unwanted drug release, arising as an artefact during homogenization [5], and, therefore, the investigation of individual concentration profiles is limited.

This thesis aims to provide new insights into the PK of liposomal drug delivery systems, by measuring encapsulated and released drug concentrations in blood, tumor and healthy tissues separately. To do so, polyethylene glycol (PEG)-coated liposomal prednisolone phosphate was chosen as a model formulation. Rapid dephosphorylation of prednisolone phosphate (PP) into prednisolone (P) after release from the liposomes *in vivo* is assumed to enable the accurate differentiation and quantification of encapsulated and released drug ([6]; chapters 2, 4-6). This chapter of this thesis provides a general discussion of the development, semi-validation and implementation of such methodology, which is followed by future perspectives and an overall conclusion.

Rate of prednisolone phosphate dephosphorylation after release

PP is known for its extremely rapid and complete dephosphorylation into P *in vivo* [7-9]. The hydrolysis of PP into P after release form the liposomes enables the accurate quantification of encapsulated and released drug concentrations because the dephosphorylation process is considerably faster than the rate of release of drug from the liposomes. This is verified in chapter 2, at which the rate of dephosphorylation was studied using tissue homogenates. Rapid dephosphorylation was observed for PP in homogenates of liver and kidney: the majority of PP was already converted after only 10 min of incubation of a high PP concentration representing ~3000 nmol/g tissue. The converted concentration is much larger than the maximal sum total (i.e. PP + P) drug concentration in the tissues of interest after administration of PEGylated liposomal PP in mice, which approached 200 nmol/g (chapter 6). Subsequent data analysis estimated that in a worst-case scenario, at which the *in vivo* maximal sum total drug concentrations in the liver and kidneys were released at once from the liposomes, PP would be completely converted in less than 10 min. This was considered to be instantaneous as compared to the time frame of drug release from PEGylated liposomes, which is rather in the order of hours than minutes [3, 10]. Afterwards, an internal study confirmed similar results in whole blood.

Due to the limited availability of splenic tissue, PP was only incubated at a high concentration in splenic tissue homogenate. In these settings, no statistical significant decrease of PP was observed by applying the Kruskal-Wallis one-way analysis of variance test, which prohibited the possibility to draw any conclusions. However, the corresponding dephosphorylation rate constant k was not equal to zero ($k = 0.006 \pm 0.001$ min^{-1}), indicating that a significant dephosphorylation did occur. From t = 0-10 min about 200 nmol/g was dephosphorylated, which is similar to a concentration achieved by a worst-case scenario in the spleen. This is positive with regard to a possible instantaneous conversion of PP into P after release in the spleen.

Unfortunately, representative tumor tissue was not available. Additional experiments are required to confirm the rapid dephosphorylation of PP into P after release from the liposomes in the tumor. However, the efficacy of PEGylated liposomal PP is probably mainly based on the interaction with macrophages (see chapter 1). Based on the previous observed efficacy [11, 12] and the presence of phosphatases in macrophages and lysosomes [13], it is assumed that, after liposome uptake by macrophages, the drug is released in the endosomes/lysosomes and is subsequently dephosphorylated into P [11, 14, 15]. This is positive with regard to a possible rapid dephosphorylation of PP after release in the tumor.

Overall, it is likely that PP and P are a good representative of the encapsulated and released drug in blood as well as in the tissues of interest. Consequently, the accurate quantification of PP and P concentrations in these matrices yield the encapsulated and

released drug concentrations, respectively. In this way, methods in which the liposomes and released drug are separated based on their different physicochemical properties, like charge, size and hydrophobicity, can be circumvented. As discussed in chapter 1, this is very desirable, since these methods are hampered by drug release during tissue homogenization. This yields overestimations of the released drug in comparison to the *in vivo* concentration. Overall, the principle of differentiation by encapsulation of a prodrug in a carrier system can account for any prodrug which is rapidly converted in relation to its release from the carrier and the carrier should be able to protect the drug against the specific hydrolyzing enzymes.

Method development and validation

Importance of method optimization and validation

Chapters 4 and 5 describe the development and semi-validation of a quantitative method to determine the encapsulated PP and released P concentrations in whole blood and liver tissue. Subsequently, the accuracy of the method for tumor, spleen and kidneys was confirmed (see chapter 6 on unpublished data). The need for thorough method optimization and appropriate validation was stressed by preliminary studies. In one study, sample preparation by acidification to pH 2, liquid-liquid extraction using ethyl acetate [16, 17] and subsequent washing with hexane [18] was attempted. In general, this approach seemed to suffer from low recoveries for PP of roughly 35%. A second preliminary study used tetrahydrofuran (THF) to attempt sample preparation. Despite the success of THF with regard to the qualification of encapsulated and non-encapsulated PP concentrations in liposome preparations, homogenization of liver tissue in pure THF resulted in poor solubility of PP in the resulting matrix. These examples indicated that method reliability is far from self-evident, which in these cases was probably caused by the different characteristics of PP and P. Hereafter, method development was started from scratch. Since the method was intended for fundamental research, extensive validation as described by for example the U.S. Food and Drug Administration (FDA) was not required and would be rather disproportional, as indicated in chapter 4. Nevertheless, to secure suitable and reliable performance characteristics it was validated in an appropriate way using criteria adapted from the FDA guidance [19], which were in agreement with accuracy criteria from internal, industrial guidelines for preclinical bioanalytical methods at the time (see chapters 4 and 5).

Qualification of liposome preparations

In order to achieve meaningful data, the analytical method for the quantification of encapsulated PP and released P in whole blood and liver tissue should be properly developed to measure the specific parameters and adequately validated to ensure reliability. For the development and semi-validation of this method, accurate knowledge

of the encapsulated and non-encapsulated PP concentrations in the liposome preparation itself was required. Hence, chapter 3 describes the systematic development and cross-validation of a simple but reliable and precise method for the determination of these individual concentrations. This included the differentiation of the non-encapsulated PP from the encapsulated PP by dephosphorylation of the non-encapsulated PP using alkaline phosphatase (AP). The amount of AP and the incubation time were thoroughly chosen in order to ensure dephosphorylation of all non-encapsulated PP even when small changes in these parameters occur. During sample preparation prior to high-performance liquid chromatography, prevention of the significant hydrolysis of PP after liposome rupture is crucial to prevent overestimations of the non-encapsulated drug. The use of THF for rapid deactivation of AP as well as complete liposome rupture in one single step yielded accurate results. It was concluded that, possibly, liposome rupture by THF is slower than enzyme deactivation by THF. Thus, the encapsulated drug is still protected by the liposome until the AP in the sample is fully deactivated by THF. Finally, the accuracy of the developed method is comparable to the accuracy determined by dialysis, while clearly the method using AP is more precise.

In practice, the developed method for the quantification of encapsulated and non-encapsulated drug in liposome preparations of PP as described in chapter 3 appeared to be an easy but valuable tool to verify the sufficient removal of the non-encapsulated drug leaving only small amounts in the liposome preparation. The presence of only small amounts of non-encapsulated drug is, of course, a crucial characteristic of liposome preparations and it should be secured at all times to obtain reliable results.

Quantification in blood and tissue samples

Like the method for quantification of encapsulated and non-encapsulated drug in the liposome preparation itself, the developed method for the quantification of encapsulated PP and released P in blood and tissues was also designed to induce complete liposome rupture and prevent significant enzymatic hydrolysis of "encapsulated" drug during sample preparation. This was to avoid significant under- and overestimations of the encapsulated PP and released P concentrations, respectively. This was accomplished by the determination of a well-chosen amount of methanol as tissue homogenization and precipitation solvent. Together with the use of two representative internal standards, protein precipitation, optimized chromatography, negative electrospray and Orbitrap-MS analysis, this yielded suitable recovery, specificity, selectivity, sensitivity, accuracy (80-120%) and precision (20%).

Liposome rupture

As discussed above, the solvents used during sample preparation should induce complete liposome rupture and prevent enzymatic hydrolysis. It was shown in chapter 3

that liposome rupture by two equivalents of acetonitrile of a 100 times diluted liposome preparation was inferior due to a recovery of 79 ± 7%. It was also reported that the addition of one aliquot of methanol to one aliquot of pure liposome preparation resulted in a useless jelly. Unpublished results described a recovery of 81 ± 5% (related to liposome rupture by THF) after the addition of two equivalents of methanol to one equivalent of a 10 times diluted liposome preparation. However, in chapter 4, a recovery of 106 ± 0.2% has also been observed after the addition of two equivalents of methanol to one equivalent of a 20 times diluted liposome preparation. Overall, these results suggest that the complete liposome rupture by solvents is not self-evident and, logically, may also depend on the liposome concentration. Insufficient liposome rupture reduces the recovery, sensitivity and possibly also the accuracy of the method. While such deviations still can be acceptable during bioanalysis, during analysis of the liposome product they become more critical. Then, knowledge and optimization of the liposome rupture during sample preparation is wanted.

Enzyme deactivation

The rapid deactivation of enzymes during sample preparation is also important. Whereas THF provided good results with regard to the qualification of encapsulated and non-encapsulated PP of liposome preparations, methanol proved very suitable for the immediate enzyme deactivation in blood and tissue samples. Also other solvents and inhibitors were tested for their capability to deactivate liver phosphatases. It was shown in chapter 4 that acetonitrile, which is widely used as precipitation solvent and assumed to denaturate enzymes, seems not to deactivate the liver phosphatases completely: 47 area% was converted into P. Moreover, chapter 4 also mentions that a mixture of commercial available phosphatase and protease inhibitor cocktails, which are often applied to prevent dephosphorylation of prodrugs, seems not to prevent hydrolysis at all: 82 area% was converted into P as compared to 81 area% for the control (values were not shown). Care should be taken to ensure phosphatase deactivation in tissue matrices like liver, while the phosphatase activity itself in ethylenediaminetetraacetic acid-stabilized plasma is low (unpublished results).

PEGylated liposomal 4-methylumbelliferyl phosphate

Simultaneously with the realization of this dissertation, Kohli et al. provided a similar approach for a liposomal preparation of 4-methylumbelliferyl phosphate [20]. The encapsulated drug was represented by the phosphate compound 4-methylumbelliferyl phosphate (MU-P) and the released drug was represented by the parent compound 4-methylumbelliferone (MU). Additionally, the metabolite 4-methylumbelliferyl glucuronide (MU-G) was also taken into account. To our knowledge, the authors provided no verification of sufficient liposome rupture and deactivation of tissue phosphatases

during storage and sample preparation. However, the authors were able to measure small amounts of MU (1% of the injected dose/g tissue or even less) in the liver and spleen. This suggests that, maximally, an overestimation of the released drug due to hydrolysis of the prodrug during storage and sample preparation would be as large as these small amounts. Furthermore, to our knowledge, the MU-P tissue concentrations were not corrected for the compound in the residual blood. As already indicated in chapter 6, large blood concentrations can lead to overestimations of the tissue concentrations when not corrected. More specific, at 1 h after injection of PEGylated liposomal PP at a dose of 36 μmol PP/kg, the uncorrected encapsulated PP tumor concentration is 128% related to the corrected concentration (unpublished results). At different points of time for other tissues, even larger deviations were observed up to 268% (unpublished results). Since large concentrations of MU-P were observed in the serum of mice after administration of 20 mg/kg MU-P equivalents [20], this probably leads to overestimations of the MU-P tissue concentrations and the MU-P tissue concentrations will not be taken into consideration. The parent compound MU was not observed in the serum [20].

Pharmacokinetics

The implementation of the developed methodology as discussed in chapters 4 and 5 is described in chapter 6. Encapsulated PP and released P concentrations in blood, tumor, liver, spleen and kidneys were measured after i.v. injection of PEGylated liposomal PP in tumor-bearing mice. Subsequent kinetic analysis yielded also the tissue influx of encapsulated drug and the release of drug from the liposomes with time. The PK features are discussed in this section.

Extravasation of encapsulated PP

Comparison of the results from the different tissues learned that the rate of tumor influx of encapsulated drug is not larger in comparison to the rates corresponding to the liver and spleen. As is discussed in chapter 6, the prominent uptake by liver and spleen is still probably due to the uptake by tissue macrophages, since it was observed previously that PEGylated liposomal PP localizes in the macrophages of liver and spleen [21, 22] and the PEG coating is only able to reduce the uptake by the mononuclear phagocyte system and cannot avoid it [23]. A significant, large rate of tissue influx was clearly observed per gram of spleen. This could not be fully explained by the larger macrophage density in the spleen in comparison to most other tissues like the liver [24, 25]. Most probably, other characteristics of the spleen also play an important role: the spleen exhibits an enormous contact surface area for blood cells and particulates and can reduce the blood flow resulting in extended contact with the macrophages [25].

Drug delivery by liposomes

The rate of drug release from the liposomes in the tumor seems rather smaller instead of larger in comparison to the liver and the spleen. At 6 h after injection, significant smaller released P concentrations were observed in the tumor than in the other tissues. However, drug release in the tumor seems prolonged and the released P concentration decreases more gradually as compared to the liver and spleen. Assuming the drug is released after digestion of the liposomes in macrophages, it is concluded in chapter 6 that this could indicate that the tumor contains (1) less, (2) different, and/or (3) less accessible macrophages compared to the liver and spleen. However, during the verification of the rapid dephosphorylation of PP after release from the liposomes as described in chapter 2, no representative tumor tissue was available. Although it is likely that PP is also rapidly hydrolyzed into P in the tumor as discussed above, additional experiments are required to confirm this. Hence, the prolonged drug release and prolonged released P concentrations in the tumor might be (partially) an artifact, if the dephosphorylation rate of PP in the tumor tissue is not adequate.

As described in chapter 1, Laginha et al. used the affinity of doxorubicin for DNA in the cell nucleus to approximate available doxorubicin levels in the nuclei of tumor cells [3]. Based on an area under the concentration-time curve from 0 to 7 days for drug in the tumor cell nuclei relative to the total tumor, Doxil® resulted in an availability of 49.4 and 41.3% for a dose of 9 and 16 mg/kg, respectively. This indicates that on average, roughly half of the doxorubicin in the tumor is present in the released state within the seven day time frame, which is in the same order of magnitude as the released P percentage in tumor tissue (see chapter 6, Figure 3a). For both doses, the maximal concentration of doxorubicin in the tumor cell nuclei occurred at two to three days after injection. This in comparison to the four hours observed for non-encapsulated doxorubicin. This was contributed to the slow rate of release of doxorubicin from the liposomes prior to transfer to the nucleus.

Kohli et al. encapsulated the phosphate compound MU-P in various PEGylated liposomes with different acyl chains and with either free or covalently attached cholesterol (covalently attached cholesterol decreases drug release in tissues) [20]. At t = 3 and 48 h after i.v. administration of 20 mg/kg MU-P equivalents in mice, the released MU was quantified in liver, spleen and kidneys [20]. In general, a higher concentration of the released MU was observed in the spleen as compared to the liver and the kidneys for both points in time. More specific, for the PEGylated liposome preparation containing 2-diarachidoyl-sn-glycero-3-phosphocholine and free cholesterol, which is most similar to the liposomes used in chapter 6, the released MU was about a factor three or four larger in the spleen than in the liver and kidneys at 3 h after injection. This is in line with the results from chapter 6, in which a significant larger concentration of released P was described in the spleen in comparison to liver and kidneys at 6 h after injection. At 48 h

after injection the released MU concentrations in the three organs were small (about 1% of the injected dose/g tissue) and differences between the organs were not clear.

Redistribution of released P

Remarkably, chapter 6 describes an extremely large rate of release per gram of spleen. It is about 17-74 fold larger than in the other investigated tissues. Maximally, the released P concentration in the spleen was about 1.8-4.4 fold larger. Thus, the released P concentrations remained relatively small in comparison with as expected by the extremely large rate of release per gram. Because of the properties of P to pass membranes [26], P probably distributed quickly out of the spleen. In general, a rapid redistribution of P is expected as hypothesized previously [6, 12]. This would explain the P concentrations observed in the blood as well as relatively large and persistent P concentrations in the kidneys in comparison to the calculated drug release per gram of kidneys.

It was concluded that a rapid redistribution of the released P could counteract the targeted drug delivery effect by the liposomes. However, chapter 6 also describes that the release of drug from the liposomes in the tumor seemed slower but prolonged compared with the liver and spleen. Likely due to the sustained release, the released P concentration in the tumor remained at a relatively constant level in comparison to the released P in the circulation, liver and spleen despite the possible redistribution towards the blood and other tissues. For a compound like doxorubicin, redistribution from the tissues after release might be less likely since it is known for its affinity for tissue [3, 27]. These differences for P and doxorubicin indicate the important role of the characteristics of the drug itself in the field of drug delivery. As repeatedly mentioned in this thesis, only the released drug can exert biological activity. As discussed in chapter 6, released drug concentrations depend on the PK of the liposomal carrier, the drug release from the carrier as well as on the PK of the drug itself (e.g. retention, distribution, metabolism and elimination). Drug release from the liposomes and released drug concentrations are two different concepts. Rapid drug release from the liposomes does not automatically result in large released drug concentrations. It is also dependent on the PK of the drug itself after release. Therefore, from a PD point of view the released drug concentration is wat should be measured and not the release of the drug.

Future perspectives and concluding remarks

In summary, this thesis focuses on the optimization, adequate validation and implementation of a reliable method to quantify encapsulated and released drug concentrations in blood and tissues after administration of a liposome formulation. It demonstrated that the encapsulation of prodrugs into carriers can enable the quantification of encapsulated and released drug in blood and tissues. Hereto, the

prodrug should be rapidly converted after release and the carrier should protect the enclosed drug against enzymatic conversion. This thesis also demonstrates the value of appropriate method development and validation in an academic setting. In the case of liposome and/or phosphate prodrug containing samples verification of complete liposome rupture and especially enzyme deactivation during sample preparation showed to be crucial. Finally, the thesis provides new insights into the liposomal PK. Targeted drug delivery by PEGylated liposomal PP did not avoid the significant presence of released P in healthy tissues: larger peak concentrations of released P were measured in liver, spleen and kidneys than in the tumor. In general, released P probably quickly redistributed after release in the tissues and this could counteract the targeted drug delivery by the liposomes. However, drug release in the tumor seems to be maintained for an extended period and seems to maintain fairly constant levels of released P. This in contrast to the liver and spleen. These extended release characteristics in the tumor most likely contribute to the beneficial effect.

A probably fast redistribution of P from the tissues after release emphasizes the significance of the particular PK properties of the drug compound itself after delivery by the liposomes. For example, a quick redistribution or extensive metabolism can strongly influence the released drug concentrations in a tissue. It is therefore pointed out that from a PD point of view, further research should focus on released drug concentrations instead of drug release out of the carrier.

REFERENCES

1. U.S. Food and Drug Administration, The drug development process, https://www.fda.gov/ForPatients/Approvals/Drugs/default.htm, (accessed January 2019).
2. H.M. Kieler-Ferguson, D. Chanc, J. Sockolosky, L. Finney, E. Maxey, S. Vogt and F.C. Szoka Jr., Encapsulation, controlled release, and antitumor efficacy of cisplatin delivered in liposomes composed of sterol-modified phospholipids, *Eur. J. Pharm. Sci.*, 2017, **103**, 85-93.
3. K.M. Laginha, S. Verwoert, G.J.R. Charrois and T.M. Allen, Determination of doxorubicin levels in whole tumor and tumor nuclei in murine breast cancer tumors, *Clin. Cancer Res.*, 2005, **11**, 6944-6949.
4. W.C. Zamboni, A.C. Gervais, M.J. Egorin, J.H.M. Schellens, E.G. Zuhowski, D. Pluim, E. Joseph, D.R. Hamburger, P.K. Working, G. Colbern, M.E. Tonda, D.M. Potter and J.L. Eiseman, Systemic and tumor disposition of platinum after administration of cisplatin or Stealth liposomal-cisplatin formulations (SPI-077 and SPI-077 B103) in a preclinical tumor model of melanoma, *Cancer Chemother. Pharmacol.*, 2004, **53**, 329-336.
5. A.N. Schorzman, A.T. Lucas, J.R. Kagel and W.C. Zamboni, Methods and study designs for characterizing the pharmacokinetics and pharmacodynamics of carrier-mediated agents, in *Targeted drug delivery methods and protocols*, eds. R.W. Sirianni and B. Behkam, Humana Press, New York, 2018, pp 201-228.
6. J.M. Metselaar, M.H.M. Wauben, J.P.A. Wagenaar-Hilbers, O.C. Boerman and G. Storm, Complete remission of experimental arthritis by joint targeting of glucocorticoids with long-circulating liposomes, *Arthritis Rheum.*, 2003, **48**, 2059-2066.
7. J.Q. Rose, A.M. Yurchak and W.J. Jusko, Dose dependent pharmacokinetics of prednisone and prednisolone in man, *J. Pharmacokinet. Biopharm.*, 1981, **9**, 389-417.
8. V. Garg and W.J. Jusko, (1994) Bioavailability and reversible metabolism of prednisone and prednisolone in man, *Biopharm. Drug Dispos.*, 1994, **15**, 163-172.
9. H. Möllmann, S. Balbach, G. Hochhaus, J. Barth and H. Derendorf, Pharmacokinetic-pharmacodynamic correlations of corticosteroids, in *Handbook of pharmacokinetic/ pharmacodynamic correlation*, eds. H. Derendorf and G. Hochhaus, CRC Press, Boca Raton, 1995, pp 323-361.
10. A. El-Kareh and T.W. Secomb, A mathematical model for comparison of bolus injection, continuous infusion, and liposomal delivery of doxorubicin to tumor cells, *Neoplasia*, 2000, **2**, 325-338.
11. B.J. Crielaard, T. Lammers, M.E. Morgan, L. Chaabane, S. Carboni, B. Greco, P. Zaratin, A.D. Kraneveld and G. Storm, Macrophages and liposomes in inflammatory disease: friends or foes?, *Int. J. Pharm.*, 2011, **416**, 499-506.
12. R.M. Schiffelers, J.M. Metselaar, M.H.A.M. Fens, A.P.C.A. Janssen, G. Molema and G. Storm, Liposome-encapsulated prednisolone phosphate inhibits growth of established tumors in mice, *Neoplasia*, 2005, **7**, 118-127.
13. H. Bull, P.G. Murray, D. Thomas, A.M. Fraser and P.N. Nelson, Acid phosphatases, *J. Clin. Pathol.: Mol. Pathol.*, 2002, **55**, 65-72.
14. P. Barrera, J.M. Metselaar, J.M. van den Hoven, S. Mulder, B. Nuijen, C. Wortel, G. Storm, J.H. Beijnen and P.L.C.M. van Riel, Long-circulating liposomal prednisolone versus pulse intramuscular methylprednisolone in patients with active rheumatoid arthritis, in J.M. van den Hoven, *Liposomal glucocorticoids: pharmaceutical, preclinical and clinical aspects*, PhD thesis, Utrecht University, 2012, pp 101-116.

15. C.W. Wong, B. Czarny, J.M. Metselaar, C. Ho, S.R. Ng, A.V. Barathi, G. Storm and T.T. Wong, Evaluation of subconjunctival liposomal steroids for the treatment of experimental uveitis, *Sci. Rep.*, 2018, **8**, e6604.
16. H. Derendorf, P. Rohdewald, G. Hochhaus and H. Möllmann, HPLC determination of glucocorticoid alcohols, their phosphates and hydrocortisone in aqueous solutions and biological fluids, *J. Pharm. Biomed. Anal.*, 1986, **4**, 197-206.
17. P.N. Schild and B.G. Charles, Determination of dexamethasone in plasma of premature neonates using high-performance liquid chromatography, *J. Chromatogr. B*, 1994, **658**, 189-192.
18. Y. Iglesias, C. Fente, S. Mayo, B. Vázquez, C. Franco and A. Cepeda, Chemiluminescence detection of nine corticosteroids in liver, *Analyst*, 2000, **125**, 2071-2074.
19. U.S. Department of Health and Human Services, Food and Drug Administration, Center for Drug Evaluation and Research, Center for Veterinary Medicine, Guidance for industry: bioanalytical method validation, http://www.fda.gov/downloads/Drugs/Guidances/ucm070107.pdf, 2001.
20. A.G. Kohli, H.M. Kieler-Ferguson, D. Chan and F.C. Szoka, A robust and quantitative method for tracking liposome contents after intravenous administration, *J. Controlled Release*, 2014, **176**, 86-93.
21. B. Ozbakir, B.J. Crielaard, J.M. Metselaar, G. Storm and T. Lammers, Liposomal corticosteroids for the treatment of inflammatory disorders and cancer, *J. Controlled Release*, 2014, **190**, 624-636.
22. J. Schmidt, J.M. Metselaar, M.H.M Wauben, K.V. Toyka, G. Storm and R. Gold, Drug targeting by long-circulating liposomal glucocorticosteroids increases therapeutic efficacy in a model of multiple sclerosis, *Brain*, 2003, **126**, 1895-1904.
23. J.W. Nichols and Y.H. Bae, EPR: evidence and fallacy, *J. Controlled Release*, 2014, **190**, 451-464.
24. S.H. Lee, P.M. Starkey and S. Gordon, Quantitative analysis of total macrophage content in adult mouse tissues: immunochemical studies with monoclonal antibody F4/80, *J. Exp. Med.*, 1985, **161**, 475-489.
25. S.M. Moghimi, Mechanisms of splenic clearance of blood cells and particles: towards development of new splenotropic agents, *Adv. Drug Delivery Rev.*, 1995, **17**, 103-115.
26. C.R. Yates, C. Chang, J.D. Kearbey, K. Yasuda, E.G. Schuetz, D.D. Miller, J.T. Dalton and P.W. Swaan, Structural determinants of P-glycoprotein-mediated transport of glucocorticoids, *Pharm. Res.*, 2003, **20**, 1794-1803.
27. M. de Smet, E. Heijman, S. Langereis, N.M. Hijnen and H. Grüll, Magnetic resonance imaging of high intensity focused ultrasound mediated drug delivery from temperature-sensitive liposomes: an *in vivo* proof-of-concept study, *J. Controlled Release*, 2011, **150**, 102-110.

Appendix

Supplementary data chapter 5

Supplementary material chapter 6

Summary

Samenvatting in het Nederlands

List of publications corresponding to this thesis

Dankwoord

Curriculum vitae

Appendix A.1

Supplementary data chapter 5

Table A.1.1: Prednisolone phosphate (PP) and prednisolone (P) concentrations in the calibration standards containing matrix from whole blood or liver

	PP concentration (µmol/L blood) (nmol/g liver)	P concentration (µmol/L blood) (nmol/g liver)
Blood	0.0176	0.0186
	0.0352	0.0373
	0.0705	0.0745
	0.141	0.149
	0.282	0.298
	0.564	0.596
	1.13	1.19
	2.26	2.39
	4.51	4.77
	9.02	9.54
	18.0	19.1
	36.1	38.2
	72.2	76.3
	144	153
	289	305
	578	611
	1155	1221
Liver	0.107	0.113
	0.214	0.226
	0.427	0.451
	0.855	0.903
	1.71	1.81
	3.42	3.61
	6.84	7.22
	13.7	14.4
	27.4	28.9
	54.7	57.8
	109	116
	219	231
	438	462
	875	924

(A)

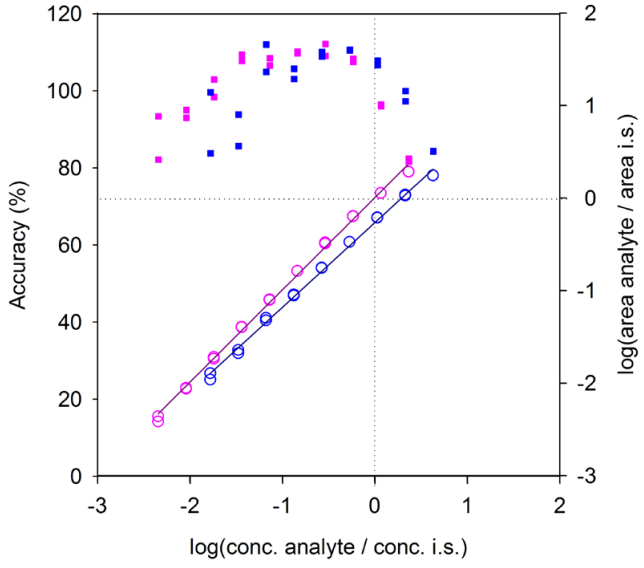
120
100
80
60
40
20
0
2
1
0
-1
-2
-3
-3
-2
-1
0
1
2
Accuracy (%)
log(area analyte / area i.s.)
log(conc. analyte / conc. i.s.)

(B)

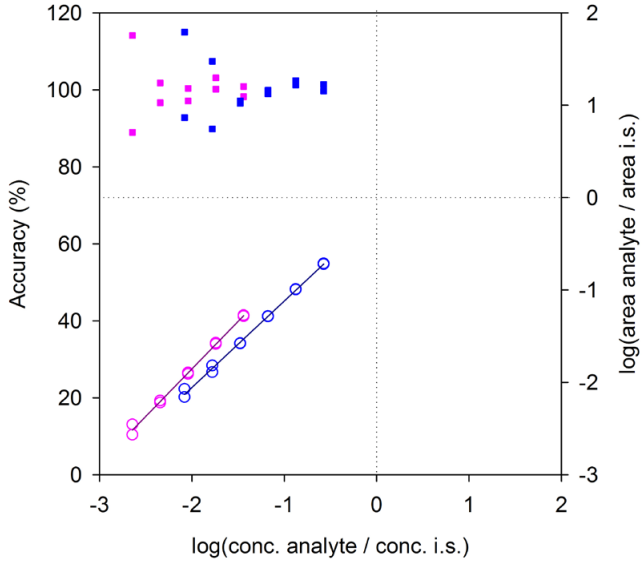
120
100
80
60
40
20
0
2
1
0
-1
-2
-3
-3
-2
-1
0
1
2
Accuracy (%)
log(area analyte / area i.s.)
log(conc. analyte / conc. i.s.)

(C)

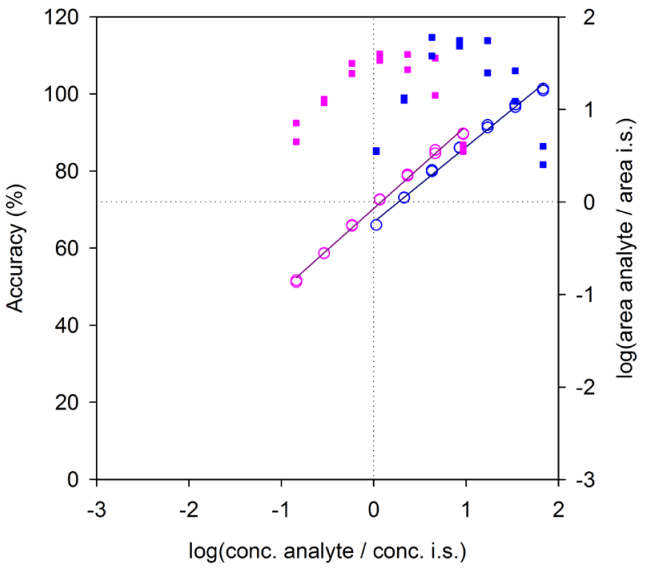
120
100
80
60
40
20
0
Accuracy (%)
2
1
0
-1
-2
-3
log(area analyte / area i.s.)
-3
-2
-1
0
1
2
log(conc. analyte / conc. i.s.)

(D)

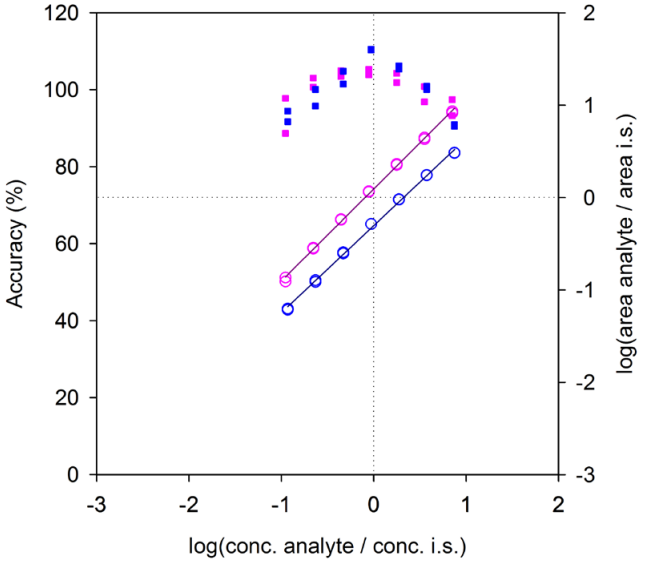
120
100
80
60
40
20
0
Accuracy (%)
2
1
0
-1
-2
-3
log(area analyte / area i.s.)
-3
-2
-1
0
1
2
log(conc. analyte / conc. i.s.)

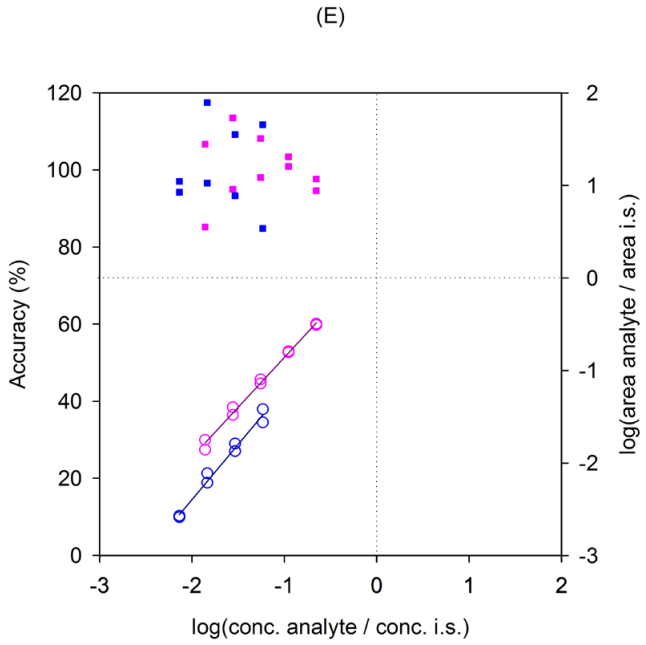

Figure A.1.1: Observed linear ranges for the prednisolone phosphate (PP) (pink circles) and prednisolone (P) (blue circles) calibration standards, corresponding accuracies for PP (pink squares) and P (blue squares), and corresponding coefficients of determination (R^2):

(a)	Blood injection volume 5 µL	PP: 0.564-289 µmol/L blood, $R^2 = 0.997$ P: 0.298-76.3 µmol/L blood, $R^2 = 0.997$
(b)	Blood injection volume 30 µL	PP: 0.282-4.51 µmol/L blood, $R^2 = 0.996$ P: 0.149-4.77 µmol/L blood, $R^2 = 0.997$
(c)	Blood injection volume 5 µL after 5× sample dilution	PP: 18.0-1155 µmol/L blood, $R^2 = 0.996$ P: 19.1-1221 µmol/L blood, $R^2 = 0.993$
(d)	Liver injection volume 5 µL	PP: 3.42-219 nmol/g liver, $R^2 = 0.999$ P: 3.61-231 nmol/g liver, $R^2 = 0.998$
(e)	Liver injection volume 30 µL	PP: 0.427-6.84 nmol/g liver, $R^2 = 0.994$ P: 0.226-1.81 nmol/g liver, $R^2 = 0.983$

conc., concentration; i.s., internal standard; log, logarithm to base 10

Appendix A.2

Supplementary material chapter 6

Tumor pharmacokinetics of encapsulated drug

Non-linear regression of the tumor concentration of encapsulated prednisolone phosphate (encapsulated PP) versus time was performed using Equations (8) and (9) as described in chapter 6. Note, Equations (8) and (9) were derived from Equations (6) and (7), which express the change of the amount of encapsulated PP with time. Figure A.2.1a shows there is no trend discerned between the amounts of encapsulated PP in the tumor and the time, whereas a relationship between the encapsulated PP concentration and the time is evident from Figure A.2.1b. Moreover, non-linear regression of the encapsulated PP tumor concentrations using Equations (12) and (13) results in better fits. These equations were derived from differential Equations (10) and (11) describing the change of the encapsulated PP tumor concentration with time. The corresponding *S*-values were 6.3 (zero-order release) and 5.5 (first-order release) for the concentration-based regression models, compared to 9.5 and 9.3, respectively, for the amounts-based regression models.

Differences between the results obtained for amounts- and concentration-based regression models can occur when the mass of the tissue is not constant with time as is expected for the tumor tissue. In this case, k_{PPBT} and k_{relT} are rather constant per gram of tumor and not per tumor as such. This indicates that the amounts of entities causing the different kinetic processes is rather similar per gram of tumor and not per whole tumor. With regard to the encapsulated PP tumor influx, this is in line with tumor physiology: during tumor growth new blood vessels with wide fenestrations, through which liposomes extravasate [A.2.1], are formed [A.2.2]. Thus, upon tumor growth the amount of entrances for liposomes also increases.

When comparing Equation (15) describing the rate of tumor influx and Equation (17) describing the rate of influx per gram of tumor to the corresponding equations for the other tissues (Equations (14) and (16), respectively), such kinetics for the influx of encapsulated PP towards the tumor appears to be a handicap. Assuming whole blood and tissue densities are 1 g/mL, V_{DPP} is about 2.5 times m_T and $\frac{V_{DPP}}{m_{L/S/K}}$ is always larger than one. Consequently, the encapsulated PP influx towards the tumor and the encapsulated PP influx towards one gram of tumor, respectively, are at a quantitative disadvantage.

Hepatomegaly

The mass of the liver was not constant with time (see chapter 6, Table 1). Most plausible, the observed increase in liver mass is caused by hepatomegaly due to hepatocytic accumulation of glycogen, which was also observed after short-term high-dose corticosteroid therapy [A.2.3], and was caused by prednisolone released by macrophages in the liver.

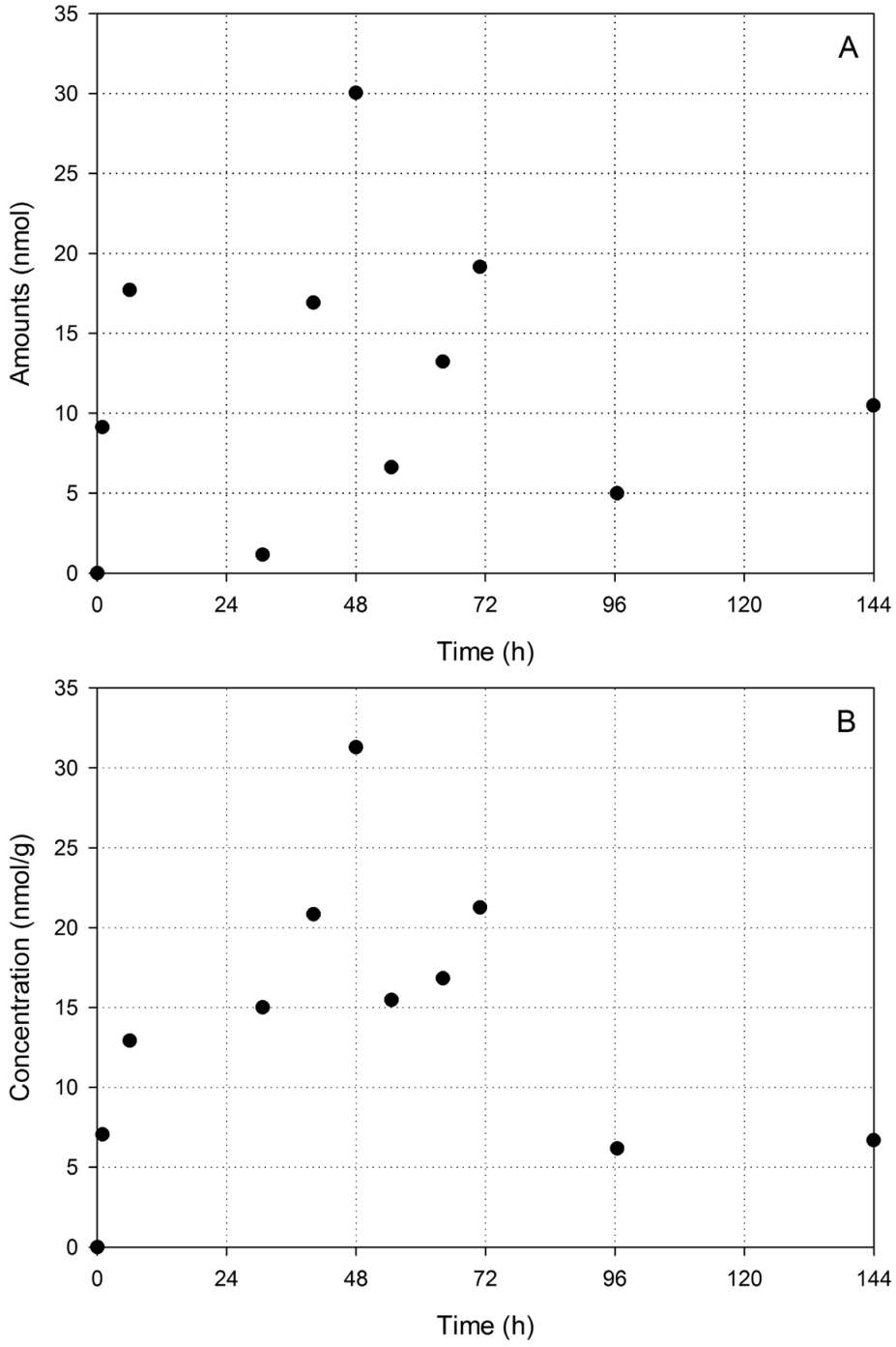

Figure A.2.1: Amounts (a) and concentrations (b) of encapsulated PP in the tumor as a function of time

REFERENCES

A.2.1 J.W. Nichols and Y.H Bae, EPR: evidence and fallacy, *J. Controlled Release*, 2014, **190**, 451-464.

A.2.2 N. Nishida, H. Yano, T. Nishida, T. Kamura and M. Kojiro, Angiogenesis in cancer, *Vasc. Health Risk Manage.*, 2006, **2**, 213-219.

A.2.3 T.C. Iancu, H. Shiloh and L. Dembo, Hepatomegaly following short-term high-dose steroid therapy, *J. Pediatr. Gastroenterol. Nutr.*, 1996, **5**, 41-46.

Appendix A.3

Summary

SUMMARY

During the development of a drug product, knowledge about the pharmacokinetics (PK) and pharmacodynamics (PD) supports the optimization of the effective dosage form and corresponding regimen. PK involves the processes of absorption, distribution, metabolism and excretion (ADME), which strongly influence the performance of the drug. This thesis focuses on the targeting of solid tumors by liposomal drug delivery systems. Due to the encapsulation of drugs into liposomes, the PK processes of distribution and elimination can change, yielding an improved therapeutic index. However, for liposomal formulations an additional PK parameter is of major importance, which involves the liberation of the drug from the liposomal carrier and subsequent fate of the drug.

Liposomes are vesicles which consist of one or more (phospho)lipid bilayers. After encapsulation of drug into the vesicles, these are deployed as drug delivery systems for the treatment of cancer and inflammations. Ideally, tumor targeted drug delivery results in the specific accumulation of liposomes at the target cells and avoidance of healthy tissue. At the target tissue, controlled release of the drug induces levels within the therapeutic window for a desired period of time. This minimizes toxicity and optimizes the therapeutic activity. Liposomes can alter the PK and can increase the therapeutic index successfully, mainly through the reduction of side effects. Nevertheless, liposomes do not meet all the criteria of an ideal drug delivery system. **Chapter 1** discusses the successes and remaining challenges of tumor targeted drug delivery by liposomes.

Successes and challenges of drug products are determined by the PK and PD. However, the PKPD of liposomal formulations intended for targeted drug delivery to solid tumors is not completely known. The drug has to be released from the liposome to become available and exert its effect. Thus, to gain more insights into the PKPD of liposomal drug delivery, individual concentration profiles of encapsulated and released drug are required. Such individual concentrations in plasma have been reported, but due to practical complications encapsulated and released concentrations in tissues are less commonly measured.

However, the encapsulation of phosphate prodrugs like prednisolone phosphate (PP) can allow the individual quantification of encapsulated and release drug concentrations in tissues after administration of a liposome formulation. Rapid conversion of PP into prednisolone (P) after release from the liposomes *in vivo* can provide a means to differentiate between encapsulated and released drug in blood and tissues, at which PP represents the encapsulated drug, while P represents the released drug. This thesis describes the development and implementation of a method for the quantification of encapsulated PP and released P concentrations in blood, tumor and healthy tissues after administration of polyethylene glycol (PEG)-coated liposomes containing PP in mice.

In **chapter 2** the rapid dephosphorylation of PP into P by murine liver and kidney phosphatases is verified *in vitro* using tissue homogenates and data analysis. PP incubation in the homogenates resulted in a rapid conversion into P: the majority of PP was already dephosphorylated after only 10 min of incubation using a high PP concentration representing ~3000 nmol/g tissue. The *in vivo* maximal released drug concentrations in liver and kidneys were calculated to be converted in less than 10 min. The time frame of drug release from PEGylated liposomes is rather in the order of hours than in the order of minutes. Related to the drug release from PEGylated liposomes, the *in vivo* conversion of PP into P is considered instantaneous. Thus, the dephosphorylation of PP into P in the excretory organs seems sufficiently fast to enable the determination of encapsulated and released drug concentrations in these tissues after administration of PEGylated liposomal PP in mice.

Chapter 3 presents the development of a method for the simple and reliable quantification of the encapsulated and non-encapsulated PP amounts in preparations of PEGylated liposomal PP. The evaluation of the non-encapsulated drug amount is an important part during the quality assurance of liposomal formulations. In addition, in this thesis, quantitative information about the encapsulated and non-encapsulated drug amounts in the liposome preparation itself was required in order to determine the accuracy of the method for the quantification of individual encapsulated and released drug concentrations in blood and tissues as described in chapter 4 and 5.

The method uses alkaline phosphatase (AP) to distinguish the non-encapsulated PP from the encapsulated PP by conversion of the non-encapsulated PP into P. During method development reaction progress curves were measured to determine the required amount of AP and the corresponding incubation time to achieve dephosphorylation of all non-encapsulated PP even when small changes in these parameters occur. In addition, several organic solvents were tested as precipitation solvent for their ability to yield clean chromatograms, rapid AP deactivation and complete liposome rupture to prevent under- and overestimations of the encapsulated and non-encapsulated drug concentrations. While tetrahydrofuran (THF) meets these three requirements, remarkably, acetonitrile was inferior to THF yielding a recovery of PP of 79 ± 7%. The performance of the developed method was evaluated by cross-validation involving dialysis: the accuracy of the method using AP is comparable to the accuracy of dialysis, while the method using AP is more precise. In conclusion, systematic method development yielded a reliable method for the quantification of the non-encapsulated drug fraction in preparations of liposomal PP.

The development and appropriate validation of the method for the quantification of encapsulated PP and released P in blood, tumor, liver, spleen and kidneys after

administration of PEGylated liposomal PP in mice is described in **chapter 4 and 5**. To obtain reliable results the methodology was thoroughly developed and validated using criteria adapted from the "Bioanalytical method validation guidance for industry" by the U.S. Food and Drug Administration. These criteria are in agreement with accuracy criteria from internal, industrial guidelines for preclinical bioanalytical methods at the time. In short, the accuracy and precision were anticipated to comply with an accuracy of 80-120% and a precision of maximally 20%.

Chapter 4 describes the development of the sample preparation methods for blood and liver tissue samples. The homogenization and precipitation solvent was anticipated to induce complete liposome rupture and prevent significant enzymatic hydrolysis of "encapsulated" PP during sample preparation to prevent significant under- and overestimations of the encapsulated PP and released P concentration, respectively. Further, it was anticipated to yield sufficient clean supernatants, sufficient extraction of P and PP and sufficient accuracy and precision. These requirements are met by the use of 10 mL methanol/g tissue during homogenization of liver tissue and protein precipitation of blood samples with four equivalents of methanol, at which the methanol contains the internal standards dexamethasone and dexamethasone phosphate. In contradiction to what was expected, acetonitrile and commercial available inhibitor cocktails were not able to deactivate liver phosphatase activity completely.

The sample preparation methods were coupled to a method involving liquid chromatography-mass spectrometry (LC-MS), of which the development is described in **chapter 5**. During LC-MS method optimization, the interference by (biological) impurities is avoided by optimization of the chromatography, negative electrospray ionization and high-resolution accurate mass Orbitrap analysis. This resulted in highly accurate and sensitive detection of PP and P in the complex matrices. Together, the sample preparation and LC-MS methods resulted in the following method specifications. The lower limits of quantitation were 0.99 µmol/L blood and 0.53 nmol/g liver for PP, and 229 nmol/L blood and 0.514 nmol/g liver for P. The accuracies were between 84-118% and the intrarun precision was ≤11%. Postliminary, the suitability of this methodology for tumor, kidney and splenic tissue samples is verified by similar qualification (internal study). These specifications are sufficient to measure encapsulated PP and released P concentrations in blood, tumor, liver, spleen and kidneys after administration of PEGylated liposomal PP at a dose of 36 µmol/kg PP (= 18 mg/kg of prednisolone disodium phosphate).

Chapter 6 focusses on the implementation of the developed methodology as described in chapter 4 and 5. To better understand the underlying PK of the targeted drug delivery by liposomes the developed method was applied after i.v. administration of PEGylated liposomal PP as a model formulation in mice. Encapsulated PP and released P drug concentrations in blood, tumor, liver, spleen and kidneys were quantified. Additionally,

the tissue influx of encapsulated drug and the drug release from the liposomes were calculated for each of the tissues separately using kinetic modelling.

After comparison of the results observed for the different tissues, it seems that a high affinity for the uptake of encapsulated drug as well as the release of drug is mainly observed for the spleen and not for the tumor. Moreover, from a quantitative point of view, the availability of released drug in the tumor after liposomal delivery is not pronounced as compared to availability in the other tissues of interest, because significantly larger peak concentrations of released P were measured in liver, spleen and kidneys than in the tumor. After release of drug from the liposomes in the tissues, the released P is probably rapid redistributed to the circulation and other tissues which could counteract the drug delivery effect of the liposomes. However, drug release in the tumor seems more extended than in the other tissues and the released drug concentration in the tumor remains at a fairly constant level in contradiction to the levels in the circulation, liver and spleen. These sustained release characteristics in the tumor most probably contribute to the beneficial effect. Nevertheless, larger released drug concentrations are present in other tissues.

In summary, this thesis focuses on the development, adequate validation and implementation of a reliable method to quantify encapsulated and released drug concentrations in blood and tissues after administration of a liposome formulation. As discussed in **chapter 7**, it shows that the fast dephosphorylation of a phosphate prodrug into its parent compound after release from the liposomal carrier allows the individual quantification of encapsulated and released drug in blood and tissues. In addition, the importance of appropriate method development and validation in an academic setting is demonstrated. More specific for liposomes and phosphate prodrugs, the verification of complete liposome rupture and particularly enzyme deactivation during sample preparation seems to be crucial. Finally, the thesis shows new insights into the PK of PEGylated liposomal PP as a model formulation. While larger peak concentrations of released P were observed in the liver, spleen and kidneys than in the tumor, extended release characteristics in the tumor probably contributes to the beneficial effect. The probably rapid redistribution of P from the tissues after drug release from the liposomes, highlights the impact of the PK properties of the drug compound itself on the liposomal drug delivery effect. It is therefore suggested that, from a PD point of view, further research should focus on released drug concentrations instead of the drug release.

Appendix A.4

Samenvatting in het Nederlands

Begrippenlijst

eiwitprecipitatie	het bewust laten bezinken van eiwitten in een monster met als doel dit op te schonen voorafgaand aan de analyse
farmaca	het meervoud van farmacon
farmacodynamiek (PD)	het verband tussen de farmaconconcentratie en de therapeutische activiteit/bijwerkingen als functie van de tijd
farmacokinetiek (PK)	de processen die het farmacon in het lichaam ondergaat na toediening van een geneesmiddel als functie van de tijd
farmacon	het werkzame bestanddeel in een geneesmiddel
fosfaatprodrug	een farmacon waaraan een fosfaatgroep is gekoppeld, waardoor een wateroplosbaar, maar therapeutisch niet-actief molecuul ontstaat; Dit wordt in het lichaam door specifieke enzymen (fosfatasen) weer omgezet (defosforylering) naar het oorspronkelijke farmacon.
(fosfo)lipide bilaag	een membraan bestaande uit twee lagen lipiden; Dit zijn meestal lipiden met een fosfaatgroep.
interne standaard	een andere maar representatieve stof voor de te analyseren stof; Hiervan wordt een bekende, constante hoeveelheid toegevoegd aan de standaarden van de kalibratielijn en de monsters om te corrigeren voor variaties tijdens de monstervoorbewerking en/of de analyse.
juistheid	de mate waarin de (gemiddelde) resultaten van een kwantitatieve analyse overeenkomen met de werkelijke waarde
LC-MS	afkorting voor "liquid chromatography-mass spectrometry", een techniek waarbij stoffen in een monster worden gescheiden met behulp van vloeistofchromatografie en vervolgens worden geanalyseerd met behulp van massaspectrometrie
macrofaag	een type witte bloedcel die ongewenste deeltjes in zich opneemt en afbreekt
precisie	de spreiding tussen de afzonderlijke resultaten van een kwantitatieve analyse
recovery	de terugvindbaarheid van de te analyseren stof; Deze bedraagt het percentage te analyseren stof in het te analyseren deel van het monster na de monstervoorbewerking ten opzichte van de totale te analyseren stof in het oorspronkelijke, onbewerkte monster.

	Hierbij bevat het onbewerkte monster een bekende (toegevoegde) concentratie van de te analyseren stof.
therapeutische index	de verhouding tussen de bijwerkingen en het therapeutisch effect van een farmacon
therapeutisch venster	de concentratierange die resulteert in een optimale verhouding tussen de bijwerkingen en het therapeutisch effect van een farmacon
validatie	aan de hand van vooraf gestelde eisen voor een specifiek doel aantonen dat de methode de gewenste resultaten oplevert
(weefsel)homogenisatie	het verpulveren van een weefsel zodat de samenstelling van het monster overal gelijk is en het, doorgaans na verdere monstervoorbewerking, kan worden geanalyseerd

SAMENVATTING

Tijdens het ontwikkelen van geneesmiddelen is kennis van de farmacokinetiek (PK) en farmacodynamiek (PD) belangrijk voor de optimalisatie van de farmaceutische formulering en de bijbehorende dosering. Tot de PK behoren de processen absorptie, distributie, metabolisme en excretie (ADME), welke de werking van het geneesmiddel sterk beïnvloeden. Dit proefschrift richt zich op de selectieve aflevering van farmaca in solide tumoren met behulp van liposomen. Door het farmacon te verpakken in liposomen kan de distributie en eliminatie veranderen. Hiervan probeert men gebruik te maken om het farmacon specifiek bij of in de tumorcellen af te leveren en het gezonde weefsel hierbij te ontzien. Dit kan vervolgens resulteren in een verbeterde therapeutische index. Naast de ADME van de liposomen, is een extra PK proces van groot belang voor liposomale formuleringen, namelijk het vrijkomen van het farmacon uit de liposomen, als ook de PK van het vrijgekomen farmacon.

Liposomen zijn hele kleine blaasjes die bestaan uit één of meerdere (fosfo)lipide bilagen. In deze blaasjes kunnen farmaca worden ingesloten. Zolang het farmacon is ingesloten vertoont het geen bijwerkingen, maar kan het zijn therapeutische werking ook niet uitoefenen. Liposomale formuleringen worden ingezet tijdens de behandeling van kanker en ontstekingen om het farmacon op specifieke locaties in het lichaam af te leveren. In het ideale geval accumuleren de liposomen selectief in of nabij specifieke cellen (bijvoorbeeld tumorcellen) en niet in gezond weefsel. In het specifieke weefsel zorgt een gereguleerde afgifte van het farmacon uit de liposomen vervolgens voor een plaatselijke concentratie binnen het therapeutische venster gedurende een gewenste periode. Deze specifieke, plaatselijke levering van farmacon minimaliseert de bijwerkingen en optimaliseert de therapeutische activiteit. In de praktijk kunnen liposomen de PK daadwerkelijk veranderen en de therapeutische index met succes verbeteren voornamelijk door een vermindering van bijwerkingen. Desalniettemin resulteert het gebruik van liposomen niet in de volledig ideale situatie zoals hierboven beschreven. **Hoofdstuk 1** beschrijft de successen en resterende uitdagingen wat betreft de selectieve aflevering van farmaca in tumoren met behulp van liposomen.

In het algemeen worden de effectiviteit en bijwerkingen van geneesmiddelen bepaald door de PK en PD. De PKPD van liposomale formuleringen die zijn bedoeld voor de specifieke, plaatselijke medicijnafgifte in solide tumoren is echter niet volledig bekend. Het ingesloten farmacon moet eerst vrijkomen uit de liposomen om beschikbaar te zijn en zijn effect te kunnen uitoefenen. Om meer inzicht te krijgen in de PKPD van dergelijke liposomale formuleringen is het dus nodig de concentraties van het ingesloten en vrijgekomen farmacon apart van elkaar te kwantificeren. Ofschoon dergelijke, afzonderlijke concentraties zijn gepubliceerd voor plasmamonsters, is het

meten van ingesloten en vrijgekomen concentraties in weefsels minder standaard vanwege praktische complicaties.

Het insluiten van fosfaatprodrugs zoals prednisolonfosfaat (PP) maakt de afzonderlijke kwantificatie van ingesloten en vrijgekomen farmacon in weefsels na toediening van een liposomale formulering echter mogelijk. Een snelle *in vivo* omzetting van PP in prednisolon (P) na afgifte uit de liposomen biedt de mogelijkheid om te differentiëren tussen ingesloten en vrijgekomen farmacon in bloed en weefsels. Hierbij is PP representatief voor het ingesloten farmacon en is P representatief voor het vrijgekomen farmacon. Dit proefschrift beschrijft de ontwikkeling en implementatie van een methode voor de kwantificering van ingesloten PP en vrijgekomen P concentraties in bloed, tumor en gezonde weefsels van muizen na toediening van polyethyleenglycol (PEG) gecoate liposomen met PP.

In **hoofdstuk 2** is de snelle defosforylering van PP in P door lever- en nierfosfatasen van muizen met behulp van weefselhomogenaten en data-analyse geverifieerd *in vitro*. De incubatie van PP met de homogenaten resulteerde in een snelle omzetting in P: tijdens de eerste 10 min van de incubatie met een hoge PP concentratie, die representatief was voor 3000 nmol/g weefsel, was de meerderheid van het PP al gedefosforyleerd. Uit berekeningen volgde dat de tijd die nodig is om de maximale, vrijgekomen, *in vivo* farmaconconcentraties in de lever en nieren om te zetten kleiner is dan 10 min. Het tijdsbestek van de medicijnafgifte uit gePEGyleerde liposomen is eerder in de ordegrootte van uren dan minuten. Vergeleken met de afgifte van farmacon uit gePEGyleerde liposomen, wordt de *in vivo* omzetting van PP in P als instantaan beschouwd. De defosforylering van PP in P in de uitscheidingsorganen lijkt dus voldoende snel om de bepaling van de ingesloten en vrijgekomen farmaconconcentraties in deze weefsels na toediening van gePEGyleerde liposomen met PP in muizen mogelijk te maken.

Hoofdstuk 3 beschrijft de ontwikkeling van een analytische methode voor de eenvoudige maar betrouwbare kwantificatie van de hoeveelheden ingesloten en niet-ingesloten PP in bereidingen van gePEGyleerde liposomen met PP. De evaluatie van de hoeveelheid niet-ingesloten farmacon is een belangrijk onderdeel van de kwaliteitsborging van liposomale formuleringen. Bovendien was tijdens dit promotieonderzoek kwantitatieve informatie vereist over de hoeveelheid ingesloten en niet-ingesloten farmacon in de liposoombereiding om de juistheid te bepalen van de methode voor de afzonderlijke kwantificatie van ingesloten en vrijgekomen farmacon in bloed en weefsels zoals beschreven in hoofdstuk 4 en 5.

De methode onderscheidt het niet-ingesloten PP van het ingesloten PP door het niet-ingesloten PP om te zetten in P met behulp van het enzym alkalische fosfatase (AP). Tijdens de methodeontwikkeling zijn omzetting-tijdcurves gemeten om de

hoeveelheid AP en de bijbehorende incubatietijd te bepalen die nodig zijn om al het niet-ingesloten PP te defosforyleren. Zelfs wanneer er kleine veranderingen in deze parameters optreden. Hieruit volgde dat de volledige omzetting van al het niet-ingesloten PP kan worden gegarandeerd door middel van incubatie van (1) 100 µL van de liposoombereiding (of verdunning) met maximaal 500 µM niet-ingesloten PP met (2) 100 µL van een AP oplossing (minimaal 6,960 mg AP (bevroren afgewogen) + 1,5 mL van een fosfaatgebufferde zoutoplossing van pH 7,4) gedurende 60 min. Verder zijn verschillende organische oplosmiddelen als precipitatiemiddel getest op hun capaciteit om schone chromatogrammen, een snelle deactivatie van AP en een volledige degradatie van de liposomen te verzorgen om onder- en overschattingen van de ingesloten en niet-ingesloten farmaconconcentratie te voorkomen. Tetrahydrofuraan (THF) voldoet aan deze drie eisen. Hierbij is het opmerkelijk dat acetonitril ondergeschikt was aan THF en resulteerde in een PP recovery van 79 ± 7% ten opzichte van 100 ± 1% voor THF. Het functioneren van de ontwikkelde methode is geëvalueerd door middel van een kruisvalidatie met dialyse: de juistheid van de methode met AP is vergelijkbaar met de juistheid van dialyse, terwijl de precisie beter is voor de methode met AP. Concluderend kan gesteld worden dat de beschreven systematische methodeontwikkeling een betrouwbare methode voor de kwantificering van de niet-ingesloten fractie PP in bereidingen van liposomaal PP heeft opgeleverd.

De ontwikkeling en gepaste validatie van de methode voor de kwantitatieve analyse van ingesloten PP en vrijgekomen P in bloed, tumor, lever, milt en nieren van muizen die gePEGyleerde liposomen met PP toegediend hebben gekregen, is beschreven in **hoofdstuk 4 en 5**. Om betrouwbare resultaten te verkrijgen is de methodologie zorgvuldig ontwikkeld en gevalideerd volgens aangepaste criteria van de "Bioanalytical method validation guidance for industry" van de U.S. Food and Drug Administration. Deze criteria zijn in overeenstemming met de nauwkeurigheidscriteria van de interne, industriële richtlijnen voor preklinische, bioanalytische methoden destijds. In het kort betekent dit dat er werd gestreefd naar een juistheid van 80-120% en een precisie van maximaal 20%.

Hoofdstuk 4 omschrijft de ontwikkeling van de monstervoorbewerkingsmethodes voor bloed- en levermonsters. Het oplosmiddel voor homogenisatie en precipitatie dient tijdens de monstervoorbewerking een volledige degradatie van de liposomen te induceren en een significante enzymatische hydrolyse van "ingesloten" PP te voorkomen. Dit om significante onder- en overschattingen van respectievelijk de ingesloten PP en vrijgekomen P concentratie te voorkomen. Verder dient het te resulteren in voldoende schone supernatanten, een voldoende extractie van P en PP en een voldoende juistheid en precisie. Aan deze eisen wordt voldaan door tijdens de homogenisatie van levermonsters 10 mL methanol/g weefsel te gebruiken en tijdens de eiwitprecipitatie

van bloedmonsters vier equivalenten methanol. Hierbij bevat de methanol de interne standaarden dexamethason en dexamethasonfosfaat. In tegenstelling tot wat werd verwacht, waren acetonitril en commercieel verkrijgbare inhibitor cocktails niet in staat om de activiteit van leverfosfatasen volledig te deactiveren.

Deze monstervoorbewerkingsmethodes werden gecombineerd met een LC-MS methode, waarvan de ontwikkeling is beschreven in **hoofdstuk 5**. Om de interferentie door (biologische) onzuiverheden te vermijden, is de LC-MS methode geoptimaliseerd door middel van optimalisatie van de chromatografie, negatieve elektrospray ionisatie en hoge resolutie accurate massaspectrometrie met de Orbitrap. Dit resulteerde in een zeer accurate en gevoelige detectie van PP en P in de complexe matrices. De monstervoorbewerking in combinatie met de LC-MS methode resulteerde in de volgende gezamenlijke specificaties. De onderste kwantificatielimieten waren 0,99 µmol/L bloed en 0,53 nmol/g lever voor PP en 229 nmol/L bloed en 0,514 nmol/g lever voor P. De juistheid lag tussen 84-118% en de "intrarun" precisie was ≤11%. Naderhand is de geschiktheid van deze methodologie geverifieerd voor tumor, nieren en milt door middel van een vergelijkbare kwalificatie (interne studie). Deze specificaties zijn voldoende om ingesloten PP en vrijgekomen P concentraties te meten in het bloed, de tumor, lever, milt en nieren van muizen die een dosis van 36 µmol/kg PP (= 18 mg/kg prednisolondinatriumfosfaat) aan gePEGyleerde liposomen met PP toegediend hebben gekregen.

Hoofdstuk 6 richt zich op de implementatie van de ontwikkelde methode die beschreven is in hoofdstuk 4 en 5. Om de PK van liposomale formuleringen die zijn bedoeld voor de specifieke, plaatselijke medicijnafgifte in solide tumoren beter te begrijpen, werden gePEGyleerde liposomen met PP toegediend als modelformulering aan muizen waarna de ontwikkelde methode werd toegepast. De ingesloten PP en vrijgekomen P concentraties in bloed, tumor, lever, milt en nieren zijn gekwantificeerd. Verder zijn de influx van het ingesloten farmacon richting de weefsels en de medicijnafgifte uit de liposomen gemodelleerd voor elk van de weefsels afzonderlijk.

Als we de resultaten voor de verschillende weefsels vergelijken, lijkt voornamelijk de milt en niet de tumor een hoge affiniteit te tonen voor de opname van ingesloten farmacon als ook de afgifte van farmacon uit de liposomen. Dit komt waarschijnlijk door de anatomie en hoge macrofaagdichtheid van de milt. Bovendien is vanuit een kwantitatief oogpunt de beschikbaarheid van vrijgekomen farmacon in de tumor niet uitgesproken in vergelijking met de beschikbaarheid in de andere onderzochte weefsels. In de lever, milt en nieren werden namelijk significant hogere piekconcentraties van vrijgekomen P gemeten dan in de tumor. Hierbij spelen onder andere de dichtheid, het type en/of de bereikbaarheid van de macrofagen in de verschillende weefsels mogelijk een rol. Na afgifte uit de liposomen in de weefsels, distribueert het vrijgekomen P

waarschijnlijk snel richting de circulatie en andere weefsels. Dit kan de selectieve aflevering van farmacon door de liposomen (deels) teniet doen. Echter, het vrijkomen van het farmacon houdt langer aan in de tumor dan in de andere weefsels en de vrijgekomen farmaconconcentratie in de tumor blijft redelijk constant ten opzichte van de concentraties in de circulatie, lever en milt. Deze verlengde afgifte in de tumor draagt zeer waarschijnlijk bij aan het therapeutisch effect. Niettemin zijn er grotere vrijgekomen farmaconconcentraties aanwezig in andere weefsels.

Samengevat richt dit proefschrift zich op de ontwikkeling, gepaste validatie en implementatie van een betrouwbare methode om ingesloten en vrijgekomen farmaconconcentraties in bloed en weefsels te kwantificeren na toediening van een liposoomformulering. Zoals besproken in **hoofdstuk 7**, laat dit proefschrift zien dat de snelle defosforylering van een fosfaatprodrug na het vrijkomen uit de liposomen de afzonderlijke kwantificering van ingesloten en vrijgekomen farmacon in bloed en weefsels mogelijk maakt. Verder wordt het belang van gepaste methodeontwikkeling en validatie in een academische omgeving getoond. In het geval van liposomen en fosfaatprodrugs lijkt de verificatie van een volledige degradatie van de liposomen en vooral ook van de deactivatie van enzymen essentieel te zijn tijdens de monstervoorbewerking. Ten slotte toont het proefschrift nieuwe inzichten in de PK van de modelformulering, i.e. gePEGyleerde liposomen met PP. Hoewel in de lever, milt en nieren hogere piekconcentraties van vrijgekomen P zijn waargenomen dan in de tumor, draagt de verlengde afgifte van farmacon in de tumor waarschijnlijk bij aan het therapeutisch effect. De waarschijnlijk snelle herverdeling van P na afgifte van PP uit de liposomen, benadrukt de invloed van de PK eigenschappen van het farmacon zelf op de uitwerking van de selectieve aflevering van farmacon door liposomen. Vanuit een PD oogpunt luidt dan ook het voorstel dat verder onderzoek zich zou moeten richten op de vrijgekomen farmaconconcentraties en niet op de farmaconafgifte uit de liposomen.

Appendix A.5

List of publications corresponding to this thesis

LIST OF PUBLICATIONS CORRESPONDING TO THIS THESIS

- The development of a method to quantify encapsulated and free prednisolone phosphate in liposomal formulations
  Evelien A.W. Smits, Coen J.P. Smits and Herman Vromans
  Journal of Pharmaceutical and Biomedical Analysis, 2013, **75**, 47-54

- *In vitro* confirmation of the quantitative differentiation of liposomal encapsulated and non-encapsulated prednisolone (phosphate) tissue concentrations by murine phosphatases
  Evelien A.W. Smits, José A. Soetekouw and Herman Vromans
  Journal of Liposome Research, 2014, **24,** 130-135

- Plasma, blood and liver tissue sample preparation methods for the separate quantification of liposomal-encapsulated prednisolone phosphate and non-encapsulated prednisolone
  Evelien A.W. Smits, José A. Soetekouw, Peter F.A. Bakker, Bart J.H. Baijens and Herman Vromans
  Journal of Liposome Research, 2015, **25**, 46-57

- Quantitative LC-MS determination of liposomal encapsulated prednisolone phosphate and non-encapsulated prednisolone concentrations in murine whole blood and liver tissue
  Evelien A.W. Smits, José A. Soetekouw, Irene van Doormalen, Bart H.J. van den Berg, Marcel P. van der Woude, Nicolette de Wijs-Rot and Herman Vromans
  Journal of Pharmaceutical and Biomedical Analysis, 2015, **115**, 552-561

- The availability of drug by liposomal drug delivery
  Individual kinetics and tissue distribution of encapsulated and released drug in mice after administration of PEGylated liposomal prednisolone phosphate
  Evelien A.W. Smits, José A. Soetekouw, Ebel H.E. Pieters, Coen J.P. Smits, Nicolette de Wijs-Rot and Herman Vromans
  Investigational New Drugs, 2018, https://doi.org/10.1007/s10637-018-0708-4

Appendix A.6

Dankwoord

DANKWOORD

Het voelt nog maar relatief kort geleden dat ik een vacature in de krant zag staan voor een positie als promovendus bij Organon in Oss. Eigenlijk was ik op dat moment tevreden met mijn toen huidige baan, maar het leek me meteen geweldig om een aantal jaren in een dergelijke multinational te mogen rondlopen. Ik ging er vanuit dat er veel andere kandidaten zouden zijn en schatte mijn kansen dan ook niet zo hoog in. Zelfvertrouwen is niet mijn allergrootste talent, maar toch besloot ik te solliciteren. En ik werd aangenomen.

Daarop volgde een aantal bewogen jaren, waarbij de sporthalbijeenkomst op donderdag 8 juli nog steeds op mijn netvlies staat gebrand. Maar ik heb er ook de mogelijkheid gekregen om samen te werken met specialisten uit verschillende vakgebieden. Stuk voor stuk collegiale, vakbekwame mensen voor wie ik grote bewondering en respect heb. Het zijn de herinneringen aan deze personen die ik meeneem.

Promoveren doe je niet alleen. Dit proefschrift is tot stand gekomen met hulp van collega's van o.a. Organon en Universiteit Utrecht en MediTrans. Ook familie en vrienden hebben een belangrijke bijdrage geleverd. Via deze weg wil ik dan ook iedereen hartelijk danken voor hun betrokkenheid. Een aantal mensen wil ik graag specifiek noemen zonder de intentie anderen te kort te doen.

Prof. dr. Herman Vromans, promotor. Beste Herman, allereerst bedankt dat je iets in mij zag en mij hebt aangenomen. Bedankt ook voor je begeleiding, vertrouwen, geduld en voor de vrijheid die ik heb gekregen. Ik heb veel bewondering voor je strategisch inzicht en je affiniteit voor het selecteren van innovatieve onderzoeksthema's. Ik durf wel te zeggen dat dit het succes van dit promotieonderzoek mede heeft bepaald.

Dr. Nicolette de Wijs-Rot, copromotor. Beste Nicolette, als groepshoofd maakte je ruimte voor mijn project. Jouw keuze voor de LTQ Orbitrap bleek vervolgens de sleutel te zijn. Ik heb enorme bewondering voor je professionaliteit. Bedankt voor het delen van je expertise, begeleiding en betrokkenheid.

Via deze weg wil ik ook de beoordelingscommissie, welke bestond uit prof. dr. Gert Storm, prof. dr. Daan Crommelin, prof. dr. Jos Beijnen, prof. dr. Stefaan De Smedt en prof. dr. Erik Frijlink, hartelijk bedanken voor het beoordelen van het manuscript.

José Soetekouw, zonder jouw hulp waren de experimenten waarschijnlijk nooit klaar geweest voor de reorganisatie van Merck. Bedankt voor je vakkundige en tomeloze inzet

tijdens het halen van deze harde deadline. Daarnaast kon ik ook altijd bij je terecht voor deskundig advies op analytisch danwel persoonlijk vlak. En nog steeds. Dank je wel José!

Bart van den Berg, je leverde een belangrijke bijdrage aan de ontwikkeling van de MS methode. Na je vertrek bleef je beschikbaar om de desbetreffende publicatie tot een goed einde te brengen. Bedankt voor het delen van je expertise, de inzichtelijke discussies en je betrokkenheid. Ik heb veel van je mogen leren.

Irene van Doormalen, na het vertrek van Bart nam jij het stokje over. Samen met Marcel, Wouter, Theo en Nicolette hebben we een betrouwbare MS methode ontwikkelt, wat resulteerde in de publicatie beschreven elders in dit proefschrift. Dank je wel voor jullie inzet. Ik had dit niet zonder jullie ervaring en specialisme kunnen doen.

Coen Smits, mijn broer. Doorgaans passeren familieleden pas de revue aan het einde van het dankwoord. Ik heb het geluk een grote broer te hebben met een wetenschappelijke achtergrond en die altijd voor me klaar staat. Tijdens het schrijven van dit proefschrift was je mijn vraagbaak voor o.a. statistische en wiskundige kwesties. Ik heb er enorm veel van geleerd. Je rust en relativeringsvermogen heb ik graag opgezocht. Dank je wel! Uiteindelijk ben je coauteur van twee publicaties. Ik vind het heel bijzonder dit samen met jou gedaan te mogen hebben.

Bart Baijens, je was de eerste collega die zich aansloot bij het project. Ik heb dat altijd beschouwd als een enorme luxe. Dank je wel voor je bijdrage tijdens de ontwikkeling van de monstervoorbewerking- en LC-MS methode, als ook voor je enthousiasme en begrip.

Peter Bakker, ook jij hebt me werk uit handen genomen. Je hebt me ook heel veel geleerd over HPLC en laboratoriumpraktijken in zijn algemeenheid. Ik kon je altijd even een vraag stellen of even sparren. Dank je wel daarvoor! Ook bedankt voor je betrokkenheid en de gezellige pauzes samen met de anderen van de Biofarmacie.

Een woord van waardering ten aanzien van de collega's van de Universiteit Utrecht mag in dit dankwoord zeker niet ontbreken. Hun expertise op het gebied van liposomen en de bereidheid deze te willen delen, vormden belangrijke input voor dit promotieonderzoek. Niet in de laatste plaats, mocht ik gebruik maken van een aan de universiteit ontwikkelde liposoomformulering. Heel veel dank hiervoor. Een aantal personen wil ik graag specifiek vermelden.

Prof. dr. Gert Storm. Beste Gert, bedankt voor je hartelijke ontvangst op de universiteit. Bedankt ook voor je begeleiding en betrokkenheid tijdens mijn promotieonderzoek en in het bijzonder tijdens mijn verblijf op de universiteit.

Raymond Schiffelers, ik kon altijd bij je terecht voor extra informatie over dierexperimentele vraagstukken omtrent liposomen. Bedankt voor het delen van je expertise.

Ebel Pieters, jouw bijdrage als art. 9 functionaris tijdens het *in vivo* werk was essentieel. Dank je wel voor je hulp bij het opzetten van deze proef en het uitvoeren ervan. Ik vond het prettig om met je samen te werken.

Louis van Bloois, jij hebt me geleerd liposomen te maken. Als er iets mis was gegaan, kon ik altijd bij je terecht en had je een oplossing. Dank je wel voor het delen van je kennis en ervaring.

Karin Hens en Barbara de Jong, bedankt voor jullie snelle antwoorden op mijn e-mails en jullie hulp met het MyPhD systeem.

Verder wil ik de bewoners van kamer Z509 van het F.A.F.C. Wentgebouw bedanken voor hun collegialiteit en gezelligheid.

Voor zover nog niet genoemd, wil ik graag mijn oud-collega's van d'n Organon bedanken voor hun collegialiteit. In het bijzonder, wil ik graag de volgende personen met naam noemen.

Roel Arends, ik kon altijd bij je terecht met vragen op het gebied van de farmacologie. Ook na je vertrek bleef je deur open staan. Dank je wel voor het delen van je expertise.

Cees van Dongen, Hans van Laarhoven, Miranda de Jager, Foppe Bakker en Frans Spanjers, dank jullie wel voor jullie hulp, voor het delen van jullie kennis en ervaring, voor de prettige discussies, voor jullie gezelligheid en humor, en voor jullie goede zorgen en wijsheid. Kortom, ik heb het ervaren als een zeer fijne habitat voor mij als promovenda. Dat zal ik altijd blijven waarderen. Miranda, bedankt voor je support de laatste jaren op farmaceutisch gebied danwel privé. Dank je wel voor de gezellige uitstapjes samen met José naar de martelkelder en zo.

Verder wil ik nog bedanken: Henny Bruinewoud, Fried Faassen, Michel Heisen, Siene Schoonus, Jasminka Franjković-Džafić, Lisa Holmdahl, Chris Dirks, Mari Jansen en de solids, Ineke van den Brink-Kleefsman, Bianca Matthee, Jolanda van Turnhout, Premie Krom-Govender, Jurgen Ketelaars, John den Engelsman, Michiel Damen, Ad Gerich, Harrie Peters, Hester Kramer, de groep Modeling & Simulation, Ilse Mommers, John Dulos, Frank Wijnands, John Fundter, Freek Bourgondiën, Laura Hermens, Bianca Huisman, Mijntje Biermann en Jannie Bloemers.

Graag wil ik de andere promovendi van o.a. Organon en de Universiteit Utrecht bedanken voor hun gezelschap en support. In het bijzonder wil ik Tofan Willemsz noemen. Tofan, bedankt voor het bieden van een luisterend oor, het delen van je optimisme en de culinaire uitstapjes. Raween Kalicharan en Ton van Heugten, dank jullie wel voor alle

informatie omtrent het afronden van het proefschrift en het beantwoorden van al mijn vragen daarover.

I would also like to thank the students Krishan Kharagjitsing, Andhyk Halim, Dionne David and Daphne van Dijk for their interest in the project. Thank you for all the hard work you have done and thank you for providing the opportunity for me to practice my people skills as a supervisor.

Annelieke Paantjens, naast een zeer goede vriendin, was je ook even mijn collega en ervaringsdeskundige als het om promoveren aan de UU gaat. Ik kan altijd bij je terecht met werk gerelateerde vragen danwel issues op het persoonlijk vlak. Dank je wel!

Beste vrienden, familie en schoonfamilie, bedankt voor het tonen van jullie interesse in mij en het promotieonderzoek. Bedankt voor jullie support maar zeker ook voor de afleiding en ontspanning. Femke Langenkamp, we kennen elkaar al sinds de meisjes E. Leuk dat je vandaag een van mijn paranimfen wilt zijn.

Pap en mam, het moge duidelijk zijn dat zonder jullie dit proefschrift er nooit was geweest. Dank je wel dat jullie ons de mogelijkheid hebben gegeven om te studeren. Bedankt ook voor jullie onvoorwaardelijk steun, vertrouwen en liefde. Nu, in het verleden en in de toekomst. Ik prijs me gelukkig met jullie als ouders. En… sorry voor de grijze haren.

Lieve Ruud, woorden gaan hier sowieso te kort schieten. Dank je wel voor je onbaatzuchtigheid en geduld, dat je het me hebt gegund om dit af te maken en altijd achter me bent blijven staan. Dank je wel voor de inhoudelijke discussies tijdens het eten, de we-gaan-het-nu-eens-over-iets-anders-hebben momenten en je flauwe, heerlijke grappen. Dank je wel dat je er voor me bent, hoe lastig het ook voor jou geweest moet zijn. Je bent een mooi mens. Ik hou van jou.

Appendix A.7

Curriculum vitae

CURRICULUM VITAE

Evelien Smits werd geboren in Velden en rondde het Gymnasium af aan het Valuascollege te Venlo. Zij behaalde haar MSc diploma in Moleculaire Wetenschappen aan de Wageningen Universiteit met als specialisatie Fysische Chemie. Hierbij deed zij afstudeeronderzoeken bij de vakgroep Organische Chemie en bij Agrotechnology and Food Sciences Group, welke beide zijn verbonden aan het Wageningen Universiteit en Research Centrum. Ze liep stage bij Organische en Fysische Chemie aan de Carl von Ossietszky Universiteit in Oldenburg, Duitsland. Haar promotietraject in de Farmaceutische Wetenschappen vond plaats bij Organon Biosciences[7] in Oss in samenwerking met Utrecht Universiteit en onder begeleiding van de promotor prof. dr. Herman Vromans en de copromotor dr. Nicolette de Wijs-Rot. Dit resulteerde in dit proefschrift. Daarnaast was ze werkzaam als "Prof. Eveline Adrenaline" bij Mad Science Brabant en was ze ook geïnteresseerd in andere vakgebieden zoals de dermatologie, voedingswetenschappen en psychologie.

Evelien Smits was born in Velden, The Netherlands, and graduated at the Gymnasium department of the Valuascollege in Venlo. She obtained her MSc degree in Molecular Sciences with a specialization in Physical Chemistry at Wageningen University and completed a first MSc thesis at the Laboratory of Organic Chemistry, a second MSc thesis at the Agrotechnology and Food Sciences Group, which were both at Wageningen University and Research Centre, and a scientific internship in Organic and Physical Chemistry at the Carl von Ossietszky University of Oldenburg, Germany. Her PhD project in Pharmaceutical Sciences was performed at Organon Biosciences[8] in Oss in collaboration with Utrecht University and supervised by Prof. Dr. Herman Vromans and Dr. Nicolette de Wijs-Rot. This resulted in the current dissertation. In addition, she worked as "Prof. Eveline Adrenaline" at Mad Science Brabant and was also interested into other disciplines like dermatology, nutrition and psychology.

7 In de loop van het promotieonderzoek werd Organon Biosciences overgenomen door Schering-Plough wat op zijn beurt fuseerde met MSD.

8 During the PhD project Organon Biosciences was acquired by Schering-Plough, which merged with MSD.